The role of α-tubulin acetylation in the regulation of murine sperm motility

FRANCIS, SARAH,LOUISE

The role of α-tubulin acetylation in the regulation of murine sperm motility

Sarah Louise Francis

A thesis submitted for the degree of Doctor of Philosophy

Department of Biosciences

Durham University

2018

Abstract

The role of α-tubulin acetylation in the regulation of murine sperm motility

Sperm motility is a vital function required for fertility and is a consequence of interactions between components of the axoneme in the sperm flagellum. Microtubules, made up of α- and β-tubulin, are a central component of the axoneme and undergo various post-translational modifications. One such modification is the acetylation of the lysine 40 residue of α-tubulin which is carried out by α-tubulin acetyltransferase (α-TAT1), and is deacetylated by the activities of histone deacetylase 6 (HDAC6) and SIRT2. Recently, research has implicated α-tubulin acetylation in the regulation of sperm motility. The work presented in this thesis therefore aimed to study the influence that the state of α-tubulin acetylation has on sperm function by assessing the role of α-tubulin deacetylation in sperm motility modulation. To do this, murine sperm were treated with the HDAC6-specific inhibitor, tubacin; the general Class I and II HDAC inhibitor trichostatin A (TSA); and the general Class III HDAC inhibitor, nicotinamide. Exposure to the inhibitors did not significantly affect sperm motility or levels of acetylated α-tubulin. Furthermore, high baseline levels of acetylated α-tubulin were found in sperm. Subsequent examination of HDAC activity demonstrated that HDAC6 was active and could be inhibited in live murine sperm. Taken together, the results indicated that HDAC6 activity in sperm was low, suggesting that highly acetylated α-tubulin may be important for sperm function. As acetylation is indicative of microtubule stability, the effect of microtubule destabilisation using the drug, nocodazole, was assessed. Both α-tubulin organisation and acetylation remained intact in sperm following treatment, though nocodazole was found to significantly enhance certain motility parameters. This thesis therefore reports the novel finding that treatment with a microtubule depolymerising drug can alter sperm motility, indicating that subtle changes in microtubule conformation may influence flagellar motion which could have important implications for infertility caused by impaired sperm motility.

Acknowledgements

I would like to thank Professor Stuart Wilson for granting me the opportunity to undertake this PhD and supervising me in the first instance. I would also like to thank Dr Adam Benham for taking over my supervision and providing invaluable guidance that allowed me to complete this thesis. I am extremely grateful for your support, encouragement and allowing me to join your lab. My gratitude is also extended to Dr Susan Pyner and Dr Jason Gill for your helpful guidance in relation to my project, and to Dr Morag Mansley for teaching and supporting me whilst I found my feet in the lab. I also thank Durham University for providing the funding to support this project.

I would like to thank Dr Steve Publicover and Professor Chris Barratt and lab members for allowing me to visit and learn sperm-related techniques - I am very grateful for your time and expertise. I am also grateful to staff at both the LSSU and the Microscopy and Bioimaging Facility in Durham for your invaluable assistance and knowledge. Thank you also to the technical team at Queen's Campus, particularly Mr George Otterson, without whom the relocation to Biosciences would have been even more stressful and chaotic!

To the friends I made whilst completing this PhD, I extend my heartfelt thanks. Thank you for supporting me when times were difficult, learning my tea colour preferences, and for providing a safe haven in G115. I know I wouldn't have got through it without you. Thank you also to members of my new lab group for welcoming me and helping me to settle in. In particular, I am grateful to Naomi for keeping me sane on the final leg - I am very thankful that we were able to share the end of our PhD journeys.

I would like to thank my friends for listening to me complain for 4 years, and humouring me whilst I talk about sperm. Thank you to Stuart for learning "HDAC6," keeping me grounded, and reminding me there's more to life. I promise I will get a job! Finally, my biggest thanks go

to my parents for your patience, understanding and encouragement. Thank you for your unconditional support during this PhD and everything that came before.

Statement of copyright

Contents

List of figures

Chapter 1

Chapter 2

Chapter 3

Chapter 4

Chapter 5

Chapter 6

List of tables

List of abbreviations

+TIPs	Plus end tracking proteins
AAA	ATPase family associated with diverse cellular activities
ABHD2	alpha/beta hydrolase domain containing protein 2
AKAP	A-kinase anchoring protein
ALH	Amplitude of lateral head displacement
ART	Assisted Reproductive Technology
ATP	Adenosine triphosphate
BCF	Beat cross frequency
cAMP	Cyclic adenosine monophosphate
CASA	Computer-assisted sperm analysis
CatSper	Cation channel of sperm
CCP	Cytosolic carboxypeptidase
CP	Central pair of microtubules
CTT	C-terminal tails
DA	Dynein arms
DAPI	4', 6-diamidino-2-phenylindole
DMEM	Dulbecco's Modified Eagle's Medium
ECL	Enhanced chemiluminescence

EDTA	Ethylenediaminetetraacetic acid
EGTA	Ethylene glycol-bis-N,N,N',N'-tetraacetic acid
FBS	Foetal bovine serum
FS	Fibrous sheath
GCN5	General control nonderepressible 5
GDP	Guanosine diphosphate
GR	Glucocorticoid receptor
GTP	Guanosine triphosphate
HDAC	Histone deacetylase
HEK-MSR	Human embryonic kidney – macrophage scavenger receptor
HEPES	4-(2-hydroxyethyl)-1-piperazineethanesulfonic acid
HFEA	Human Fertilisation and Embryology Authority
HSP90	Heat shock protein 90
IAM	Inner acrosomal membrane
ICSI	Intracytoplasmic sperm injection
IVF	*In vitro* fertilisation
LC	Longitudinal columns
LIN	Linearity
MAP	Microtubule associated protein
MEF2	Myocyte enhancer factor 2

MS	Mitochondrial sheath
NICE	National Institute of Clinical Excellence
OAM	Outer acrosomal membrane
ODF	Outer dense fibres
OMDA	Outer microtubule doublets of the axoneme
PBS	Phosphate buffered saline
PKA	Protein kinase A
PM	Plasma membrane
PTM	Post-translational modification
PVDF	Polyvinylidene difluoride
RS	Radial spokes
sAC	Soluble adenylyl cyclase
SCA	Sperm Class Analyser
SDS	Sodium dodecyl sulfate
SETD2	SET-domain containing 2
SIRT	Sirtuin (silent information regulator)
STORM	Stochastic optical reconstruction microscopy
STR	Straightness
TBS-T	Tris-buffered saline with Tween-20
TE	Trypsin/EDTA

TEM	Transmission electron microscopy
TGF-β	Transforming growth factor β
TNP	Transition protein
TR	Transverse ribs
TSA	Trichostatin A
TTL	Tubulin tyrosine ligase
TTLL	Tubulin tyrosine ligase-like
VAP	Average path velocity
VCL	Curvilinear velocity
VSL	Straight line velocity
WH	Whittens-HEPES media
WH-cap	Whittens-HEPES capacitating media
WHO	World Health Organisation
WOB	Wobble
ZP	Zona pellucida
α-TAT1	α-tubulin acetyltransferase 1

Chapter 1

Chapter 1 – Introduction

1.1 Infertility

Infertility is broadly defined by the World Health Organisation (WHO), National Institute of Clinical Excellence (NICE) and the Human Fertilisation and Embryology Authority (HFEA) as the inability of a couple to achieve a clinical pregnancy after one year of regular unprotected sexual intercourse (NICE, 2013; HFEA, 2016). Studies estimate that between 8% and 12% of reproductive-aged couples globally are affected by infertility (Vander Borght and Wyns, 2018). In the UK, approximately one in seven couples experience subfertility (HFEA, 2016), equating to 3.5 million people of reproductive age (NICE, 2013). Such figures prompted the recognition of infertility as a worldwide public health issue by the WHO (Boivin *et al.*, 2007; Mascarenhas *et al.*, 2012). In addition, a recent comprehensive report showing a significant unexplained decline in sperm counts over the last 40 years (Levine *et al.*, 2017) has brought male reproductive health to the forefront and highlighted the requirement for further understanding of this under-researched area.

1.2 Male infertility

It is estimated that upwards of 33 million men worldwide are infertile (Agarwal *et al.*, 2015), with male factors contributing to the decision to undertake fertility treatment in approximately 40% of infertility cases (NICE, 2013). In the most recent data from the HFEA, male infertility was reported as the most common reason for a couple to undertake cycles of *in vitro* fertilisation (IVF) (HFEA, 2018). These statistics highlight the role of male factors as an important contributor to the requirement for fertility treatment. The aetiology of male infertility is wide-ranging, arising from the abnormal functioning of various parts of the reproductive tract, and including disorders such as cryptorchidism, tract obstructions, varicocele, or genetic conditions such as Klinefelter Syndrome. However, the single most common identified cause of infertility is sperm dysfunction, defined as sperm lacking 'normal'

function (Hull *et al.*, 1985; Barratt *et al.*, 2011). The term 'sperm dysfunction' can encompass a range of sperm abnormalities including those shown in **Table 1.1**; a semen analysis is used clinically to attempt to identify specific sperm defects.

1.2.1 Diagnosis of male factor infertility

A routine semen analysis assesses semen volume and pH, and sperm concentration, motility, and morphology. Guidelines set out by the WHO indicate that a 'normal' semen classification (normozoospermia) requires a sperm concentration of ≥15 million/ml, sperm motility ≥40%, with 32% progressively motile, and sperm morphology ≥4% normal forms (Cooper *et al.*, 2010). If sperm parameters fall outside of these ranges, a classification system exists to describe the abnormality (**Table 1.1**), and forms the basis of the recommended treatment.

Table 1.1: Classification of sperm abnormalities

Parameter	Range	Classification
Sperm concentration	0 million/ml	Azoospermia
	<15 million/ml	Oligozoospermia
	≥250 million/ml	Polyzoospermia
Sperm motility	<40% motile, <32% progressively motile	Asthenozoospermia
Sperm morphology	<4% normal forms	Teratozoospermia

1.2.2 Assisted Reproductive Technology (ART) for the treatment of male infertility

Individuals found to exhibit defects in any sperm parameter currently only have one treatment option - Assisted Reproductive Technology (ART). The use of such technology has grown globally over the past few decades and it is now estimated that over 7 million babies have been born as a result of ART (ESHRE, 2018). In the UK, *in vitro* fertilisation (IVF) accounts for more than 2% of all babies born (HFEA, 2014). For male factor infertility, two types of

treatment are usually recommended depending on the severity of the abnormality. For mild sperm dysfunction, conventional IVF may be advised, during which oocytes and sperm are brought into close proximity and fertilisation allowed to occur. Alternatively, for severe sperm defects such as very low concentrations or poor motility, intracytoplasmic sperm injection (ICSI) may be recommended which involves the injection of a single sperm directly into the egg. The latest data from the HFEA indicates that 36% of all treatment cycles in the UK in 2016 involved the use of ICSI, with male factor infertility being a main reason for choosing an ICSI cycle (HFEA, 2018). These figures demonstrate the importance of ICSI in aiding couples with male infertility. However, the willingness of couples to undergo such invasive, expensive, and emotionally demanding procedures also indicates a lack of alternative treatment options and helpful diagnoses arising from the incomplete understanding of fertility in males.

1.2.3 Limitations in the diagnosis and treatment of male factor infertility

Knowledge of the mechanisms underlying sperm functionality is lacking. As such, questions have been raised over the clinical value of the current semen analysis (Barratt *et al.*, 2011). Whilst current procedures can aid in detecting the cause of the subfertility broadly, semen analysis gives only a description of the abnormality; the underlying structural or molecular defect is usually not identified. As a consequence, treatment options remain the same regardless of the semen analysis result. In addition, overlaps exist between the sperm parameters of infertile and fertile men (Nallella *et al.*, 2006; Lefièvre *et al.*, 2007), making it difficult to define the parameter boundaries between 'fertile' and 'subfertile.' To further confound the difficulty in diagnosing male infertility, routine semen analysis assesses freshly ejaculated sperm. However, sperm must reside in the female reproductive tract before they acquire the ability to fertilise an oocyte in a process known as capacitation (see section 1.1.4) (Lishko *et al.*, 2012). This means that sperm parameters in a freshly ejaculated sample may not provide an accurate representation of the fertilising capacity of the sperm once inside the female reproductive tract. Both the limitations in diagnosis and treatment of male factor

infertility result from a lack of understanding of the complex processes underlying sperm function, making it difficult to identify problems and develop appropriate treatments. In particular, there is a dearth of knowledge regarding the fundamental function of sperm motility. Whilst the overall mechanical mechanism is well-characterised, many questions concerning the regulation of this motility remain to be addressed, including the identification and characterisation of all involved signalling pathways, and the role of post-translational modifications (PTMs) in the workings of the structural components of the sperm flagellum. Indeed, aberrant acetylation in the sperm microtubules has been correlated with impaired motility (Gentleman *et al.*, 1996; Bhagwat *et al.*, 2014). However, the impact of protein modifications on sperm functions such as motility requires further evaluation and an understanding of the specialised sperm structure.

1.3 Development of the highly specialised sperm structure

Sperm have the essential function of delivering DNA to an oocyte in order to propagate paternal genes and are highly specialised for this role, with an extremely streamlined structure. A strong flagellum allows the sperm to be propelled through the aqueous environment of the reproductive tract, and the lack of cytoplasmic organelles such as Golgi apparatus, endoplasmic reticulum, and ribosomes permits high motility as sperm do not carry any organelles unnecessary for their function (Alberts *et al.*, 2002). Sperm comprise two distinct regions enclosed by a single plasma membrane: the head and the tail, with both regions exhibiting morphological specialisations required for their distinct functions. The head contains the extremely condensed paternal DNA - a function of the histone-to-protamine transition during development (see section 1.3.1.1), whilst the tail is a long, powerful structure designed to propel the sperm to the oocyte to fulfil its role of fertilisation. Development of this unique structure occurs through the process of spermatogenesis in the testes, where spermatogonial stem cells transition into mature haploid spermatozoa.

1.3.1 Spermatogenesis

Spermatozoa develop from primordial germ cells that migrate into the testes during embryogenesis. In contrast to the female oogonia which only develop in the foetus and become arrested in meiosis as oocytes before birth, proliferation of spermatogonia takes place only at the onset of puberty, and sperm production occurs continuously throughout life (Alberts *et al.*, 2002). Spermatogenesis takes place in the seminiferous tubules of the testes. These highly coiled, complex structures contain germ cells at many different stages of development, as well as Sertoli cells which provide nourishment to the developing sperm through the transport and secretion of nutrients and regulatory factors (**Figure 1.1**). The seminiferous tubules are surrounded by a basement membrane and myoid cells, with blood vessels and the Leydig cells responsible for androgen synthesis found in the interstitial space (Nishimura and L'Hernault, 2017).

Two types of spermatogonial stem cells are located on the basement membrane: Type A and Type B. Type A spermatogonia undergo mitotic divisions to produce either two new Type A cells for self-renewal, or various intermediate spermatogonia which subsequently divide producing Type B spermatogonia (Fayomi and Orwig, 2018). These cells then divide mitotically producing primary spermatocytes which successively undergo meiosis I to produce diploid secondary spermatocytes. Completion of meiosis II in every diploid spermatocyte results in two haploid round spermatids (**Figure 1.1**) (Nishimura and L'Hernault, 2017) which subsequently undergo spermiogenesis.

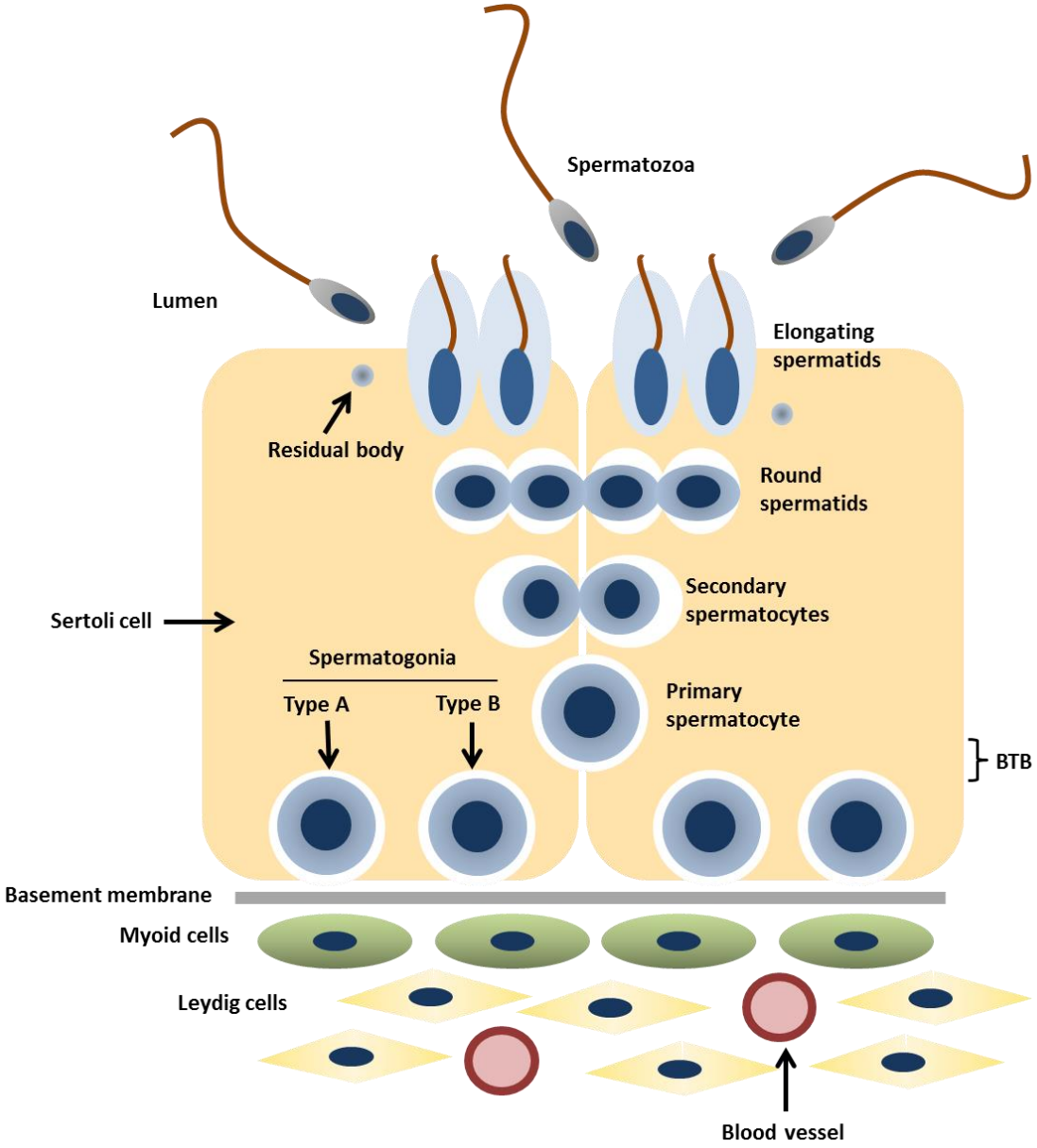

Figure 1.1: Schematic representation of spermatogenesis in the seminiferous tubules.

Male germ cells differentiate from spermatogonia to spermatids during various stages of mitosis and meiosis. During elongation, spermatids undergo chromatin condensation and acrosome development, forming their characteristic head shape, as well as losing unnecessary organelles in a residual body. Once developed, the spermatozoa are released into the tubule lumen. A close interaction with Sertoli cells is maintained throughout spermatogenesis; the cells provide developing sperm with the required nutrients and regulatory factors. In addition, Leydig cells in the interstitial space synthesise androgens required for development. BTB - blood-testis barrier. Self-drawn figure adapted from reference (Nishimura and L'Hernault, 2017).

1.3.1.1 Spermiogenesis

Following differentiation into round spermatids, the cells then undergo the final stage of spermatogenesis, known as spermiogenesis, which results in the production of mature spermatozoa. Throughout the development of the sperm, the differentiating cells remain in contact with one another via cytoplasmic bridges, which result from incomplete cytokinesis during meiosis. This contact ensures that the haploid sperm can be supplied with the components of a diploid genome, for example, sperm bearing a Y chromosome can be supplied with products encoded by the X chromosome from their neighbouring sperm. This is especially important during spermiogenesis and ensures that all spermatozoa have the required proteins for development (Greenbaum *et al.*, 2011).

During the first stages of spermiogenesis, structures known as the axoneme and acrosome are assembled. Polarisation of the acrosome and the nucleus to one side of the cell then signals the commencement of the elongating phase of the spermatid (O'Donnell, 2014). During this stage, the sperm head is shaped by the manchette - a transient microtubule-based structure, and by the condensation of nuclear chromatin via a well-characterised but complex process known as the histone-to-protamine transition (Boskovic and Torres-Padilla, 2013). Briefly, histones associated with spermatid DNA are hyperacetylated to reduce their DNA binding affinity, and are replaced by transition proteins (TNPs). TNPs are subsequently replaced by small, highly basic protamines which produces toroidal structures in the chromatin, increasing DNA packaging and chromatin condensation to levels six times that found in somatic cells (Balhorn, Brewer and Corzett, 2000; Fuentes-Mascorro, Serrano and Rosado, 2000). As a consequence, the integrity of the paternal genome is protected during sperm transport (Carrell, Emery and Hammoud, 2007). This process is vital as abnormal protamination has been linked with sperm DNA fragmentation and male infertility (García-Peiró *et al.*, 2011; Francis *et al.*, 2014).

The replacement of histones with protamines also means that sperm become transcriptionally quiescent at this stage of development; mRNAs required at a later stage are transcribed earlier and can be subjected to translational repression to ensure required proteins are available when necessary (Braun, 1998). Related to the loss of transcription function, spermiogenesis also involves the removal of organelles that are not required in the mature sperm including ribosomes, excess mitochondria and lipids. These cellular components, along with cytoplasm, are displaced towards the tail end of the sperm head and are later shed from the sperm in a 'residual body,' leaving behind only a small remnant known as the cytoplasmic droplet (Breucker, Schafer and Holstein, 1985).

An additional event that takes place during spermiogenesis is the formation of the flagellum. Whilst the cytoskeletal axoneme is assembled earlier, further components including the fibrous sheath (FS) and outer dense fibres (ODFs) are constructed around the axoneme, producing the structure of a functional sperm tail (see section 1.3.2.2) (O'Donnell, 2014). In the final stage of spermiogenesis known as spermiation, spermatids undergo restructuring and remodelling to produce streamlined spermatozoa. Spermatozoa with their complete structure are then released from the Sertoli cells into the seminiferous tubule lumen, ready for transport to the epididymis for further maturation (O'Donnell *et al.*, 2011).

1.3.2 Specialised structure of the mature spermatozoon

The events taking place during the latter stages of spermatogenesis are required for the development of mature sperm endowed with all of the structural adaptations necessary for their function. Both the sperm head and tail exhibit such specialisations that facilitate the fulfilment of their purpose in reproduction.

1.3.2.1 Structure of the sperm head

As previously described, the sperm head is formed into its final shape during the elongation phase of spermiogenesis, with the histone-to-protamine transition responsible for the highly condensed paternal DNA in the nucleus. Lying at the anterior end of the sperm head is an

important structure known as the acrosome. This organelle is a Golgi-derived secretory structure which forms a 'cap' over the sperm head (Abou-Haila and Tulsiani, 2000), and is bound by a continuous membrane which ensures containment of its contents. This membrane is described as having two regions: the inner acrosomal membrane (IAM), which lies above the nuclear envelope, and the outer acrosomal membrane (OAM) which is closely associated with the sperm plasma membrane. The acrosome has been reported to contain a variety of enzymes including hyaluronidase (Kim *et al.*, 2005) and N-acetylglucosaminidase (Miller, Gong and Shur, 1993). The best characterised component of the mammalian sperm acrosome is the sperm-specific, serine protease, acrosin which is reported to be involved in the digestion of the zona pellucida (ZP) of the oocyte (Ferrer *et al.*, 2012). When in close contact with the oocyte, capacitated sperm are triggered to undergo the acrosome reaction, allowing exocytosis of the acrosome contents by fusion of the OAM with the sperm plasma membrane. Where these initiating signals originate is now debated (Buffone, Hirohashi and Gerton, 2014). The accepted explanation for many years involved the view that sperm bind to a glycoprotein receptor in the ZP which triggers exocytosis (Saling, Sowinski and Storey, 1979). However, sperm binding to the ZP may only initiate the acrosome reaction in fertilising sperm; Baibakov and colleagues demonstrated that *Acr3*-EGFP sperm bound to the ZP of mouse eggs for 2-3 hours following fertilisation with their acrosomes intact. The group therefore concluded that the interaction of a ZP ligand with a sperm receptor may not alone be sufficient to induce acrosomal exocytosis (Baibakov *et al.*, 2007). Other reports suggest the acrosome reaction may take place in the cumulus cell mass or in its vicinity (Jin *et al.*, 2011). Regardless of site, current research agrees that acrosomal exocytosis allows the fertilising sperm to penetrate layers surrounding the oocyte to gain access to the oolemma (plasma membrane) (Buffone, Hirohashi and Gerton, 2014).

A further feature of the sperm head is the presence of cytoskeletal structures in three different regions. The subacrosomal cytoskeleton lies between the nucleus and acrosome, whilst the postacrosomal cytoskeleton is located between the sperm plasma membrane and the

acrosome. Both of these structures together make up the perinuclear theca which is composed of cytosolic and nuclear proteins (Oko and Sutovsky, 2009), as well as other cytoskeletal proteins including tubulin, actin and spectrin (Dvoráková *et al.*, 2005). The perinuclear theca surrounds the nucleus except in the region of tail attachment, and is suggested to have roles in acrosomal assembly, and sperm-egg interactions (Oko and Sutovsky, 2009). The third cytoskeletal structure, the para-acrosomal cytoskeleton, is a filamentous complex between the acrosome and plasma membrane and its presence has only been reported in a few species such as the hamster (Olson and Winfrey, 1985).

Whilst mammalian sperm all exhibit a condensed nucleus and acrosome, some variations in sperm head morphology are found between species. Four main sperm head morphologies are found in mammals: spatulate, found in species such as rabbit; ovate, seen in humans and other primates; falciform, found in mouse, rat and other rodent sperm; and sperm with large acrosomes, found in species such as chinchilla and guinea pigs (**Figure 1.2**). Reasons for this diversity remain unclear but various factors influencing the evolution of these morphologies include differences in the size and shape of the female reproductive tract, and competition between sperm. The falciform (hook-like) shape of rodent sperm is suggested to be an evolutionary response to sperm competition, whereby sperm are able to use the hooks to form 'trains' which swim faster than individual sperm in some species (Moore *et al.*, 2002). However, this notion of altruism in sperm has been criticised, particularly following the finding that sperm conjugates only occur in certain species of muroid rodent (Firman *et al.*, 2013; Tourmente, Zarka-Trigo and Roldan, 2016). Nevertheless, the morphology of the hook may confer an advantage in sperm performance as hook length and curvature are positively associated with swimming velocity (Varea-Sanchez *et al.*, 2016). Whilst there are noticeable differences in head shape between mammalian sperm, the basic structural plan of the sperm tail varies little between species, with only changes to the thickness and length apparent in the flagellum (Fawcett, 1970).

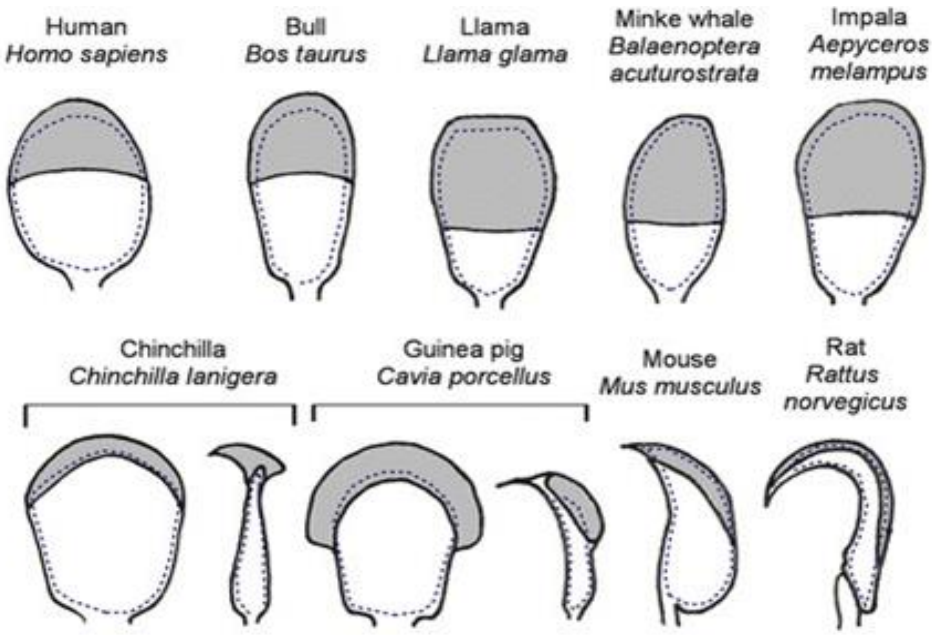

Figure 1.2: Schematic representation of variations in mammalian sperm head morphologies.

The ovate head shape is found in the sperm of many mammals including humans, whist the sperm of rodents such as mice and rats display a falciform (hook-like) shape. Some mammalian species exhibit other characteristics such as the large acrosomal caps present in chinchilla and guinea pig sperm. Acrosomal regions are shown in grey; the dashed line represents the nucleus outline. Adapted from reference (Skinner and Johnson, 2017).

1.3.2.2 Structure of the sperm tail

On the basis of ultrastructure, the sperm tail can be sub-divided into four sections: the connecting piece, midpiece, principal piece and end-piece (**Figure 1.3**). The connecting piece, or neck of the sperm, forms the junction between the head and the tail. Adherent to the outer membrane of the sperm nuclear envelope is a dense plaque of material known as the basal plate. The nuclear envelope and the basal plate form an articular structure known as the capitulum which is the implantation site of the tail (Fawcett, 1970). Extending from the capitulum are two major and five minor columns of a cross-striated fibrous protein. The two major columns each divide in two, producing nine columns that connect to the nine ODFs that begin at the midpiece. In the interior of the connecting piece, the microtubules of the axoneme begin in close relation to the segmented columns (Fawcett, 1970).

The axoneme is a cytoskeletal structure that runs throughout the subdivisions of the sperm tail and is central to motility (**Figure 1.3**). This structure consists of microtubules made from α- and β-tubulin (Turner, 2006) arranged in a 9+2 formation - nine doublet microtubules surrounding one central microtubule pair. Radial spokes project from each outer microtubule pair inwards to the central pair and each microtubule pair is also connected to the adjacent microtubule pair via two rows of dynein arms (inner and outer arms) (Lindemann and Lesich, 2016). ODFs composed of a keratin-like substance surround the axoneme providing structural support (Calvin, Hwang and Wohlrab, 1975; Kierszenbaum, 2002). Each ODF is paired with a microtubule doublet in the midpeice; however ODFs associated with doublet 3 and 8 end at the junction between the midpiece and principal piece (Lindemann and Lesich, 2016). A distinction between the midpiece and principal piece is also evident in the structures surrounding the ODFs. In the midpiece, the axoneme is surrounded by the mitochondrial sheath (MS) made up of many helically-coiled mitochondria. At the principal piece, the MS is replaced by the FS, which is known to play an important role in motility. The FS tapers and terminates at the end-piece, where the plasma membrane surrounds only the axoneme (Fawcett, 1975; Turner, 2006).

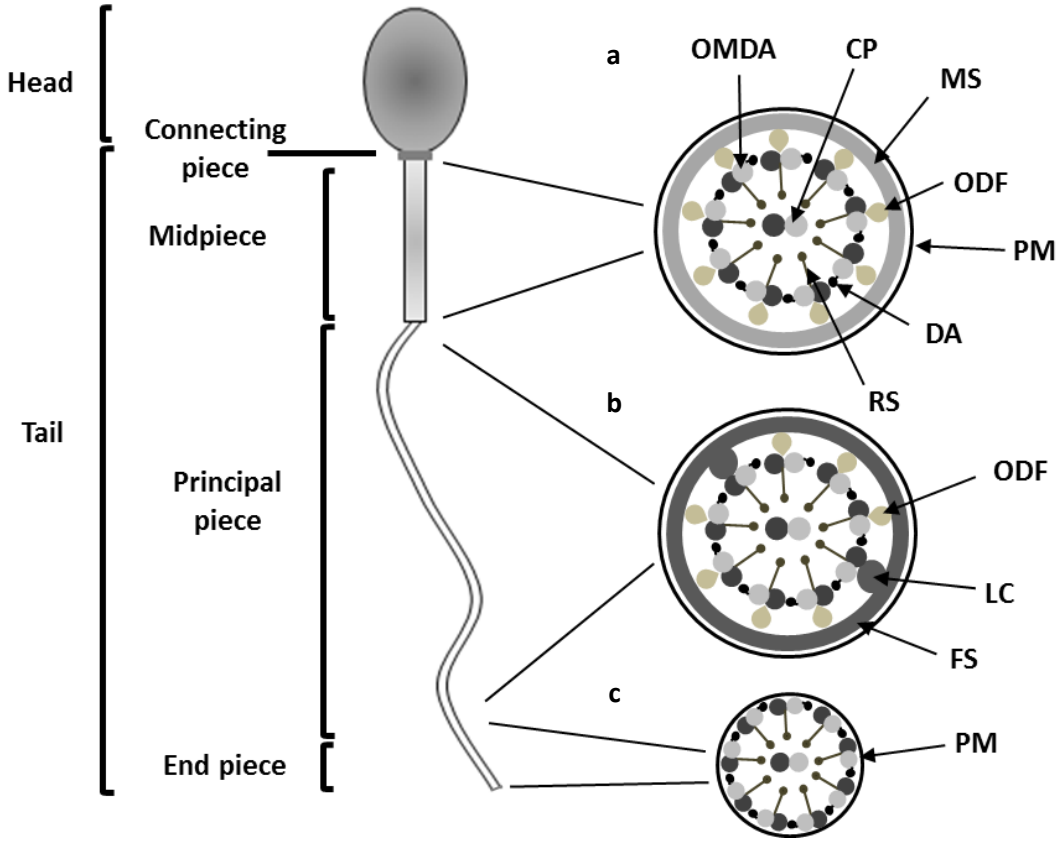

Figure 1.3: Schematic representation of the ultrastructure of a mammalian sperm tail.

The sperm tail can be divided into 4 areas: the connecting piece, the midpiece, the principal piece and the end piece. (a) Cross-section through a representation of the sperm midpiece showing the components of the axoneme in the centre: the 9 outer microtubule doublets of the axoneme (OMDA) with associated dynein arms (DA) and radial spokes (RS), surrounding the central pair of microtubules (CP). Around the axoneme are the outer dense fibres (ODF), surrounded by the mitochondrial sheath (MS) and the plasma membrane (PM). (b) Schematic cross-section through the principal piece showing the axoneme components and the replacement of the MS with the fibrous sheath (FS). Longitudinal columns (LC) of the FS replace two ODFs. (c) Schematic cross-section of a representative end piece. The ODFs and FS ceased at the end of the principal piece so that only the PM surrounds the axoneme. Self-drawn figure adapted from reference (Turner, 2003).

The role of the MS in sperm function is unclear; debate exists regarding the location of energy production for motility. Many reports have concluded that energy production for sperm motility is produced via glycolysis in the principal piece as opposed to oxidative phosphorylation in the mitochondria (Storey and Kayne, 1975; Fraser and Quinn, 1981; Miki *et al.*, 2004). Nevertheless, mitochondrial function correlates with sperm functionality and fertilisation capacity which suggests roles for mitochondria in other aspects of sperm physiology (Amaral *et al.*, 2013). One such function of the MS is in the maintenance of the structural integrity of the sperm tail; removal of the MS results in the disintegration of the ODFs and axoneme (Lindemann and Lesich, 2016). The FS also plays a mechanical role in sperm motility as well as a role in facilitating signal transduction and glycolysis. The FS structure comprises longitudinal columns (LC) of protein, of which two replace the lost ODFs in the principal piece, and these LCs are stabilised by transverse ribs (TR) of protein. The main proteins making up the FS are members of the A-kinase anchoring protein (AKAP) family, specifically AKAP-3 and AKAP-4 (Luconi *et al.*, 2011). For motility, the FS along with the central and outer microtubule pairs provide structural support, helping to organise the planar beat (Lindemann, Orlando and Kanous, 1992). The FS also anchors enzymes involved in glycolysis such as hexokinase, lactate dehydrogenase and glyceraldehyde-3-phosphate dehydrogenase (Westhoff and Kamp, 1997; Travis *et al.*, 1998), and compartmentalises signalling proteins such as protein kinase-A (PKA) (Luconi *et al.*, 2011). All sperm structural components therefore have vital individual roles, which work in collaboration to ensure essential sperm functions such as motility can proceed.

1.4 Fundamental sperm functions prior to fertilisation

The structural features of sperm described above provide the necessary machinery required to fulfil the cell's purpose of delivering the paternal genome to the oocyte. Once sperm are released from the epididymis, signals from the female reproductive tract contribute to the activation of this machinery to initiate important sperm processes and functions. These include

the initiation of capacitation, which prepares the sperm for fertilisation, and the activation of motility, required for navigation and access to the oocyte.

1.4.1 Sperm capacitation

In the 1950's, Austin and Chang identified independently that sperm were unable to fertilise oocytes until they had resided in the female reproductive tract for a period of time (Austin, 1951; Chang, 1951), introducing the term 'capacitation' to the literature to describe the acquisition of fertilising capacity (Austin, 1952). Research into capacitation has now revealed that various molecular processes take place to prepare the sperm for fertilisation. These include the removal of non-covalently attached glycoproteins and seminal proteins acquired in the epididymis, and the removal of cholesterol from the sperm membrane, increasing fluidity (De Jonge, 2005). In addition, increased intracellular pH, cyclic adenosine monophosphate (cAMP) levels, and tyrosine phosphorylation are found in capacitated sperm (Lishko *et al.*, 2012; Battistone *et al.*, 2013). These changes facilitate the sperm's ability to undergo the acrosome reaction, a process characterised by the release of hydrolytic enzymes from the acrosomal cap on the sperm head. This release of enzymes is one of the mechanisms that allows sperm to penetrate through the layers surrounding the oocyte (Roldan, Murase and Shi, 1994). Another requirement is the development of specific patterns of motility.

1.4.2 Sperm motility

Motility is an essential sperm characteristic, improper functioning of which can result in infertility (Boyle *et al.*, 1992). Two types of motility have been found in sperm: activated and hyperactivated motility, both serving different purposes in conveying the sperm to the egg. Activated motility is exhibited by freshly ejaculated sperm following the process of functional maturation in the epididymis (Dacheux and Dacheux, 2014). This form of motility is characterised by a symmetrical, lower amplitude waveform produced by the flagellum, which drives the sperm in a relatively straight line. This form of motility is considered to propel the sperm through the female reproductive tract to the oviduct (Turner, 2003). Hyperactivated

motility on the other hand, develops alongside capacitation after the sperm have resided in the female reproductive tract for a period of time. First identified by Yanagimachi (Yanagimachi, 1970), this form of motility is characterised by an asymmetrical increase in the amplitude of the flagellar bend resulting in whip-like motions of the tail, and vigorous side-to-side movements of the head. Hyperactivated sperm also swim in star-spin or figure-of-eight trajectories (Ho and Suarez, 2001). Various purposes for hyperactivation have been demonstrated including easier migration through the viscous fluid in the female reproductive tract; detachment from the oviductal epithelium; and penetration of cumulus cells and outer layers surrounding the egg (Ho and Suarez, 2001; Suarez, 2008). Knowledge of the molecular processes occurring during activated and hyperactivated motility is incomplete. However, the predominant mechanical mechanism and various relevant molecular pathways underlying motility have been characterised and are described below.

1.4.2.1 Mechanism of sperm motility

The mechanical process underlying motility arises from the interaction of axonemal components described in section 1.3.2.2; doublet microtubules of the axoneme make contact with one another via the action of dynein arms. These dynein arms can be regarded as either inner arm dyneins or outer arm dyneins based on their positions on the axoneme, and power the beating of cilia and flagella (Cho and Vale, 2012). Disruption of the inner arm dynein heavy chain in mice caused low motility in sperm and an inability to move from the uterus to the oviduct, resulting in infertility (Neesen *et al.*, 2001), indicating the importance of the dynein motor proteins in sperm motility.

The dynein arms comprise heavy, intermediate and light chains which assemble to form head and stem regions (Mohri *et al.*, 2012). The dynein heavy chains are members of the ATPase family associated with diverse cellular activities (AAA) superfamily and associate to form a ring-like structure, producing the head region. Two extended α-helices project from the head to form a stalk that acts as an ATP-sensitive microtubule-binding site (Mohri *et al.*, 2012). In

this way, the dynein heavy chains are responsible for motor activity; activation of the dynein heavy chain ATPase results in the transient interaction of the arms with adjacent microtubules via the microtubule-binding domain (Gibbons and Rowe, 1965). A downwards power stroke is generated causing the microtubules to slide past one another. As the axoneme is anchored to the sperm head, this force is converted to a bend in the tail, and subsequent motility (Turner, 2006) (**Figure 1.4**). The regulation of these processes is controlled by intracellular molecular processes that are initiated in response to environmental cues, as described herein.

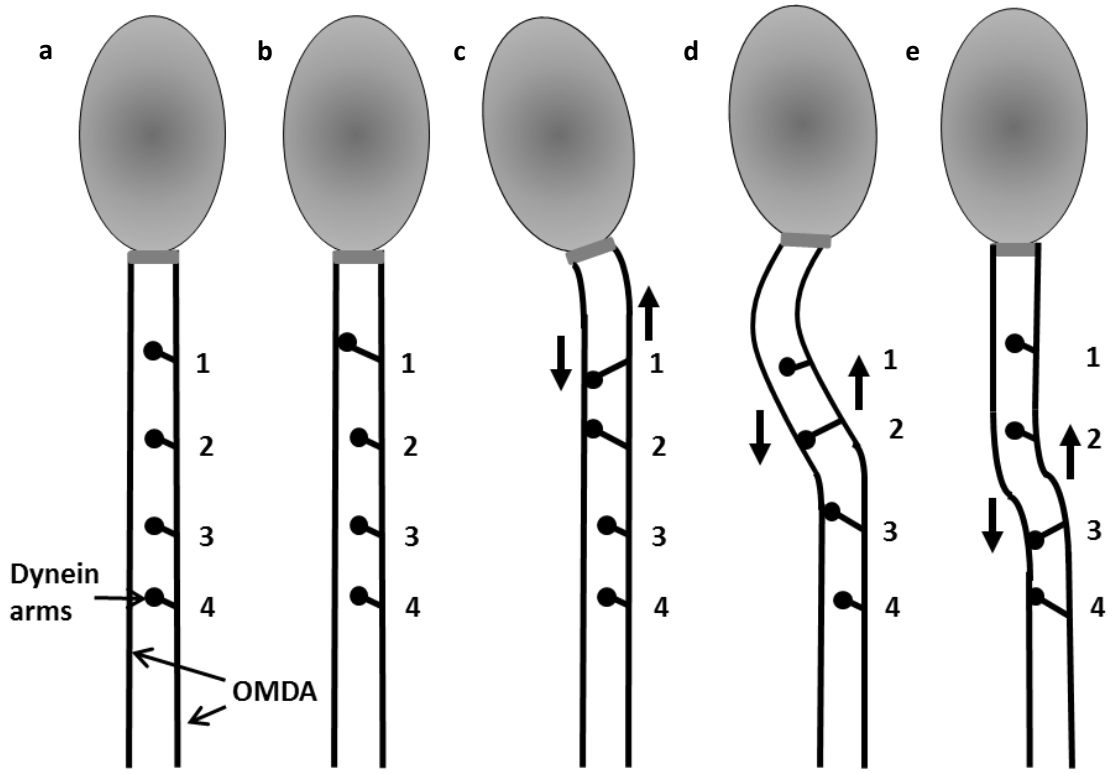

Figure 1.4: Representation of the generation of the sperm flagellar bend by the action of dynein arms.

For simplicity, only 2 outer microtubule doublets of the axoneme (OMDA) are shown as parallel lines, and the central pair and accessory structures are omitted. A pair of inner and outer dynein arms are represented by the numbered symbol projecting from the microtubule on the right. (a) Dynein arms are not active, therefore the microtubules are straight with no bend in the flagellum. (b) The first dynein arm is activated and interacts with the adjacent microtubule pair. (c) Generation of a downwards stroke from the first interacting dynein arm causes the microtubules to slide past one another and creates a bend in the axoneme. The second dynein arm interacts. (d) Release of the microtubule by the first dynein arm, and generation of a downwards stroke in the second, propagates the bend down the length of the axoneme. (e) The third dynein arm interacts, propagating the bend further down the axoneme. This process continues with all dynein arms down the length of the flagellum and around the circumference on all 9 microtubule doublets in 3 dimensions. Self-drawn figure adapted from reference (Turner, 2003).

1.4.2.2 Current knowledge of the main molecular mechanisms regulating sperm motility

The regulation of sperm motility, including the initiation of the specialised hyperactivated pattern of motility, during the transit of the sperm towards the oocyte is an extremely complex process that is yet to be fully elucidated. Research to date has identified the importance of various signalling pathways in the regulation of sperm motility, most notably the cAMP/PKA pathway and calcium signalling.

The cAMP/PKA pathway is recognised as a central signalling pathway in the regulation of sperm motility. Sperm entry into the female reproductive tract results in an increase in intracellular cAMP production via the activation of the soluble adenylyl cyclase (sAC). The sAC is activated by the increased pH in the seminal plasma and female reproductive tract compared to the epididymis, which leads to the transport of HCO_3^- into the sperm and a subsequent increase in intracellular pH (Lishko *et al.*, 2012). High levels of CO_2 present in the oviduct are also converted to HCO_3^- by the sperm (Okamura *et al.*, 1985; Wandernoth *et al.*, 2010). An increase in cAMP in the sperm results in the phosphorylation and activation of PKA bound to AKAPs in the FS via regulatory subunits. PKA catalytic subunits are released to exert effects on downstream proteins (Luconi *et al.*, 2004). Most targets of PKA remain unidentified; however one known target is axonemal dynein. Phosphorylation and activation of dynein is a crucial regulatory point in sperm motility as described previously (section 1.4.2.1).

The sAC is also activated by calcium. Whilst normal activated motility does not require an elevation of calcium (Lishko *et al.*, 2012), extracellular calcium is required for the increase in beat frequency initiated by HCO_3^- dependent sAC activation (Carlson, Hille and Babcock, 2007). This means that Ca^{2+} entry is vital for changes in the motion of the tail manifested during hyperactivation. As a result, a large body of research has focussed on determining the method by which calcium enters the sperm. In 2001, the first subunit of a sperm-specific, pH-sensitive, Ca^{2+}-selective ion channel known as CatSper (cation channel of sperm) was ascertained (Ren *et al.*, 2001), with specificity to the principal piece (Lishko *et al.*, 2012). Whilst the channel has

been found to be Ca^{2+}-selective, CatSper is also permeable to monovalent ions such as sodium (Lishko and Kirichok, 2010). Progesterone is a potent activator of this channel in human sperm, inducing Ca^{2+} influx and triggering physiological processes such as hyperactivation (Lishko, Botchkina and Kirichok, 2011) by activation of its recently identified receptor, alpha/beta hydrolase domain containing protein 2 (ABHD2) (Miller *et al.*, 2016). Progesterone released by cumulus cells surrounding the oocyte is thought to activate ABHD2, which hydrolyses endocannabinoid 2-arachidonoylglycerol in the sperm membrane, leading to its removal from CatSper, and allowing Ca^{2+} influx through the channel (Miller *et al.*, 2016). CatSper channels have been shown to form four linear 'stripes' that run the length of the principal piece of the sperm flagellum (Chung *et al.*, 2014). Recent evidence has suggested that the selective activation of these pH-sensitive channels may underlie the asymmetry of the flagellar beat in hyperactivated motility. Miller and colleagues found that Hv1 channels in human sperm which are responsible for H^+ extrusion and consequential increased intracellular pH, form longitudinal bilateral lines in the principal piece (Miller *et al.*, 2018). The group concluded that the off-centre distribution of these channels may serve to alkalinise only a portion of the sperm axoneme, in turn activating only a sub-set of CatSper channels. As a consequence, the unilateral influx of Ca^{2+} through the channels then results in the asymmetric flagellar motion that characterises hyperactivated motility (Miller *et al.*, 2018).

Although various signalling pathways have been implicated in the control of sperm motility, they do not individually provide a complete explanation for motility modulation, indicating the contribution of other mechanisms of regulation. The molecular signalling processes involved in sperm motility described above allow the sperm to react to cues in their environment. Activation of these pathways culminates in adjustments to the intracellular axonemal machinery - the central mechanical process underlying sperm motility. Therefore, whilst studies have identified molecular pathways that contribute to the regulation of sperm microtubule movement, a full understanding of the sperm axoneme and knowledge of the regulatory mechanisms that microtubules may themselves exhibit is lacking.

1.5 Microtubules

Microtubules are vital cytoskeletal structures present in all eukaryotes, which assemble from heterodimers of the 50 kDa α- and β-tubulin proteins. Microtubule structure and the sequences of α- and β-tubulin are highly conserved in evolution and as a result, look alike in most species (Janke, 2014). As well as being a central component of flagella, they are also vital constituents of other cellular structures including mitotic spindles, centrioles and the cytoskeleton. As such, microtubules play a variety of important roles in cellular functions including mitosis, intracellular transport, maintenance of cell morphology, and cell migration. Their role in these varied functions is permitted by the existence of regulatory mechanisms that generate microtubule diversity. One such mechanism is the presence of PTMs such as detyrosination/tyrosination, polyglutamylation, polyglycylation and acetylation, the roles of which will be discussed in section 1.5.2. Another mechanism conferring microtubule diversity is the expression of different α- and β-tubulin isoforms resulting from the existence of multiple genes coding for the proteins. The isoforms differ by subtle variations in the amino acid sequence mainly in the C-terminal tail (CTT), which protrudes out from the microtubule. The most diverse CTTs are exhibited by β-tubulin (Sirajuddin, Rice and Vale, 2014). Research has suggested that β-tubulin isoforms can function interchangeably and copolymerise into heterogeneous microtubules (Lewis, Gu and Cowan, 1987). However, certain specialised cell types such as platelets (Schwer *et al.*, 2001) and neuronal cells (Joshi and Cleveland, 1989) have been found to express specific β-tubulin isoforms required for functional microtubules. Studies of β-tubulin in sperm flagella have shown an enrichment of the βII isoform (Dutcher, 2001; Konno *et al.*, 2015) which is required for correct assembly and structural arrangement of the flagellar microtubules (Raff *et al.*, 1997, 2000). In addition, a crucial role for glycine 56 of the βII-tubulin isoform in allowing attachment of outer dynein arms to the microtubule has been identified in *Drosophila* sperm (Raff *et al.*, 2008). Incorporation of the appropriate tubulin isoforms into the microtubule therefore appears important in conferring functionality to the microtubule and ensuring that the correct structure is assembled.

1.5.1 Microtubule structure and dynamics

Molecules of α- and β-tubulin making up the microtubules consist of a predominantly globular core and a short CTT when correctly folded. These α- and β-tubulin molecules join together to form heterodimers, which subsequently stack head-to-tail to generate protofilaments. Tubulin protofilaments then associate laterally forming sheets that roll to create tubes 25 nm in diameter, with a central lumen approximately 17 nm in diameter. The lateral associations exhibit a small offset such that tubulin subunits in adjacent protofilaments display a left-handed helical pathway around the microtubule (Meurer-Grob, Kasparian and Wade, 2001) (**Figure 1.5a**).

Microtubules are dynamic structures and can therefore rapidly polymerise and depolymerise, switching between polymer growth and shrinkage in a process known as 'dynamic instability.' Nucleation of the polymer begins with the formation of a template for microtubule growth by γ-tubulin, to which a few hundred α-β tubulin heterodimers bind (Moritz *et al.*, 1995). Further dimers are then able to associate to or dissociate from either end of the microtubule; the end displaying faster growth and shrinkage is known as the 'plus-end,' whilst the less dynamic end is the 'minus end.' Stochastic net addition or loss of heterodimers leads to the growth or shrinkage of the microtubule, respectively, with the stability of a microtubule depending on the frequency of transition between these two processes (Hawkins *et al.*, 2010) (**Figure 1.5b**).

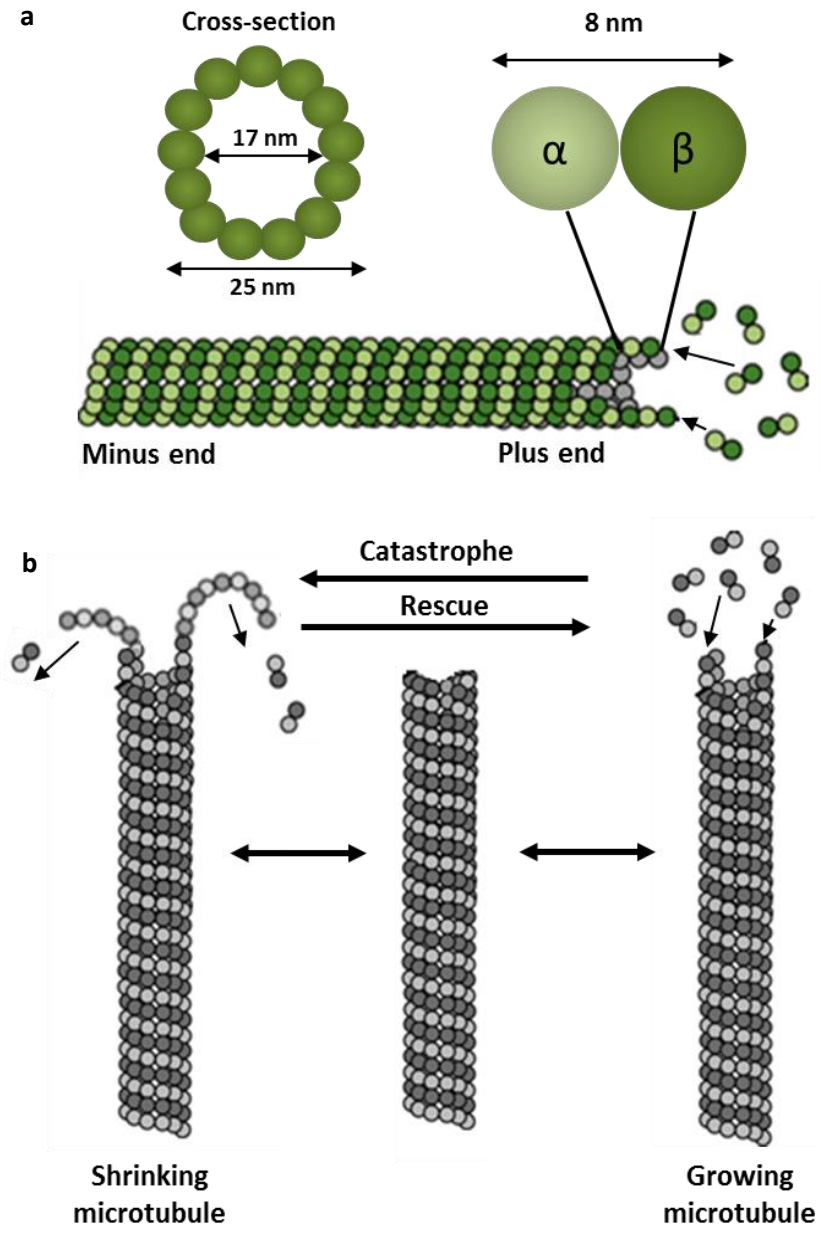

Figure 1.5: Structure and dynamics of microtubules.

(a) Microtubules are made up of heterodimers of α-tubulin (light green) and β-tubulin (dark green) which join together end-to-end to form protofilaments. These filaments join laterally, generating cylindrical tubes to which further α-β-tubulin heterodimers can associate to, or dissociate from. The end of the microtubule with the fastest growth and shrinkage is known as the 'plus-end'; the minus end is less dynamic. (b) Net addition or loss of heterodimers determines growth and shrinkage of the microtubule. A transition from shrinkage to growth is termed 'rescue,' whilst a transition from growth to shrinkage is known as 'catastrophe.' Adapted from reference (Hawkins *et al.*, 2010).

This dynamic instability is based on the binding and hydrolysis of guanosine triphosphate (GTP) by tubulin in a theory known as the GTP cap model. Every tubulin monomer can bind one GTP molecule, positioned at the interface between α- and β-tubulin subunits. The orientation of the microtubules is such that the plus-end is crowned by β-tubulin subunits, exposing their GTP nucleotide (Nogales *et al.*, 1999). During microtubule growth, incoming heterodimers of tubulin interact with the GTP of the receiving β-tubulin via their α-tubulin subunit. GTP is subsequently hydrolysed, and GDP (guanosine diphosphate)-tubulin is formed. As the incoming heterodimer also bears a GTP nucleotide on its β-tubulin subunit which is unaffected by the polymerisation, the plus-end of the microtubule generally retains a GTP-cap (Nogales, 2000). Attempts to measure the size of this cap are ongoing, with the first studies indicating that the cap consisted of a single layer of GTP-tubulin (Nogales, 2000). More recent evidence obtained during experiments in kidney epithelial cells using fluorescently-labelled microtubule end-binding proteins demonstrated that the cap spread over approximately 55 rows of tubulin, with the average cap size measuring approximately 750 tubulin subunits (Seetapun *et al.*, 2012). As the binding of GTP to tubulin transitions through steps including the hydrolysis of GTP to GDP-Pi, and the release of phosphate (GDP-Pi to GDP), it is possible that the end-binding proteins recognise different nucleotide states. Therefore, the GTP cap may comprise a variety of nucleotide and structural states which work in collaboration to stabilise the plus-end of the microtubule (Brouhard and Sept, 2012). In general, no GTP-cap exists at the minus-end of the microtubule; the addition of tubulin heterodimers to the minus-end occurs through the interaction of the GTP-β-tubulin of the incoming subunit, and α-tubulin of the polymerised subunit, so no GTP-tubulin is left exposed (Nogales *et al.*, 1999).

The GDP-tubulin making up the body of the microtubule is regarded as unstable as its natural conformation is a ring structure composed of one protofilament, which does not conform to the straight structure of the microtubule (Hawkins *et al.*, 2010). The GTP-cap with a more straight conformation is therefore thought to stabilise the microtubule structure (Nogales, 2000). When the cap is stochastically lost, lateral interactions between protofilaments weaken

(Nogales *et al.*, 1999) and the GDP-tubulin begins to return to its preferred kinked conformation (Hawkins *et al.*, 2010). This destabilises the microtubule and leads to the rapid depolymerisation seen following removal of the GTP-cap (Nogales, 2000). The assembly and disassembly of tubulin subunits appears to be self-regulated by the nucleotide state of the protein. However, this dynamic instability is under the influence of other factors that may stabilise or destabilise the microtubules and regulate their function. One mechanism by which microtubules are able to fulfil their diverse range of functions is by the presence of a variety of tubulin PTMs.

1.5.2 Post-translational modifications of tubulin

As previously highlighted, PTMs of tubulin can act as regulatory mechanisms allowing microtubules to perform their varied functions. Various PTMs have been identified and the pattern of these modifications on the microtubule surface is referred to as the 'tubulin code,' which is analogous to the histone code. Much like how histone PTMs direct chromatin function, the tubulin code can be read by various microtubule-interacting proteins in order to determine particular associations and functions. Three major classes of these microtubule binding proteins are: microtubule associated proteins (MAPs); plus-end tracking proteins (+TIPs); and molecular motors. MAPs bind statically to tubulin subunits and are thought to play a variety of roles including contributing to the stability of the microtubules and facilitating interactions of the microtubules with other proteins (Verhey and Gaertig, 2007). For example, the MAP, p58, mediates the binding of the Golgi complex to the microtubules for organisation (Haggarty *et al.*, 2003); and tau, a MAP with predominant expression in neurons has been shown to enhance microtubule stability and polymerisation (Ramkumar, Jong and Ori-McKenney, 2018). The +TIPs bind transiently to the plus-end of microtubules to modulate microtubule dynamics and regulate interactions between the microtubules and other cellular components (Galjart, 2010). For example, the $p150^{Glued}$ subunit of dynactin binds to both soluble tubulin and the microtubule to enhance polymerisation, and subsequently, the

formation of microtubules (Lazarus *et al.*, 2013). Motor proteins such as kinesin aid in the transport of intracellular cargo along microtubules. By moving through a cycle of binding ATP, hydrolysing the nucleotide, and then releasing the products, the kinesin molecule moves each of its two 'heads' (motor domains) alternately along a protofilament of the microtubule. The cargo linked to the other end of the polypeptide chain is then conveyed along the microtubule to the appropriate site. The interaction of microtubules with microtubule binding proteins therefore regulates particular functions such as assembly of the microtubules, intracellular trafficking, microtubule dynamics and motility of cilia and flagella (Verhey and Gaertig, 2007). These interactions are in turn regulated by the pattern of PTMs on the microtubule surface. Discovery of new tubulin PTMs is still taking place and many functions of known and new modifications remain to be elucidated. However, some of the best characterised PTMs include detyrosination, Δ2 modification, polyglutamylation, polyglycylation and acetylation, all of which have been found in spermatozoa (Bré *et al.*, 1996).

1.5.2.1 Detyrosination and the Δ2 modification

In most species, the α-tubulin gene encodes a final tyrosine residue at the C-terminus (Valenzuela *et al.*, 1981) which is enzymatically removed in the detyrosination process (Hallak *et al.*, 1977) (**Figure 1.6**). The removed tyrosine residue is then available to undergo ligation to free tubulin heterodimers by the action of tubulin tyrosine ligase (TTL) (Prota *et al.*, 2013). The carboxypeptidase responsible for the removal of the tyrosine has remained unidentified until recently. Both Aillaud *et al.* and Nieuwenhuis *et al.* have implicated vasohibins in this role. They identified that vasohibin 1 and vasohibin 2, when complexed with the regulating peptide, small vasohibin binding protein, exhibited tubulin tyrosine carboxypeptidase activity (Aillaud *et al.*, 2017). Furthermore, purified vasohibins are able to remove the C-terminal tyrosine of α-tubulin (Nieuwenhuis *et al.*, 2017), indicating vasohibins as the tubulin carboxypeptidase.

Removal of the terminal tyrosine exposes the penultimate glutamic acid residue of α-tubulin (Wloga, Joachimiak and Fabczak, 2017). Detyrosinated α-tubulin can undergo further

modification by the removal of this glutamic acid residue (Paturle-Lafanechère *et al.*, 1991) by the action of cytosolic carboxypeptidases (CCPs) (Kalinina *et al.*, 2007). This generates Δ2 α-tubulin (two C-terminal amino acids missing) which cannot be retyrosinated (Prota *et al.*, 2013) and as such is an irreversible PTM (Janke and Montagnac, 2017). Older, more long-lived microtubules exhibit increased detyrosination compared to recently assembled microtubules (Brown *et al.*, 1993); however, detyrosination has not been found to promote microtubule stability (Webster *et al.*, 1990). Instead, detyrosination may play a role in regulating the dynamic instability of microtubules by inhibiting depolymerisation. A kinesin-13 motor protein, MCAK, which performs ATP-driven microtubule depolymerisation, has preferential activity for tyrosinated rather than detyrosinated microtubules (Sirajuddin, Rice and Vale, 2014). In addition, detyrosination is also associated with an increase in kinesin-1 landing rate (Kaul, Soppina and Verhey, 2014), indicating a role for tyrosination/detyrosination in mediating interactions between tubulin and other proteins required for microtubule function.

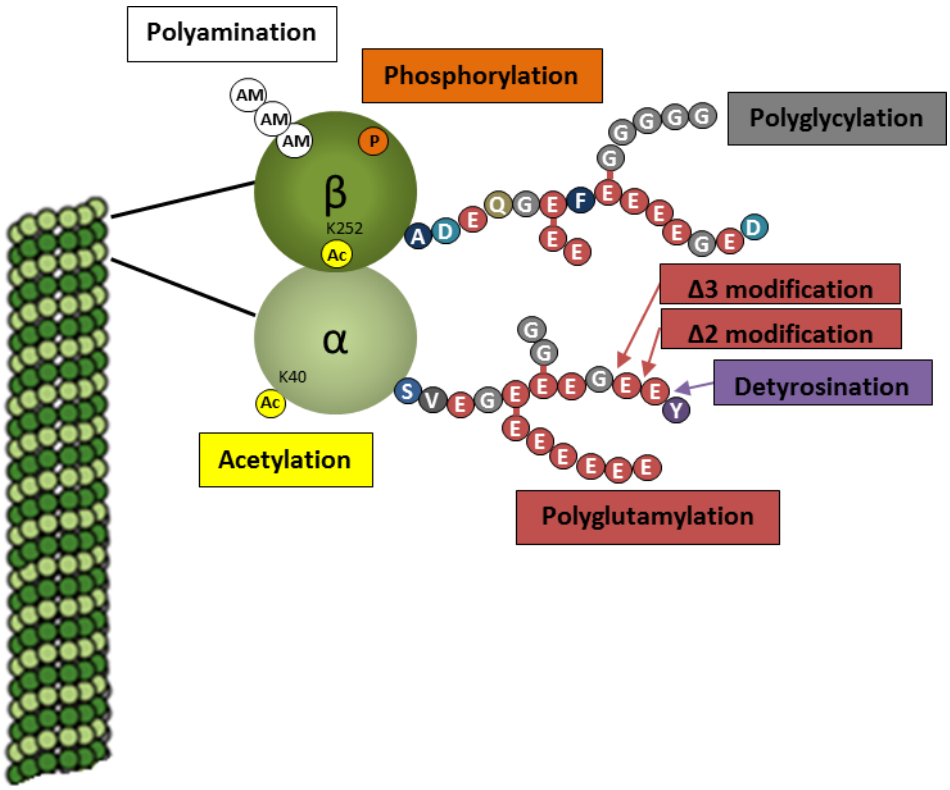

Figure 1.6: Schematic illustration of the location of various tubulin post-translational modifications.

The C-terminal tails of α- and β-tubulin exhibit various PTMs, which are located at the outer surface of the microtubule. Detyrosination and the Δ2/Δ3 modification are present in α-tubulin, whereas glutamylation and glycylation occur in both α- and β-tubulin and can be either in mono- or polymeric forms. Acetylation occurs at the N-terminus of α-tubulin, on the K40 residue, and is the only known PTM to reside on the luminal side of the microtubules. Acetylation of K252 in β-tubulin has also been found. Phosphorylation and polyamination have been demonstrated in both α- and β-tubulin; the best-studied site of phosphorylation is S172 of β-tubulin, and the main site of polyamination is Q15 of β-tubulin. Self-drawn figure adapted from reference (Janke, 2014).

1.5.2.2 Polyglutamylation and polyglycylation

Like detyrosination and the Δ2 modification, polyglutamylation and polyglycylation are modifications to the CTT. However, these PTMs can occur in both α- and β-tubulin. Glutamylation and glycylation occur upon the ligation of glutamate or glycine residues respectively, to the γ-carboxyl group of glutamic acid residues in the CTT (**Figure 1.6**). The modifications are polymeric and so following initiation, further glutamyl or glycyl residues can be ligated to form side chains of varying lengths (Wloga, Joachimiak and Fabczak, 2017). Glutamylation and glycylation are carried out by distinct members of the tubulin tyrosine ligase-like (TTLL) family (Wloga, Joachimiak and Fabczak, 2017), with members playing roles in initiation or elongation, and also exhibiting preferences for modification of the α- or β-tubulin CTTs (van Dijk *et al.*, 2007). Glutamylation is a reversible reaction; removal of glutamate residues is carried out by members of the CCP family. These CCPs also catalyse the removal of the gene-encoded penultimate glutamate residue of the C-terminus of α-tubulin, producing the Δ2 modification (Rogowski *et al.*, 2010). The enzyme catalysing the removal of glycine residues is yet to be identified; however, deglycylase activity has been shown in metallocarboxypeptidases of protozoa (Lalle *et al.*, 2011).

Whilst functions of polyglutamylation remain to be elucidated, this modification has recently been shown to play a role in the interaction of tubulin with dynein. Deletion of two TTLL paralogs responsible for glutamylation caused abnormal waveforms and reduced beat frequency in the cilia of *Tetrahymena,* thought to arise from the dysregulation of inner arm dynein (Suryavanshi *et al.*, 2010). Similarly, *Chlamydomonas* lacking a tubulin polyglutamylating enzyme exhibited lowered flagellar motility, but a complete loss of motility in flagella lacking outer arm dynein (Kubo *et al.*, 2010). Although these studies suggest a role for polyglutamylation in the regulation of inner arm dynein and microtubule interactions, further research is required to confirm this function.

Whilst polyglutamylation is present in cytoplasmic and axonemal microtubules, polyglycylation is particularly predominant in the axonemes of cilia and flagella (Bré *et al.*, 1996; Iftode *et al.*, 2000). Polyglycylation occurs as one of the final PTMs to occur in sperm differentiation of *Drosophila*, suggesting that it may act as a developmental signalling device (Bressac *et al.*, 1995; Bré *et al.*, 1996). Antibody labelling of tubulin polyglycylation in sea urchin sperm caused an inhibition of motility, an effect not seen with use of antibodies directed against epitopes a few amino acids from the polyglycylation site, and was suggested to arise from the interference with tubulin-dynein interactions (Bré *et al.*, 1996). Interestingly, long glycine side chains appear to be absent in human sperm tubulin (Bré *et al.*, 1996), which may result from mutations in the elongating glycylase, TTLL10, that render the enzyme inactive in humans (Rogowski *et al.*, 2009). Nevertheless, aberrant polyglycylation of tubulin has been implicated in human disease, with findings that TTLL3, a human glycylase, is down-regulated in colon carcinomas (Rocha *et al.*, 2014). Overall, the functions of polyglycylation and polyglutamylation of α- and β-tubulin are only just emerging, and so knowledge of the role that these PTMs play in directing microtubule function is incomplete.

1.5.2.3 Acetylation

All PTMs described previously are known to occur on tubulin CTTs. However, acetylation is unique in that this modification is present at the N-terminus, and as such, projects into the lumen of the microtubule (**Figure 1.6**). Acetylation of α-tubulin is associated with stable microtubules, however the function and mechanism of acetylation is still under investigation and will be discussed in section 1.6.

1.5.2.4 Other post-translational modifications of tubulin

In ongoing research attempting to understand the regulation of many cell processes involving microtubules, further tubulin PTMs are emerging. One such modification found on tubulin is phosphorylation, which can occur on serine, threonine and tyrosine residues of both α- and β-tubulin. However, the biological significance of this modification has yet to be determined. The

most studied phosphorylation event takes place on serine 172 of β-tubulin and is catalysed by cyclin-dependent kinase 1. This phosphorylation may interfere with interactions between heterodimers and GTP binding, indicating a role for the modification in microtubule dynamics during cell division (Fourest-Lieuvin *et al.*, 2006; Caudron *et al.*, 2010). A further PTM observed is polyamination (**Figure 1.6**). This covalent linkage of polyamine to tubulin is abundant in the axons of neuronal cells, and in the testes (Song *et al.*, 2013). The main site of polyamination is glutamine 15 of β-tubulin, however, other sites in both α- and β-tubulin have also been mapped. The polyamination sites found suggest a role for the modification in the interaction of α-β-tubulin heterodimers via an involvement in GTP binding or hydrolysis, and lattice stabilisation (Song *et al.*, 2013). Methylation of tubulin has also been discovered in mitotic cells where the lysine 40 (K40) site of α-tubulin in the central spindle is trimethylated by SET-domain-containing 2 (SETD2) methyltransferase (Park, Chowdhury, *et al.*, 2016; Park, Powell, *et al.*, 2016). Deletion of SETD2 caused mitotic spindle and cytokinesis defects, and polyploidy (Park, Powell, *et al.*, 2016). The emerging discoveries of a variety of tubulin PTMs further support the role of the tubulin code in directing the function of microtubules, with future research hopefully elucidating the role of these and other PTMs.

1.6 Acetylation and deacetylation of α-tubulin

Acetylation of lysine residues was first discovered in the 1960s (Gershey, Vidali and Allfrey, 1968), and refers to the transfer of an acetyl moiety from acetyl coenzyme A (Li and Yang, 2015). The scale of proteins adorned with the acetylation PTM is slowly coming to light. Approximately 2500 acetylated proteins have been detected in humans, making the human acetylome comparable to the phosphoproteome in number (Kim and Yang, 2011), and potentially importance. One of these proteins in which acetylation may play a key role is α-tubulin. As previously mentioned, acetylation of α-tubulin occurs at the N-terminus of the protein, specifically at the ε-amino group of lysine 40.

1.6.1 Identification of the α-tubulin acetylation site

Elucidation of the specific site of α-tubulin acetylation began in 1981, when McKeithan and Rosenbaum found that α-tubulin from the cytoplasm and flagella of the alga *Polytomella* possessed different isoelectric points (McKeithan and Rosenbaum, 1981). It was subsequently determined that conversion between the two types of α-tubulin in both *Polytomella* and *Chlamydomonas* arose from a PTM (L'Hernault and Joel L Rosenbaum, 1983; McKeithan *et al.*, 1983). Further research identified that the PTM under question involved an acetyl group, and that this acetylation was located on the ε-amino group of a lysine residue in flagellar α-tubulin (L'Hernault and Rosenbaum, 1985). Development of a monoclonal antibody raised against the acetylated form of α-tubulin from sea urchin sperm axonemes demonstrated that acetylation of α-tubulin could be found in many organisms (Piperno and Fuller, 1985). Specificity of the antibody for acetylated α-tubulin was further confirmed by the finding that the antibody did not react with soluble α-tubulin but would recognise sea urchin egg extract and *Chlamydomonas* cytoplasmic tubulin following *in vitro* acetylation (Piperno and Fuller, 1985). This monoclonal antibody (clone 6-11B-1) remains commercially available and has been widely used to identify stable microtubules. In 1987, LeDizet and Piperno determined the binding site of the 6-11B-1 antibody and subsequently demonstrated lysine 40 as the α-tubulin lysine residue bearing the acetylation (LeDizet and Piperno, 1987). Whilst the development of this antibody has allowed for research into the distribution of α-tubulin acetylation, the majority of studies to date have focussed on the K40 site. However, additional sites of acetylation have been identified in α- and β-tubulin (Choudhary *et al.*, 2009) but these require further confirmation. A novel acetylation site on lysine 252 in β-tubulin has recently been found which, when acetylated by the acetyltransferase, San, impedes tubulin incorporation into the microtubule (Chu *et al.*, 2011). This acetylation may therefore play a role in the regulation of microtubule assembly. However, by virtue, the modification only exists in soluble heterodimers (Chu *et al.*, 2011), and as such, acetylation of α-tubulin K40 remains the only acetylation site known on polymerised microtubules.

The luminal location of the K40 acetylation site, together with the finding that the modification only occurs on α-β-tubulin heterodimers that are incorporated into the microtubule lattice, not cytosolic heterodimers, has made it challenging to identify the precise mechanism by which α-tubulin is acetylated. As a result, the acetyltransferase responsible for the K40 modification has only recently been elucidated.

1.6.2 Acetylation of α-tubulin by α-TAT1

Acetyltransferase activity was detected in *Chlamydomonas* flagella as early as 1985 (Greer *et al.*, 1985), however the identity of this enzyme has remained unknown until recently. Various candidates for the role were identified including a transcription regulator, elongator protein 3 (Creppe *et al.*, 2009; Solinger *et al.*, 2010), an N^{α}-acetyltransferase complex (Ohkawa *et al.*, 2008), and the GCN5 (homolog of yeast general control nonderepressible 5) family of lysine acetyltransferases (Conacci-Sorrell, Ngouenet and Eisenman, 2010). The identity of the acetyltransferase involved in α-tubulin acetylation was elucidated based on the findings that MEC-12 (α-tubulin) is required for touch sensitivity in *Caenorhabditis elegans,* and that this α-tubulin exhibits acetylation (Fukushige *et al.*, 1999) and requires the activity of MEC-17 for maintenance (Zhang *et al.*, 2002). MEC-17 was found to contain a protein domain which is related to the catalytic subunit of the GCN5 family (Steczkiewicz *et al.*, 2006), and subsequently MEC-17, and its mammalian ortholog, α-TAT1 (α-tubulin acetyltransferase) were identified as the α-tubulin acetyltransferases (Akella *et al.*, 2010; Shida *et al.*, 2010). Confirmation of the function of α-TAT1 *in vivo* came from Kim *et al.* and Kalebic *et al*. who demonstrated that genetic ablation of α-TAT1 in mice led to the loss of detectable K40 α-tubulin acetylation in a variety of tissues including the brain, testes, liver, and pancreas (Kim *et al.*, 2013; Nereo Kalebic *et al.*, 2013). However, the mice were viable and developed normally, with the only defects being detected in the dentate gyrus (part of the hippocampus) (Kim *et al.*, 2013) and in sperm motility, subsequently affecting the fertility of male mice (Nereo Kalebic *et al.*, 2013). Whilst it has been suggested that the other acetyltransferase candidates

may be responsible for minor tubulin acetylation *in vivo* (Akella *et al.*, 2010), the lack of α-tubulin acetylation in α-TAT1 knockout mice indicates that other enzymes are not able to rescue the deficiency (Nereo Kalebic *et al.*, 2013). Therefore, α-TAT1 appears to be the predominant mammalian α-tubulin acetyltransferase.

Structurally, α-TAT1 shares sequence motifs with members of the GCN5 acetyltransferase family, which function to acetylate histones. However, the α-tubulin binding site of α-TAT1 is very basic (Friedmann *et al.*, 2012), whereas the substrate binding sites of histone acetyltransferases are largely acidic or apolar, allowing binding to the basic histone tails which harbour many lysine and arginine residues (Rojas *et al.*, 1999). This variation in substrate binding site is consistent with the finding that α-TAT1 has no detectable acetylation activity towards histones (Shida *et al.*, 2010). Structural analysis of α-TAT1 has also provided insights into the interaction of the acetyltransferase with the α-β-tubulin dimer. α-TAT1 shows a preference for acetylation of α-tubulin in polymerised microtubules (Friedmann *et al.*, 2012), with catalytic activity more than 100 times higher towards polymerised tubulin than free tubulin (Janke and Montagnac, 2017). This is consistent with previous research suggesting that the K40 acetylation site might sit at the interface between tubulin protofilaments; the tubulin acetyltransferase may recognise elements from both α-tubulin and its β-tubulin lateral neighbour (Nogales *et al.*, 1999). Therefore, the microtubule lateral contacts may be required for α-TAT1 recognition of the site and as such, acetylation proceeds on polymerised, rather than free tubulin.

The mechanism underlying the entry of α-TAT1 to the K40 acetylation site, given its luminal localisation, is still under investigation. At present, two predominant hypotheses exist to attempt to explain how α-TAT1 reaches its target (**Figure 1.7**). One possibility is that α-TAT1 enters through the ends of the microtubule and moves throughout the lumen (Akella *et al.*, 2010). This is supported by the finding of high concentrations of α-TAT1 at microtubule ends, possibly due to the high density of exposed luminal K40 sites (Coombes *et al.*, 2016). Ly and

colleagues found that α-tubulin acetylation began from the open extremities of *ex vivo* microtubules, and demonstrated that acetylation spread progressively and longitudinally along the microtubule length (Ly *et al.*, 2016). Szyk *et al.* also found that α-TAT1 entered the microtubules at the open extremities but proposed that α-TAT1 diffuses rapidly throughout the lumen, stochastically acetylating tubulin units (Szyk *et al.*, 2014a). However, mathematical modelling predicted that diffusion of an antibody specific for a luminal epitope would take years to reach equilibrium, suggesting that a diffusion model for α-TAT1 may be problematic (Odde, 1998). Furthermore, the random distribution of acetylation patterns in the microtubules reported by Szyk *et al.* better fits with a second, but not exclusive, hypothesis of α-TAT1 entry in which defects in the microtubule lattice provide entry sites for α-TAT1. The existence of defects in the microtubule wall has been reported and includes the loss of tubulin dimers, fractures in the wall, and increased spacing between protofilaments creating a 'split' (Schaap, De Pablo and Schmidt, 2004). In addition, switches in the number of protofilaments making up the microtubules have also been reported (Chretien *et al.*, 1992). These defects are therefore proposed to create transient sites for α-TAT1 to enter the microtubule lumen and acetylate α-tubulin, with subsequent restoration of microtubule integrity by self-repair mechanisms (Schaedel *et al.*, 2015). Therefore, α-TAT1 may scan the outer surface of the microtubule for possible luminal entry sites; a theory supported by the reported binding of α-TAT1 to the external microtubule surface (Howes *et al.*, 2014). Research to date therefore suggests that α-TAT1 gains access to the K40 acetylation site using both microtubule ends and breaks in the lattice (Coombes *et al.*, 2016) (**Figure 1.7**).

Mechanisms governing the regulation of α-TAT1 activity are unclear; however a recent study has revealed a role for the transforming growth factor-β (TGF-β) signalling pathway in microtubule acetylation. TGF-β-activated kinase 1 has been shown to directly interact with and phosphorylate α-TAT1 following activation by TGF-β superfamily ligands, leading to microtubule acetylation, and highlighting this pathway as a potential regulatory mechanism of microtubule acetylation (Shah *et al.*, 2018). Further work is required to elucidate the factors

involved in the regulation of α-TAT1, and to further clarify the mechanism by which α-tubulin is acetylated. Whilst α-TAT1 is responsible for the acetylation of α-tubulin, overall levels of microtubule acetylation are determined by a balance between the activities of this acetyltransferase and deacetylase enzymes.

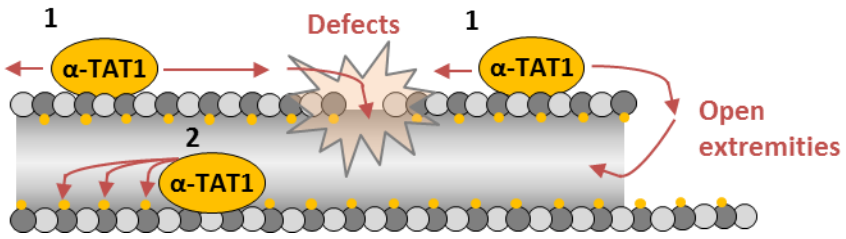

Figure 1.7: Potential mechanisms of α-TAT1 microtubule lumen access for K40 acetylation.

(1) α-tubulin acetyltransferase (α-TAT1) may bind to and scan the outer surface of the microtubule for possible entry sites. (2) α-TAT1 may enter the lumen through either breaks or defects in the lattice, or at microtubule ends, and subsequently modifies available K40 sites. Self-drawn figure adapted from reference (Janke and Montagnac, 2017).

1.6.3 Deacetylation of α-tubulin by histone deacetylases

To maintain the appropriate levels of α-tubulin acetylation required for microtubule function, the acetyltransferase activity of α-TAT1 is counterbalanced by the deacetylase activity of members of the histone deacetylase (HDAC) family. The HDACs comprise four classes based on their homology to yeast histone deacetylases, and play varying roles in cellular functions. Class I HDACs include HDAC1, 2, 3 and 8, and are localised mainly to the nucleus with ubiquitous expression. Class II comprises six HDAC isoforms which are split into Class IIa (HDAC4, 5, 7 and 9), and Class IIb (HDAC6 and 10). Class IIa HDACs have large N-terminal extensions with conserved regions for the binding of transcription factors and chaperone proteins. For example, 12 conserved amino acids are required for the binding of Class IIa HDACs to their best-characterised partners, the myocyte enhancer factor 2 (MEF2) transcription factors (Wang and Yang, 2001). The MEF2 family play roles in cell growth, differentiation, and survival; interactions between MEF2 and HDAC4 and 5 in skeletal muscle were shown to repress MEF2 activity, blocking the muscle-inducing action of MyoD, resulting in an inhibition of myoblast differentiation (Lu *et al.*, 2000). Class IIa HDACs also possess both a nuclear localisation signal and a nuclear export signal (McKinsey, Zhang and Olson, 2001; Wang and Yang, 2001) enabling the HDACs in this class to shuttle between the nucleus and cytoplasm, providing a mechanism for transcriptional responses to extracellular signals (Haberland, Montgomery and Olson, 2009). Class IIb HDACs are mainly cytoplasmic. Although little is known about the function of HDAC10, HDAC6 is known to be an important cytoplasmic deacetylase with a structure distinct from all other HDACs (Haberland, Montgomery and Olson, 2009); the role of HDAC6 will be discussed in further detail in section 1.6.3.1. HDAC11 is the only Class IV HDAC, and is enriched in certain tissues including brain, heart and muscle, though knowledge of its function is limited. All aforementioned HDACs display Zn^{2+}-dependent enzymatic activity. In contrast, Class III is comprised of a family known as the sirtuins, which are NAD^{+}-dependent deacetylases. Sirtuins, or SIRTs, are named after the yeast silent information regulator 2 (Sir2) with which they share sequence homology, and the family in humans is comprised of seven isoforms (SIRT1-7).

Sirtuins are present in various subcellular locations such as the nucleus (SIRT1, 2, 3, 6 and 7), cytoplasm (SIRT1 and 2), and mitochondria (SIRT3, 4 and 5) (Michishita *et al.*, 2005). While certain members of the family have been shown to exhibit other enzymatic functions such as ADP-ribosylation (Haigis *et al.*, 2006), the SIRTs, like other HDACs show robust deacetylase activity.

As their name suggests, the primary function of HDACs was initially identified as the deacetylation of histone proteins. In this way, the HDACs play a role in the regulation of gene expression as deacetylation exposes the positive charge of histone tails, increasing the binding affinity for DNA, and causing transcriptional repression through limiting the accessibility of transcription factors to their target genes (Shahbazian and Grunstein, 2007). Histone acetylation sites also act as binding regions for transcriptional regulators (Haberland, Montgomery and Olson, 2009). However, it has emerged that in addition to histones, HDACs have a variety of other cellular targets. The Class IIb HDACs in particular possess only slight activity against acetylated histone substrates, despite their conserved deacetylase site, indicating that other cellular substrates may be the targets of their action (Haberland, Montgomery and Olson, 2009). This is certainly true for HDAC6, which is known to have various cytoplasmic substrates; one significant target being α-tubulin.

1.6.3.1 Structure and function of HDAC6

HDAC6 was first found to deacetylate α-tubulin by Hubbert and colleagues. They reported that the overexpression of HDAC6 led to a reduction in global acetylated α-tubulin levels in NIH-3T3 cells, whilst inhibition of HDAC6 led to an increase in acetylation of the microtubule network. Furthermore, HDAC6 was shown to deacetylate polymerised microtubules *in vitro* (Hubbert *et al.*, 2002). In accordance with these findings, Matsuyama *et al.* used the HDAC inhibitor trichostatin A (TSA) to identify acetylated proteins and found α-tubulin to exhibit the modification. They subsequently identified HDAC6 as the α-tubulin deacetylase (Matsuyama *et al.*, 2002b). Zhang *et al.* also confirmed the α-tubulin deacetylase activity of HDAC6 by

demonstrating that inhibition and targeted inactivation of the deacetylase led to hyperacetylation of tubulin in mammalian cells. Furthermore, HDAC6 was shown to associate with the microtubule network (Zhang *et al.*, 2003). However, while the ability of HDAC6 to deacetylate polymerised microtubules has been demonstrated, HDAC6-mediated deacetylation is more effective on tubulin heterodimers (Miyake *et al.*, 2016).

As previously stated, HDAC6 exhibits variations in its structure compared to the other HDACs. One of these differences is the duplication of the HDAC-homology domain in HDAC6, meaning that there are two sites present for deacetylase activity (Grozinger, Hassig and Schreiber, 1999). Various studies have sought to determine whether both domains are a requirement for the deacetylase activity of HDAC6. Whilst some findings have suggested that the catalytic domains may function independently (Grozinger, Hassig and Schreiber, 1999), others have found that both domains are required to confer the activity of the whole enzyme (Zhang *et al.*, 2006). Further uncertainty about the function of the two sites arises from evidence that the second domain possesses a crucial motif required for HDAC6 function. Whilst both catalytic domains exhibit this substrate recognition site, its presence in the second domain is critical for the whole enzymatic activity of HDAC6 (Zhang *et al.*, 2006). Regardless of function, the double deacetylase domain structure of HDAC6 is conserved in various species (Yang and Grégoire, 2005), and this conservation throughout evolution indicates a critical role for this duplication (Boyault *et al.*, 2007).

Another notable feature of HDAC6 is the presence of a cysteine- and histidine-rich region at the C-terminus. This zinc-finger domain constitutes a high-affinity ubiquitin-binding motif known as ZnF-UBP, and is conserved in HDAC6 orthologs in many species (Boyault *et al.*, 2007). HDAC6 has been demonstrated to bind to both mono- and polyubiquitin chains (Boyault *et al.*, 2006), and to form a complex with proteins with known functions in ubiquitin-dependent cellular processes (Seigneurin-Berny *et al.*, 2001). In this way, HDAC6 plays a role in conveying misfolded proteins along microtubules to the aggresome by interaction with the ubiquitinated

proteins and dynein motors, allowing the misfolded proteins to be processed (Kawaguchi *et al.*, 2003).

In addition to the catalytic activities of HDAC6, the structure of the deacetylase is also important in determining its cellular location. HDAC6 possesses a strong nuclear export signal which functions to anchor the enzyme in the cytoplasm (Boyault *et al.*, 2007). In addition, human HDAC6 has been shown to have a tetradecapeptide repeat domain known as SE14 which functions as an intrinsic mechanism for retention of HDAC6 in the cytoplasm (Bertos *et al.*, 2004). Whilst HDAC6 was initially regarded as exclusively cytoplasmic, findings have suggested a role for the HDAC in nuclear activities (M. Zhang *et al.*, 2014), and demonstrated that HDAC6 can shuttle between the nucleus and cytoplasm (Verdel *et al.*, 2000). However, the primary targets of HDAC6 deacetylase activity are mainly cytoplasmic proteins and in addition to α-tubulin include the chaperone protein, heat-shock protein 90 (HSP90), and the cytoskeletal protein, cortactin (cortical actin binding protein). HSP90 facilitates the structural maturation of client proteins, the best-characterised being the glucocorticoid receptor (GR). The GR is a member of the steroid hormone receptor family which when activated, translocates to the nucleus to act as a transcription factor. HDAC6 has been shown to deacetylate HSP90, regulating its activity; inactivation of HDAC6 led to a loss of HSP90 chaperone activity towards the GR and consequential impairment of GR-ligand binding and gene activation (Kovacs *et al.*, 2005). Cortactin plays a vital role in the regulation of cell motility by interacting with F-actin to promote actin polymerisation, and is mostly found at areas of actin assembly such as the leading edge of migrating cells. Hyperacetylation of cortactin has been shown to prevent its association with F-actin leading to impaired cell motility, and implicating cortactin deacetylation by HDAC6 as an important modulator of actin-dependent motility (Zhang *et al.*, 2007). HDAC6 therefore interacts with important regulatory proteins that have vital roles in controlling a variety of cellular processes, implicating the deacetylase in functions such as cell migration and microtubule-dependent intracellular trafficking.

1.6.3.2 SIRT2 as an α-tubulin deacetylase

As previously mentioned, the Class III HDAC family have been shown to exhibit deacetylase activity. In particular, the cytoplasmic localisation of human SIRT2 (Perrod *et al.*, 2001) suggested that it may be involved in the deacetylation of cytosolic proteins. This was confirmed with the identification of SIRT2 as an α-tubulin deacetylase (North *et al.*, 2003). Knockdown of both HDAC6 and SIRT2 led to an increase in acetylation of α-tubulin and were both shown to co-localise on the microtubule network, indicating that they function as α-tubulin deacetylases and may interact with one another either directly or as part of a complex (North *et al.*, 2003). Whilst SIRT2 has been shown to deacetylate α-tubulin *in vitro* (North *et al.*, 2003), knockdown of SIRT2 appears to have no effect on acetylation of α-tubulin in the nervous system of mice (Bobrowska *et al.*, 2012; Taes *et al.*, 2013). Furthermore, the finding that HDAC6 functions as an α-tubulin deacetylase independently (Zhang *et al.*, 2008; Zhao, Xu and Gong, 2010), while SIRT2 interactions with tubulin involve other proteins including HDAC6 (North *et al.*, 2003), implicates HDAC6 as the central tubulin deacetylase. However, Skoge and Ziegler demonstrated that inhibition of SIRT2 led to hyperacetylation of perinuclear microtubules, whereas HDAC6 did not deacetylate these microtubules. This indicates that SIRT2 and HDAC6 may deacetylate α-tubulin in distinct microtubule structures (Skoge and Ziegler, 2016). Findings to date are therefore unclear on the context in which α-tubulin is deacetylated by SIRT2. Further research is required to identify the role and extent of the contribution of SIRT2 deacetylation to the regulation of net acetylated α-tubulin levels *in vivo*.

1.6.4 Functions of α-tubulin acetylation

The identification of the acetylation of α-tubulin at the K40 site initiated many studies into the biological function of this PTM. Despite much research, the impact of acetylation on microtubule properties and subsequent functions in cellular processes is only beginning to emerge. One dominant role identified for α-tubulin acetylation has been in microtubule

stability. However, the question of whether microtubules are acetylated because they are stable, or are stable because they are acetylated has drawn the focus of numerous research studies to date.

1.6.4.1 Acetylation of α-tubulin marks stable microtubules

Initial research into the role of α-tubulin acetylation indicated that this PTM may be the feature that leads to stabilisation of the microtubules. Evidence for this notion came from findings that acetylation was usually found in stable, long-lived microtubules (Webster and Borisy, 1989), and acetylated microtubules were resistant to cold-induced depolymerisation (Cambray-Deakin and Burgoyne, 1987). However, subsequent data indicated that α-tubulin acetylation may be a consequence rather than a cause of microtubule stability. Palazzo and colleagues demonstrated that chemically stabilising microtubules led to an increase in acetylation, whereas artificially increasing acetylation did not increase markers of microtubule stability (Palazzo, Ackerman and Gundersen, 2003). Furthermore, silencing of HDAC6 led to complete acetylation of microtubules, however, microtubule growth velocities were unaffected (Zilberman *et al.*, 2009), suggesting that acetylation itself may not be the mechanism through which microtubules are stabilised. In addition, acetylation of microtubules appears to be a function of their longevity; α-TAT1 exhibits slow enzymatic activity and so only those microtubules that are stable enough to remain are acetylated by the acetyltransferase (Szyk *et al.*, 2014a). Acetylation of α-tubulin is therefore found in microtubules with a slow turnover, and research to date indicates that acetylation marks stable microtubules but is not the causative factor of microtubule stability.

1.6.4.2 α-tubulin acetylation is implicated in a variety of cellular processes

Investigations into the role of α-tubulin acetylation has mainly been carried out by modifying the activities of the deacetylases HDAC6 or SIRT2, or by manipulation of the α-TAT1 gene, as specific inhibitors of the acetyltransferase are currently unavailable (Al-Bassam and Corbett, 2012). Roles for acetylation of α-tubulin have been reported in a variety of cellular processes

including: cell adhesion (Aguilar *et al.*, 2014), intracellular trafficking (Reed *et al.*, 2006) and touch sensation (Shida *et al.*, 2010; Morley *et al.*, 2016). Acetylation of α-tubulin is also implicated in the mechanism of cell motility. Piperno and colleagues found that dynamic microtubules at the leading edge of fibroblasts lack acetylation (Piperno, LeDizet and Chang, 1987). Furthermore, fibroblasts overexpressing HDAC6 move significantly faster in response to serum than those expressing catalytically-inactive HDAC6 (Hubbert *et al.*, 2002). Therefore, it was proposed that HDAC6-mediated deacetylation enhances microtubule-dependent motility by reducing microtubule stability through a decrease in tubulin acetylation (Hubbert *et al.*, 2002). However, others have postulated that the observed increase in cell motility is due to the alteration in the degree of tubulin acetylation itself and is not a result of changes in microtubule stability (Palazzo, Ackerman and Gundersen, 2003). Microtubule acetylation has also been implicated in promoting the direction of cell motility; selectively acetylated microtubules were found orientated towards the leading edge of cell, defining the direction of migration (Montagnac *et al.*, 2013). Microtubule acetylation therefore appears to be involved in the regulation of cell motility as well as various other cellular processes. However, understanding exactly how acetylation of α-tubulin participates in such a diverse range of cellular functions has been a focus of much research.

One possible mechanism has recently come to light, which may aid in explaining the functional consequences of microtubule acetylation. Acetylation of α-tubulin may play a role in protecting the microtubules from mechanical breakage. Portran *et al.* demonstrated that K40 acetylation weakens lateral interactions between tubulin protofilaments which prevents any pre-existing defects from spreading (Portran *et al.*, 2017). As microtubules are rigid structures that rupture under flexural stress (Hawkins *et al.*, 2010), they proposed that acetylation softens the microtubules, rendering them less susceptible to breakage in areas subject to repeated bending (Portran *et al.*, 2017). In addition, Xu *et al.* demonstrated enhanced acetylation in microtubule regions undergoing high curvature, which increased flexibility, allowing resistance against breakage as a result of mechanical stress (Xu *et al.*, 2017).

Therefore, the acquisition of α-tubulin acetylation in long-lived microtubules confers resistance to breakage and limits the ageing of the microtubules (Portran *et al.*, 2017). The notion that acetylation acts as a microtubule protective mechanism may help to explain how cellular processes can be influenced by changes in the acetylation state of α-tubulin. However, interestingly, mice lacking α-TAT1 display no major defects in development, behaviour or homeostasis despite an almost total loss of α-tubulin acetylation in all examined tissues (Nereo Kalebic *et al.*, 2013). The only detected defects following loss of α-TAT1 were a slight distortion of the dentate gyrus (Kim *et al.*, 2013), and deficits in sperm morphology and motility leading to a reduction in litter sizes (Nereo Kalebic *et al.*, 2013). The results of these studies show that α-TAT1 is a requirement for acetylation in the sperm flagellum, and that this is necessary for normal sperm function (Kim *et al.*, 2013; Nereo Kalebic *et al.*, 2013). The lack of effect observed in all other aspects of development and physiology of the mice following ablation of α-TAT1 raises further questions regarding the function of microtubule acetylation. Nevertheless, the reported subfertility of male mice lacking α-TAT1 indicates that acetylation of α-tubulin may contribute a function vital for sperm performance.

1.6.4.3 The role of α-tubulin acetylation in sperm motility and development

Initial evidence for the role of tubulin acetylation in sperm function arose from a case study of an infertile male with retinal degeneration. Hypoacetylation of α-tubulin was reported in the individual's sperm with a concurrent impairment of motility (Gentleman *et al.*, 1996). Further research demonstrated that the sperm of asthenozoospermic individuals exhibited a reduction in acetylated α-tubulin, again highlighting a link between sperm motility and microtubule acetylation (Bhagwat *et al.*, 2014). However, these studies indicated only an association between the acetylation state of α-tubulin and sperm motility; further exploration of the influence of microtubule acetylation/deacetylation on sperm function has come from studies of α-TAT1- or HDAC6-deficient mice.

Male mice lacking α-TAT1 exhibit a subfertile phenotype (Nereo Kalebic *et al.*, 2013), indicating that acetylation of α-tubulin is necessary for normal sperm functioning. Indeed, sperm from α-TAT1-deficient mice display a loss of microtubule acetylation (Kim *et al.*, 2013), and significant reductions in progressive motility and beat lateral amplitude compared to their control counterparts (Nereo Kalebic *et al.*, 2013). Defects in sperm morphology were also found, with a dramatic increase in the presence of cytoplasmic droplets (associated with impaired sperm maturation), and a significant decrease in flagellar length associated with loss of acetylation, although the axonemal microtubule structure maintained a 9+2 arrangement (Nereo Kalebic *et al.*, 2013). These results, together with a reduction in cauda epididymal sperm number following α-TAT1 deletion, indicate that the acetyltransferase is a requirement for normal sperm development, with the loss of α-TAT1 detrimentally affecting the fertility of the male mice. Conversely, knockout of HDAC6 in mice resulted in fertility characteristics comparable to wild-type mice including sperm number and litter sizes, indicative of normal sperm function (Zhang *et al.*, 2008). During spermatogenesis, developing spermatids from HDAC6-deficient mice were noted to exhibit high levels of acetylation throughout all differentiation stages. In contrast, wild-type spermatogenic cells only began to show increased α-tubulin acetylation at the beginning of the elongation phase which persisted into the condensing phase (Zhang *et al.*, 2008). The results indicate that although an increased level of α-tubulin acetylation was present in the sperm from HDAC6-deficient mice throughout development, this effect did not influence the functionality of the resulting mature sperm. Furthermore, apart from small changes to bone mineral density and the immune response, no significant effects on viability or development of the HDAC6 knockout mice were observed, despite the greatly elevated levels of tubulin acetylation found in most tissues. The group therefore concluded that HDAC6 may be dispensable, and that the level of α-tubulin is not critical in adult mouse homeostasis (Zhang *et al.*, 2008).

The results from the knockout studies appear to suggest that either the presence or activity of α-TAT1 is required for normal sperm development and subsequent function. However,

removal of the counteractive HDAC6 does not affect fertility of the mice, indicating that increased α-tubulin acetylation throughout sperm development does not exert detrimental effects. However, only one study to date has examined the effect of manipulating deacetylase activity directly in mature sperm and the results showed that this can influence sperm swimming behaviour. Parab and colleagues demonstrated the co-localisation of HDAC6 and acetylated α-tubulin in the flagella of testicular and epididymal sperm from rats. Inhibition of HDAC6 in epididymal sperm led to an increase in acetylation of α-tubulin, a significant reduction in progressive motility, and an increase in beat frequency. The group suggested that inhibition of HDAC6 prevented its dissociation from the tubulin binding site, hindering the microtubule molecular processes and interfering with sperm movement as a consequence (Parab *et al.*, 2015). The group further postulated that the stability of the microtubules may be the factor defining sperm motility; HDAC6 may act as a MAP and could regulate the dynamic instability of the flagellar microtubules, subsequently influencing sperm movement (Parab *et al.*, 2015). Taken together, the results from studies reporting on the effects of acetylation/deacetylation in sperm appear to suggest that this modification does exert an influence on sperm motility; however research in this area is extremely limited. The emerging recognition of acetylation as an important microtubule regulatory mechanism in cell motility and other functions highlights the necessity for further research into the role of the PTM in sperm motility.

1.7 Aims

Motility is a fundamental sperm function vital for natural fertilisation, however, knowledge of the mechanisms underlying its regulation is limited. As the sperm microtubules are responsible for the mechanical process involved in motility, and previous research has strongly suggested a link between motility and the acetylation state of α-tubulin, the overall aim of the work presented in this thesis was to explore the role that this PTM plays in the regulation of motility in murine sperm. Investigation of the contribution of this potential mechanism to sperm

motility modulation will allow further comprehension of the regulatory processes involved in the essential sperm function.

To achieve the aim, the function of deacetylation was first examined using inhibitors of the α-tubulin deacetylases, HDAC6 and SIRT2 to assess their activity and determine whether deacetylation of α-tubulin plays an important part in motility modulation. Secondly, the role of microtubule stability which has been correlated with the presence of acetylation on α-tubulin was examined to determine whether stability plays a regulatory role in motility. To do this, a microtubule depolymerising drug was used to assess whether stable microtubules are a requirement for murine sperm motility.

Chapter 2

Chapter 2 – Materials and Methods

2.1 Materials

All chemicals and reagents were obtained from Sigma-Aldrich, UK, unless otherwise stated.

2.2 Preparation of murine spermatozoa and spermatids

2.2.1 Extraction of murine tissues

Male BALB/c or C57 mice aged 8-12 weeks were sacrificed in accordance with the Animals (Scientific Procedures) Act (1986) by trained personnel at the Life Sciences Support Unit, Durham University. Reproductive tracts of the mice were dissected out and placed in Whittens-HEPES media (WH; 4.4 mM KCl, 1.2 mM KH_2PO_4, 1.2 mM $MgSO_4$, 5.4 mM glucose, 99.2 mM NaCl, 4.8mM lactic acid, 2.4 mM $CaCl_2$, 0.8 mM sodium pyruvate, 20 mM HEPES, 30 mM sodium bicarbonate, pH 7.2). Epididymal tissue and testicular tissue were separated, and adipose tissue removed.

2.2.2 Preparation and treatment of epididymal spermatozoa

Each epididymis was placed into 1 ml of Whittens-HEPES capacitating media (WH-cap; WH media supplemented with 10 mg/ml protease-, fatty acid-, and globulin-free BSA), and cut approximately 10 times along the length of the tissue. Media and epididymal tissues were transferred into 1.5 ml microcentrifuge tubes (Eppendorf, UK) and sperm were then allowed to swim out of the tissue for approximately 1 hour at room temperature. Epididymal tissue was removed from the tubes and sperm from two epididymides were pooled. Each sperm sample was then counted by diluting a small sample with deionised water (1:10) to inhibit sperm motility, and counting using a Neubauer improved bright line haemocytometer (0.100 mm depth, Marienfeld, Germany) according to manufacturer's instructions.

Following counting, sperm were prepared for treatments by centrifuging at 300 xg for 5 minutes at room temperature and resuspending in WH-cap at a concentration of 6 million/ml.

Sperm (1.5 million per condition) were then either treated with various inhibitors/drugs (**Table 2.1**) for 3 hours, or were allowed to capacitate for approximately 3 hours and then treated for 1 hour at 37°C, 5% CO_2. Control sperm were treated with the appropriate volumes of vehicle (DMSO/diH_2O). Following treatments, sperm underwent motility analysis using computer-assisted sperm analysis (CASA) or Kremer assay (section 2.4), were lysed for Western Blot analysis (section 2.5), or were fixed for immunofluorescence (section 2.7).

Table 2.1: Drugs used in the treatment of cells

Inhibitor/drug	Concentrations used	Company	Catalogue number
Trichostatin A (TSA)	1 µM, 10 µM	Tocris Bio-Techne, UK	1406
Tubacin	5 µM	Sigma Aldrich, UK	SML0065
Nicotinamide	5 mM	Sigma Aldrich, UK	T2340
Nocodazole	25 µM	Sigma Aldrich, UK	M1404

2.2.3 Preparation and treatment of spermatids

Following excision of the reproductive tract, outer capsules were removed from the testes, and the tissue spread out to allow spermatids to be released from the tubules. The tissue was placed on a 70 µm cell strainer (Corning, UK) on top of a 50 ml Falcon tube, and cells pushed through using the barrel of a 3 ml syringe and approximately 1.5 ml of WH media to produce a single cell suspension. A small sample of this suspension was removed and mixed in a 1:1 ratio with trypan blue; spermatids were subsequently counted using a haemocytometer.

For treatments, spermatids were centrifuged at 300 xg for 5 minutes and approximately 3 million resuspended in 500 µl warm WH media (concentration of 6 million/ml). This was then split equally between control and experimental conditions so that approximately 1.5 million spermatids were treated with the drugs listed in **Table 2.1** or vehicle (DMSO/diH_2O) for 1 or 3 hours at 37˚C, 5% CO_2. Following treatment, spermatids were lysed for Western blotting analysis (see section 2.5).

2.3 Cell culture

2.3.1 Growth and maintenance of HEK-MSR cell line

Human Embryonic Kidney-Macrophage Scavenger Receptor (HEK-MSR) cells were grown in serial culture under sterile conditions. Cells were maintained at 37˚C in a 5% CO_2 humidified incubator in Dulbecco's Modified Eagle's Medium (DMEM GlutaMax, high glucose, Gibco Thermofisher, UK) supplemented with foetal bovine serum (FBS, 10% v/v), penicillin (100 units/ml), streptomycin (100 µg/ml) and the selection antibiotic, G418 sulfate (0.5 µg/µl; InvivoGen, USA). Cells were split once they had reached approximately 70-80% confluency to maintain growth in the exponential phase. Growth medium was aspirated from the flasks and cells were washed with 10 ml of phosphate buffered saline (PBS; Gibco, UK) to remove residual media. To detach cells from the base of the flask, trypsin/EDTA (TE; trypsin - 0.5%; Gibco Thermofisher, UK) was applied and the cells were incubated at 37˚C 5% CO_2 for 5 minutes. Growth medium (9 ml) was subsequently added to the flask to inactivate the TE, and cell suspensions were centrifuged at 1000 xg for 5 minutes at room temperature. Media was then discarded and cell pellets resuspended in 10 ml of growth media. Cells were then either passaged or used for experimental analysis. For passaging, cells were seeded into new cell culture flasks in a 1:20 ratio. Media was replaced every 3-4 days.

For experimental analysis, 10 µl of cell suspension was applied to a haemocytometer (Marienfeld, Germany) and cells were counted in five 1 mm^2 areas then averaged to obtain cell number x 10^4/ml. Cell suspensions were next adjusted to 200,000 cells/ml and 2 ml of cell suspension plated into each well of a six-well plate. Plates were incubated at 37˚C, 5% CO_2 for 24 hours prior to treatments. Cells were treated with the drugs listed in **Table 2.1**, or appropriate concentrations of vehicle (DMSO/diH_2O), and incubated at 37˚C, 5% CO_2 for 1 or 3 hours depending on the treatment regimen. Following treatment, media was removed from the wells and cells were washed with 2 ml ice-cold PBS. Cells were either scraped into 100 µl of SDS lysis buffer (50 mM Tris-HCl pH 7.5, 150 mM NaCl, 6% SDS w/v, 50 µM sodium fluoride, 50

µM sodium pyrophosphate, 0.2 mM sodium orthovandate, 0.1% β-mercaptoethanol v/v, 1 Roche protease inhibitor tablet per 50ml, product number 04693132001) or MRC lysis buffer (50 mM Tris-HCl pH 7.5, 1 mM EGTA, 1 mM EDTA, 1 mM sodium ortho vandate, 10 mM β-glycerol phosphate, 50 mM sodium fluoride, 5 mM sodium pyrophosphate, 0.27 M sucrose, 1% Triton x100 v/v, 0.1% β-mercaptoethanol v/v, 1 Roche protease inhibitor tablet per 50 ml), and vortexed to assist cell lysis. Cell lysates were stored at -20˚C until required for analysis.

2.3.2 Cryopreservation of cells

Cells that were not passaged were frozen for later use. Confluent HEK-MSR cells were treated with TE for 5 minutes at 37˚C. Media (5 ml) was then added, and cells were centrifuged at 1000 xg for 5 minutes before discarding the supernatant. The cell pellet was resuspended in 1 ml of FBS containing 10% DMSO and transferred to a 1.5 ml cryovial. Cells were frozen at -20˚C for 1 hour, before being placed in a -80˚C freezer overnight. Cells were then transferred to a liquid nitrogen dewar for long-term storage.

2.4 Sperm motility assessment

2.4.1 Computer-assisted sperm analysis

For assessment of motility, CASA was utilised using a Sperm Class Analyser (SCA) system (Microptics, Spain) with external microscope (Primo Star, Zeiss, UK) and attached camera (Basler, Germany). To perform the sperm analysis, 3 µl of the appropriate sperm sample was placed into a pre-warmed chamber of a Leja 4-chamber 20 micron depth counting chamber (Microm, UK). The chamber was placed onto the heated stage of the microscope (37˚C) and left to equilibrate for approximately 2 minutes prior to analysis to allow 'drift' to cease. For every treatment, between 800 and 900 sperm were assessed at random across three different samples, using a 10x negative phase objective and SCA inbuilt frame rate of 25 fps. Settings were defined as follows: minimum head area – 2 μm^2; maximum head area – 70 μm^2; and minimum number of VAP (average path velocity) points – 9. Motion parameters assessed for individual spermatozoa are illustrated in **Figure 2.1** and included: VAP, curvilinear velocity

(VCL), straight line velocity (VSL), straightness (STR, defined as VSL/VAP), linearity (LIN, defined as VSL/VCL), wobble (WOB, defined as VAP/VCL), amplitude of lateral head displacement (ALH), and beat cross frequency (BCF). General motility classification included: immotile (VAP <20 μm/s); moderate (VAP 20-80 μm/s), and rapid (VAP >120 μm/s). Progressively motile sperm were defined as those with a VAP >120 μm/s and STR >80%. Sperm hyperactivation was assessed using the criteria: VCL ≥ 120 μm/s, LIN < 50%, and ALH ≥ 7 μm, and expressed as a percentage of the total number of motile cells. To reduce any inaccuracy during assessment, the SCA playback system was used and any erroneous sperm identifications were removed from the analysis.

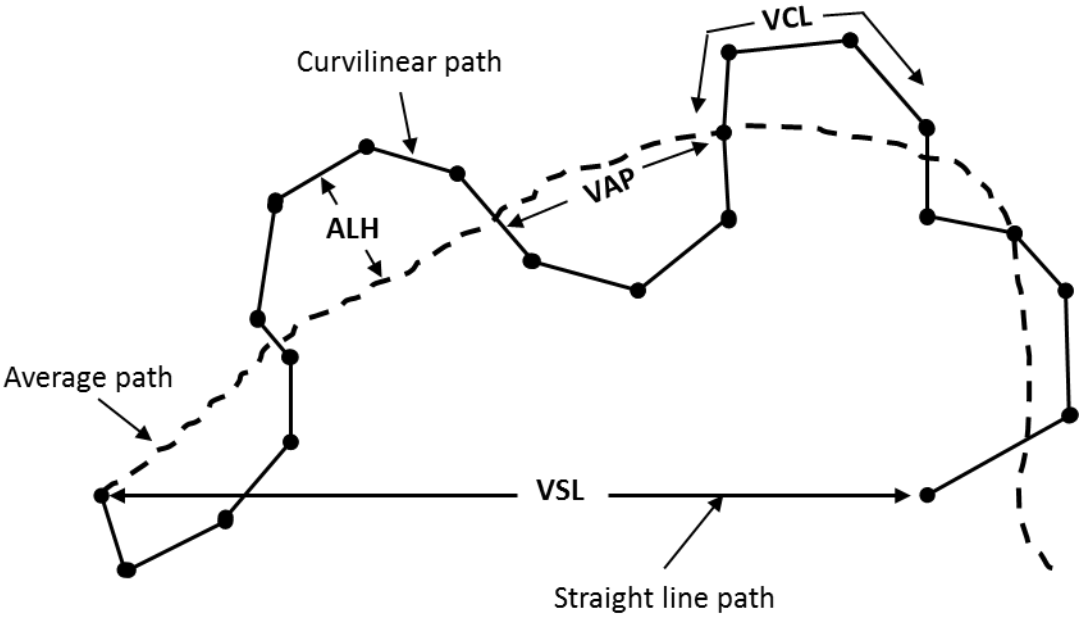

Figure 2.1: Various parameters of sperm motility assessed by computer-aided sperm analysis.

ALH – amplitude of lateral head displacement; VAP – average path velocity; VCL – curvilinear velocity; VSL – straight line velocity. Self-drawn figure adapted from reference (WHO, 2010).

2.4.2 Kremer assay

Murine sperm were assessed for their ability to penetrate artificial cervical mucus using the Kremer assay. To do this, viscous media was prepared by the addition of 1% methyl cellulose to the WH-cap media. To dissolve, media was vortexed and then placed on a roller overnight at 4˚C. Before use, Kremer media was brought up to room temperature and poured into 2 ml microcentrifuge tubes (Sarstedt, Germany). Rectangular borosilicate glass capillary tubes (0.4x4 mm ID, 50 mm L; VitroCom, USA) were placed into the Kremer media and allowed to fill by capillary action. Once filled, tubes were cleaned with tissue to remove media on the outer surface, and one end sealed with Cristaseal wax (Hawksley, UK).

Sperm were prepared and treated with drugs/inhibitors as previously described (section 2.2.2) in 2 ml microcentrifuge tubes. Kremer media-filled capillary tubes were then placed into the sperm either immediately or following an appropriate period of incubation for the treatment. Tubes were incubated at an approximate 30˚ angle, at 37˚C, 5% CO_2 for 1 hour to allow sperm to enter the media. Following incubation, capillary tubes were removed and the open end sealed with Cristaseal wax. Tubes were then placed on a marked slide and the number of sperm across six fields of view that entered the tube at 0 cm, and penetrated to 1 cm were counted using a Primo Star microscope and 40x phase objective (Zeiss, UK).

2.5 Western blotting

2.5.1 Preparation of sperm and spermatid samples for Western blotting

Following treatment and/or motility analysis, sperm were centrifuged at 10,000 xg for 10 minutes and resuspended in SDS lysis buffer in a ratio of 10 µl per 1 million sperm. Vortexing was used to ensure complete resuspension of pellets and subsequent lysis of all sperm. For spermatid lysis, spermatids were centrifuged at 10,000 xg for 10 minutes and resuspended in 300 µl SDS lysis buffer. Spermatid lysates were run through a 23 guage 1.25” needle (BD, UK) 5 times and 1 µl DNase (10 mg/ml) added for DNA degradation. Lysates were then stored

at -20˚C until required. If protein amount in the sperm and spermatid lysates was to be determined, the bicinchoninic acid (BCA) assay was used (see section 2.5.3).

Samples for Western blotting were typically prepared at either a protein concentration of 1 µg/µl, or 0.5 million sperm per 20 µl sample depending on analysis. For preparation, sperm and spermatid lysates were thawed, and required volumes mixed with 4x SDS-sample buffer (240 mM Tris HCl pH 6.8, 8% SDS w/v, 40% glycerol v/v, 0.04% bromophenol blue w/v, supplemented with 10% β-mercaptoethanol v/v or 50 mM dithiothreitol; DTT)**.** Samples were brought up to the required volume with deionised water, and heated to 95˚C for 5 minutes. Samples then underwent SDS-PAGE immediately, or were stored at -20˚C.

2.5.2 Preparation of HEK-MSR cell samples for Western blotting

HEK-MSR cell lysates were thawed on ice and vortexed to mix contents. Protein concentration of the sample was determined using either the Bradford or BCA assay (see section 2.5.3). Samples were typically prepared at a protein concentration of 0.5 µg/µl, by mixing appropriate volumes of the sample with 4x SDS sample buffer and bringing up to volume with deionised water. Samples were then denatured at 95˚C for 5 minutes, vortexed, and either underwent SDS-PAGE immediately or were stored at -20˚C until required.

2.5.3 Protein assay

To assess protein concentration, a small volume of sperm, spermatid or HEK cell samples were diluted 1:10 with deionised water. Protein standards were made from bovine serum albumin in a 1:10 dilution of the appropriate lysis buffer in deionised water to produce protein concentrations of 0.05, 0.1, 0.2, 0.3, 0.4, 0.5, 0.7, and 1.0 µg/µl. Diluted samples and standards were added to a 96 well plate, each in duplicate 10 µl volumes. For the Bradford assay, 200 µl of Bradford Reagent (BioRad, UK), which had previously been diluted 1:5 in deionised water and filtered (Whatman No.1 filter paper), was added to the protein samples. Plates were then incubated at room temperature for 5 minutes and the absorbance of the samples at 595 nm was read using a microplate reader (MultiSkan GO, Thermo Scientific, Finland). For the BCA

assay, 200 µl of pre-mixed BCA reagent (1:50 solution A: solution B; Pierce, UK) was added to samples and standards, and the plates were incubated at 37˚C for 30 minutes before reading the absorbance at 562 nm using a microplate reader. Values obtained for the protein standards were input into a Microsoft Excel spreadsheet to generate a standard curve, from which the protein concentrations of the samples were calculated.

2.5.4 Preparation of SDS-polyacrylamide gels

SDS-polyacrylamide gels were prepared by pouring a 15% resolving gel (**Table 2.2**) into glass plates (BioRad, Hertfordshire, UK), overlaying with 500 µl of butanol or deionised water to ensure a level surface, and leaving to set for approximately 25 minutes. Once set, the butanol/water was poured off and the gel washed with deionised water. Residual liquid was removed using absorbent paper. Stacking gels (5%) (**Table 2.3**) were then poured on top, and 10-well combs inserted before leaving to set. Gels were used for electrophoresis immediately or stored overnight at 4˚C.

Table 2.2: Composition of 15% resolving gel

Chemical	Concentration
Bis/acrylamide (BioRad, UK)	15% (v/v)
Tris HCl pH 8.8	375 mM
SDS	0.1% (v/v)
Ammonium persulfate	0.1% (v/v)
TEMED	0.4 µl/ml
diH_2O	To volume

Table 2.3: Composition of 5% stacking gel

Chemical	Concentration
Bis/acrylamide (BioRad, UK)	5% (v/v)
Tris HCl pH 8.8	62.5 mM
SDS	0.1% (v/v)
Ammonium persulfate	0.1% (v/v)
TEMED	1 µl/ml
diH_2O	To volume

2.5.5 SDS-polyacrylamide gel electrophoresis

Gels were placed into gel tanks (XCell Sure Lock, Invitrogen, USA) and running buffer (250 mM Trizma base, 190 mM glycine, 0.1% SDS w/v) was poured into the tanks to cover the wells. Wells were then loaded with fixed volumes of protein samples, and a Precision Plus protein ladder (BioRad, Hertfordshire, UK) was included to allow determination of protein size. Unused wells were filled with the same volume of 1x SDS-sample buffer. Gels were run at 200 V for 60-70 minutes at room temperature.

2.5.6 Western blot

After running, gels were removed from the tank and rinsed thoroughly in deionised water. Polyvinylidene fluoride (PVDF) membranes (Amersham Hybond, GE Healthcare Life Sciences, UK) cut to 8.5x6.5 cm were activated in methanol for 15 seconds, rinsed in deionised water, and placed in transfer buffer (20 mM Trizma base, 150 mM glycine, 20% methanol v/v) until required. Short glass plates were removed from gels, and a piece of PVDF placed carefully onto the gel surface. Blotting paper (9x7 cm) was dipped in transfer buffer and placed on top of the PVDF. Gels were flipped over and the glass plate removed. Another piece of blotting paper was placed on to the surface of the gel, and air bubbles were removed. Sponges that had been

pre-soaked in transfer buffer were placed into a transfer cassette (XCell II Blot Module, Invitrogen, USA) with the blot in the centre; a pre-soaked sponge was used between blots if two were being transferred. Cassettes were placed back into the gel tank and the cassette filled with transfer buffer. Deionised water was used to fill the rest of the tank to approximately 2 cm from the top. Transfer was carried out at 30V for 2 hours at room temperature.

2.5.7 Blocking and antibodies

Following transfer, PVDF membranes were placed into a blocking solution consisting of 5% non-fat dried milk in Tris-buffered saline with Tween-20 (TBS-T; 20 mM Trizma Base, 150 mM sodium chloride, 0.1% Tween-20, pH 7.6), and incubated on a rocker (Bibby Scientific, Staffordshire, UK) for 60 minutes at room temperature. Primary antibodies were made up in 1% milk in TBS-T at appropriate concentrations in 50 ml Falcon tubes (**Table 2.4**). Following blocking, PVDF membranes were placed into the tubes and incubated in primary antibody either overnight at 4˚C, or for 1 hour at room temperature on a rotating roller (Bibby Scientific, Staffordshire, UK). Following incubation, membranes were removed from the tubes and washed in TBS-T three times for 15 minutes each on a rocker at room temperature. HRP-conjugated secondary antibodies were made up in 1% non-fat dried milk in TBS-T to appropriate concentrations in 50 ml Falcon tubes (**Table 2.4**). PVDF membranes were placed into the secondary antibody solution to incubate for 1 hour at room temperature on a rotating roller. Following incubation, membranes were removed and washed three times in TBS-T for 15 minutes on a rocker at room temperature.

Table 2.4: Primary and secondary antibodies

	Antibody	Type	Company	Dilution	Molecular weight (kDa)
Primary	Anti-acetylated α-tubulin (clone 6-11B-1)	Mouse monoclonal	Sigma T7451	1:50000	~55
	Anti-α-tubulin	Rabbit polyclonal	Abcam ab4074	1:50000	~55
Secondary	Anti-mouse	Horse	Vector Laboratories PI-2000	1:2000	-
	Anti-rabbit	Goat	Vector Laboratories PI-1000	1:2/3000	-

2.5.8 ECL and detection of protein

After washing, excess TBS-T was removed from membranes by touching corners lightly on to tissue paper. Membranes were then either covered with an enhanced chemiluminescence (ECL) solution (1 ml of each solution per blot; **Table 2.5**) and allowed to react for 3 minutes in the dark, or 500 µl of pre-mixed ECL reagents (Amersham ECL Prime Western blotting detection reagent, GE Healthcare, UK) were applied. Excess ECL was removed from membranes using tissue paper. Blots were covered with cling film and wiped over to remove further excess ECL. Exposure was then performed using either a ChemiDoc MP System (BioRad, UK) and ImageLab software (BioRad, UK), or membranes were exposed to CL-X Posure film (ThermoScientific, Belgium) under dark room conditions. Films were developed using a Compact X4 film processor (Xograph, UK).

Table 2.5: Composition of enhanced chemiluminescence (ECL) solutions

	Chemical	Concentration
Solution 1	Luminol	2.5 mM
	p-Coumaric acid	0.4 mM
	Tris HCl pH 8.5	885 mM
	diH_2O	To volume
Solution 2	H_2O_2	30% (v/v)
	Tris HCl pH 8.5	100 mM
	diH_2O	To volume

2.5.9 Stripping and re-probing membranes

To ensure primary antibodies were removed from membranes before re-probing with another, membranes underwent two 30 minute washes at room temperature in 1x acid stripping buffer (400 mM glycine, 7 mM SDS, 2% Tween-20 v/v, pH 2.2). Membranes were then washed in 1x PBS three times for 3 minutes each to bring back up to pH. Subsequently, membranes were blocked and incubated with primary antibody as previously described.

2.5.10 Densitometry

Protein bands visualised on membranes were semi-quantitatively analysed using ImageJ image processing software (NIH, USA) to measure pixel density. Changes in protein levels were expressed as fold change relative to protein levels in the vehicle control.

2.6 HDAC activity assay

HDAC enzymatic activity in sperm and HEK-MSR cells was assessed using the HDAC Cell-based Activity Assay Kit (Cayman Chemical, 600150, USA), which allows measurement of deacetylase activity in whole cells using a cell-permeable HDAC substrate. A schematic of the experimental procedure is shown in **Chapter 4, Figure 4.15a**. To prepare HEK-MSR cells for the assay, cells

were seeded at a density of $2x10^4$ cells/well in 100 µl of growth media in the 96-well plate provided with the kit. Cells were cultured for 24 hours at 37°C, 5% CO_2 prior to undergoing treatment. To prepare sperm for the assay, epididymal sperm were extracted on the day of the assay as previously described (section 2.2.2). Sperm were resuspended to 6 million/ml in WH-cap media, and 100 µl placed into 1.5 ml microcentrifuge tubes to undergo treatment. To determine whether HDAC activity could be inhibited in sperm and HEK-MSR cells, both cell types were treated with 1 µM TSA, 5 µM tubacin or vehicle in duplicate for 1 hour at 37°C, 5% CO_2. Untreated cells were also cultured under the same conditions for later inclusion of controls to test assay specificity.

Following treatment, the manufacturer instructions were followed for the preparation of reagents and assay procedure. Briefly, HEK cells in the 96-well plate, and sperm in microcentrifuge tubes were centrifuged at 500 xg for 5 minutes and washed in the provided assay buffer. Cells that had undergone inhibitor treatments were then resuspended in the appropriate media. Untreated cells were either resuspended in the provided human recombinant HDAC1 positive control, or media plus the provided TSA to ensure specificity of the assay. At this point, sperm were transferred from microcentrifuge tubes to the 96-well plate. HDAC reactions were initiated by addition of the HDAC substrate (Boc-Lys(AC)-AMC), and the plate was incubated for 2 hours at 37°C, 5% CO_2. At the end of the incubation, deacetylated standards were added to the plate to allow a standard curve to be produced. Lysis/developer solution was subsequently applied to every well, and the plate shaken for 2 minutes on a plate shaker before incubating for 15 minutes at 37°C. Fluorescence intensity was subsequently measured at excitation and emission wavelengths of 360 nm and 465 nm, respectively, using a Synergy H4 hybrid plate reader (BioTek, USA) and Gen5 software (version 2.01.12, BioTek, USA).

To determine HDAC activity in the samples, a standard curve was plotted from the average fluorescence values of the deacetylated standards, and the linear regression calculated.

Corrected sample fluorescence was then calculated for each condition by finding the average fluorescence of the duplicate readings for each condition, and subtracting the average fluorescence of the TSA control sample. The values were then entered into the following calculation to determine the HDAC activity of the samples:

$$\text{HDAC activity (nmol/min/ml)} = \frac{[\text{Corrected sample fluorescence} - (\text{y-intercept})/\text{slope}]}{15 \text{ minutes}}$$

2.7 Immunofluorescence

2.7.1 Preparation of mouse sperm for immunofluorescence

First, circular glass coverslips 18 mm in diameter were pre-coated with 0.001% poly-d-lysine (Corning, UK) to allow sperm to adhere. Coverslips were placed in 6 cm cell culture dishes and a 50 µl drop of poly-d-lysine was pipetted on to the centre of the coverslip. This was left to air dry for approximately 1 hour. Coverslips were rinsed with 2 ml PBS (Gibco, UK) before use to remove any residual poly-d-lysine solution.

Following treatment for 3 hours with vehicle, 25 µM nocodazole, or 1 µM TSA as a control, sperm were washed in PBS by centrifuging at 700 xg for 5 minutes at room temperature and resuspending in 1 ml PBS. Sperm were centrifuged again, and resuspended in 500 µl of fixative (3.7% paraformaldehyde v/v, 0.02% glutaraldehyde v/v, 50 mM PIPES, 5 mM EGTA, 2 mM magnesium sulphate) containing constituents to maintain the definition of microtubules (Baur and Stacey, 1977). Sperm were fixed in solution for 10 minutes at room temperature, then centrifuged at 700 xg for 5 minutes at room temperature, and washed in 1 ml PBS. Sperm were centrifuged again and resuspended in PBS to a concentration of 12 million/ml. A 50 µl drop of sperm was placed onto the centre of poly-d-lysine-coated coverslips, and sperm were allowed to adhere at room temperature for approximately 30 minutes. Unbound sperm were washed away with PBS, and adherent sperm were permeabilised with 0.5% Triton X-100 (v/v) in PBS for 5 minutes at room temperature. Coverslips were then washed three times by gently

pipetting 2 ml PBS into the dishes containing the coverslips. Blocking was then performed using 3% BSA (w/v) in PBS for 30 minutes at room temperature. Overnight incubation (at 4°C) of sperm in 70 µl of anti-α-tubulin antibody (per coverslip) at a dilution of 1:1000 in 1% BSA (w/v) in PBS followed. Details of the primary antibody are shown in **Table 2.4**.

Following primary antibody incubation, coverslips were washed three times in 2 ml PBS for 5 minutes, then incubated at room temperature with 70 µl (per coverslip) of secondary antibody (Alexo Fluor 488 donkey anti-rabbit A21206, 1:500 dilution; ThermoFisher, UK) diluted in 1% BSA in PBS for 1 hour in a humidified chamber. Coverslips were then washed three times by incubation in 2 ml PBS for 10 minutes in a humidified chamber. Sperm nuclei were stained using 50 µl (per coverslip) of 4',6-diamidino-2-phenylindole solution (DAPI; 40ng/ml in PBS) for 10 minutes in a humidified chamber, followed by rinsing with 2 ml PBS. Excess liquid was removed using tissue paper, and the coverslips were mounted onto microscope slides (VWR, UK) using 10 µl of soft-set Vectashield (Vector Laboratories, USA), before sealing around the edges with clear nail polish. Slides were allowed to dry overnight at 4˚C in the dark before staining was visualised using a Zeiss LSM 880 confocal microscope with airyscan and Zeiss Zen Black 2.3 software (Zeiss, Germany). Z-stack images were obtained and maximum intensity projections produced for examination of α-tubulin localisation. Coverslips incubated without primary antibody confirmed the specificity of secondary antibody.

2.7.2 Preparation of HEK-MSR cells for immunofluorescence

Sterile circular glass coverslips 18 mm in diameter were placed in 6 cm cell culture dishes. Following trypsinisation and resuspension, HEK-MSR cells were seeded at a 1:4 dilution and left to adhere to the coverslips overnight. Cells were treated the following day with vehicle, 25 µM nocodazole, or 1 µM TSA as a control for 3 hours. Following treatment, cells were washed three times with 2 ml PBS, fixed for 10 minutes at room temperature with 2ml of fixative, and then washed with 2 ml PBS. HEK cells then underwent the same experimental procedures as described for sperm. Briefly, cells were permeabilised with 0.5% Triton X-100 (v/v) in PBS for 5

minutes at room temperature, blocked using 3% BSA (w/v) in PBS for 30 minutes at room temperature, and incubated in anti-α-tubulin antibody at 4°C overnight (1:1000 dilution in 1% BSA in PBS; see **Table 2.4** for antibody details). After incubation, coverslips were washed in PBS and subsequently incubated with secondary antibody (Alexo Fluor 488 donkey anti-rabbit A21206, 1:500 dilution in 1% BSA in PBS) in a humidified chamber for 1 hour at room temperature. Cells were then washed three times in PBS for 10 minutes, and nuclei were stained by incubating each coverslip with 50 µl of DAPI solution for 10 minutes at room temperature in a humidified chamber. Coverslips were then mounted onto slides and sealed as described in section 2.7.1, then allowed to dry overnight at 4˚C in the dark. A Zeiss LSM 880 confocal microscope with airyscan and Zeiss Zen Black 2.3 software were used to visualise labelling and obtain Z-stack images, which were subsequently used to produce maximum intensity projections for examination of microtubule organisation.

2.8 Transmission Electron Microscopy (TEM)

Following treatment with vehicle, 25 µM nocodazole, or 1 µM TSA, sperm were prepared for TEM analysis by centrifuging at 700 xg for 5 minutes at room temperature, and then fixing in Karnovsky's fixative (2% paraformaldehyde v/v, 2.5% glutaraldehyde v/v, 0.1 M sodium cacodylate buffer pH 7.4) for 45 minutes at room temperature. Sperm were then centrifuged at 1000 xg for 5 minutes, and washed three times in 0.1 M sodium cacodylate buffer. Post-fixation of the sperm was carried out by resuspension in 1% osmium tetroxide v/v in 0.1 M sodium cacodylate buffer for 1 hour at room temperature, before centrifuging again at 700 xg for 5 minutes. Sperm pellets were then enrobed in 2% gelatin and left to set overnight at 4°C. Once set, samples were removed from the tubes and excess gelatin surrounding the pellet was trimmed. Samples embedded in gelatin were then placed in glass vials and dehydrated by covering in pre-chilled 50% alcohol for 5 minutes on a rotator at 4°C. The alcohol was removed and replaced and the sample left to incubate again on a rotator for 5 minutes. This step was performed three times in total. The procedure was repeated with 70% and 95% alcohol

sequentially, before dehydration in 100% alcohol, 100% alcohol and propylene oxide solution (1:1), and propylene oxide, three times each for 10 minutes. Araldite resin was made up using the Agar 100 resin kit (Agar Scientific, UK) according to manufacturer's instructions, ensuring the resin was well-mixed before proceeding. A small amount of the resin was mixed in a 1:1 ratio with propylene oxide in a glass vial which was subsequently placed in the vials containing the samples for 1 hour at 37°C. Remaining resin/propylene oxide was removed from the glass vials and replaced with 100% araldite resin for 1 hour at 37°C, with a resin change after 30 minutes. Samples were then embedded into moulds and covered with fresh resin, ensuring all air bubbles were removed, before allowing to polymerise for 48 hours at 60°C. Ultrathin sections were then cut using a Leica UC6 ultramicrotome (Leica Microsystems Ltd., UK), counterstained with 1% uranyl acetate/lead citrate, and viewed using an Hitachi H-7600 Transmission electron microscope (Hitachi High-Technologies, UK) by trained personnel in the Microscopy and Bioimaging Facility, Durham University.

2.9 Statistical analysis

Mean values for sperm motility parameters, sperm numbers and fold change in relative protein abundance were compared by unpaired T-test with significance level set at $P < 0.05$ in Microsoft Excel (2016). When more than two conditions were being compared, GraphPad Prism (Version 7.04, GraphPad Software, Inc.) was utilised to perform a one-way analysis of variance (ANOVA), with a Dunnett's post-hoc test to identify which groups were significantly different from one another ($P < 0.05$).

Chapter 3

Chapter 3 – The role of α-tubulin deacetylases in sperm motility

3.1 Introduction

Microtubules are a central component of the sperm axoneme, and a fundamental structure required for the mechanical mechanism underlying sperm motility. Since the discovery in *Chlamydomonas reinhardtii* that the microtubule protein, α-tubulin has an acetylation site on the K40 residue (L'Hernault and Joel L Rosenbaum, 1983; LeDizet and Piperno, 1987), the role of this post-translational modification in microtubule function has been under question. Whilst the exact mechanism by which this PTM regulates microtubule function remains unclear, the acetylation state has been linked to a variety of cellular processes including cell migration. These findings, coupled with the knowledge that the K40 site is present in the cilia and flagella of a variety of species (Piperno and Fuller, 1985), raised the possibility that this PTM may have an influence on the regulation of sperm motility. The existence of α-tubulin hypoacetylation in individuals with impaired sperm motility (Gentleman *et al.*, 1996; Bhagwat *et al.*, 2014) further suggested that α-tubulin acetylation/deacetylation may play a part in sperm motility modulation. This implicated the counterbalancing actions of the α-tubulin acetyltransferase, α-TAT1, and the deacetylases, HDAC6 and SIRT2 (**Figure 3.1**) in potential regulatory roles for sperm motility. Whilst a few groups have assessed the impact of α-TAT1 and HDAC6 knockout on sperm development and function in mouse models (Zhang *et al.*, 2008; Kim *et al.*, 2013; Nereo Kalebic *et al.*, 2013), only one study to date has investigated the role of HDAC6 in the motility of mature sperm via inhibition of the deacetylase. An increase in acetylation of α-tubulin, together with a reduction in progressive motility was found in sperm from Holtzman rats following HDAC6 inhibition (Parab *et al.*, 2015), which indicates a role for microtubule deacetylation in the regulation of sperm motility. However, research into the function of microtubule acetylation/deacetylation in sperm is extremely limited, and given the recent

emergence of studies indicating the importance of the acetylome in cellular functions, is an area that requires further investigation.

3.1.1 Aims

The primary aim of the investigations in this chapter was to explore the role that HDAC6 plays in the regulation of sperm motility by exposing sperm to the HDAC6-specific inhibitor, tubacin, and examining motility parameters and levels of acetylated α-tubulin. Secondly, the lesser-understood α-tubulin deacetylase, SIRT2, was also examined for its role in sperm motility via use of the general Class III HDAC inhibitor, nicotinamide.

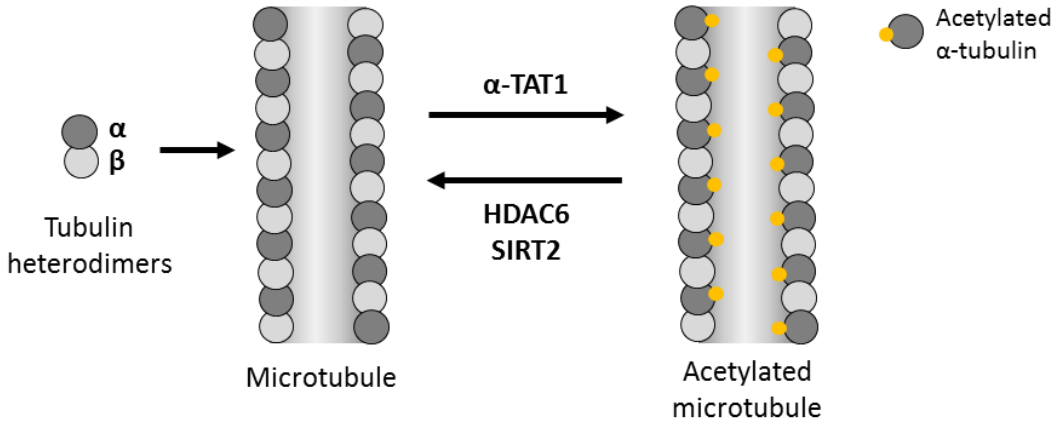

Figure 3.1: Acetylation and deacetylation of microtubules.

Heterodimers of α- and β-tubulin assemble to form microtubules. The acetyltransferase, α-TAT1 acetylates α-tubulin whilst the activities of HDAC6 and SIRT2 act to deacetylate α-tubulin. Self-drawn figure adapted from reference (Leroux, 2010).

3.2 Results

3.2.1 Impact of tubacin treatment on sperm from BALB/c mice

To explore the role of HDAC6 in sperm, sperm from BALB/c mice were treated with the HDAC6-specific inhibitor, tubacin, both during and following the period of capacitation. Sperm were then analysed to determine the effect of this inhibition on motility parameters and acetylation of α-tubulin. The results of these experiments are reported in the following sections.

3.2.1.1 Motility parameters of murine sperm are insensitive to treatment with tubacin

To investigate whether HDAC6 played a role in sperm motility, epididymal sperm were treated with 5 μM tubacin for either 1 hour following capacitation, or for 3 hours during capacitation. Assessment of motility parameters was then carried out using CASA. As shown in **Figure 3.2**, slight increases in mean curvilinear, straight line, and average path velocities, as well as amplitude of lateral head displacement and beat cross frequency were found following treatment of sperm with tubacin for 1 hour in 6 independent experiments. However, these increases were not significant. Straightness, linearity and wobble were all unaffected by treatment with tubacin for 1 hour. In addition, the percentage of sperm exhibiting hyperactivation following tubacin treatment for 1 hour showed a small but non-significant decrease compared to control, whilst progressive motility was very slightly increased (**Figure 3.3**).

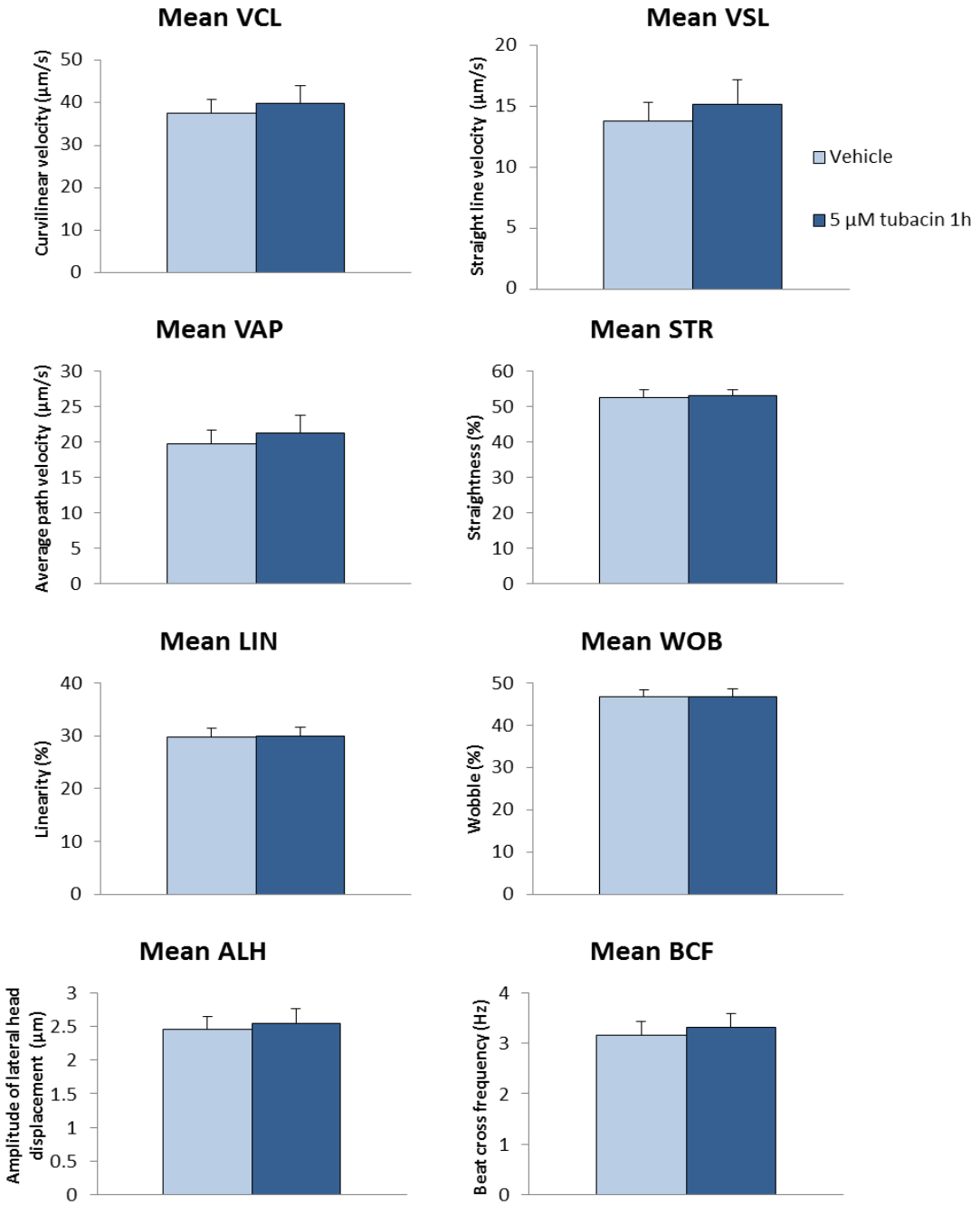

Figure 3.2: Motility parameters following treatment of sperm with tubacin for 1 hour following capacitation.

Epididymal sperm were treated with 5 µM tubacin for 1 hour and motility characteristics were assessed using computer-assisted sperm analysis. Treated sperm exhibited slight increases in: VCL – curvilinear velocity, VSL - straight line velocity, VAP - average path velocity, ALH - amplitude of lateral head displacement and BCF - beat cross frequency, whilst STR - straightness, LIN - linearity and WOB – wobble were comparable to control. Values are shown as mean ± SEM, n=6, and were compared by unpaired T-test.

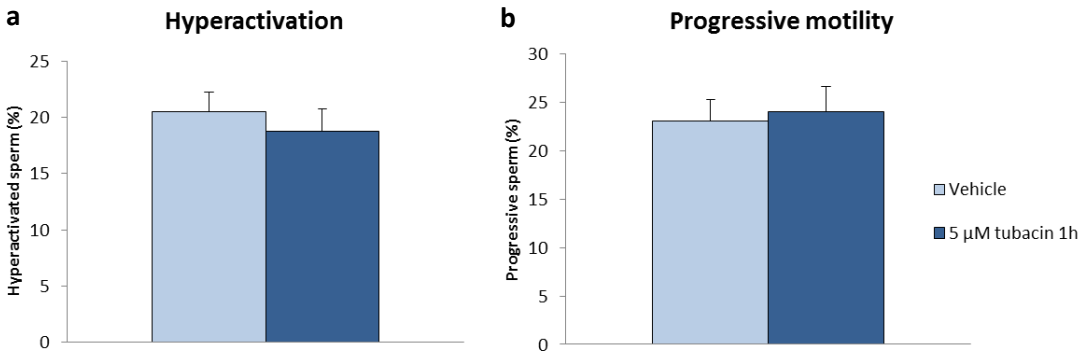

Figure 3.3: Hyperactivation and progressive motility in sperm following treatment with tubacin for 1 hour following capacitation.

Analysis of sperm motility following treatment with vehicle or 5 µM tubacin for 1 hour after capacitation showed the percentage of sperm exhibiting (a) hyperactivated motility was slightly decreased compared to control, and (b) progressive motility was comparable to control. Hyperactivated sperm are shown as a percentage of the total motile sperm; progressive sperm are shown as a percentage of total sperm in the analysed sample. Values shown are mean ± SEM, n=6, and were compared by unpaired T-test.

As various changes to the sperm take place during capacitation including an increase in another PTM, tyrosine phosphorylation, it was hypothesised that changes to the sperm protein acetylation state may also occur during the capacitation period. Therefore, sperm were treated with tubacin for 3 hours during capacitation and the effect on motility examined. Exposure to tubacin resulted in very slight reductions in all motility parameters, however these differences were not statistically significant (**Figure 3.4**). Additionally, a reduction in the percentages of sperm exhibiting hyperactivated and progressive motility was found following exposure to tubacin for 3 hours, however these changes were small and non-significant (**Figure 3.5**). The results demonstrate that murine sperm motility is insensitive to treatment with tubacin following capacitation, and when treatment was applied during the capacitation process. Overall the findings do not support a role for HDAC6 in the regulation of sperm motility.

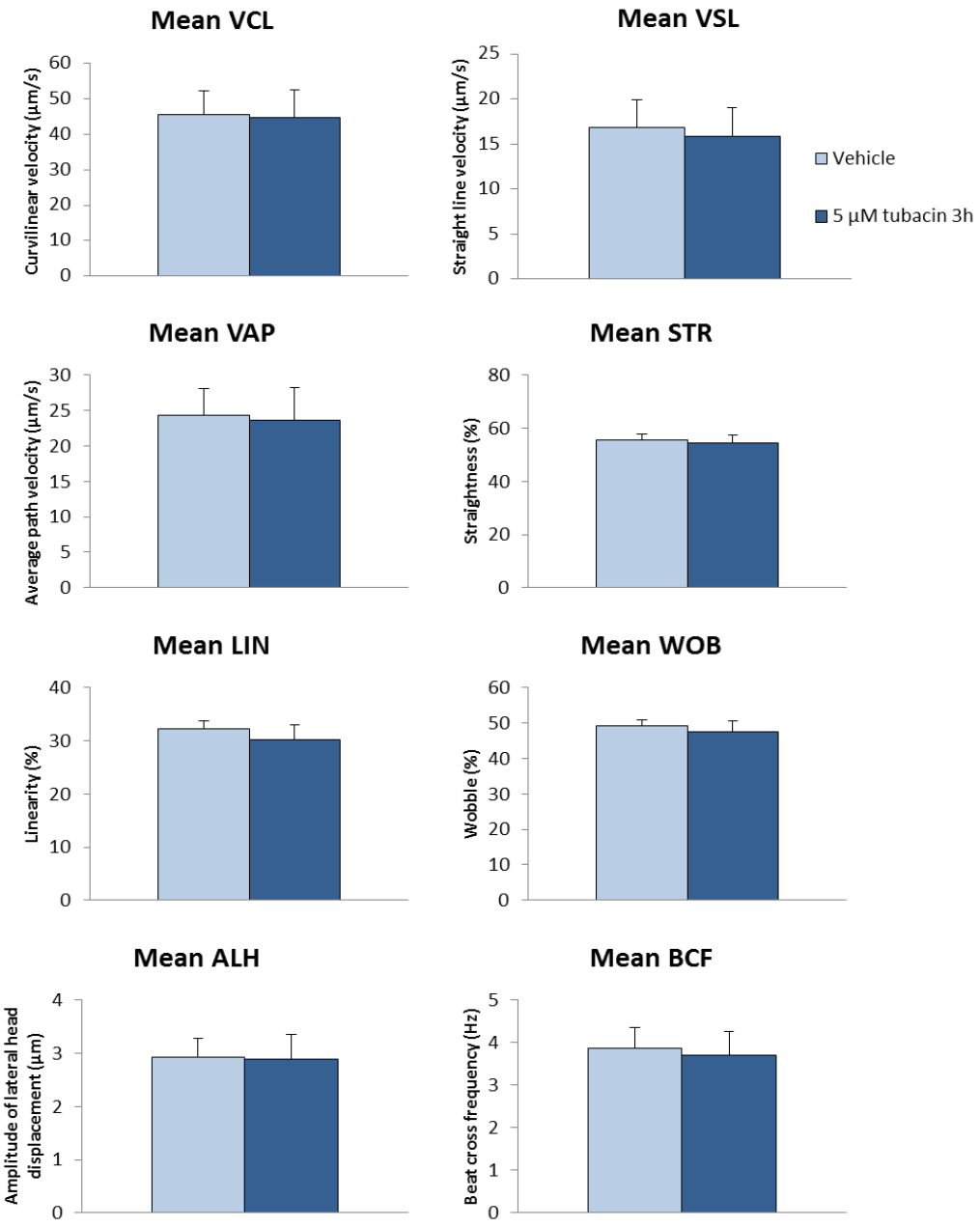

Figure 3.4: Motility parameters following treatment of sperm with tubacin for 3 hours during capacitation.

Epididymal sperm were treated with vehicle or 5 µM tubacin for 3 hours during capacitation, and motility characteristics were assessed using computer-assisted sperm analysis. All examined motility parameters were comparable between control and treated sperm. VCL – curvilinear velocity, VSL - straight line velocity, VAP - average path velocity, STR - straightness, LIN - linearity, WOB - wobble, ALH - amplitude of lateral head displacement and, BCF - beat cross frequency. Values are shown as mean ± SEM, n=3, and were compared by unpaired T-test.

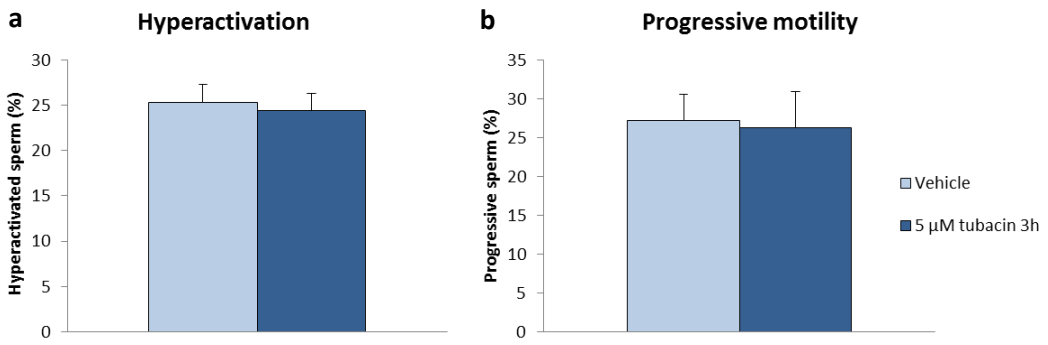

Figure 3.5: Hyperactivation and progressive motility in sperm following treatment with tubacin for 3 hours during capacitation.

Analysis of sperm exposed to 5 µM tubacin for 3 hours during capacitation showed the percentages of sperm exhibiting (a) hyperactivated and (b) progressive motility were not affected by the treatment. Hyperactivated sperm are shown as a percentage of the total motile sperm; progressive sperm are shown as a percentage of total sperm in the analysed sample. Values shown are mean ± SEM, n=3, and were compared by unpaired T-test.

3.2.1.2 Sperm motility in viscous media is unaffected by treatment with tubacin

To investigate whether sperm motility was altered by exposure to tubacin under conditions more comparable to the female reproductive tract, sperm were assessed for their ability to penetrate viscous media following treatment using a Kremer assay. A schematic illustration of the experimental approach is shown in **Figure 3.6a**. Epididymal sperm were first allowed to capacitate, and were then treated with 5 μM tubacin for 1 hour, with subsequent examination of their ability to penetrate artificial mucus in 1 hour. Overall, the mean number of sperm reaching 1 cm in the viscous media was less than the mean number of sperm entering the media at 0 cm by approximately 25% and 31% in vehicle- and tubacin-treated conditions respectively (**Figure 3.6b**). Analysis of the effects of tubacin treatment revealed a slight but non-significant increase in the number of sperm entering the media at 0 cm following tubacin exposure. The number of sperm reaching 1 cm after treatment was comparable to vehicle-treated sperm (**Figure 3.6b**). The results indicate that exposure to tubacin does not impact upon the ability of capacitated sperm to swim through viscous media.

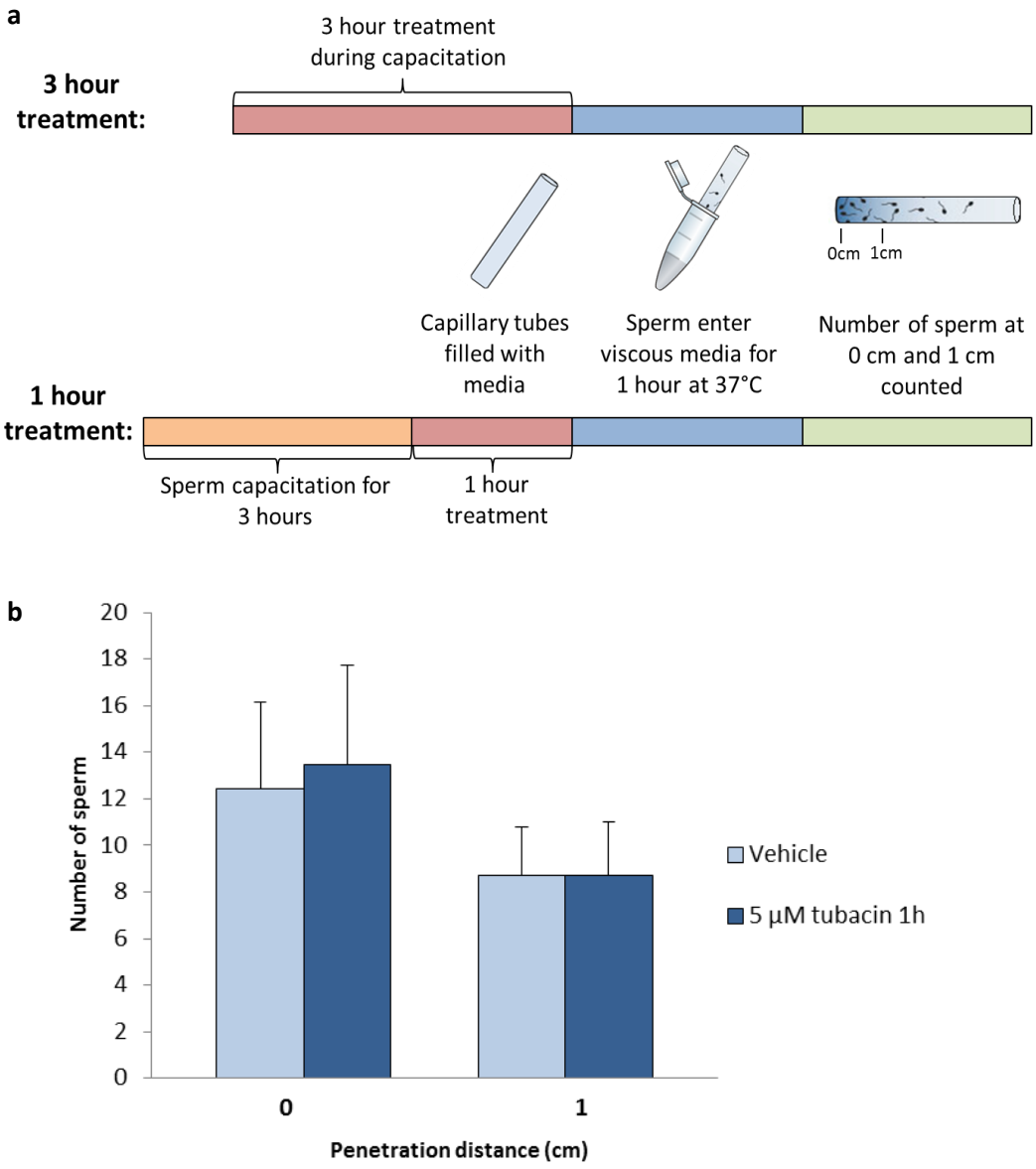

Figure 3.6: Assessment of sperm motility in viscous media using the Kremer assay.

(a) Schematic diagram of the experimental procedure for the Kremer assay in which sperm either underwent 1 hour or 3 hour drug treatments. (b) Capacitated sperm treated with vehicle or 5 µM tubacin for 1 hour were assessed for their ability to enter and penetrate viscous media. The mean number of sperm entering the media at 0 cm and penetrating to 1 cm was not significantly affected by treatment with tubacin. Values are shown as mean ± SEM, n=3, and were compared by unpaired T-test.

To determine whether treatment with an inhibitor of HDAC6 during capacitation had any subsequent effects on motility in viscous media, capacitating sperm were exposed to 5 µM tubacin for 3 hours, and then allowed to swim into the media for 1 hour. Firstly, like the 1 hour treatment, the mean number of sperm reaching 1 cm was less than the mean number of sperm entering the viscous media at 0 cm by approximately 53% and 63% in vehicle- and tubacin-treated conditions respectively (**Figure 3.7**). With regard to the effects of tubacin treatment, the number of sperm entering the media at 0 cm and penetrating to 1 cm showed slight reductions upon exposure to tubacin, however these differences were not statistically significant (**Figure 3.7**). This indicates that exposure to tubacin during capacitation does not significantly affect the ability of sperm to swim through viscous media. As such, no evidence was found to support a regulatory role for HDAC6 in murine sperm motility in the female reproductive tract.

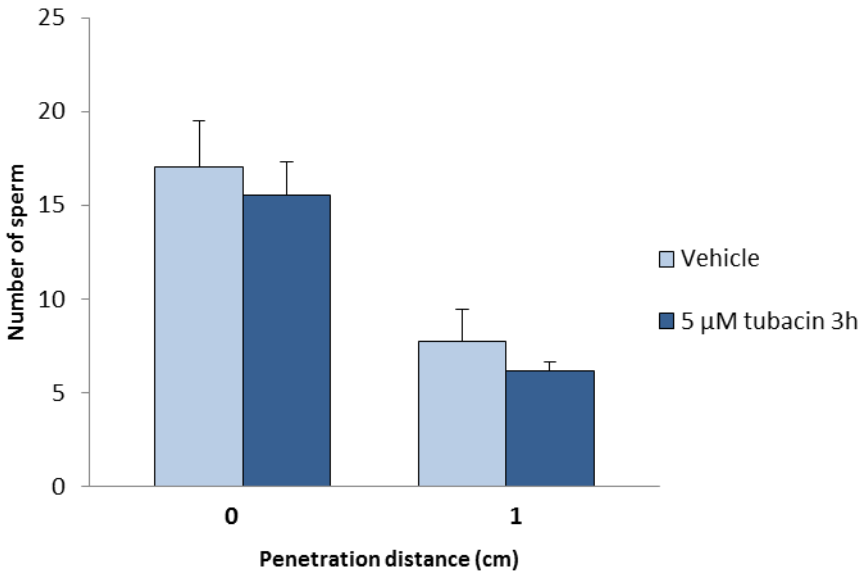

Figure 3.7: Penetration distance of sperm in viscous media following treatment with tubacin for 3 hours during capacitation.

Sperm treated with vehicle or 5 µM tubacin for 3 hours during capacitation were assessed for their ability to enter and penetrate viscous media. The mean number of sperm entering the media at 0 cm and penetrating to 1 cm was slightly lower in the treated condition compared to control sperm. Values are shown as mean ± SEM, n=5, and were compared by unpaired T-test.

3.2.1.3 Levels of α-tubulin acetylation in sperm are unaffected by treatment with tubacin

The results of the motility analysis demonstrated that sperm motility was insensitive to treatment with an inhibitor of HDAC6. To determine the acetylation status of sperm α-tubulin and the effect of tubacin treatment upon this, sperm treated with 5 μM tubacin for either 1 hour after capacitation or 3 hours during capacitation were lysed for Western blot analysis.

Figure 3.8a shows a representative Western blot of sperm lysates from 3 independent experiments in which capacitated sperm were treated with either vehicle or tubacin for 1 hour. Bands at approximately 55 kDa corresponding to acetylated α-tubulin in both vehicle- and tubacin-treated conditions from 6 independent experiments were subject to densitometric analysis (**Figure 3.8c**). Both the Western blot and densitometry demonstrate that the abundance of acetylated α-tubulin in murine sperm was unaffected by treatment with tubacin for 1 hour (**Figure 3.8a, c**). Blots were reprobed for total α-tubulin (**Figure 3.8b**), and bands at approximately 55 kDa were again subject to densitometric analysis (**Figure 3.8d**) which demonstrated that loading was comparable across conditions.

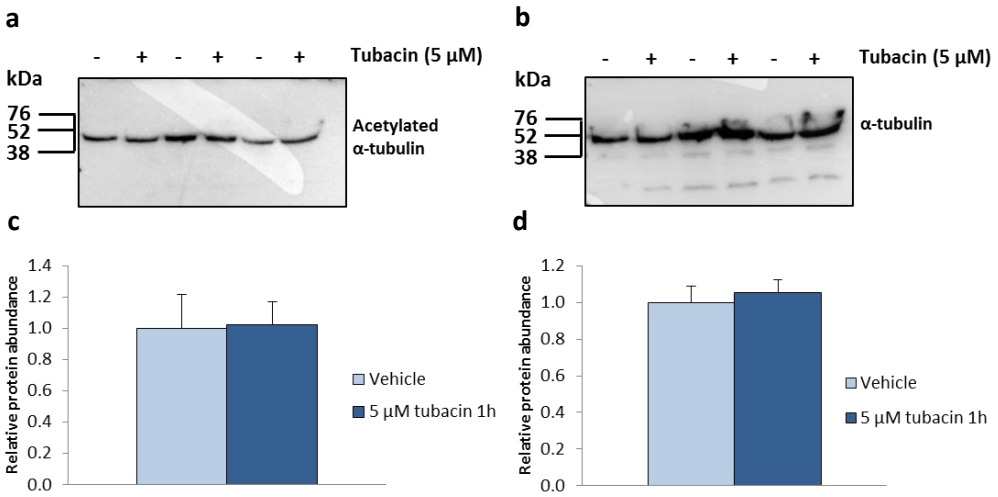

Figure 3.8: Acetylation of α-tubulin in sperm following treatment with tubacin for 1 hour following capacitation.

(a) Representative Western blot of acetylated protein from capacitated sperm treated with either vehicle or 5 µM tubacin for 1 hour in 3 independent experiments. Protein from approximately 0.5 million sperm was loaded in each lane. Bands at approximately 55 kDa correspond to acetylated α-tubulin. (b) All blots were reprobed for total α-tubulin as a loading control; bands at approximately 55 kDa correspond to α-tubulin. (c) Bar graph shows densitometric analysis of bands corresponding to acetylated α-tubulin (n=6). (d) Bar graph shows densitometric analysis of bands corresponding to total α-tubulin (n=6). Values are shown as mean ± SEM and were compared by an unpaired T-test.

To determine whether exposure to tubacin during capacitation had any effect on acetylation of α-tubulin, sperm were treated with 5 μM tubacin for 3 hours and lysed for Western blot analysis. **Figure 3.9a** shows a representative Western blot of sperm lysates from 3 independent experiments in which sperm were treated with either vehicle or tubacin. Bands at approximately 55 kDa corresponding to acetylated α-tubulin in both the vehicle- and tubacin-treated conditions were subject to densitometric analysis (**Figure 3.9c**). Both the Western blot and densitometry showed that the abundance of acetylated α-tubulin remained comparable to control following the treatment (**Figure 3.9a, c**). The blot was reprobed for total α-tubulin (**Figure 3.9b**), and bands at approximately 55 kDa were again analysed using densitometry to demonstrate equal loading between conditions (**Figure 3.9d**).

Overall, the results indicated that treatment of sperm with 5 μM tubacin both during and following capacitation did not impact upon the abundance of acetylated α-tubulin, therefore suggesting that α-tubulin may not be actively deacetylated by HDAC6 in murine sperm.

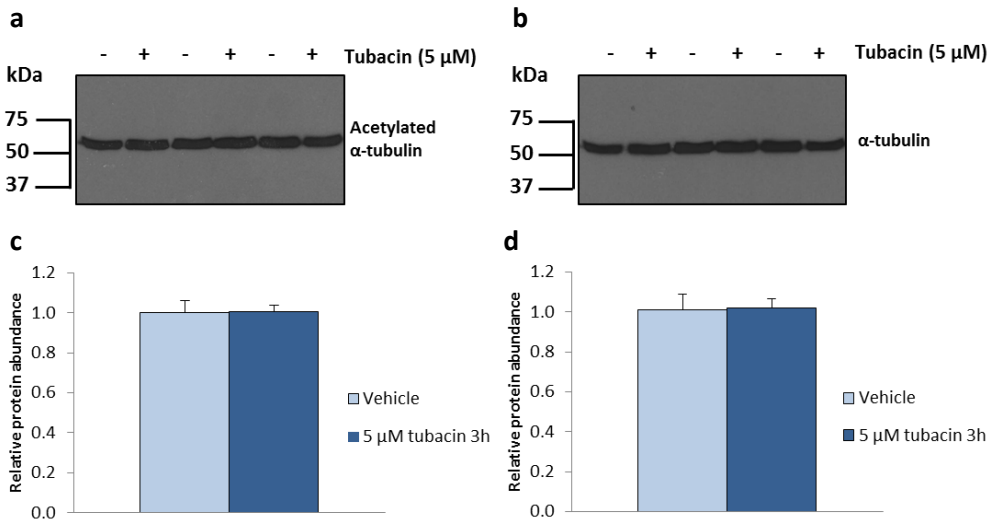

Figure 3.9: Acetylation of α-tubulin in sperm following treatment with tubacin for 3 hours during capacitation.

(a) Western blot of acetylated protein from sperm treated with either vehicle or 5 µM tubacin for 3 hours during capacitation in 3 independent experiments. Protein from approximately 0.5 million sperm was loaded in each lane. Bands at approximately 55 kDa correspond to acetylated α-tubulin. (b) Blots were reprobed for total α-tubulin as a loading control; bands at approximately 55 kDa correspond to α-tubulin. (c) Bar graph shows densitometric analysis of bands corresponding to acetylated α-tubulin (n=3). (d) Bar graph shows densitometric analysis of bands corresponding to total α-tubulin (n=3). Values are shown as mean ± SEM and were compared using an unpaired T-test.

3.2.1.4 Treatment with tubacin increases acetylated α-tubulin abundance in HEK cells

As the results obtained previously demonstrated that levels of α-tubulin acetylation in sperm were insensitive to treatment with tubacin, the HEK-MSR cell line was utilised to determine the response of another cell type to the inhibitor as a control. HEK cells were treated with 5 μM tubacin for up to 3 hours in 4 independent experiments, and were analysed by Western blot to determine the levels of acetylated α-tubulin. **Figure 3.10a** shows a representative Western blot from one of these time courses. Bands at approximately 55 kDa corresponding to acetylated α-tubulin in the 4 time courses were subject to densitometric analysis which is represented in **Figure 3.10c**. HEK cells exhibited an approximate 12- and 21-fold increase in acetylated α-tubulin abundance compared to control after treatment for 1 and 3 hours, respectively (**Figure 3.10a, c**). Statistical analysis using one-way ANOVA/Dunnett's post-hoc test determined these differences to be significant ($P < 0.0001$). Reprobing the Western blots for total α-tubulin and subsequent analysis of bands by densitometry showed that the abundance of α-tubulin remained comparable across conditions and demonstrated equal loading (**Figure 3.10b, d**). The data therefore indicated that treatment of HEK cells with tubacin resulted in an increase in acetylation of α-tubulin. This suggested that the deacetylase activity of HDAC6 in HEK cells could be inhibited by treatment with tubacin.

In addition to the effects of tubacin, a further observation regarding the baseline levels of acetylated α-tubulin in HEK cells was made during the experiments. It was noted that the levels of acetylated α-tubulin in control HEK cells appeared much lower than the levels previously observed in control sperm. This could explain the disparity in the effects of the inhibitor between sperm and HEK cells; α-tubulin in sperm may be highly acetylated and as such may not be responsive to tubacin. However, as it was not possible to compare the levels directly across different Western blots, lysates from HEK cells were included in subsequent blots presented in this section, and the hypothesis was investigated in experiments described in the next chapter.

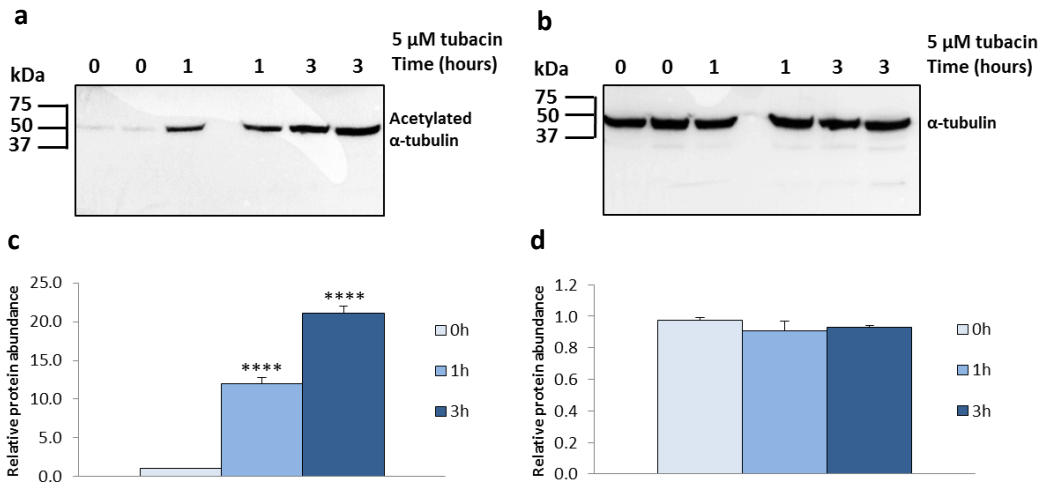

Figure 3.10: Acetylation of α-tubulin in HEK-MSR cells following tubacin time courses.

(a) Representative Western blot of acetylated protein from HEK-MSR cells treated with 5 µM tubacin for up to 3 hours. Approximately 20 µg of protein was loaded in each lane. Bands at approximately 55 kDa correspond to acetylated α-tubulin. (b) All blots were reprobed for total α-tubulin as a loading control; bands at approximately 55 kDa correspond to α-tubulin. (c) Bar graph shows densitometric analysis of bands corresponding to acetylated α-tubulin (n=4). (d) Bar graph shows densitometric analysis of bands corresponding to total α-tubulin (n=4). Values are shown as mean ± SEM compared by one-way ANOVA/Dunnett's post hoc test, ****$P < 0.0001$.

3.2.1.5 Levels of α-tubulin acetylation in spermatids are unaffected by treatment with tubacin

To determine whether developing spermatozoa were sensitive to tubacin, and investigate their state of α-tubulin acetylation, spermatids from the testes of BALB/c mice were treated with 5 μM tubacin for 1 hour in 3 independent experiments, and lysed for Western blot analysis. A representative Western blot showing lysates of spermatids, sperm and HEK cells treated with either vehicle or tubacin is shown in **Figure 3.11a**, and demonstrates that the levels of α-tubulin acetylation in spermatids were insensitive to treatment with tubacin for 1 hour. Bands at approximately 55 kDa corresponding to acetylated α-tubulin in spermatid lanes from 3 independent experiments were subject to densitometric analysis. The densitometry revealed a small 0.2-fold increase in the abundance of acetylated α-tubulin following treatment, although this was not significant (**Figure 3.11c**). Reprobing the blots for total α-tubulin (**Figure 3.11b**), and subsequent analysis of spermatid bands by densitometry demonstrated a 0.1-fold increase in the abundance of α-tubulin (**Figure 3.11d**). This suggested that the increase found in acetylated α-tubulin may result from the loading of slightly more protein in the treated condition.

Alongside spermatid lysates, HEK cell and sperm lysates were loaded as controls. Sperm samples again confirmed the lack of effect of tubacin. HEK cell lysates loaded as a positive control demonstrated the increase in acetylated α-tubulin in this cell line following treatment with 5 μM tubacin for 1 hour (**Figure 3.11a**). Notably, vehicle-treated HEK cells exhibited lower levels of α-tubulin acetylation compared to sperm and spermatids (**Figure 3.11a**).

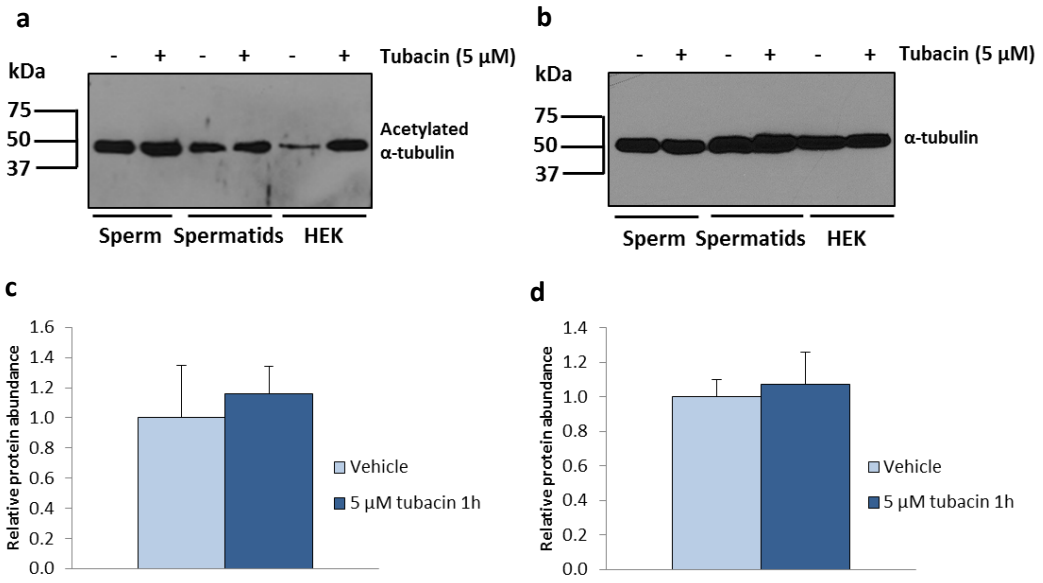

Figure 3.11: Acetylation of α-tubulin in spermatids following treatment with tubacin for 1 hour.

(a) Representative Western blot of acetylated protein in spermatids treated with 5 µM tubacin for 1 hour. HEK cell samples were loaded as a positive control; sperm samples were loaded as a negative control for the effects of tubacin. Approximately 20 µg of protein was loaded in each lane. Bands at approximately 55 kDa correspond to acetylated α-tubulin. (b) All blots were reprobed for total α-tubulin as a loading control; bands at approximately 55 kDa correspond to α-tubulin. (c) Bar graph shows densitometric analysis of bands corresponding to acetylated α-tubulin in spermatids (n=3). (d) Bar graph shows densitometric analysis of bands corresponding to total α-tubulin in spermatids (n=3). Values are shown as mean ± SEM and were compared by unpaired T-test.

To determine whether inhibition of HDAC6 for a longer time period would affect the levels of acetylated α-tubulin, spermatids were treated with 5 μM tubacin for 3 hours. A representative Western blot showing lysates of spermatids treated with either vehicle or tubacin for 3 hours in 2 independent experiments is shown in **Figure 3.12a**. Bands at approximately 55 kDa corresponding to acetylated α-tubulin in spermatid lysates from 3 independent experiments were subject to densitometric analysis (**Figure 3.12c**). In accordance with the results of the 1 hour treatment, the abundance of acetylated α-tubulin in spermatids treated for 3 hours was comparable to control (**Figure 3.12a, c**). Lysates of HEK cells treated with vehicle or tubacin for 3 hours were also loaded as a positive control to demonstrate the effects of tubacin treatment in this cell line. Vehicle-treated HEK cells were again noted to exhibit lower levels of acetylated α-tubulin than spermatid controls (**Figure 3.12a**). Reprobing the blots for total α-tubulin (**Figure 3.12b**), and subsequent densitometric analysis of bands corresponding to α-tubulin in spermatid lanes demonstrated equal loading between the conditions (**Figure 3.12b, d**). These results indicated that treatment of spermatids with tubacin did not influence the levels of α-tubulin acetylation, in accordance with the results observed in epididymal sperm. The data therefore suggest that HDAC6 may not be actively deacetylating α-tubulin in spermatids.

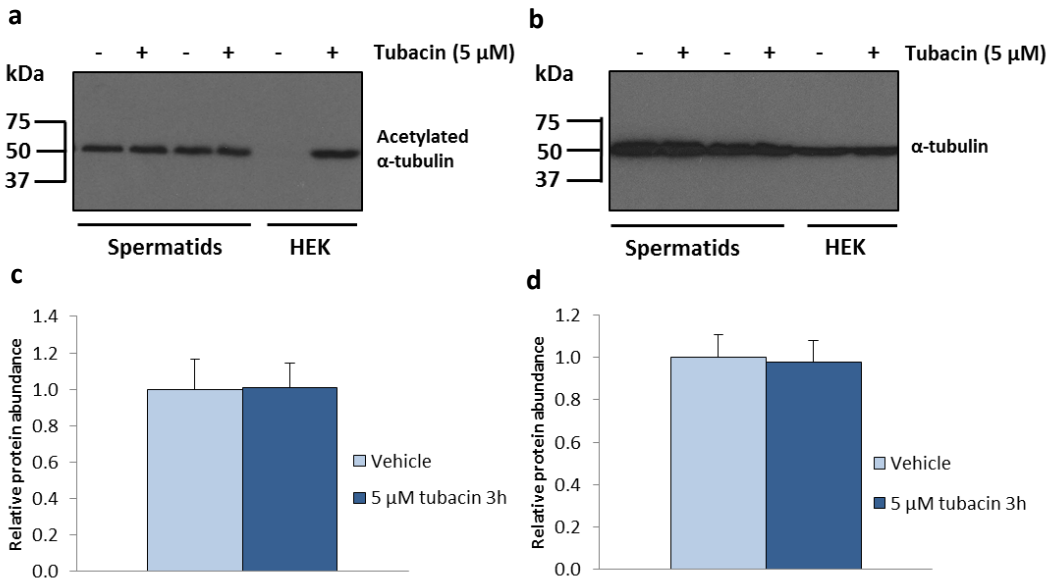

Figure 3.12: Acetylation of α-tubulin in spermatids following treatment with tubacin for 3 hours.

(a) Representative Western blot of acetylated protein from spermatids treated with 5 µM tubacin for 3 hours in 2 independent experiments. HEK cell samples were loaded as a positive control for the effects of HDAC6 inhibition. Approximately 20 µg of protein was loaded in each lane. Bands at approximately 55 kDa correspond to acetylated α-tubulin. (b) All blots were reprobed for total α-tubulin as a loading control; bands at approximately 55 kDa correspond to α-tubulin. (c) Bar graph shows densitometric analysis of bands corresponding to acetylated α-tubulin in spermatids (n=3). (d) Bar graph shows densitometric analysis of bands corresponding to total α-tubulin in spermatids (n=3). Values are shown as mean ± SEM and were compared by an unpaired T-test.

3.2.2 Impact of tubacin treatment on sperm from C57 mice

As the data presented so far were obtained using the sperm of BALB/c mice, sperm from C57 mice were treated with tubacin under the same conditions to ensure the effects observed were not strain-specific.

3.2.2.1 Motility parameters of sperm from C57 mice are insensitive to treatment with tubacin

Epididymal sperm from C57 mice were treated with 5 µM tubacin for 1 hour following capacitation. Motility analysis demonstrated that curvilinear velocity, straight line velocity, average path velocity, straightness, linearity, wobble, amplitude of lateral head displacement and beat cross frequency were all comparable to controls following treatment with tubacin (**Figure 3.13**). The percentage of sperm exhibiting hyperactivated motility was 2% lower in sperm treated with tubacin compared to control, though this small difference was not statistically significant (**Figure 3.14a**). Progressive motility was unchanged in C57 sperm following treatment with tubacin (**Figure 3.14b**). The results demonstrated that the motility of sperm from C57 mice was insensitive to treatment with tubacin, which is in accordance with the findings obtained with BALB/c sperm (Section 3.2.1.1, **Figures 3.2-3.5**). Therefore the lack of effect of tubacin on sperm motility is not restricted to BALB/c mice, further supporting the notion that HDAC6 may not play an active role in the regulation of sperm motility in mice.

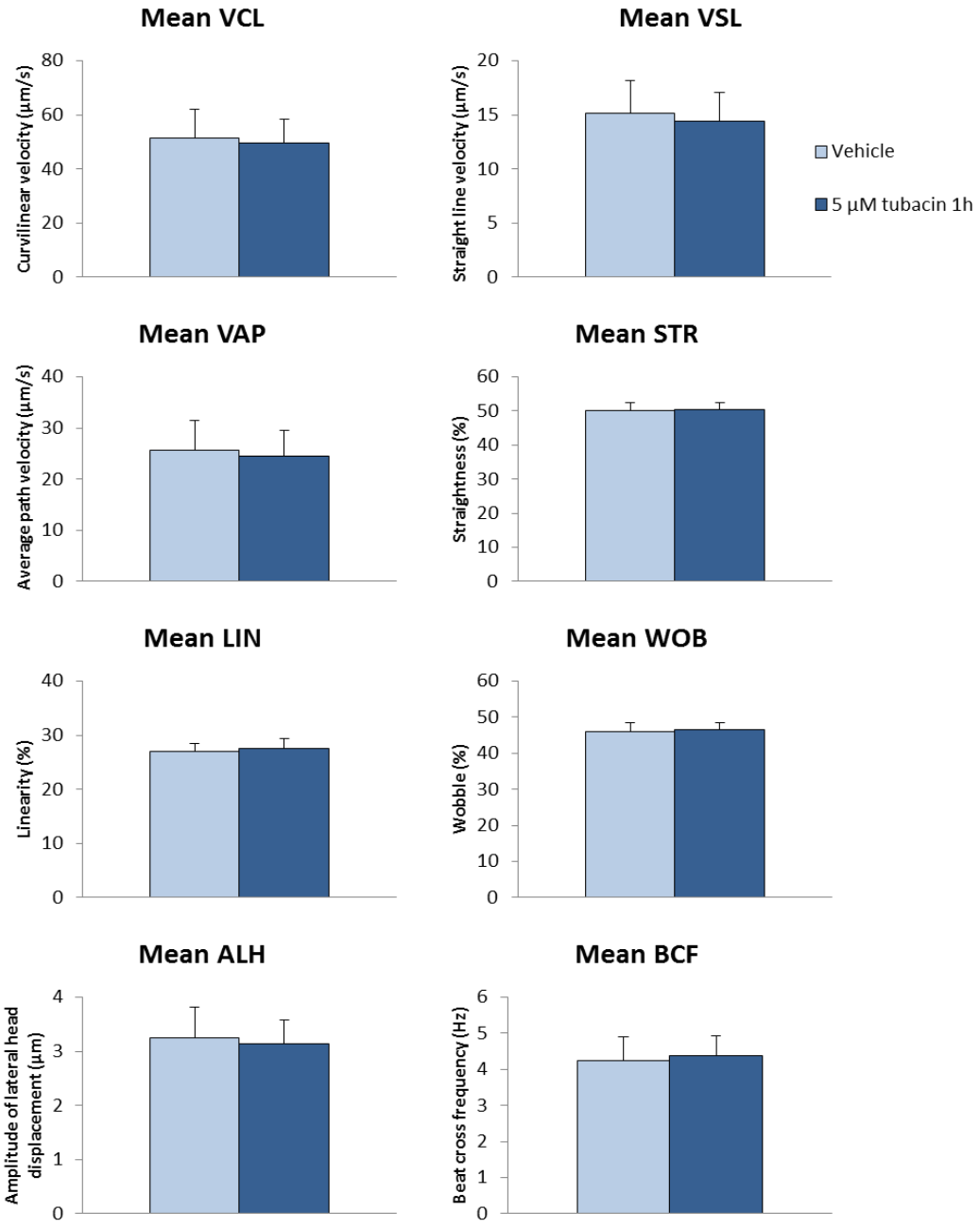

Figure 3.13: Motility parameters following treatment of C57 sperm with tubacin for 1 hour following capacitation.

Epididymal sperm were treated with 5 µM tubacin for 1 hour, and motility characteristics were assessed using computer-assisted sperm analysis. Treated sperm were comparable to control sperm in all examined motility parameters: VCL - curvilinear velocity, VSL - straight line velocity, VAP - average path velocity, STR - straightness, LIN - linearity, WOB - wobble, ALH - amplitude of lateral head displacement and, BCF - beat cross frequency. Values are shown as mean ± SEM, n=4, and were compared by unpaired T-test.

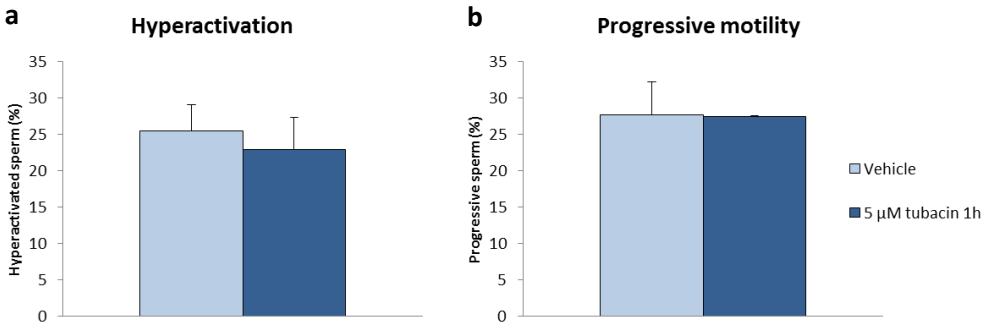

Figure 3.14: Hyperactivation and progressive motility in sperm from C57 mice following treatment with tubacin for 1 hour following capacitation.

Motility analysis of sperm treated with 5 µM tubacin for 1 hour following capacitation showed that (a) hyperactivated motility was slightly lower than control, and (b) progressive motility was comparable to control. Hyperactivated sperm are shown as a percentage of the total motile sperm; progressive sperm are shown as a percentage of total sperm in the analysed sample. Values shown are mean ± SEM, n=4, compared by unpaired T-test.

3.2.2.2 Levels of α-tubulin acetylation in sperm from C57 mice are unaffected by treatment with tubacin

To determine whether sperm from C57 mice exhibited any change in the acetylation of α-tubulin following exposure to tubacin, sperm were treated for 1 hour and lysed for Western blot. **Figure 3.15a** shows Western blot analysis of acetylated α-tubulin in sperm lysates from 4 independent experiments in which sperm were treated with either vehicle or 5 μM tubacin. Bands at approximately 55 kDa representing acetylated α-tubulin were subject to densitometric analysis (**Figure 3.15c**). The Western blot and densitometry showed that the abundance of acetylated α-tubulin in sperm from C57 mice was not affected by treatment with tubacin (**Figure 3.15a, c**). Reprobing the blot for total α-tubulin (**Figure 3.15b**) and subsequent densitometric analysis of bands corresponding to α-tubulin (**Figure 3.15d**) demonstrated that the abundance was comparable between conditions. These results showed that the levels of acetylated α-tubulin in sperm from C57 mice were insensitive to tubacin, suggesting that HDAC6 may not actively deacetylate α-tubulin in murine sperm.

The insensitivity of motility parameters and levels of acetylated α-tubulin to treatment with tubacin in the sperm of C57 mice matched the observations in sperm from BALB/c mice, indicating no difference in the response between different mouse strains. As a result, experiments from this point proceeded with the sperm from BALB/c mice. In addition, since the data demonstrated that sperm motility and α-tubulin acetylation were insensitive to an inhibitor of HDAC6, the role of another α-tubulin deacetylase, SIRT2, in sperm function was investigated.

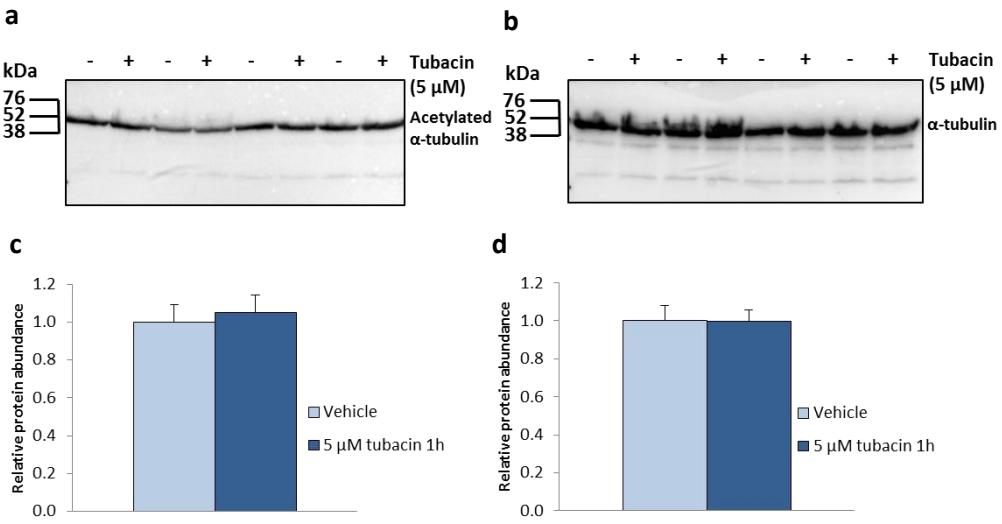

Figure 3.15: Acetylation of α-tubulin in sperm from C57 mice following treatment with tubacin for 1 hour following capacitation.

(a) Western blot of acetylated protein from the sperm of C57 mice treated with either vehicle or 5 µM tubacin for 1 hour in 4 independent experiments. Approximately 20 µg of protein was loaded in each lane. Bands at approximately 55 kDa correspond to acetylated α-tubulin. (b) All blots were reprobed for total α-tubulin as a loading control; bands at approximately 55 kDa correspond to α-tubulin. (c) Bar graph shows densitometric analysis of bands corresponding to acetylated α-tubulin (n=4). (d) Bar graph shows densitometric analysis of bands corresponding to total α-tubulin (n=4). Values are shown as mean ± SEM and were compared by an unpaired T-test.

3.2.3 Impact of nicotinamide treatment on murine sperm

Treatment of sperm with tubacin exerted no effect on motility parameters or acetylation of α-tubulin, suggesting that HDAC6 may not actively deacetylate in sperm. Therefore, the contribution of another deacetylase, SIRT2, on α-tubulin deacetylation and motility in sperm was examined using the Class III HDAC inhibitor, nicotinamide. Results from these experiments will be reported in the following sections.

3.2.3.1 Motility parameters of murine sperm are insensitive to nicotinamide treatment

Sperm were treated with 5 mM nicotinamide for 1 hour following capacitation, and motility parameters were subsequently assessed. Nicotinamide at 5 mM was selected as the drug had previously been shown to be active and non-toxic at this concentration (Bitterman *et al.*, 2002; D. Zhang *et al.*, 2014). Motility analysis demonstrated that upon treatment with nicotinamide, curvilinear, straight line, and average path velocities were comparable to control. Straightness, linearity, wobble, amplitude of lateral head displacement and beat cross frequency exhibited slight reductions following treatment, however this was not significant (**Figure 3.16**). In addition, the percentage of sperm exhibiting hyperactivated motility following exposure to nicotinamide was similar to that of vehicle-treated sperm, whilst the percentage of progressively motile sperm was slightly lower in the treated condition, although this was not significant (**Figure 3.17**). The results therefore demonstrated that treatment of sperm with 5 mM nicotinamide for 1 hour did not influence their motility.

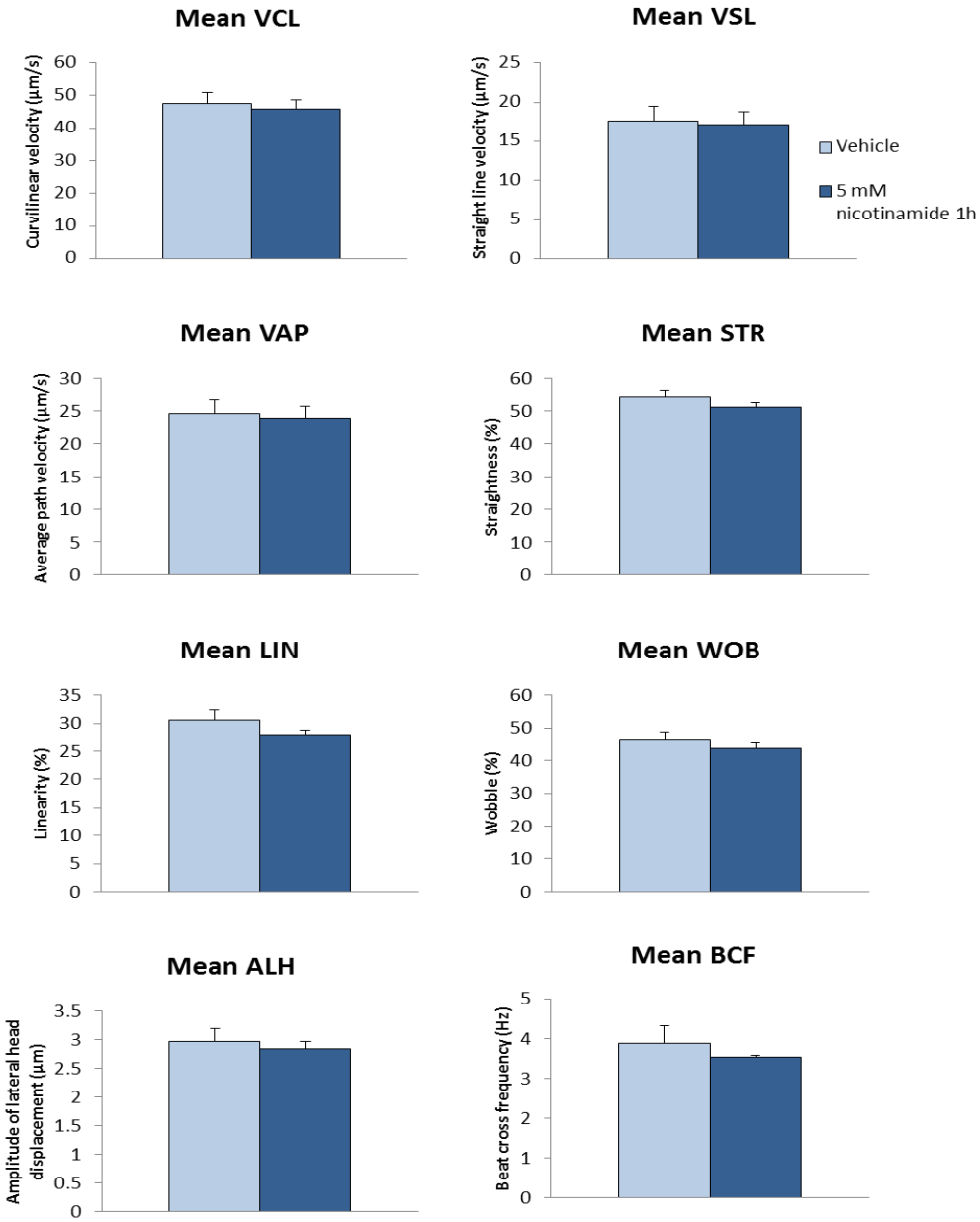

Figure 3.16: Motility parameters following treatment of sperm with nicotinamide for 1 hour following capacitation.

Epididymal sperm were treated with 5 mM nicotinamide for 1 hour and motility characteristics were assessed using computer-assisted sperm analysis. Nicotinamide-treated sperm did not exhibit any significant differences when compared to vehicle-treated sperm in all examined motility parameters: VCL – curvilinear velocity, VSL - straight line velocity, VAP - average path velocity, STR - straightness, LIN - linearity, WOB - wobble, ALH - amplitude of lateral head displacement and, BCF - beat cross frequency. Values are shown as mean ± SEM, n=3, and were compared by an unpaired T-test.

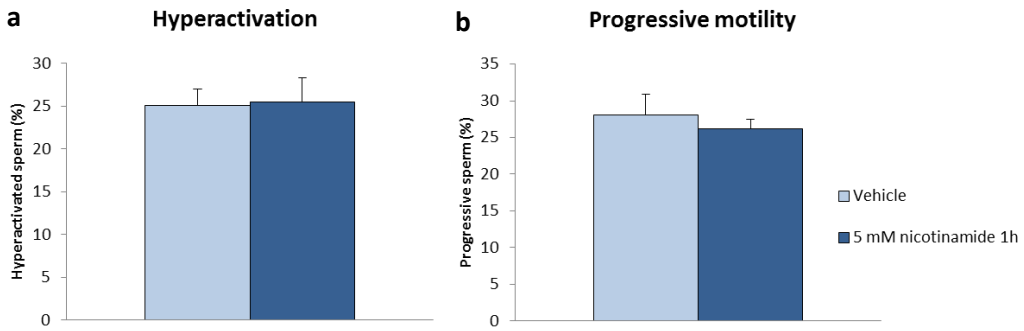

Figure 3.17: Hyperactivation and progressive motility in sperm following treatment with nicotinamide for 1 hour following capacitation.

Motility analysis of sperm treated with 5 mM nicotinamide for 1 hour following capacitation showed that the percentage of sperm exhibiting (a) hyperactivated motility was comparable to control and (b) progressive motility was slightly reduced. Hyperactivated sperm are shown as a percentage of the total motile sperm; progressive sperm are shown as a percentage of total sperm in the analysed sample. Values are shown as mean ± SEM, n=3, and were compared by an unpaired T-test.

Sperm were also treated with 5 mM nicotinamide for 3 hours during capacitation and motility parameters analysed. All parameters (curvilinear velocity, straight line velocity, average path velocity, straightness, linearity, wobble, amplitude of lateral head displacement and beat cross frequency) were slightly lower in the treated condition compared to vehicle-treated sperm (**Figure 3.18**). In addition, the percentage of sperm demonstrating hyperactivated motility was 3% lower in the nicotinamide-treated condition compared to the control condition (**Figure 3.19a**). Progressive motility following treatment was similar to control (**Figure 3.19b**). These findings are preliminary as the experiment was only repeated twice; however, nicotinamide appeared to exert only a minor effect on sperm motility after a 3 hour treatment.

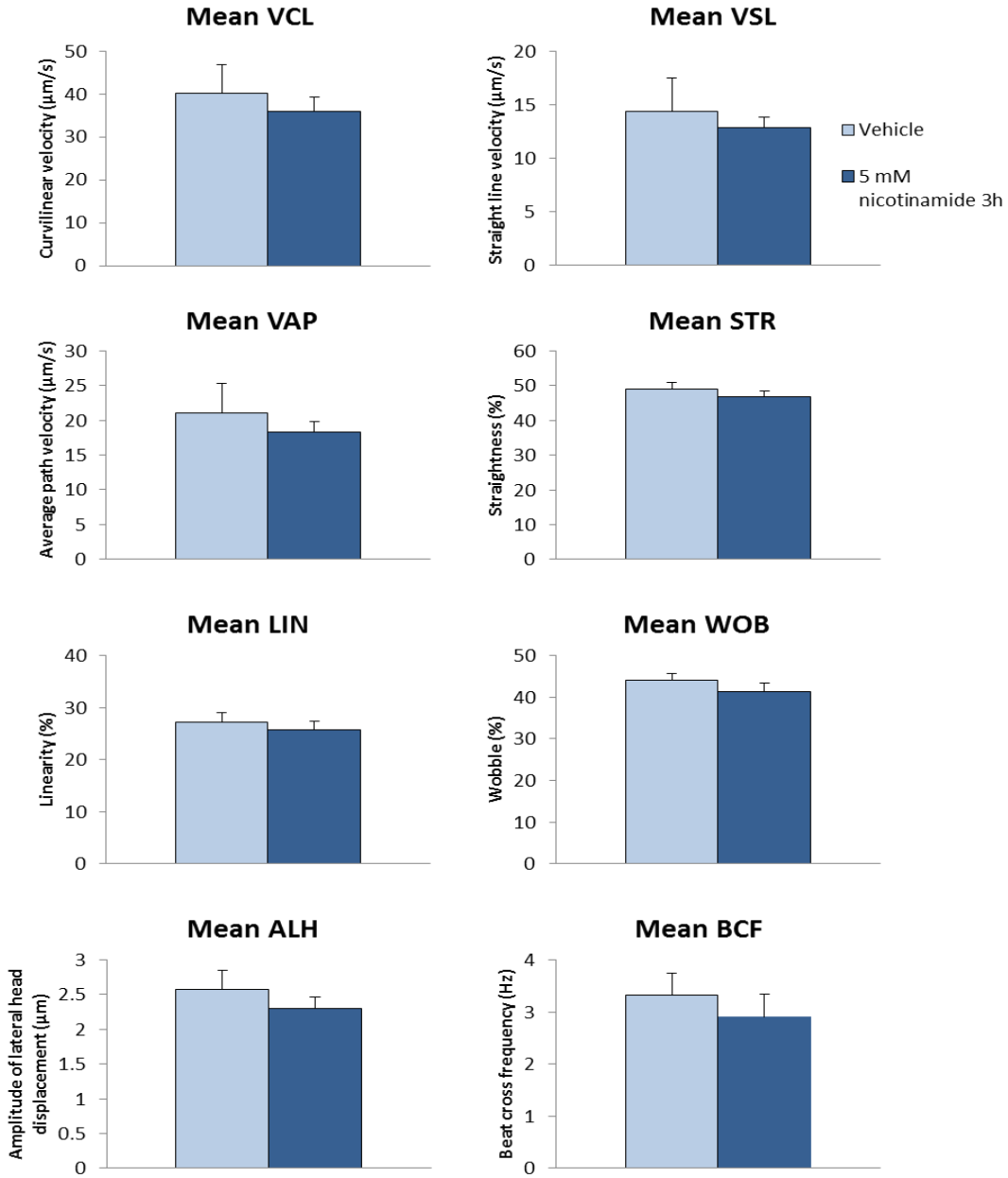

Figure 3.18: Motility parameters following treatment of sperm with nicotinamide for 3 hours during capacitation.

Sperm were treated with 5 mM nicotinamide for 3 hours during capacitation and motility characteristics were assessed using computer-assisted sperm analysis. Nicotinamide-treated sperm exhibited similar but slightly lower mean values compared to controls in all examined motility parameters: VCL – curvilinear velocity, VSL - straight line velocity, VAP - average path velocity, STR - straightness, LIN - linearity, WOB - wobble, ALH - amplitude of lateral head displacement and, BCF - beat cross frequency. Values are shown as mean ± SEM, n=2.

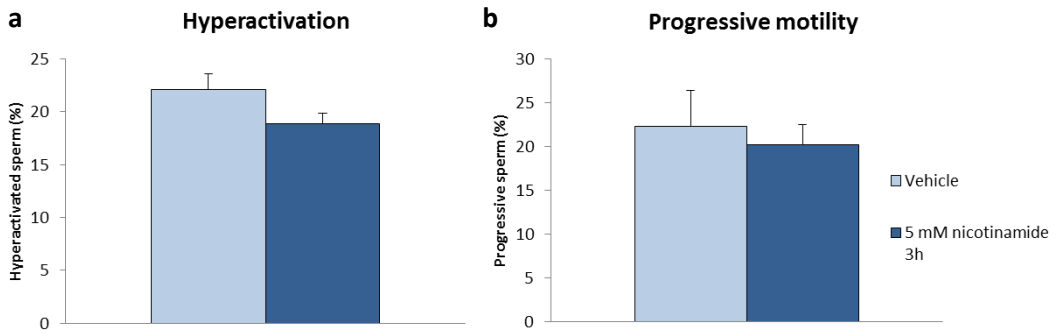

Figure 3.19: Hyperactivation and progressive motility in sperm following treatment with nicotinamide for 3 hours during capacitation.

Motility analysis of sperm treated with 5 mM nicotinamide for 3 hours during capacitation demonstrated the percentage of sperm exhibiting (a) hyperactivated and (b) progressive motility was slightly lower than controls. Hyperactivated sperm are shown as a percentage of the total motile sperm; progressive sperm are shown as a percentage of total sperm in the analysed sample. Values are shown as mean ± SEM, n=2.

3.2.3.2 Levels of α-tubulin acetylation in sperm are unaffected by nicotinamide treatment

To determine whether SIRT2 played a role in the deacetylation of α-tubulin, the effect of nicotinamide on the levels of α-tubulin acetylation was examined. Capacitated sperm treated with vehicle or 5 mM nicotinamide for 1 hour in 3 independent experiments were analysed by Western blot as shown in **Figure 3.20a**. Bands at approximately 55 kDa corresponding to acetylated α-tubulin were subject to densitometric analysis which demonstrated that the abundance of the acetylated protein was comparable between control and treated sperm (**Figure 3.20c**). Reprobing for total α-tubulin and subsequent analysis using densitometry showed a slight reduction in the abundance of α-tubulin in sperm treated with nicotinamide. However, this was only a 0.1-fold difference and was not significant (**Figure 3.20b, d**). These results therefore demonstrated that treatment with 5 mM nicotinamide for 1 hour did not affect the levels of α-tubulin acetylation in sperm.

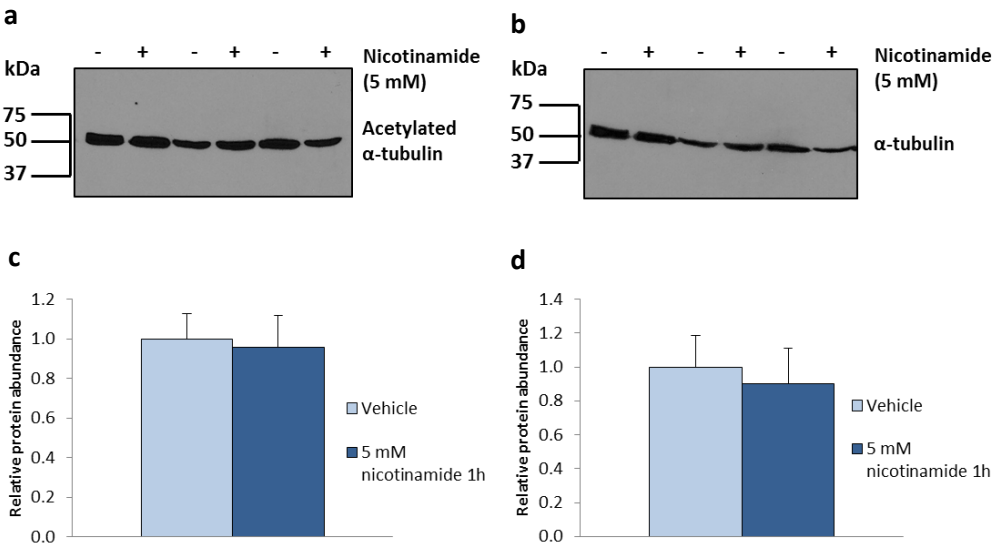

Figure 3.20: Acetylation of α-tubulin in sperm following treatment with nicotinamide for 1 hour following capacitation.

(a) Representative Western blot of acetylated protein from capacitated sperm treated with either vehicle or 5 mM nicotinamide for 1 hour. Protein from approximately 0.5 million sperm was loaded in each lane. Bands at approximately 55 kDa correspond to acetylated α-tubulin. (b) Blots were reprobed for total α-tubulin as a loading control; bands at approximately 55 kDa correspond to α-tubulin. (c) Bar graph shows densitometric analysis of bands corresponding to acetylated α-tubulin in sperm (n=3). (d) Bar graph shows densitometric analysis of bands corresponding to total α-tubulin in sperm (n=3). Values are shown as mean ± SEM and were compared by an unpaired T-test.

To determine whether exposure to nicotinamide during capacitation exerted any effect on levels of acetylated α-tubulin, sperm were treated with the inhibitor for 3 hours and lysed for Western blot analysis. Alongside this treatment, further sperm samples were exposed to 5 mM nicotinamide and 5 μM tubacin for 3 hours in combination to determine whether simultaneous treatment with inhibitors of HDAC6 and SIRT2 affected acetylated α-tubulin in sperm. As shown in **Figure 3.21**, neither the nicotinamide treatment alone, or nicotinamide and tubacin in combination caused any change to the levels of acetylated α-tubulin. Reprobing the blot demonstrated total α-tubulin levels remained equal in all conditions. These results therefore demonstrate that treatment with nicotinamide alone during capacitation did not influence the levels of α-tubulin acetylation in sperm. Furthermore, persistent acetylation of α-tubulin was exhibited following exposure to nicotinamide and tubacin in combination. The data therefore show no evidence for an active role for SIRT2 in the deacetylation of α-tubulin in sperm. However, as nicotinamide treatment did not show an effect, confirmation of the activity of this inhibitor was required using another cell line to ensure its functionality.

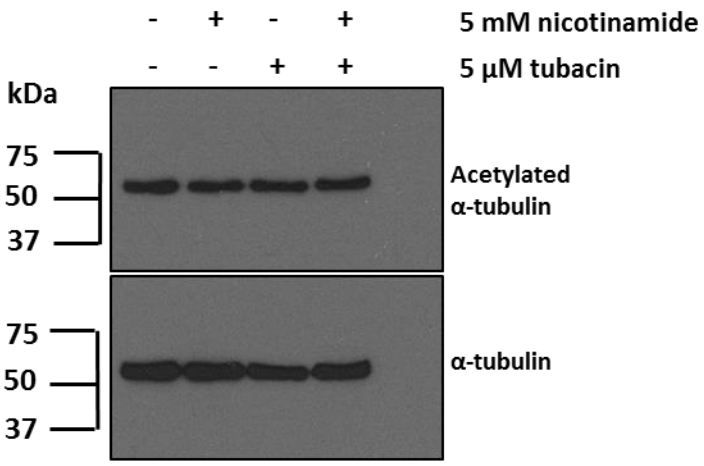

Figure 3.21: Acetylated α-tubulin in sperm following treatment with nicotinamide and tubacin for 3 hours during capacitation.

Western blot analysis of acetylated protein from sperm treated with vehicle, 5 mM nicotinamide, 5 µM tubacin, or nicotinamide and tubacin in combination to inhibit SIRT2 and HDAC6, respectively. No difference was observed in acetylation levels of α-tubulin in any condition. Reprobing the blot for total α-tubulin demonstrated equal levels in all conditions. Bands at approximately 55 kDa correspond to acetylated and total α-tubulin.

3.2.3.3 Levels of α-tubulin acetylation in HEK-MSR cells are unaffected by treatment with nicotinamide

As nicotinamide did not influence the abundance of acetylated α-tubulin in sperm, HEK-MSR cells were subjected to a nicotinamide time course to determine the response of this cell line to the inhibitor. **Figure 3.22a** shows a representative Western blot demonstrating the effects on acetylated α-tubulin during one nicotinamide time course. HEK-MSR cells treated with 5 μM tubacin for 1 hour were also loaded as a positive control. Bands corresponding to acetylated α-tubulin in 3 independent nicotinamide time courses were analysed using densitometry (**Figure 3.22c**). Cells treated with 5 mM nicotinamide for up to 3 hours did not exhibit any changes in the levels of acetylated α-tubulin (**Figure 3.22a, c**), whereas treatment of HEK-MSR cells with 5 μM tubacin for one hour caused an increase in acetylated α-tubulin abundance compared to control (**Figure 3.22a**). The Western blots were reprobed for total α-tubulin and subsequent densitometric analysis showed that the abundance of the loading control was comparable between conditions (**Figure 3.22b, d**). The data therefore demonstrated that treatment of HEK-MSR cells with 5 mM nicotinamide for up to 3 hours did not have any effect on the acetylation state of α-tubulin, suggesting SIRT2 may not play an active role in the deacetylation of α-tubulin in HEK cells.

Overall, analysis of the effects of nicotinamide indicated that this inhibitor did not have an effect on sperm motility or levels of acetylated α-tubulin in sperm, and so no evidence was found to support an active role for SIRT2 in the deacetylation of α-tubulin in sperm. However, it was not possible to control fully for the effects of nicotinamide using the HEK-MSR cell line. Whilst the data should be interpreted with this consideration, the results are consistent with the findings of HDAC inhibition previously described.

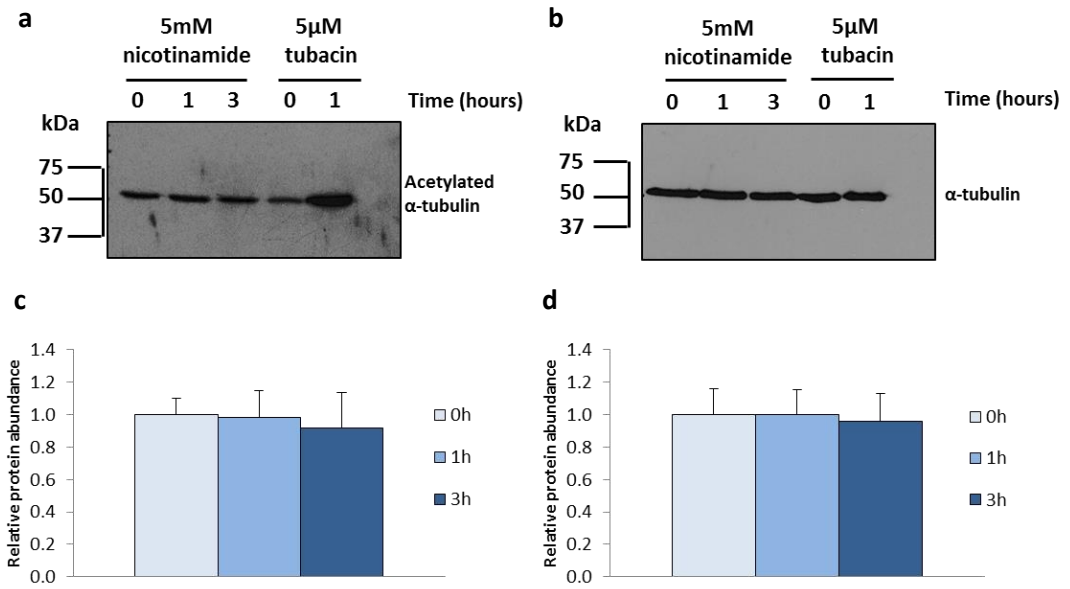

Figure 3.22: Acetylation of α-tubulin in HEK-MSR cells during nicotinamide time courses.

(a) Representative Western blot of acetylated protein from HEK-MSR cells treated with 5 mM nicotinamide for up to 3 hours. Protein from HEK cells treated with vehicle or 5 µM tubacin for 1 hour were loaded as a positive control to demonstrate the effect of α-tubulin deacetylase inhibition. Approximately 20 µg of protein was loaded in each lane. Bands at approximately 55 kDa correspond to acetylated α-tubulin. (b) All blots were reprobed for total α-tubulin as a loading control; bands at approximately 55 kDa correspond to α-tubulin. (c) Bar graph shows densitometric analysis of bands corresponding to acetylated α-tubulin following repeated nicotinamide time course blots (n=3). (d) Bar graph shows densitometric analysis of bands corresponding to total α-tubulin following repeated nicotinamide time course blots (n=3). Values are shown as mean ± SEM and were compared by an unpaired T-test.

3.3 Discussion

The α-tubulin deacetylase, HDAC6, is expressed in the testes of mice (Zhang *et al.*, 2008) and rats (Parab *et al.*, 2015; Verma *et al.*, 2017), with localisation of the deacetylase showing an overlap with acetylated α-tubulin in the rat sperm flagellum (Parab *et al.*, 2015). Therefore, one of the aims of the investigations reported in this chapter was to elucidate whether HDAC6 actively deacetylates α-tubulin in sperm. Furthermore, since the acetylation state of α-tubulin has been linked to sperm motility (Gentleman *et al.*, 1996; Nereo Kalebic *et al.*, 2013; Bhagwat *et al.*, 2014; Parab *et al.*, 2015), the central aim of the work detailed in this chapter was to determine whether HDAC6 played a role in the regulation of sperm motility.

3.3.1 The effects of tubacin on sperm motility and α-tubulin acetylation

To examine whether HDAC6 was involved in sperm motility modulation and α-tubulin deacetylation, sperm were exposed to the HDAC6-specific inhibitor, tubacin (Haggarty *et al.*, 2003). Tubacin is able to inhibit HDAC6 specifically due to variations in the structural characteristics of the ligand-binding site between members of the HDAC family. The ligand-binding channel of HDAC6 is narrower compared to that of other HDACs, meaning that tubacin can form interactions with the protein surfaces of both sides of the channel simultaneously to exert its effects, whereas this is not possible in other Class I and II HDACs (Estiu *et al.*, 2008). Analysis of sperm motility parameters demonstrated that treatment with tubacin did not influence any aspect of sperm motility, nor was progressive motility affected by the inhibitor. This finding was observed in both the sperm from BALB/c (**Figures 3.2-3.5**) and C57 (**Figures 3.13 and 3.14**) mice, indicating that the data is robust across mouse strains. Furthermore, normal motility in the presence of tubacin was found when treatment was carried out both during (**Figures 3.4 and 3.5**) and following (**Figures 3.2 and 3.3**) the period in which sperm undergo capacitation. Whilst increased tyrosine phosphorylation is the best characterised PTM reported to occur during sperm capacitation (Lishko *et al.*, 2012), there is evidence to suggest that lysine acetylation may be important during capacitation with certain sperm proteins such

as members of the AKAP family gaining acetylation during this period (Sun *et al.*, 2014; Yu *et al.*, 2015). Moreover, the concurrent development of hyperactivated motility alongside capacitation means that alterations to motility patterns take place during this period. Hyperactivation is characterised by an increase in the amplitude of the tail bend resulting in whip-like motions of the tail, and vigorous side-to-side movements of the head. This pattern of motility is a requirement for sperm penetration of the viscous mucus in the female reproductive tract and the ZP of the oocyte (Ho and Suarez, 2001). Sperm hyperactivation was normal in both BALB/c (**Figures 3.3a and 3.5a**) and C57 (**Figure 3.14a**) mice when treated with tubacin, suggesting that the inhibitor did not affect the development of this hyperactivated pattern of motility. In subsequent investigations designed to replicate the viscoelastic conditions of the female reproductive tract more closely, sperm treated with tubacin had a similar ability to control sperm to enter and penetrate the artificial viscous media (**Figures 3.6b and 3.7**). As murine sperm navigate viscoelastic substances more effectively when hyperactivated (Suarez and Dai, 1992), this result further indicates that treatment with tubacin did not affect sperm hyperactivation. The results of the motility investigations, when taken together, indicate that tubacin did not impart any effects on sperm swimming behaviour and therefore do not provide any evidence for a role for HDAC6 in the modification of any examined aspect of sperm motility.

As sperm motility appeared insensitive to treatment with a HDAC6 inhibitor, the deacetylation of α-tubulin by HDAC6 was investigated in sperm using Western blot analysis. However, the first observation of note following analysis of sperm lysates was that the sperm exhibited high baseline levels of α-tubulin acetylation in the absence of any HDAC inhibitor. This finding was subsequently supported by the analysis of sperm lysates alongside lysates from the control HEK-MSR cell line; stronger bands corresponding to acetylated α-tubulin were obtained for control sperm compared to control HEK cells when the same amount of protein was loaded for each condition (**Figure 3.11a**). This demonstrated that sperm treated only with vehicle exhibited much higher levels of acetylated α-tubulin than vehicle-treated HEK cells, indicating

high basal levels of α-tubulin acetylation in sperm. This finding was also replicated in murine spermatids which exhibited a high abundance of acetylated α-tubulin in control cells compared to HEK cells (**Figure 3.11**). Regarding the effects of tubacin exposure, the abundance of acetylated α-tubulin detected by Western blot was unchanged in the sperm of BALB/c (**Figure 3.8 and 3.9**) and C57 (**Figure 3.15**) mice following 1 and 3 hour treatments, therefore suggesting that sperm α-tubulin may be insensitive to the effects of the HDAC6 inhibitor. This finding is supported by a similar lack of response to tubacin treatment found in the spermatids of BALB/c mice following exposure for 1 and 3 hours (**Figures 3.11 and 3.12**). No change in the abundance of acetylated α-tubulin was exhibited upon Western blot analysis, suggesting that HDAC6 in both developing and mature spermatozoa may not actively deacetylate α-tubulin.

In order to confirm that the tubacin concentration and treatment times utilised were sufficient to inhibit HDAC6 activity and elicit a detectable response, the inhibitor was used on the HEK-MSR cell line, with a concentration and incubation period equivalent to that used for sperm. **Figure 3.23** summarises the effects of tubacin on acetylated α-tubulin in sperm and HEK-MSR cells. Upon Western blot analysis of the HEK cell lysates, a significant 12- and 21-fold increase in the abundance of acetylated α-tubulin was found after treatment for 1 and 3 hours, respectively (**Figure 3.10**). The substantial increase in acetylated α-tubulin exhibited by HEK cells following tubacin exposure suggested that HDAC6 was active in these cells and was responsible for a considerable degree of α-tubulin deacetylation. Furthermore, the data also showed that the tubacin concentration and treatment period investigated in sperm was sufficient to stimulate a demonstrable response in another cell line, confirming the activity of the inhibitor. This finding therefore indicated that sperm may be insensitive to treatment with tubacin. This suggested that either HDAC6 exhibits low activity in sperm and α-tubulin is maximally acetylated, or the activity of HDAC6 can be rescued by another deacetylase. Given the high baseline levels of acetylated α-tubulin in sperm, it is possible that deacetylation of α-tubulin does not take place to a great extent, and therefore inhibition of HDAC6 may not have stimulated a detectable change in α-tubulin acetylation. Alternatively, the absence of an effect

on the levels of acetylated α-tubulin and motility in sperm following tubacin treatment may result from the activity of other deacetylases substituting for that of HDAC6. Another member of the HDAC family, SIRT2, has been demonstrated to display deacetylase activity towards α-tubulin (North *et al.*, 2003). Therefore, the subsequent set of investigations sought to determine whether SIRT2 played any role in the deacetylation of α-tubulin in sperm and in sperm motility.

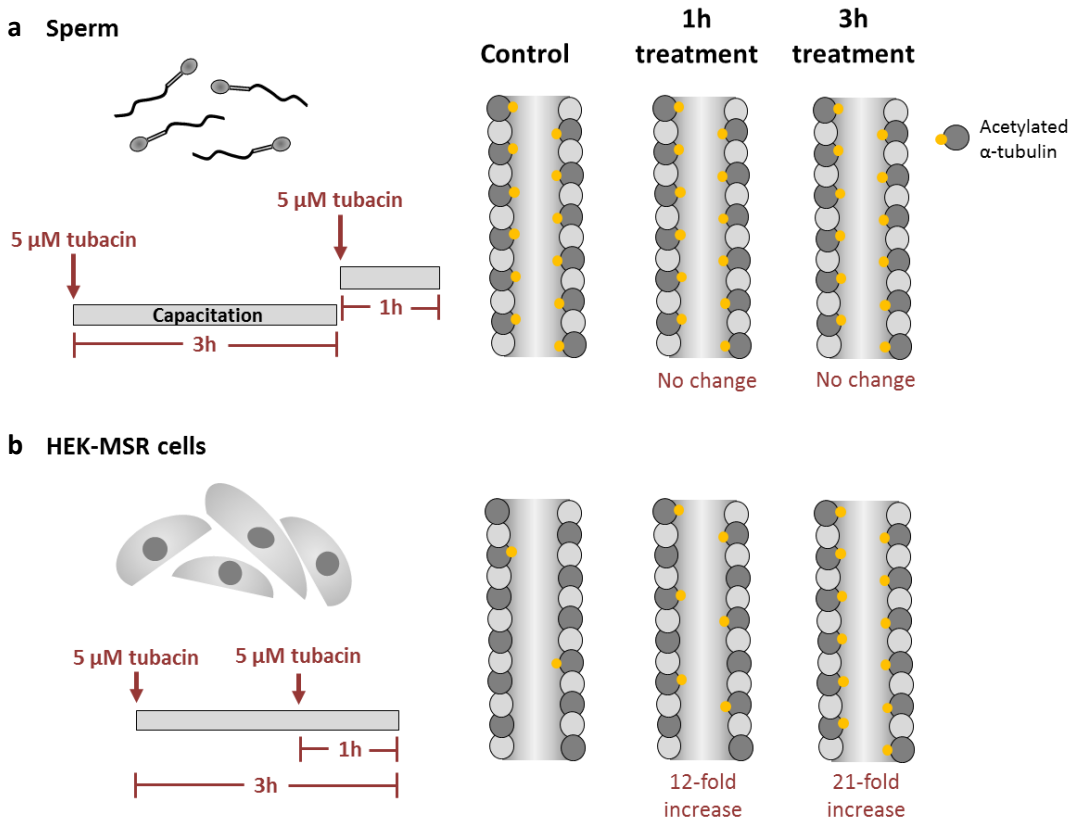

Figure 3.23: Summary schematic of the effects of tubacin on acetylated α-tubulin in sperm and HEK-MSR cells.

(a) Exposure of murine sperm to 5 µM tubacin for 3 hours during capacitation, or 1 hour following capacitation did not change the abundance of acetylated α-tubulin detected by Western blot. Sperm were also found to exhibit high baseline levels of acetylated α-tubulin. (b) HEK-MSR cells subjected to 5 µM tubacin time courses exhibited a 12- and 21-fold increase in the abundance of acetylated α-tubulin after 1 hour and 3 hour treatments, respectively. Baseline levels of acetylated α-tubulin in HEK-MSR cells appeared lower than in sperm.

3.3.2 The effects of nicotinamide on sperm motility and α-tubulin acetylation

To determine whether the cytoplasmic α-tubulin deacetylase, SIRT2 contributed any function in sperm motility and α-tubulin deacetylation, sperm were treated with the Class III HDAC inhibitor, nicotinamide (Avalos, Bever and Wolberger, 2005). Analysis of sperm motility parameters following treatment with nicotinamide for 1 and 3 hours revealed that sperm progression and all motility characteristics measured were similar to those of control sperm (**Figures 3.16-3.19**). Hyperactivation was comparable to control following 1 hour inhibition (**Figure 3.17b**), however, after the 3 hour treatment, the percentage of sperm displaying hyperactivated motility showed a 3% decrease (**Figure 3.19b**) (although this small reduction requires further verification before statistically robust conclusions can be drawn). Nevertheless, the lack of notable effect of SIRT2 inhibition on motility mirrors the observations of HDAC6 inhibition. Therefore, these results appear to indicate that inhibition of Class III HDACs using the inhibitor concentrations and incubation periods detailed does not affect sperm motility.

Research investigating the role of SIRT2 in sperm motility is lacking. The only study published to date that demonstrates the effects of nicotinamide on sperm motility comes from Sun *et al.* who used nicotinamide in combination with the Class I and II HDAC inhibitor, TSA, and assessed the effects on human sperm motility. They found a reduction in the percentage of motile sperm upon treatment, but only following a 6 hour incubation period using high concentrations of TSA and nicotinamide: 50 µM and 50 mM; and 70 µM and 70 mM, respectively (Sun *et al.*, 2014). However, the group did not expose sperm to the inhibitors individually which makes it difficult to distinguish between the effects of the Class I and II, and Class III HDAC inhibitors. Furthermore, considering the high concentrations of inhibitors being examined and the incubation time used, an evaluation of sperm viability may have been useful to determine whether a degree of the reduction in sperm motility could have resulted from cell death. Future research may therefore look to examine the role of SIRT2 in sperm motility

further, potentially using additional inhibitor studies and animal knockout models to clarify whether the deacetylase is required for normal sperm motility.

To determine whether treatment with nicotinamide exerted any effect on the levels of α-tubulin acetylation in sperm, Western blot analysis was used. After both 1 hour and 3 hour treatments, no effect on the abundance of acetylated α-tubulin was found (**Figures 3.20 and 3.21**). In addition, concurrent inhibition of HDAC6 and SIRT2 using tubacin and nicotinamide in combination did not reveal any changes in the acetylation of α-tubulin (**Figure 3.21**). This result indicated that SIRT2 and HDAC6 may not substitute for one another in deacetylase activity in sperm microtubules, despite being shown to interact on microtubule networks (North *et al.*, 2003). Overall, the results suggest that SIRT2 is not actively involved in the deacetylation of α-tubulin in the sperm flagellum. This finding is supported by work from Suzuki and Koike who tested the effect of nicotinamide treatment on cerebellar granule cells from mice. Whilst they found that treatment with 10 mM nicotinamide for 48 hours increased levels of acetylated α-tubulin in soluble fractions of protein, they did not see the same effect in the cytoskeletal fraction. In fact, treatments up to 20 mM nicotinamide for 72 hours did not produce any effects on the levels of acetylated α-tubulin in the cytoskeletal fractions of protein, suggesting that inhibition of the endogenous activity of SIRT2 was insufficient to enhance microtubule acetylation (Suzuki and Koike, 2007). The maintenance of the level of acetylated α-tubulin in the cytoskeletal fraction of granule cells following nicotinamide treatment provides support for the findings detailed in this chapter, as α-tubulin is a major part of the sperm cytoskeleton. However, the disparity in treatment periods between the studies must be taken into account; although the short-lived nature of sperm means that such long incubation times would not be possible with viable sperm. Nevertheless, the results described in this thesis demonstrate that SIRT2 inhibition did not affect levels of α-tubulin acetylation in sperm at the concentration and incubation periods used.

As treatment with a SIRT2 inhibitor demonstrated a lack of effect in sperm, the control HEK-MSR cell line was used to determine whether the nicotinamide used in this study was able to induce a detectable change in α-tubulin acetylation. **Figure 3.24** summarises the effects of exposure to nicotinamide in sperm and HEK-MSR cells. Treatment of HEK cells with nicotinamide at the same concentration and for the same time period also demonstrated a lack of effect on the abundance of acetylated α-tubulin (**Figure 3.22**). Using the same cell type, North and colleagues found that siRNA-mediated knockdown of SIRT2 in 293T cells produced an increase in the level of acetylated α-tubulin compared to controls (North *et al.*, 2003). Their study therefore suggested that loss of SIRT2 enhanced microtubule acetylation in HEK cells. However, knockdown of SIRT2 in cerebellar granule cells also resulted in an increase in acetylation of α-tubulin, even in the cytoskeletal fraction of protein, which differs from the lack of effect found on SIRT2 inhibition (Suzuki and Koike, 2007), suggesting that knockdown and inhibition may result in different outcomes for acetylation levels. Therefore, whether the concentration of nicotinamide and incubation period was insufficient to inhibit SIRT2, or whether the mechanism of α-tubulin deacetylation in HEK cells does not involve SIRT2 requires further clarification.

Overall, the results in this chapter suggest that SIRT2 is not involved in sperm motility, and does not actively deacetylate the highly acetylated α-tubulin in sperm. However, an independent positive control would be desirable to confirm that the nicotinamide used in this study was able to inhibit SIRT2 in other cell types, in order to strengthen the conclusions of the data. For this reason, nicotinamide was not used in subsequent investigations of HDAC function in this thesis.

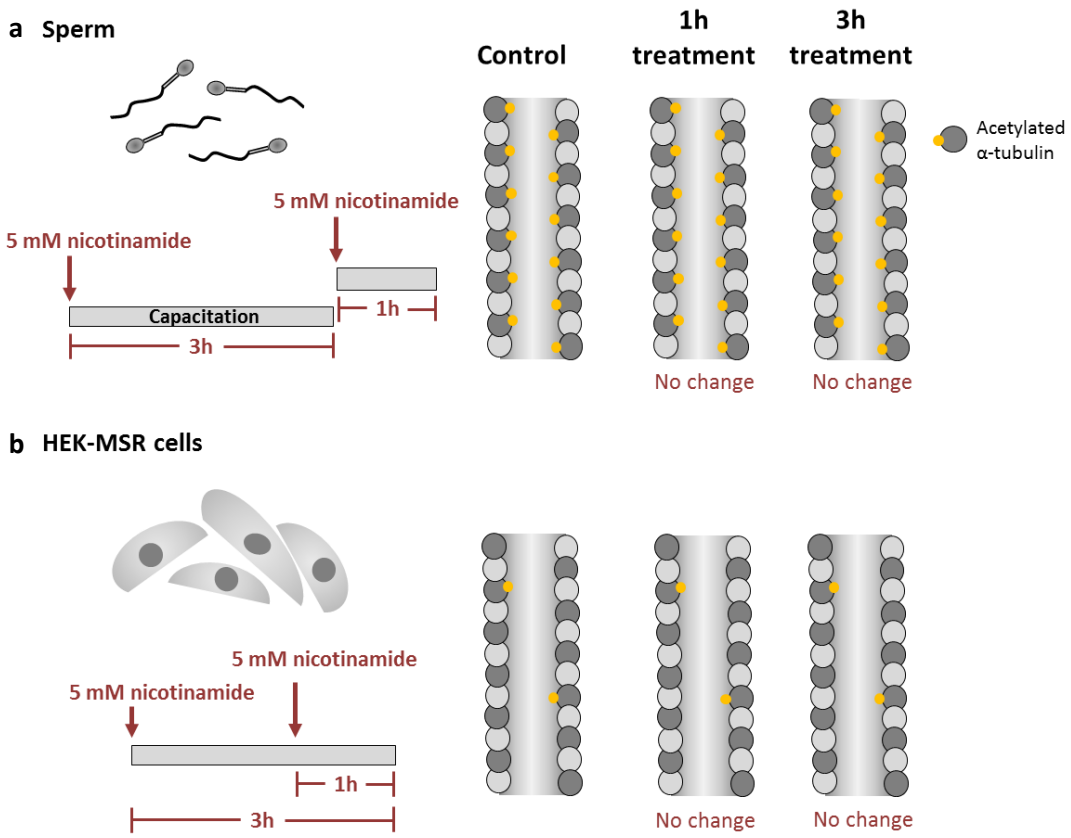

Figure 3.24: Summary schematic of the effects of nicotinamide on acetylated α-tubulin in sperm and HEK-MSR cells.

(a) Exposure of murine sperm to 5 mM nicotinamide for 3 hours during capacitation, or 1 hour following capacitation did not change the abundance of acetylated α-tubulin detected by Western blot. Sperm also exhibited high baseline levels of acetylated α-tubulin. (b) HEK-MSR cells subjected to 5 mM nicotinamide time courses also did not show any alterations to the abundance of acetylated α-tubulin after 1 hour and 3 hour treatments, with levels appearing generally lower than that of sperm.

3.3.3 Conclusions

The results reported in this chapter demonstrated that baseline levels of α-tubulin acetylation are high in murine sperm compared to HEK-MSR cells, and that HDAC6 is unlikely to actively deacetylate α-tubulin in sperm. Furthermore, HDAC6 may not be involved in the regulation of sperm motility. Similarly, SIRT2 does not appear to deacetylate α-tubulin in sperm or influence sperm motility. It is therefore suggested that deacetylation of α-tubulin in sperm may not be a mechanism by which sperm motility is modulated. Therefore, it was postulated that either another enzyme is responsible for α-tubulin deacetylation in sperm, or that HDAC6 activity is low and sperm microtubules are maintained in a highly acetylated state. To enable further conclusions to be drawn regarding the role of α-tubulin acetylation/deacetylation in sperm motility, further investigations into the activity of HDAC6 in sperm were carried out and will be detailed in the following chapter.

Chapter 4

Chapter 4 – The activity of Class I and II HDACs in sperm

4.1 Introduction

The preceding chapter detailed the results of experiments investigating the effect of inhibitors of HDAC6 and SIRT2 on the acetylation levels of the microtubule protein, α-tubulin, and motility in sperm. As described in Chapter 1 (section 1.6.3), HDAC6 is part of the Class IIb family of HDACs, along with HDAC10. While all members of the Class I and II HDAC families share the conserved deacetylase core (Finnin *et al.*, 1999), HDAC6 and HDAC10 both possess two of these deacetylase domains each (Xu, Parmigiani and Marks, 2007). The sequence homology between the deacetylase sites mean that general inhibitors of all the HDACs comprising Class I and Class II exist, such as TSA, which target this active site and interact with residues that are conserved across the HDAC family (Finnin *et al.*, 1999). Class I HDACs (HDAC1, 2, 3 and 8) are primarily localised to the nucleus and exhibit high enzymatic activity towards histones (Haberland, Montgomery and Olson, 2009). Class IIa HDACs (HDAC4, 5, 7) on the other hand can shuttle between the nucleus and cytoplasm, interacting with transcription factors and chaperone proteins to provide a link between extracellular signals and transcription (Xu, Parmigiani and Marks, 2007; Haberland, Montgomery and Olson, 2009). HDAC6 and HDAC10, making up Class IIb, are mainly cytoplasmic proteins, though both may have roles in the nucleus (Kao *et al.*, 2002; M. Zhang *et al.*, 2014). Whilst the function of HDAC6 in the deacetylation of cytoplasmic proteins including HSP90 and cortactin, alongside α-tubulin, is well-established (Valenzuela-Fernández *et al.*, 2008), very little is known about the role of HDAC10.

The findings from the previous chapter demonstrated the high baseline levels of acetylated α-tubulin in sperm, and the absence of any alteration to these acetylation levels following

treatment with the HDAC6-specific inhibitor, tubacin, and the Class III HDAC inhibitor, nicotinamide. In addition, these inhibitors were not found to exert any influence on sperm motility parameters. Normal motility and unchanged levels of α-tubulin acetylation despite treatment with inhibitors that target HDAC6 and SIRT2 indicate that tubacin and nicotinamide do not demonstrably affect α-tubulin deacetylation in sperm. The results therefore raised the possibility that deacetylase activity targeting α-tubulin may be low in sperm, particularly given the high baseline levels of α-tubulin acetylation. This therefore represented a hypothesis requiring further exploration.

4.1.1 Aims

As previous findings revealed that baseline levels of acetylated α-tubulin in sperm were high, and were insensitive to tubacin and nicotinamide treatment, the main aim of the research discussed in this chapter was to investigate whether deacetylases were active in sperm. As treatment with inhibitors of HDAC6 and Class III HDACs did not result in any changes to α-tubulin acetylation or motility in sperm, the effects of an additional inhibitor, the general Class I and II HDAC inhibitor, TSA, were also examined.

4.2 Results

4.2.1 Impact of TSA treatment on murine sperm

To explore the role of HDAC6 in sperm further, murine sperm were treated with the HDAC Class I and II inhibitor, TSA, and the effects on sperm motility and deacetylation of α-tubulin were examined. The results of these experiments will be reported in the following section.

4.2.1.1 Treatment with TSA exerts minor effects on sperm motility

Sperm were treated with TSA for either 1 hour following capacitation or 3 hours during capacitation and assessment of motility parameters was carried out using CASA. **Figure 4.1** shows the mean motility parameters from 9 independent experiments in which capacitated sperm were treated with 1 μM TSA for 1 hour. Curvilinear velocity, straight line velocity, and average path velocity exhibited increases of approximately 25%, 20%, and 20%, respectively. Slight increases in straightness, linearity and wobble were found following inhibition, whilst amplitude of lateral head displacement and beat cross frequency both exhibited a 20% increase upon exposure to TSA. However, these effects were not found to be significant when compared by an unpaired T-test. The percentage of sperm exhibiting hyperactivated motility (**Figure 4.2a**) and progressive motility (**Figure 4.2b**) increased upon treatment with TSA but the change was not significant.

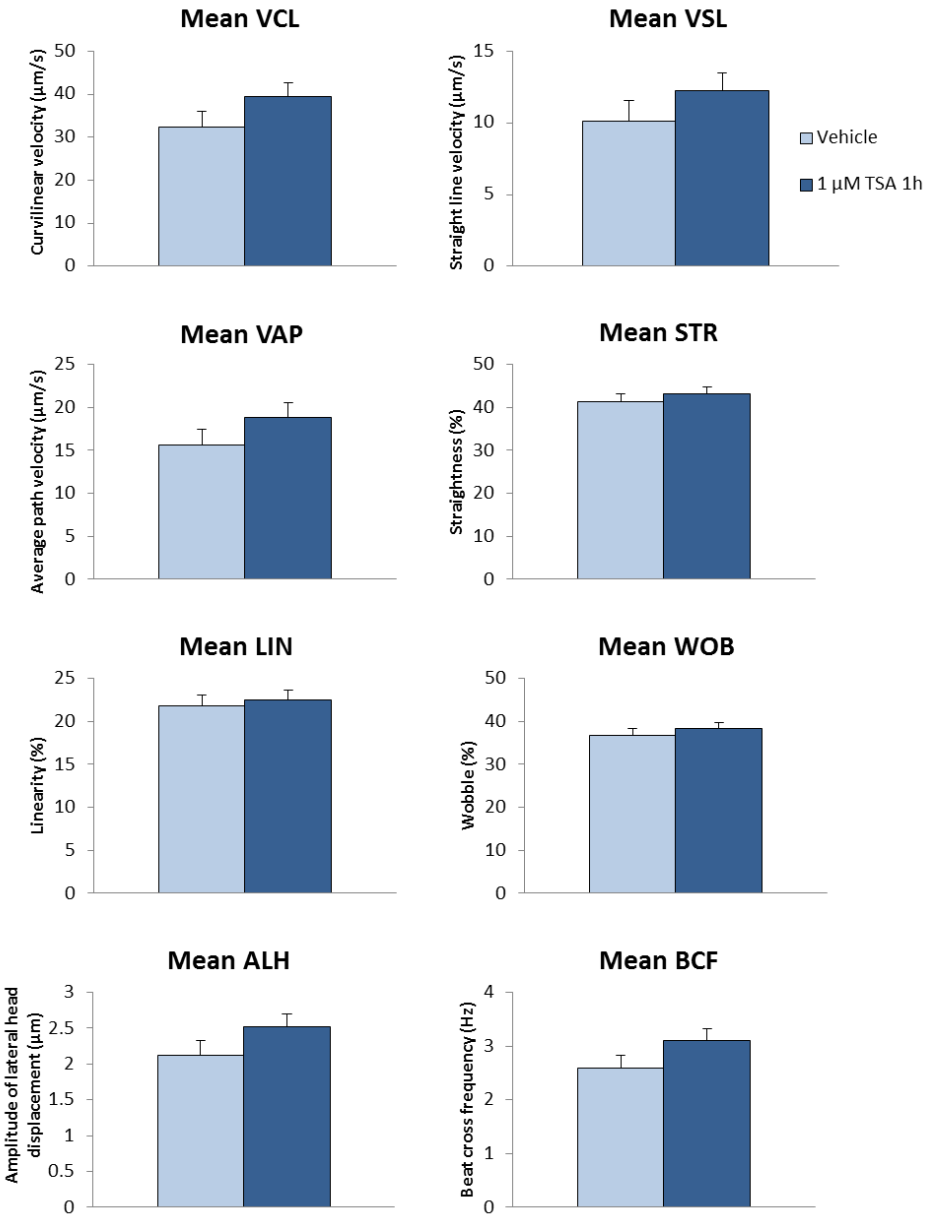

Figure 4.1: Motility parameters following treatment of sperm with 1 µM TSA for 1 hour following capacitation.

Epididymal sperm were treated with vehicle or 1 µM TSA for 1 hour and motility characteristics were assessed using computer-assisted sperm analysis. Sperm treated with TSA exhibited a small increase in all motility parameters examined: VCL – curvilinear velocity, VSL - straight line velocity, VAP - average path velocity, STR - straightness, LIN - linearity, WOB - wobble, ALH - amplitude of lateral head displacement and, BCF - beat cross frequency. Values are mean ± SEM, n=9, and were compared by an unpaired T-test.

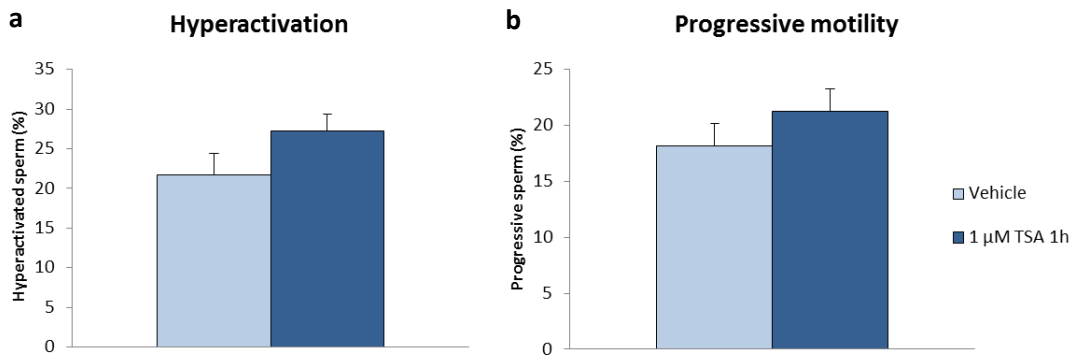

Figure 4.2: Hyperactivation and progressive motility in sperm following treatment with 1 µM TSA for 1 hour following capacitation.

Analysis of sperm motility following treatment with vehicle and 1 µM TSA for 1 hour showed the percentage of sperm exhibiting (a) hyperactivated and (b) progressive motility was higher in the sperm treated with TSA. Hyperactivated sperm are shown as a percentage of the total motile sperm; progressive sperm are shown as a percentage of total sperm in the analysed sample. Values shown are mean ± SEM, n=9, and were compared by an unpaired T-test.

As treatment with 1 µM TSA led to a small increase in sperm motility parameters, the effect of a higher concentration of TSA on motility characteristics was assessed. **Figure 4.3** shows the results of 5 independent experiments in which capacitated sperm were exposed to 10 µM TSA for 1 hour. All motility parameters were slightly increased following the treatment with 10 µM TSA, however these differences were very small and did not reach statistical significance. The percentage of sperm exhibiting hyperactivated motility was 4% higher in TSA-treated sperm compared to control (**Figure 4.4a**), whilst the percentage of sperm exhibiting progressive motility was only 1% higher following treatment (**Figure 4.4b**).

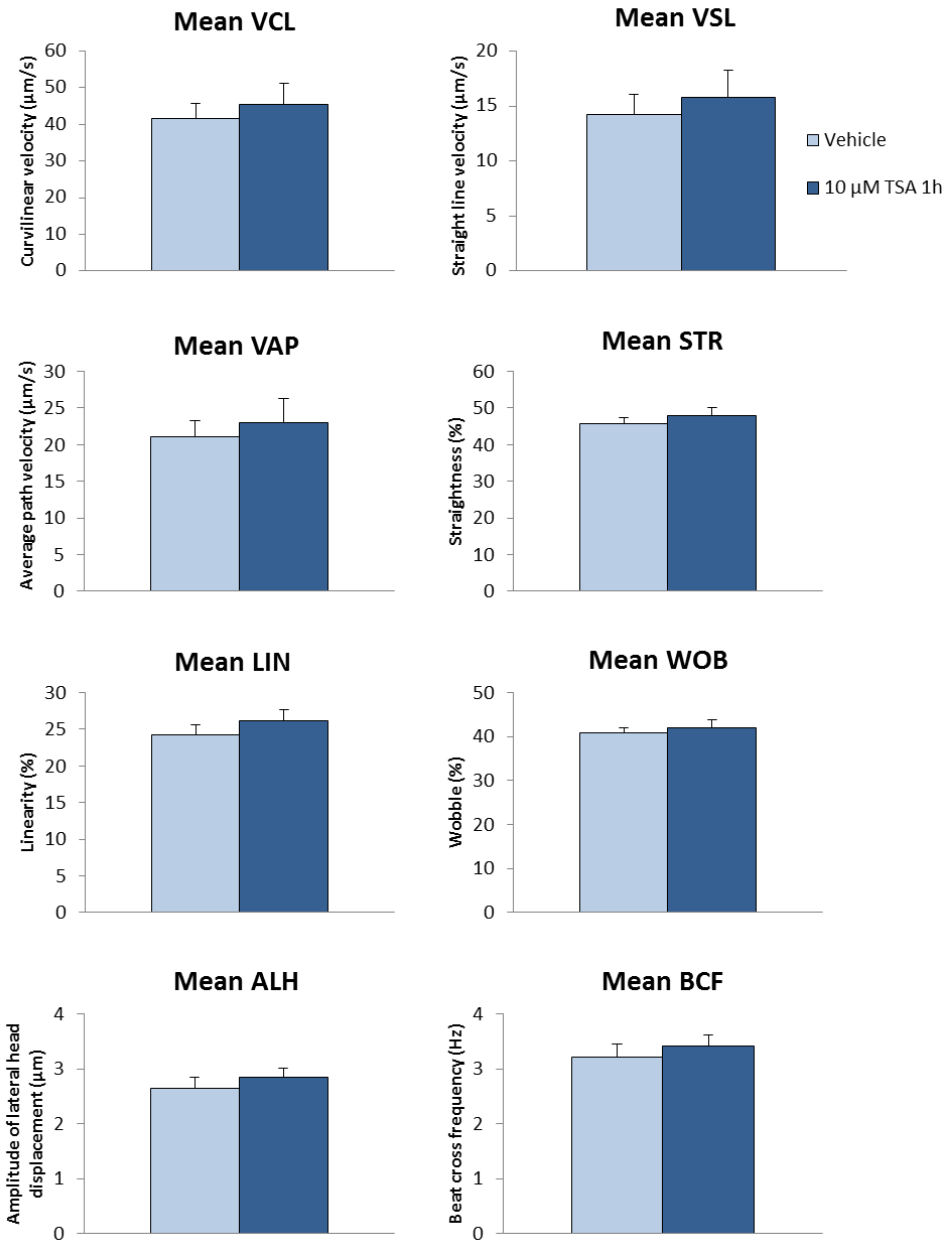

Figure 4.3: Motility parameters following treatment of sperm with 10 µM TSA for 1 hour following capacitation.

Epididymal sperm were treated with vehicle or 10 µM TSA for 1 hour, and motility characteristics were assessed using computer-assisted sperm analysis. Sperm treated with TSA exhibited slight increases in all motility parameters examined: VCL – curvilinear velocity, VSL - straight line velocity, VAP - average path velocity, STR - straightness, LIN - linearity, WOB - wobble, ALH - amplitude of lateral head displacement and, BCF - beat cross frequency. Values are mean ± SEM, n=5, and were compared by an unpaired T-test.

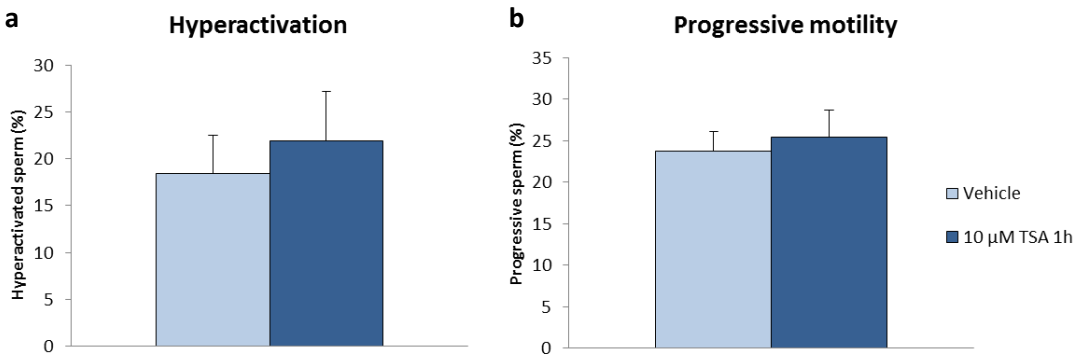

Figure 4.4: Hyperactivation and progressive motility in sperm following treatment with 10 µM TSA for 1 hour following capacitation.

Analysis of capacitated sperm motility following treatment with vehicle or 10 µM TSA for 1 hour showed the percentage of sperm exhibiting (a) hyperactivated and (b) progressive motility was slightly higher in the sperm treated with TSA. Hyperactivated sperm are shown as a percentage of the total motile sperm; progressive sperm are shown as a percentage of total sperm in the analysed sample. Values shown are mean ± SEM, n=5, and were compared by an unpaired T-test.

The previous experiments on capacitated sperm demonstrated that TSA had a minor effect on sperm motility, and so the effect of treatment for 3 hours during the sperm capacitation period was examined. **Figure 4.5** shows the mean motility parameters from 4 independent experiments in which sperm were treated with 1 μM TSA for 3 hours. All measured motility parameters (curvilinear velocity, straight line velocity, average path velocity, straightness, linearity, wobble, amplitude of lateral head displacement and beat cross frequency) were comparable to those of vehicle-treated sperm. Average path velocity exhibited the greatest change following treatment, with a small increase of 5% in sperm exposed to TSA, which was not statistically significant. Analysis of hyperactivated and progressive motility also demonstrated that sperm treated with TSA for 3 hours were comparable to vehicle-treated sperm in these motility patterns (**Figure 4.6**). The findings therefore demonstrated that treatment of sperm with TSA during capacitation did not influence their motility parameters.

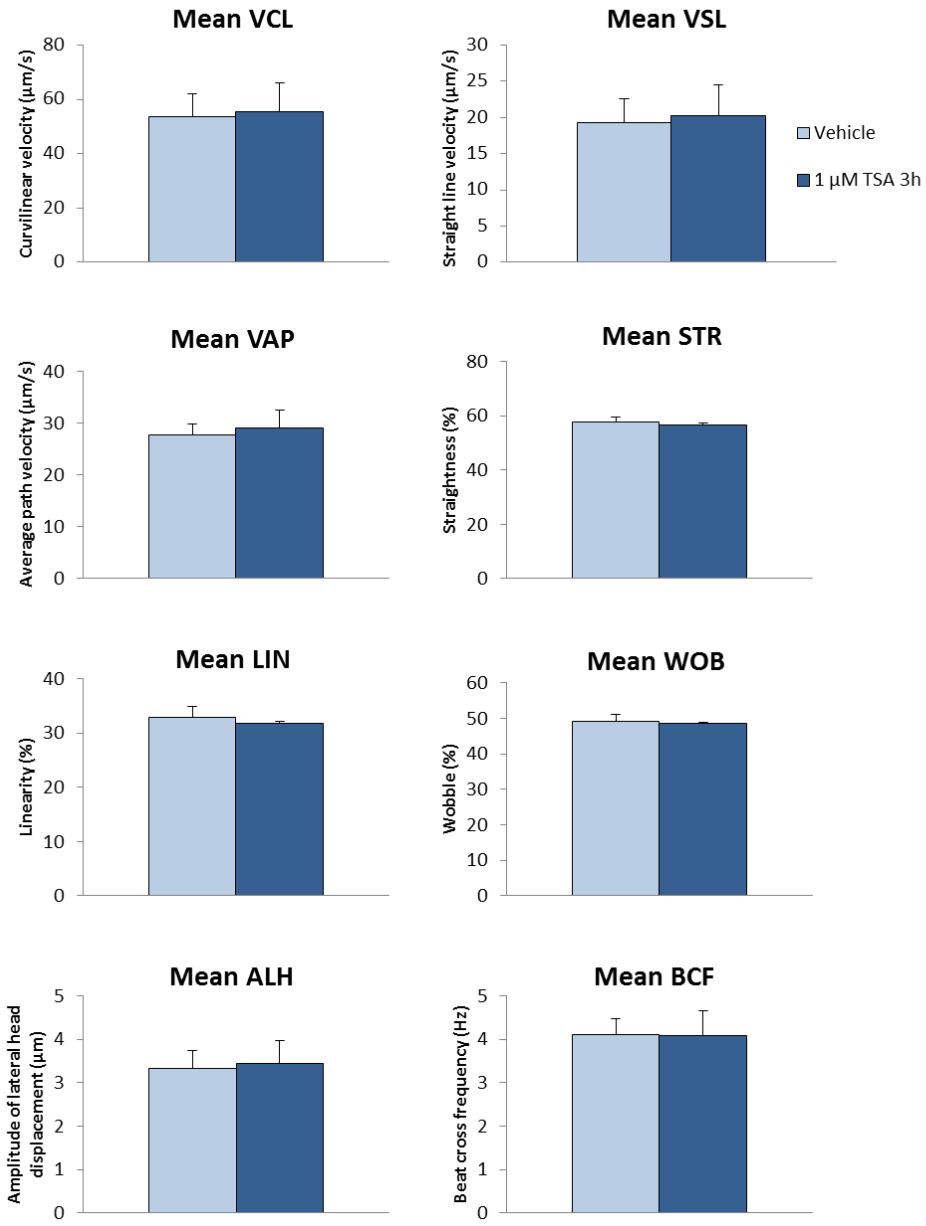

Figure 4.5: Motility parameters following treatment of sperm with 1 µM TSA for 3 hours during capacitation.

Epididymal sperm were treated with vehicle or 1 µM TSA for 3 hours, and motility characteristics were assessed using computer-assisted sperm analysis. Sperm treated with TSA were comparable to control in all motility parameters examined: VCL – curvilinear velocity, VSL - straight line velocity, VAP - average path velocity, STR - straightness, LIN - linearity, WOB - wobble, ALH - amplitude of lateral head displacement and, BCF - beat cross frequency. Values are mean ± SEM, n=4, and were compared by an unpaired T-test.

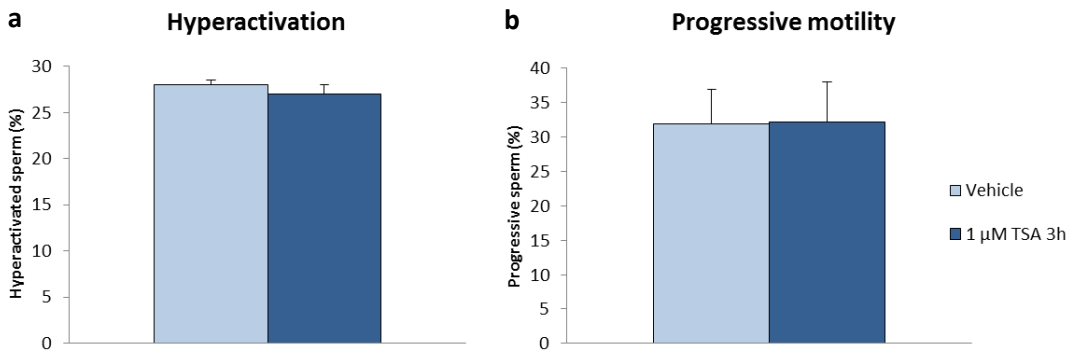

Figure 4.6: Hyperactivation and progressive motility in sperm following treatment with 1 µM TSA for 3 hours during capacitation.

Analysis of capacitated sperm motility following treatment with vehicle or 1 µM TSA for 3 hours showed the percentage of sperm exhibiting (a) hyperactivated and (b) progressive motility following treatment with TSA was comparable to controls. Hyperactivated sperm are shown as a percentage of the total motile sperm; progressive sperm are shown as a percentage of total sperm in the analysed sample. Values shown are mean ± SEM, n=4, and were compared by an unpaired T-test.

4.2.1.2 Sperm motility in viscous media is unaffected by treatment with TSA

A Kremer assay was used to investigate whether exposure to TSA altered sperm motility in conditions more comparable to the female reproductive tract by assessing the ability of sperm to penetrate viscous media. For a schematic illustration of the experimental procedure, see **Chapter 3, Figure 3.5a**. Capacitated epididymal sperm were treated with 1 µM TSA for 1 hour and subsequently examined for their ability to penetrate artificial mucus in 1 hour. Overall, approximately one third of sperm that entered the media were able to reach 1 cm in both vehicle-treated and TSA- treated conditions (**Figure 4.7**). Analysis of the effects of TSA treatment revealed that both the mean number of sperm entering the media at 0 cm, and the mean number of sperm reaching 1 cm after TSA treatment were comparable to vehicle-treated sperm (**Figure 4.7**). The results therefore indicated that treatment with TSA did not have an impact on the ability of capacitated murine sperm to swim through viscous media.

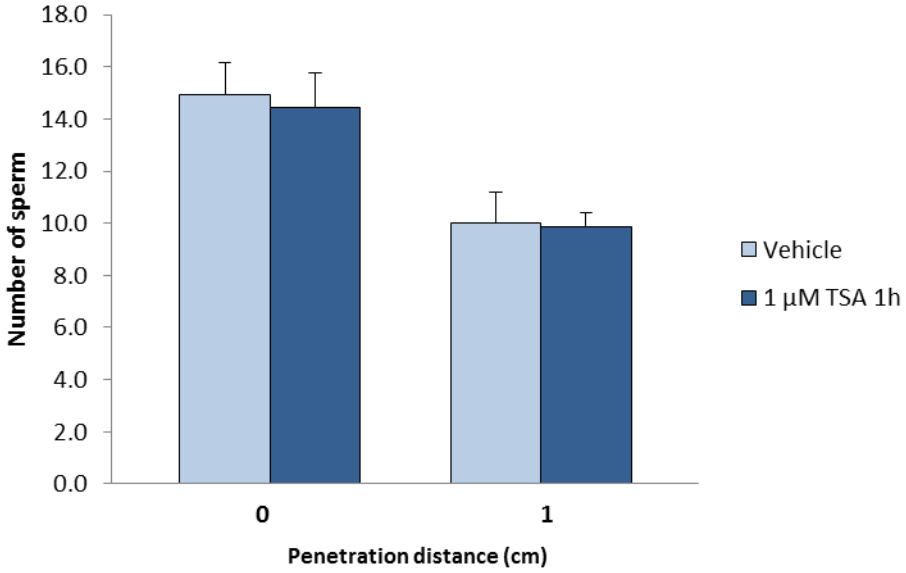

Figure 4.7: Penetration distance of sperm in viscous media following treatment with TSA for 1 hour following capacitation.

Capacitated sperm treated with vehicle or 1µM TSA for 1 hour were assessed for their ability to enter and penetrate viscous media. The mean number of sperm entering the media at 0 cm and penetrating to 1 cm was not significantly affected by treatment with TSA. Values shown are mean ± SEM, n=4, and were compared using an unpaired T-test.

To determine whether exposure to TSA during capacitation had any subsequent effects on motility in viscous media, sperm were treated with 1 µM TSA for 3 hours, and then allowed to swim into the media for 1 hour. In accordance with the results of the 1 hour treatment, the mean number of sperm reaching 1 cm was less than the mean number of sperm entering the viscous media at 0 cm by approximately 57% and 60% in vehicle- and TSA-treated conditions respectively (**Figure 4.8**). With regard to the effects of TSA treatment, the mean number of sperm entering the media at 0 cm and the mean number penetrating to 1cm showed slight reductions upon exposure to TSA; however these differences were not statistically significant (**Figure 4.8**). Therefore, treatment with TSA during capacitation did not affect the subsequent ability of sperm to enter or penetrate viscous media. This suggests that the HDACs may not be exerting a regulatory influence on murine sperm motility.

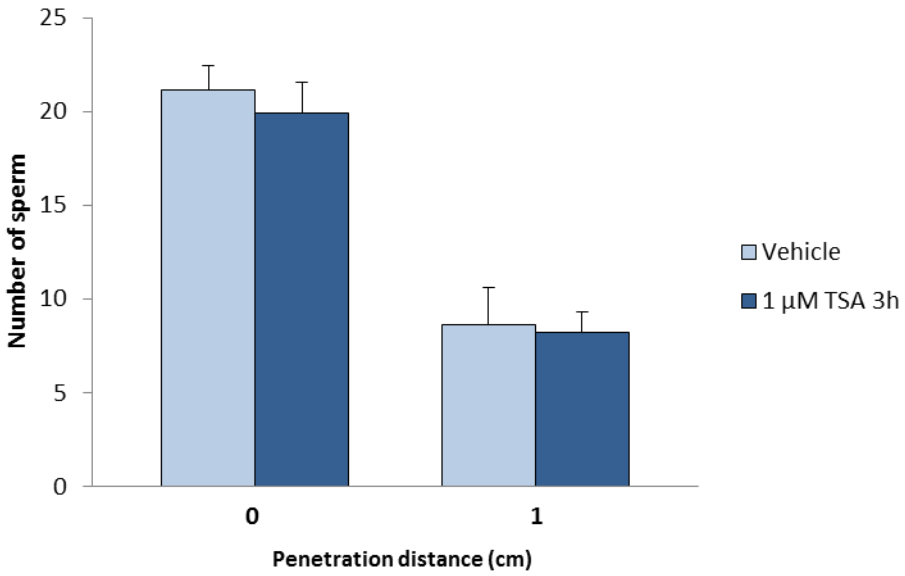

Figure 4.8: Penetration distance of sperm in viscous media following treatment with TSA for 3 hours during capacitation.

Sperm treated with vehicle or 1 µM TSA for 3 hours during capacitation were assessed for their ability to enter and penetrate viscous media. The mean number of sperm entering the media at 0 cm and penetrating to 1 cm was not significantly affected by treatment with TSA. Values are shown as mean ± SEM, n=5, and were compared using an unpaired T-test.

4.2.1.3 Levels of α-tubulin acetylation in sperm are generally unaffected by TSA

The findings described so far in this chapter demonstrated that overall, treatment with TSA did not have a significant effect on sperm motility. To determine whether TSA could influence acetylation levels of α-tubulin, capacitated sperm were exposed to 1 µM and 10 µM TSA for 1 hour and subsequently lysed for Western blot analysis.

Figure 4.9a shows a representative Western blot with sperm lysates from two independent experiments where sperm were treated with either vehicle or 1 µM TSA. The results demonstrated that levels of acetylation were comparable between treated and control sperm. Bands at approximately 55 kDa corresponding to acetylated α-tubulin were subject to densitometric analysis; **Figure 4.9c** shows the mean results from nine experiments. The data demonstrate that the mean acetylated α-tubulin abundance was slightly increased in sperm treated with TSA compared to vehicle-treated sperm; however this was not a significant change when compared by unpaired T-test. All blots were subsequently reprobed for total α-tubulin (**Figure 4.9b**), and bands at 55 kDa representing this protein from nine experiments were analysed using densitometry (**Figure 4.9d**). The results showed that α-tubulin levels were comparable in vehicle- and TSA treated sperm.

A representative Western blot from three independent experiments in which sperm were treated with either vehicle or 10 µM TSA is shown in **Figure 4.9e**, and demonstrates that levels of α-tubulin acetylation were comparable between conditions. Densitometric analysis of bands corresponding to acetylated α-tubulin from five experiments is shown in **Figure 4.9g**. The mean abundance of acetylated α-tubulin was very slightly higher in sperm exposed to 10 µM TSA compared to control, however this difference was small and not statistically significant. Reprobing the blots for total α-tubulin and subsequent densitometric analysis of bands corresponding to this protein demonstrated that lanes were equally loaded (**Figure 4.9f, h**).

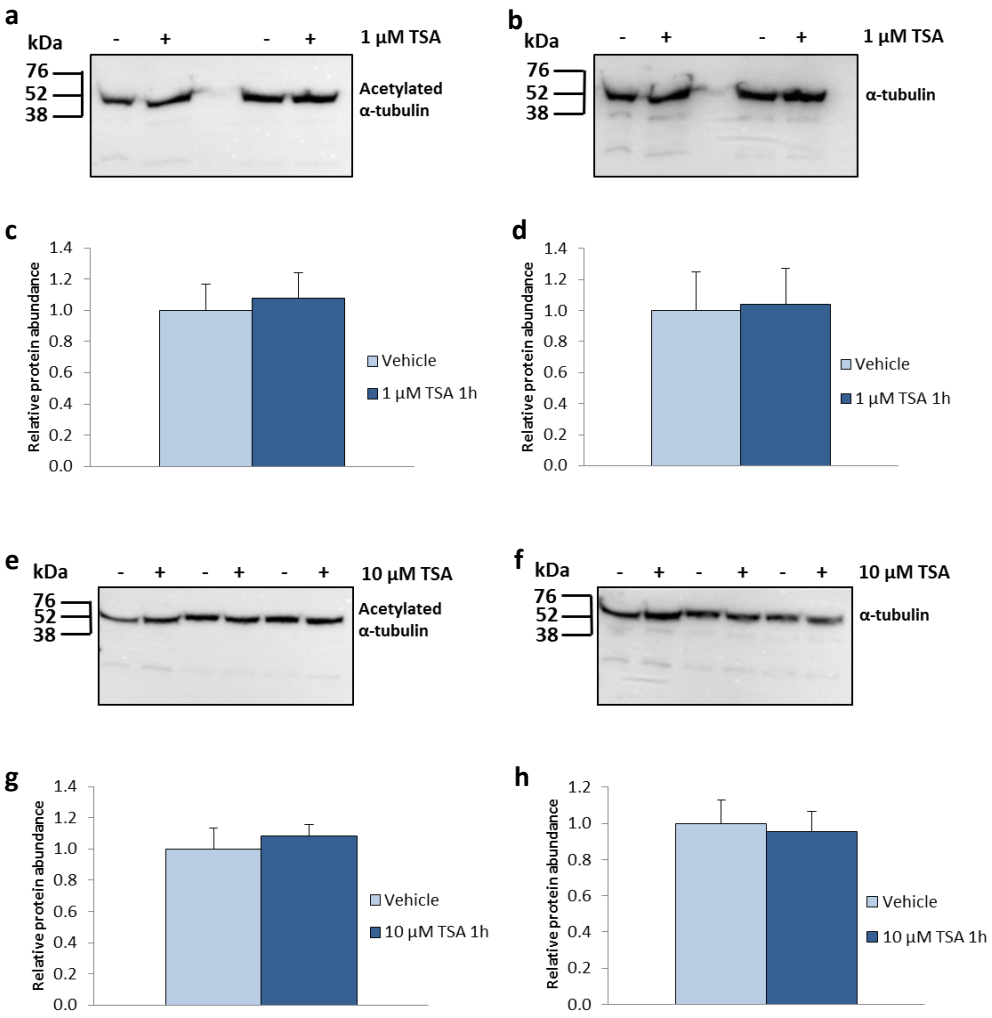

Figure 4.9: Acetylation of α-tubulin in sperm following treatment with 1 µM or 10 µM TSA for 1 hour following capacitation.

Representative Western blots and densitometry following analysis of capacitated sperm treated for 1 hour with (a-d) vehicle or 1 µM TSA, or (e-h) vehicle or 10 µM TSA. (a, e) Representative Western blots of acetylated protein in sperm lysates following treatments; bands at approximately 55 kDa correspond to acetylated α-tubulin. Protein from approximately 0.5 million sperm was loaded in each lane. (b, f) Blots were reprobed for total α-tubulin as a loading control; bands at approximately 55 kDa correspond to α-tubulin. (c, g) Bar graphs show densitometric analysis of bands corresponding to acetylated α-tubulin in sperm treated with (c) vehicle or 1 µM TSA (n=9) and (g) vehicle or 10 µM TSA (n=5). (d, h) Bar graphs show densitometric analysis of bands corresponding to total α-tubulin in sperm treated with (d) vehicle or 1 µM TSA (n=9) and (h) vehicle or 10 µM TSA (n=5). Values are shown as mean ± SEM and were compared using an unpaired T-test.

The results in **Figure 4.9** demonstrated that treatment with TSA for 1 hour following capacitation did not lead to any significant changes in the levels of α-tubulin acetylation in sperm. Therefore, the effect of TSA treatment during capacitation was examined by Western blot. **Figure 4.10a** shows the levels of acetylation in sperm lysates from two independent experiments in which sperm were treated with vehicle or 1 μM TSA for 3 hours during capacitation. This representative Western blot demonstrates that acetylation of α-tubulin is comparable between control and treated sperm. Densitometric analysis of bands corresponding to acetylated α-tubulin in sperm lysates from 4 experiments is shown in **Figure 4.10c**. This analysis showed a 0.3-fold increase in the abundance of acetylated α-tubulin of sperm treated with TSA compared to control; however this difference was not significant. All blots were subsequently reprobed for total α-tubulin; a representative blot is shown in Figure **4.10b**. Densitometry performed on 55 kDa bands corresponding to α-tubulin demonstrated equal loading between the conditions (**Figure 4.10d**). The results described indicate that treatment with TSA for 3 hours during capacitation did not significantly affect the levels of α-tubulin acetylation in sperm. The data therefore support the notion that HDAC6 does not have an active role in deacetylation of α-tubulin in sperm.

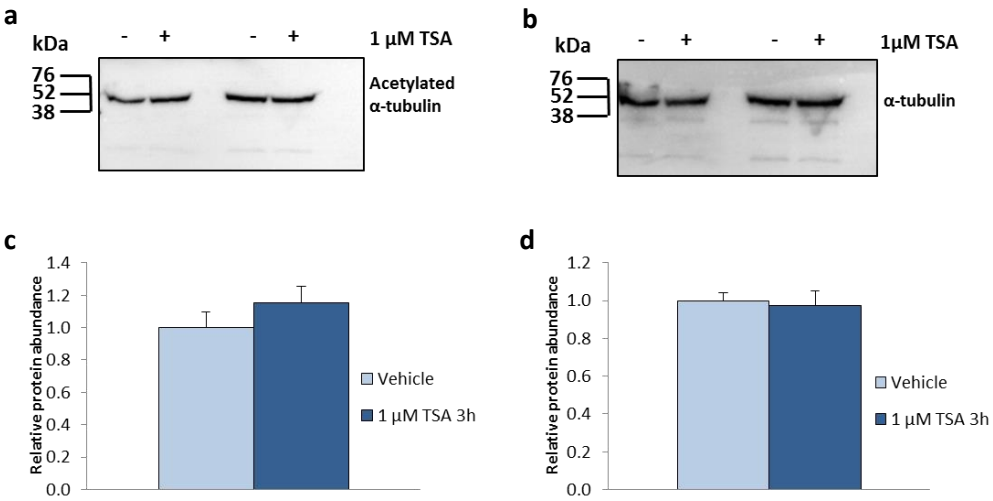

Figure 4.10: Acetylation of α-tubulin in sperm following treatment with 1 µM TSA for 3 hours during capacitation.

(a) Representative Western blot of acetylated protein from sperm treated with either vehicle or 1 µM TSA for 3 hours in 2 independent experiments. Protein from approximately 0.5 million sperm was loaded in each lane. Bands at approximately 55 kDa correspond to acetylated α-tubulin. (b) All blots were reprobed for total α-tubulin as a loading control; bands at approximately 55 kDa correspond to α-tubulin. (c) Bar graph shows densitometric analysis of bands corresponding to acetylated α-tubulin in sperm lysates (n=4). (d) Bar graph shows densitometric analysis of bands corresponding to total α-tubulin in sperm lysates (n=4). Values shown are mean ± SEM, and were compared using an unpaired T-test.

4.2.1.4 Treatment with TSA increases α-tubulin acetylation in HEK-MSR cells

As exposure to TSA did not affect the levels of α-tubulin acetylation in sperm, the HEK-MSR cell line was utilised to determine the response of another cell type to the inhibitor as a control. HEK-MSR cells were subjected to a TSA time course over 3 hours and were analysed by Western blot. **Figure 4.11a** shows a representative blot in which lysates from two independent time courses were analysed. From the Western blot, it is clear that acetylation of α-tubulin was increased upon treatment with 1 μM TSA after 1 and 3 hours. Densitometric analysis of bands corresponding to acetylated α-tubulin from 4 experiments is shown in **Figure 4.11c**. Following treatment of HEK cells with 1 μM TSA for 1 and 3 hours, the abundance of acetylated α-tubulin increased approximately 8.5-fold and 13.5-fold respectively, compared to the 0 hour condition, representing significant increases when analysed using one-way ANOVA/Dunnett's post-hoc test ($P < 0.0001$) (**Figure 4.11c**). All blots were subsequently reprobed for total α-tubulin; the representative blot following reprobing is shown in **Figure 4.11b**. Densitometric analysis of bands at approximately 55 kDa corresponding to α-tubulin demonstrated equal loading between the conditions (**Figure 4.11d**). The results indicated that treatment of HEK cells with 1 μM TSA induced an increase in acetylation of α-tubulin, suggesting that the α-tubulin deacetylase activity of HDAC6 was inhibited by this concentration of TSA over this time frame.

To determine whether 10 μM TSA affected the acetylation of α-tubulin in HEK cells in the same manner, the cell line was exposed to concentrations of 1 μM and 10 μM TSA for 1 hour and analysed by Western blot. The results of this analysis showed that levels of α-tubulin acetylation were increased to approximately the same extent above control following treatment with both TSA concentrations. A representative blot with lysates from two experiments is shown in **Figure 4.11e**. Results from the densitometric analysis of bands corresponding to acetylated α-tubulin from 4 sets of lysates are shown in **Figure 4.11g**. This indicated that the mean abundance of acetylated α-tubulin increased 6-fold and 5.7-fold following treatment with 1 μM and 10 μM TSA respectively, when compared to vehicle-treated

cells, representing a significant change as analysed using a one-way ANOVA/Dunnett's post-hoc test ($P < 0.0001$). The Western blots were reprobed for total α-tubulin; the representative blot following reprobing is shown in **Figure 4.11f**. Densitometric analysis of bands at approximately 55 kDa corresponding to α-tubulin demonstrated equal loading between the conditions (**Figure 4.11h**). The findings therefore indicate that treatment with both 1 μM and 10 μM TSA resulted in an increase in the acetylation of α-tubulin in HEK cells, but this effect was not necessarily concentration-dependent.

As observed in the preceding chapter, the basal levels of acetylated α-tubulin in HEK cells again appeared much lower than the baseline levels detected in control sperm in previous Western blots. Therefore, the differences observed between the responses of HEK-MSR cells and sperm to TSA, like tubacin in Chapter 3, may result from a disparity in basal levels of α-tubulin acetylation; if sperm α-tubulin is maximally acetylated, it may not be sensitive to HDAC inhibition by TSA. Further investigation of this hypothesis is described in section 4.2.2.

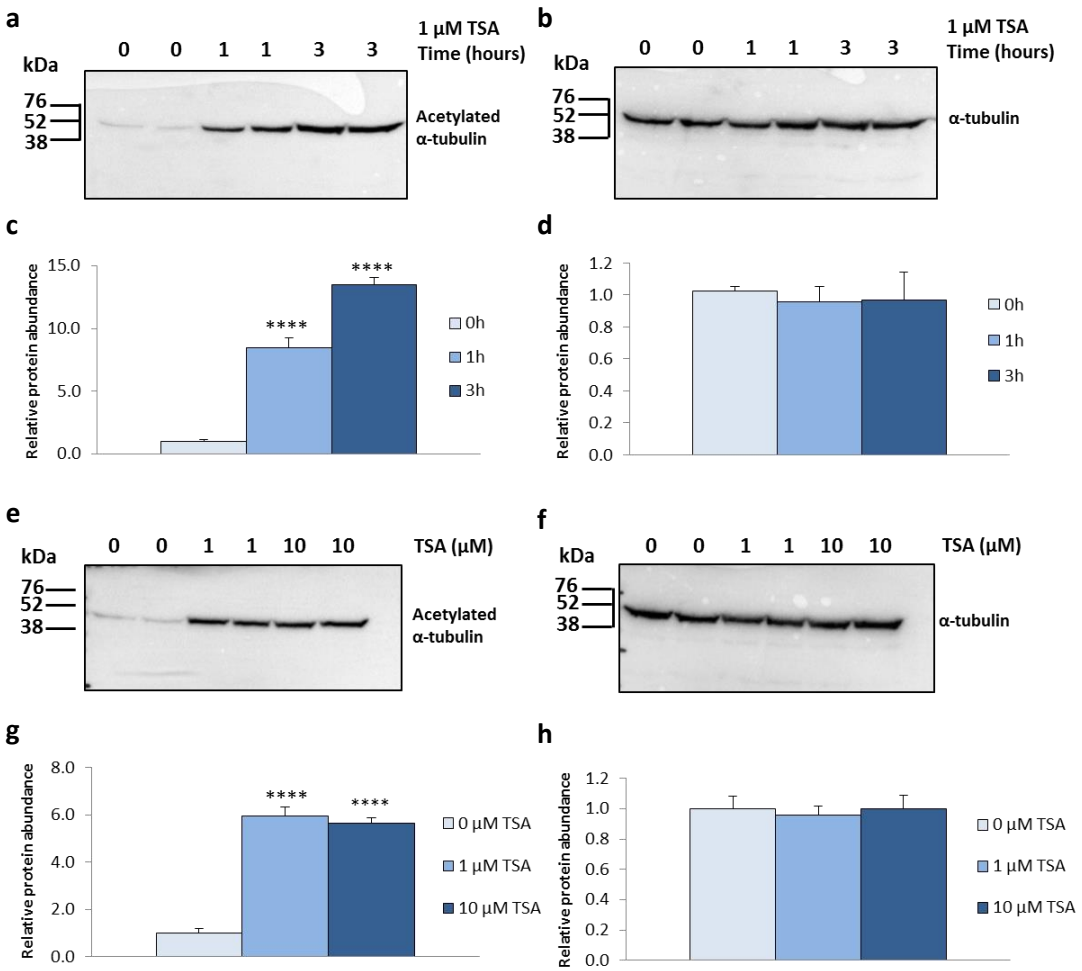

Figure 4.11: Acetylation of α-tubulin in HEK-MSR cells following treatment with TSA.

Representative Western blots of acetylated protein from HEK cells subjected to (a) a 1 µM TSA time course for 3 hours, or (e) treatment with vehicle, 1 µM TSA or 10 µM TSA for 1 hour. Approximately 20 µg of protein was loaded into each lane. Bands at approximately 55 kDa correspond to acetylated α-tubulin. (b, f) Blots were subsequently reprobed for total α-tubulin; bands at approximately 55 kDa represent the protein. (c, g) Bar graphs show densitometric analysis of bands corresponding to acetylated α-tubulin in (c) HEK cells subjected to TSA time courses (n=4) and (g) HEK cells treated with 1 µM TSA or 10 µM TSA for 1 hour (n=4). (d, h) Bar graphs show densitometric analysis of bands corresponding to total α-tubulin in (d) HEK cells subjected to TSA time courses (n=4) and (h) HEK cells treated with 1 µM TSA or 10 µM TSA for 1 hour (n=4). Values shown are mean ± SEM and were compared by one-way ANOVA/Dunnett's post-hoc test ($P < 0.0001$).

4.2.1.5 Levels of α-tubulin acetylation in spermatids are unaffected by treatment with TSA

To investigate α-tubulin deacetylation in developing spermatozoa, spermatids were treated with 1 μM TSA for 1 hour in 3 independent experiments. Western blot analysis of the lysates demonstrated that levels of acetylated α-tubulin were comparable between vehicle- and TSA-treated sperm; a representative Western blot demonstrating the results from one experiment is shown in **Figure 4.12a**. Alongside spermatid lysates, HEK-MSR cell and sperm lysates were loaded as controls. Sperm samples again confirmed the lack of effect of TSA on acetylated α-tubulin levels in male gametes, whilst HEK cell lysates loaded as a positive control demonstrated an increase in acetylation of α-tubulin following treatment with 1 μM TSA for 1 hour (**Figure 4.12a**). Notably, a band for acetylated α-tubulin was not present in the lane containing vehicle-treated HEK cells in this Western blot. This again suggested that HEK cells exhibited lower levels of α-tubulin acetylation compared to vehicle-treated sperm and spermatids (**Figure 4.12a**).

Subsequent densitometric analysis of bands corresponding to acetylated α-tubulin in three spermatid lysates determined that spermatids exhibited a 0.2–fold increase in this protein following treatment with TSA (**Figure 4.12c**). However, this was not statistically significant. Reprobing the blots for total α-tubulin followed by densitometric analysis demonstrated equal loading between vehicle-treated and TSA-treated spermatids (**Figure 4.12b, d**). Furthermore, reprobing the representative blot showed that the levels of α-tubulin were comparable between vehicle-treated and TSA-treated HEK cells, confirming the loading of protein in the vehicle-treated lane (**Figure 4.12b**). This provided further evidence for the notion that basal levels of α-tubulin acetylation in sperm are much higher than that of HEK cells. Therefore, the insensitivity of sperm and spermatids to TSA may result from the high acetylation state of their α-tubulin at baseline levels.

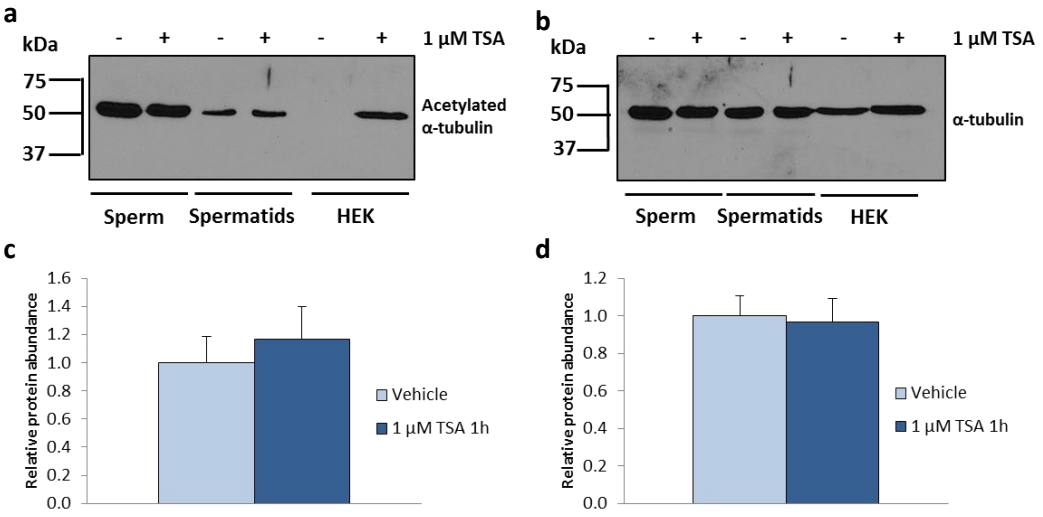

Figure 4.12: Acetylation of α-tubulin in spermatids following treatment with TSA for 1 hour.

(a) Representative Western blot of acetylated protein from spermatids treated with 1 µM TSA for 1 hour. Sperm and HEK cell lysates were loaded as controls to demonstrate the effects of TSA on these cells. Approximately 20 µg of protein was loaded into each lane. Bands at approximately 55 kDa correspond to acetylated α-tubulin. (b) All blots were reprobed for total α-tubulin as a loading control; bands at approximately 55 kDa correspond to α-tubulin. (c) Bar graph shows densitometric analysis of bands corresponding to acetylated α-tubulin in spermatid samples treated with 1 µM TSA for 1 hour (n=3). (d) Bar graph shows densitometric analysis of bands corresponding to α-tubulin in spermatids treated with 1 µM TSA for 1 hour (n=3). Values shown are mean ± SEM and were compared by unpaired T-test.

Similar effects to treatment of spermatids with 1 μM TSA for 1 hour were observed when spermatids were exposed to 1 μM TSA for 3 hours. **Figure 4.13a** shows a representative Western blot demonstrating the effect of a 3 hour vehicle or TSA treatment on spermatid lysates from two independent experiments. Acetylation of α-tubulin was comparable between vehicle-treated and TSA-treated spermatids (**Figure 4.13a**). In accordance with previous findings, acetylation of α-tubulin in HEK cell lysates (loaded as a positive control) was increased upon TSA treatment. Basal levels of acetylated α-tubulin were lower in HEK cells than spermatids when comparing between vehicle-treated conditions (**Figure 4.13a**). Densitometric analysis of bands corresponding to acetylated α-tubulin in spermatid lysates from three experiments confirmed that TSA treatment for 3 hours did not significantly alter the abundance of acetylated α-tubulin in spermatids (**Figure 4.13c**). Reprobing the Western blots for total α-tubulin showed comparable levels of protein between control and treated spermatids (**Figure 4.13b**). Likewise, levels of total α-tubulin in HEK cell conditions were similar, confirming that both lanes corresponding to HEK cell lysates were loaded with comparable amounts of protein (**Figure 4.13b**). Densitometric analysis of bands representing total α-tubulin in spermatid lysates confirmed approximately equal loading between conditions (**Figure 4.13d**). The results therefore demonstrated that treatment with 1 μM TSA for 3 hours did not alter the abundance of acetylated α-tubulin in spermatids, and reinforced the finding that spermatids exhibit high basal levels of acetylated α-tubulin compared to HEK cells.

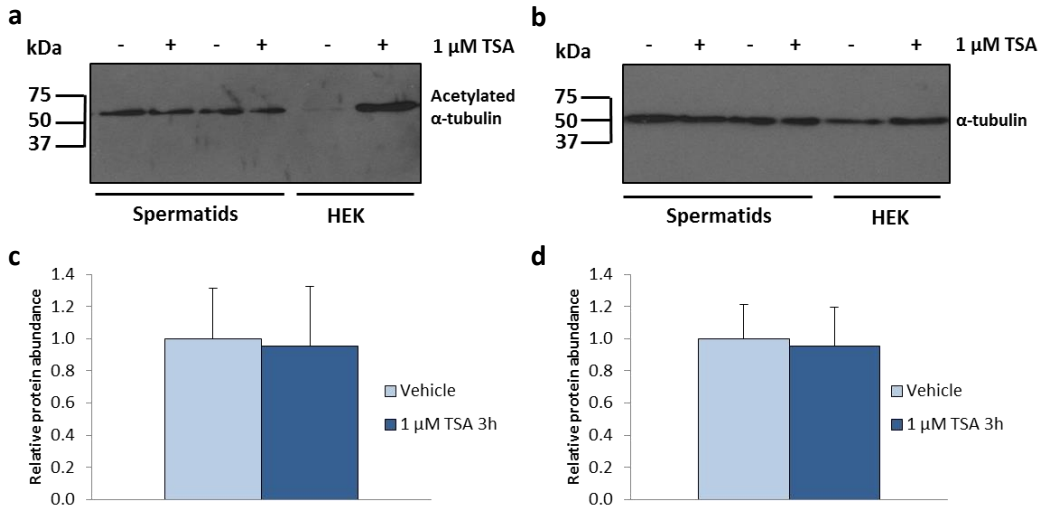

Figure 4.13: Acetylation of α-tubulin in spermatids following treatment with TSA for 3 hours.

(a) Representative Western blot of acetylated protein from spermatids treated with 1 µM TSA for 3 hours in 2 independent experiments. HEK-MSR cell lysates were loaded as a positive control to demonstrate the effects of TSA on this cell line. Approximately 20 µg of protein was loaded into each lane. Bands at approximately 55 kDa correspond to acetylated α-tubulin. (b) All blots were reprobed for total α-tubulin as a loading control; bands at approximately 55 kDa correspond to α-tubulin. (c) Bar graph shows densitometric analysis of bands corresponding to acetylated α-tubulin in spermatid samples (n=3). (d) Bar graph shows densitometric analysis of bands corresponding to total α-tubulin in spermatid samples (n=3). Values are shown as mean ± SEM and were compared by an unpaired T-test.

4.2.2 Examination of HDAC activity

As treatment of sperm with tubacin discussed in Chapter 3, and TSA reported in this chapter did not affect sperm motility or acetylation of α-tubulin, experiments to examine the activity of HDAC6 in sperm were performed; results from these investigations will be described in the following sections.

4.2.2.1 Sperm α-tubulin is highly acetylated

The absence of an increase in sperm α-tubulin acetylation following treatment with TSA and tubacin, and the low levels of acetylated α-tubulin in HEK-MSR cells compared to sperm, suggested that HDAC6 may not be active in sperm. To investigate the high acetylation state of sperm α-tubulin further, a comparison of acetylated α-tubulin in untreated sperm and untreated HEK cell lysates was carried out (with protein equalized to load 20 μg for each). **Figure 4.14a** shows a representative Western blot demonstrating the level of acetylated α-tubulin in two sperm and two HEK cell lysates. Bands at approximately 55 kDa corresponding to acetylated α-tubulin in six lysates of each cell type were subject to densitometric analysis. The abundance of acetylated α-tubulin was approximately 6-fold higher in sperm than in HEK cells, representing a significant difference in acetylation level when compared by unpaired T-test ($P < 0.0001$) (**Figure 4.14c**). Reprobing the blots for total α-tubulin (**Figure 4.14b**) and subsequent analysis by densitometry showed that levels of total α-tubulin were slightly higher in sperm than HEK cells. However, the difference was only a 0.2-fold increase, which was not statistically significant (**Figure 4.14d**). Therefore the results confirmed that sperm α-tubulin is highly acetylated compared to that of HEK cells. Furthermore, using the densitometric data, the abundance of acetylated α-tubulin in sperm was calculated as a proportion of the total sperm α-tubulin. This indicated that all of the α-tubulin analysed was acetylated (**Figure 4.14e**), suggesting that sperm α-tubulin is maximally acetylated. This finding therefore provides evidence for the notion that sperm α-tubulin is not actively deacetylated by HDAC6.

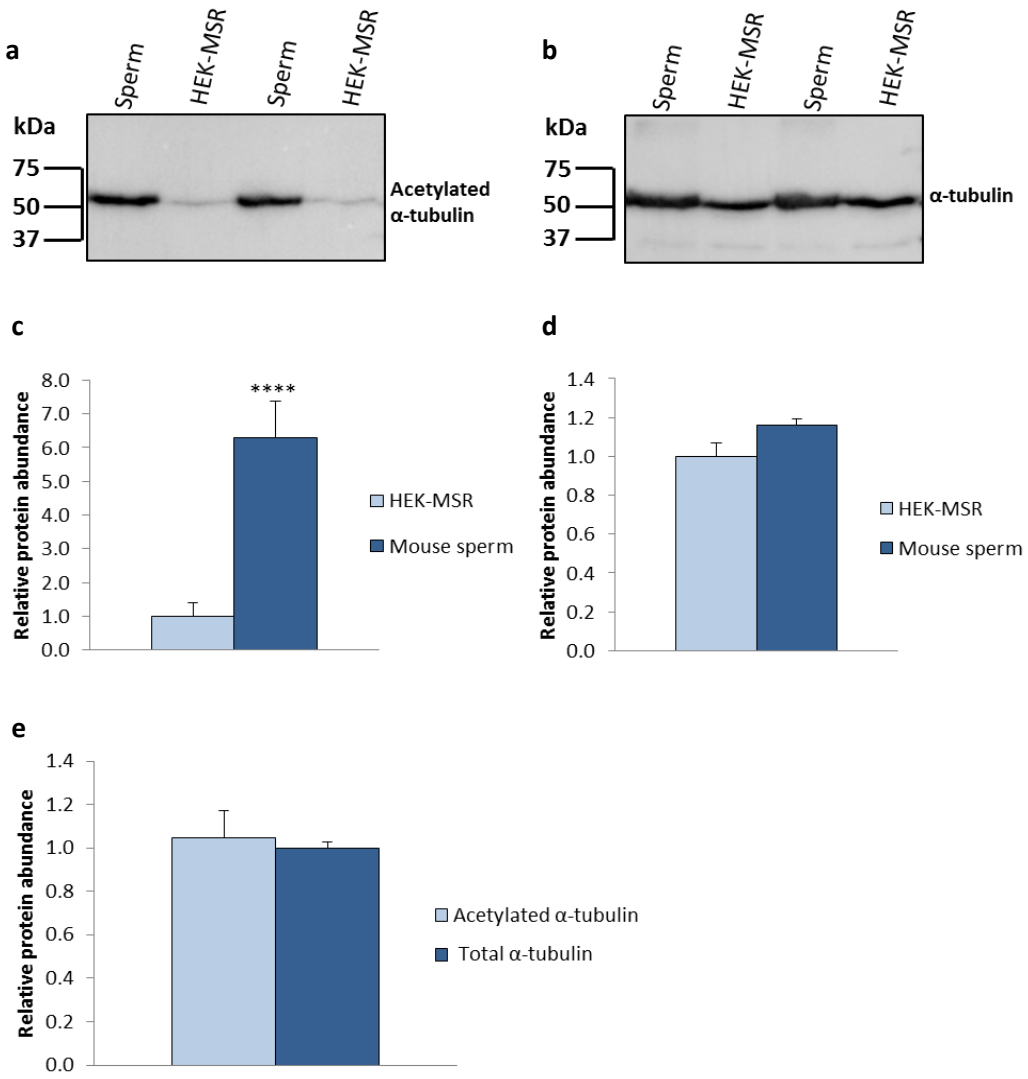

Figure 4.14: Acetylation of α-tubulin in untreated sperm and HEK-MSR cells.

(a) Representative Western blot of acetylated protein from untreated capacitated sperm and untreated HEK-MSR cells. Approximately 20 µg of protein was loaded in each lane. Bands at approximately 55 kDa correspond to acetylated α-tubulin. (b) All blots were reprobed for total α-tubulin; bands at approximately 55 kDa represent α-tubulin. (c) Bar graph shows densitometric analysis of bands corresponding to acetylated α-tubulin in sperm and HEK cell samples (n=6). (d) Bar graph shows densitometric analysis of bands corresponding to total α-tubulin in sperm and HEK cell samples (n=6). (e) Bar graph shows the abundance of acetylated α-tubulin following densitometric analysis relative to the abundance of α-tubulin (n=6). Values shown are mean ± SEM compared by unpaired T-test, **** $P < 0.0001$.

4.2.2.2 HDAC activity is detectable in sperm

As the results indicated that deacetylation of sperm α-tubulin may not be taking place, a HDAC activity assay was used to ascertain whether HDACs were, in fact, active in sperm. Sperm were incubated for 1 hour with either 1 μM TSA or 5 μM tubacin and deacetylase activity was measured fluorometrically following addition of a cell-permeable HDAC substrate for 2 hours (experimental schematic shown in **Figure 4.15a**). Mean sperm HDAC activity following three biological replicates of the assay showed reductions of approximately 45% and 33% when compared to control, following treatment with TSA and tubacin respectively (**Figure 4.15b**). However, statistical analysis using a one-way ANOVA demonstrated that no comparisons between conditions reached significance (significance level set at 0.05). The detectable inhibition of sperm HDAC activity by TSA and tubacin suggests that HDACs, including HDAC6, are active in sperm.

For control purposes, HEK cells also underwent the HDAC activity assay and following culturing, were exposed to the same experimental conditions as sperm (**Figure 4.15a**). Data demonstrated reductions in mean HDAC activity of approximately 9% and 29% when compared to control following treatment with TSA and tubacin respectively (**Figure 4.15c**). These results indicated that the two inhibitors reduced HDAC activity but these reductions did not reach statistical significance. Based on the significant effects of HDAC inhibition on acetylation of α-tubulin in HEK cells, this reduction in deacetylase activity was smaller than anticipated. Therefore, further analysis of HEK cell response to HDAC inhibition was performed to attempt to understand this unexpected outcome; results of this experiment will be detailed next.

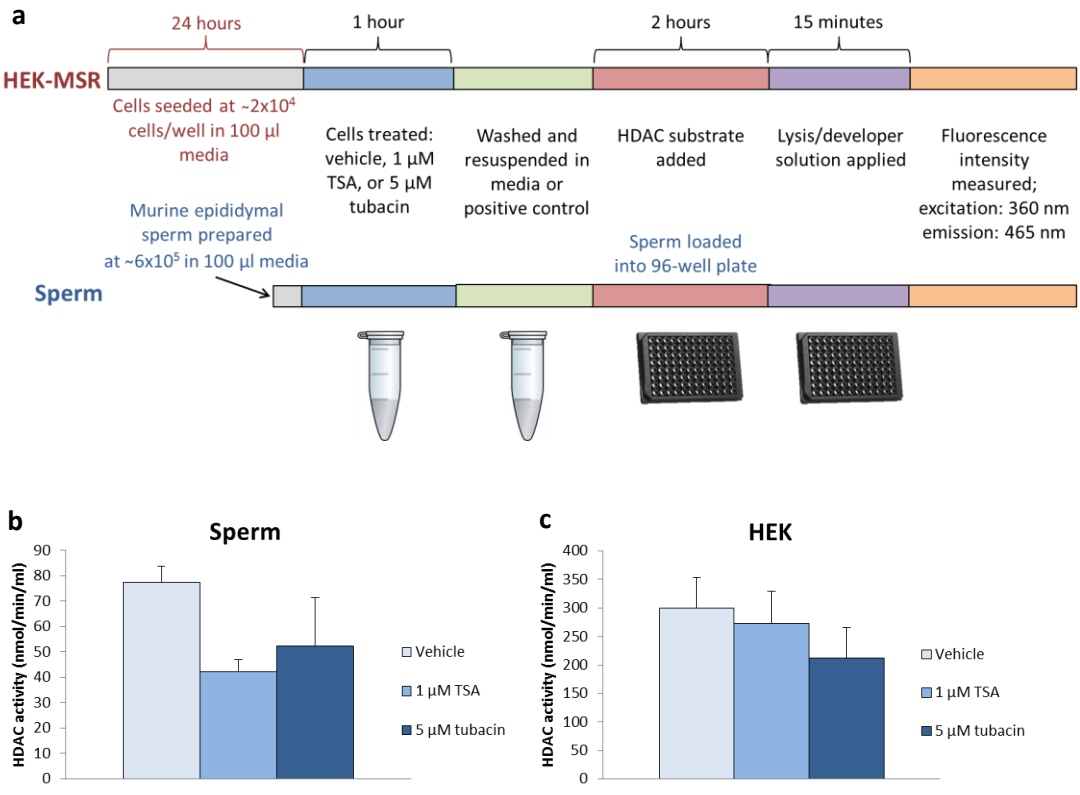

Figure 4.15: HDAC activity assay.

(a) Schematic illustration of the HDAC activity assay experimental procedure with sperm and HEK-MSR cells. HEK-MSR cells were cultured and treated in the 96-well plate throughout the experiment; sperm were transferred into the plate following treatments and washing steps as illustrated by the images. Text in black refers to procedures performed with both sperm and HEK cells. Cells were maintained at 37°C during incubation periods. Bar graphs show HDAC activity measured in (b) sperm and (c) HEK-MSR cells following treatment with vehicle, 1 µM TSA, or 5 µM tubacin. Values are shown as mean ± SEM and were compared by a one-way ANOVA.

4.2.2.3 HDAC activity recovers in HEK cells following treatment with TSA

As the reduction in HDAC activity was less than expected in HEK cells following HDAC inhibition, it was postulated that the cells may have recovered some activity following washing to remove the inhibitors, and incubation with the HDAC substrate. See **Figure 4.15a** for a schematic of the experimental procedure. To determine whether HDAC activity could be recovered in this time frame, HEK cells were treated with vehicle or 1 µM TSA for 1 hour, then washed to remove the inhibitor. Media was subsequently replaced, and cells were cultured for a further 1, 2, or 3 hours before being lysed. A representative Western blot from one recovery experiment is shown in **Figure 4.16a**, and the densitometric analysis of bands corresponding to acetylated α-tubulin from 4 independent experiments is shown in **Figure 4.16c**. Western blot analysis demonstrated that the abundance of acetylated α-tubulin was increased almost 3-fold by TSA treatment for 1 hour compared to vehicle-treated cells, representing a significant effect (unpaired T-test, $P < 0.0001$). Following removal of the inhibitor, the levels of acetylated tubulin remained higher in TSA-treated cells than their relative controls over the recovery period. The abundance of acetylated α-tubulin was 0.9-, 0.8-, and 0.5-fold higher than controls following a 1, 2, and 3 hour recovery period, respectively; the difference between control and treated α-tubulin acetylation after 1 and 2 hours recovery was statistically significant as determined by unpaired T-tests ($P < 0.01$) (**Figure 4.16a, c**). The extent of the difference in abundance of acetylated α-tubulin between control and treated HEK cells reduced over each hour of the 3 hour period of recovery, demonstrating the reversibility of HDAC inhibition with TSA in HEK cells.

Each Western blot of the 4 independent experiments was reprobed for total α-tubulin (**Figure 4.16b**), and bands at approximately 55 kDa representing α-tubulin underwent densitometric analysis. Densitometry showed that levels of α-tubulin were generally comparable between control and treated conditions; although a small 0.2-fold increase in α-tubulin was observed in the TSA-treated 3 hour recovery condition compared to its relative control (**Figure 4.16d**). This

increase was not statistically significant but should be considered when viewing the increase in acetylated α-tubulin in this condition.

The results demonstrated that following treatment with TSA, the levels of acetylated α-tubulin in HEK cells began to return to control levels within one hour of the removal of the inhibitor, and this recovery continued over the following 2 hours. This suggested that activity of HDAC6 could be regained in this time period. Therefore, with regard to the HDAC activity assay, in the 2 hour period prior to the measurement of deacetylase activity in which HEK cells were incubated in the absence of the inhibitors, partial HDAC activity may have been recovered. This finding could explain the smaller-than-expected reduction in HDAC activity in HEK cells following treatment with HDAC inhibitors.

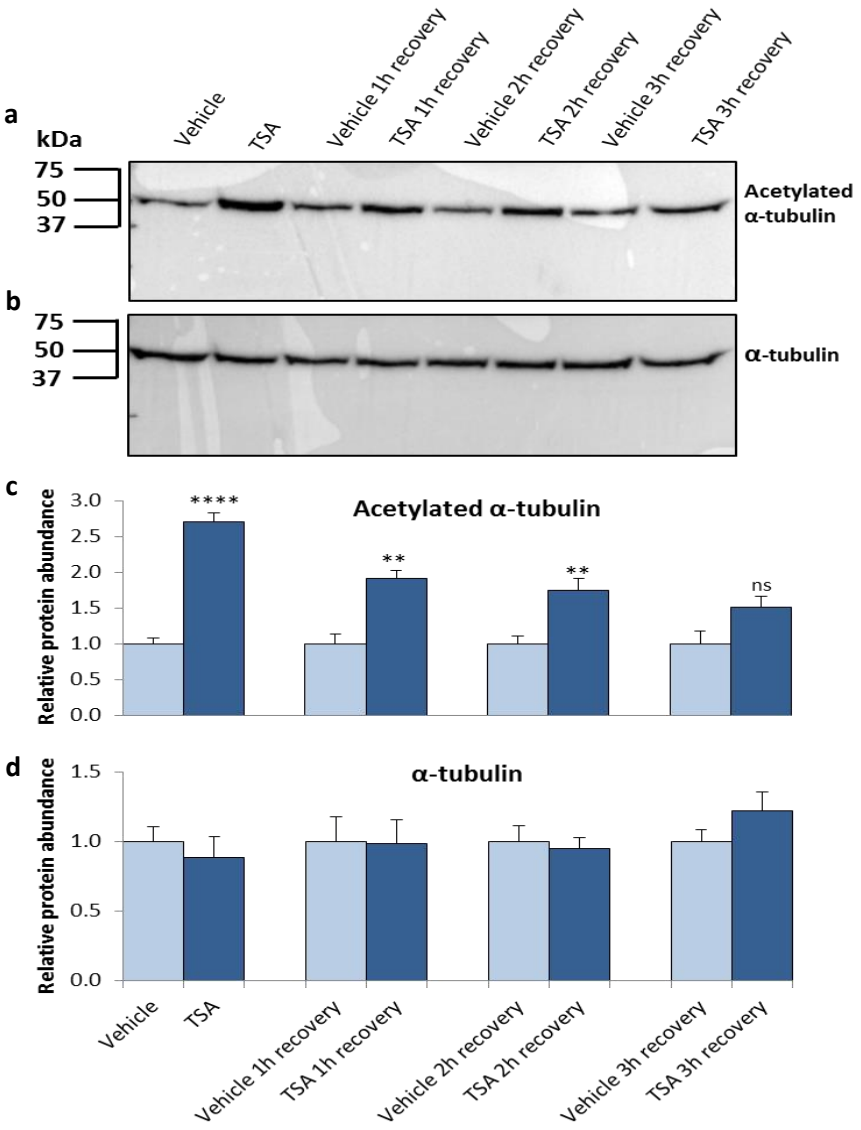

Figure 4.16: Recovery of HDAC activity in HEK-MSR cells following treatment with TSA.

(a) Representative Western blot of acetylated protein from HEK-MSR cells following treatment with vehicle or 1 µM TSA for 1 hour. Cells were washed to remove the inhibitor and media was replaced allowing recovery for 1, 2 or 3 hours. Approximately 20 µg of protein was loaded for each condition. Bands at approximately 55 kDa represent acetylated α-tubulin. (b) Blots were reprobed for total α-tubulin as a loading control; bands at approximately 55 kDa correspond to α-tubulin. (c) Bar graph shows densitometric analysis of bands corresponding to acetylated α-tubulin in HEK cell samples (n=4). (d) Bar graph shows densitometric analysis of bands corresponding to total α-tubulin in HEK cell samples (n=4). Values shown are mean ± SEM, compared by unpaired T-test, ** P <0.01, **** P < 0.0001.

4.3 Discussion

The findings presented in Chapter 3 indicated that basal levels of α-tubulin acetylation in sperm were high, and suggested that HDAC6/SIRT2 did not actively deacetylate α-tubulin in sperm or play a role in sperm motility. Therefore, the main aim of the investigations in this chapter was to examine the activity of Class I and II HDACs in order to discover whether deacetylase activity was present in sperm. The general Class I and II HDAC inhibitor, TSA, was also used to investigate whether any of the HDACs in these classes, including HDAC6, were involved in the regulation of sperm motility and the acetylation of α-tubulin, providing a second method for testing the effects of inhibitors of HDAC6 in sperm.

4.3.1 The effects of TSA on sperm motility and α-tubulin acetylation

Analysis of sperm lysates by Western blot firstly indicated that baseline levels of acetylated α-tubulin in control samples were high in the absence of any inhibitor. Secondly, treatment of capacitated sperm with 1 μM and 10 μM TSA for 1 hour did not significantly affect the abundance of acetylated α-tubulin or total α-tubulin (**Figure 4.9**). This indicated that the sperm were insensitive to treatment with TSA, supporting the findings in Chapter 3 which demonstrated a lack of response to tubacin. Both findings taken together indicate that α-tubulin in murine sperm may be fully acetylated and as such, does not show any change when deacetylation is inhibited.

Analysis of sperm motility demonstrated that exposure to TSA for 1 hour following capacitation resulted in a small increase in all parameters of motility, with amplitude of lateral head displacement, beat cross frequency, and curvilinear, straight line, and average path velocities all showing increases of at least 20% (**Figure 4.1**). In addition, the percentages of sperm exhibiting the characteristics of hyperactivation and progressive motility were both higher in the treated condition (**Figure 4.2**). Although none of these changes reached statistical significance, the data suggest that TSA may exert a small influence on sperm motility, implicating one or more Class I or II HDACs in the regulation of this function. However, analysis

of capacitated sperm exposed to 1 μM TSA for 1 hour during the Kremer assay demonstrated that the treatment did not affect the number of sperm entering or penetrating viscous media (**Figure 4.7**). Therefore, any changes observed in motility parameters following treatment with TSA may not be biologically relevant as they do not affect the ability of sperm to swim in artificial mucus. Nevertheless, as treatment with 1 μM TSA was shown to exert minor effects on motility parameters, sperm were exposed to 10 μM TSA to evaluate the influence of a higher concentration of inhibitor. Similar to the results of the 1 μM TSA treatment, exposure of sperm to 10 μM TSA resulted in small increases to motility parameters, although motility was not enhanced to the same extent as treatment with the lower concentration of TSA (**Figure 4.3**). Therefore, exposure of sperm to TSA following capacitation only appears to influence motility parameters slightly. This effect is not statistically significant and may not be biologically relevant.

To investigate whether variations in the acetylation/deacetylation of α-tubulin occur during capacitation, sperm were treated with 1 μM TSA for 3 hours during this period. The abundance of acetylated α-tubulin exhibited a small 0.2-fold increase in treated sperm, whilst levels of total α-tubulin were equal between conditions (**Figure 4.10**). This increase in abundance of acetylated α-tubulin was not statistically significant. Analysis of motility following the 3 hour treatment demonstrated that all parameters of sperm motility were normal (**Figure 4.5**), and the percentages of sperm exhibiting hyperactivated and progressive motility were comparable to controls (**Figure 4.6**). In addition, the 3 hour treatment of sperm with TSA during capacitation resulted in only a slight reduction in the number of sperm able to enter and penetrate viscous media (**Figure 4.8**). The data therefore indicate that sperm are generally insensitive to treatment with TSA during capacitation.

As sperm exhibited only slight changes to levels of α-tubulin acetylation following treatment with TSA for 1 hour, and no change during a 3 hour treatment, the HEK-MSR cell line was again utilised to determine the response of another cell type to the inhibitor as a control. Treatment

of HEK cells with 1 μM TSA increased the levels of α-tubulin acetylation approximately 8.5- and 13.5-fold after 1 and 3 hours respectively, whereas treatment with 1 μM and 10 μM TSA for 1 hour increased the abundance of acetylated α-tubulin 6- and 5.7-fold respectively (**Figure 4.11**). Therefore, treatment with TSA enhanced the levels of α-tubulin acetylation in HEK cells in a time-dependent, but not concentration-dependent manner. This is in agreement with the results from sperm that show the slight effects of 1 μM TSA on motility and α-tubulin acetylation were not enhanced by increasing the concentration of TSA to 10 μM. The findings from HEK cells also demonstrate that the treatment periods and concentrations of TSA used on sperm were sufficient to elicit a significant response in a control cell line.

In addition to HEK cells, spermatids were also used to compare the effect of TSA on α-tubulin acetylation in developing spermatozoa. Treatment with 1 μM TSA for 1 and 3 hours did not affect the abundance of acetylated α-tubulin, and Western blots also showed that spermatids and sperm had high basal levels of acetylated α-tubulin in control samples compared to HEK cells (**Figures 4.12 and 4.13**). This was in accordance with the findings described in the previous chapter, and is also consistent with the hypothesis that sperm insensitivity to HDAC inhibition may result from the high baseline level of α-tubulin acetylation. Therefore, subsequent experiments investigated this notion by examining deacetylase activity.

4.3.2 Deacetylase activity in sperm

As it was postulated that sperm α-tubulin may be maximally acetylated, and therefore insensitive to HDAC6 inhibition, levels of acetylated α-tubulin were compared between untreated sperm and HEK cells. The abundance of acetylated α-tubulin was approximately 6-fold higher in sperm than HEK cells when the same mass of protein from each cell type was analysed by Western blot (**Figure 4.14**). In addition, comparison of the levels of acetylated α-tubulin and total α-tubulin in untreated sperm indicated that all of the α-tubulin present was acetylated (**Figure 4.14e**). Levels of acetylated α-tubulin were slightly elevated above that of total α-tubulin, which may be a result of the semi-quantitative nature of Western blots. The

results from these experiments therefore provided evidence that sperm exhibit high levels of α-tubulin acetylation compared to other cell types.

The strong α-tubulin acetylation suggested that deacetylation of α-tubulin may not be taking place, and so the activity of sperm deacetylases was measured fluorometrically, in the presence or absence of HDAC inhibitors, using a cell-permeable HDAC substrate. The results showed that firstly, deacetylase activity was detectable in sperm, and secondly, this activity could be reduced by treatment with HDAC inhibitors (**Figure 4.15b**). Exposure to the HDAC6-specific inhibitor, tubacin, led to a decrease in deacetylase activity of approximately one third when compared to vehicle-treated sperm, indicating that HDAC6 is active in murine sperm, and can be inhibited. In addition, sperm exhibited approximately 45% less deacetylase activity following treatment with TSA when compared to control, confirming the activity of Class I and II HDACs, and indicating that TSA is able to inhibit HDACs in sperm. Whilst the results of the assay did not reach statistical significance, the reductions in deacetylase activity following treatment with HDAC inhibitors were reproducible in three independent experiments. Furthermore, the results are consistent with findings from Parab *et al.* who demonstrated a significant reduction in HDAC activity in sperm lysates following treatment with TSA and the HDAC6-specific inhibitor, tubastatin A (Parab *et al.*, 2015). Whilst the published findings show inhibition of HDACs in sperm lysates, the work reported in this thesis importantly demonstrates that HDAC6 activity can be inhibited in intact sperm, which has not been shown in this manner previously. The increased inhibition of activity by TSA over that of tubacin also intimated the potential presence of other active HDACs. However, additional inhibitor studies would be required to determine whether this was the case; for example, treatment with a HDAC inhibitor such as sodium butyrate to which HDAC6 is resistant would aid in distinguishing between the effects of different HDACs. Overall, the results demonstrated that activity of HDAC6 (and potentially other HDACs) is detectable in murine sperm; however the high baseline levels of α-tubulin acetylation suggests that this activity is low.

HEK cells were also subjected to HDAC inhibitor treatments with subsequent fluorometric measurement of HDAC activity as a control for the assay. Whilst the results obtained for HEK cells and sperm cannot be directly compared due to differences in cell numbers used for the assay, the findings with HEK cells were consistent with the results from sperm in that detectable levels of HDAC activity were measured. Additionally, treatment with HDAC inhibitors resulted in a reduction in deacetylase activity in HEK cells; decreases of 9% and 29% were found following exposure to TSA and tubacin, respectively (**Figure 4.15c**). This demonstrated the activity of HDAC6 in HEK cells, and showed that the HDAC could be inhibited with a detectable reduction in activity. However, given the significant effect of TSA and tubacin treatment on levels of α-tubulin acetylation demonstrated by Western blot, the extent of the reduction in deacetylase activity measured by the assay was smaller than expected in the presence of these inhibitors. As the HDAC activity assay procedure included a 2 hour period immediately prior to the measurement of fluorescence in which cells were incubated in the absence of inhibitors, it was hypothesised that HDAC activity could have recovered in this time. This notion was subsequently confirmed by the finding that the substantial increase in acetylated α-tubulin in HEK cells immediately following treatment with TSA for 1 hour reduced in extent over a 3 hour period when the inhibitor was removed (**Figure 4.16**). This indicated the recovery of HDAC activity in this cell line and suggested that the activity measured by the assay may have been lower if the inhibitor was present throughout the whole assay. A sperm HDAC recovery experiment was not possible using the same methods as a result of the insensitivity of sperm to HDAC inhibitors; the acetylation state of sperm α-tubulin is unchanged by the presence of HDAC inhibitors and so monitoring acetylation could not be used as an indicator of HDAC recovery. However, the results from HEK cells may also be applicable to sperm as the assay is not cell-type dependent; the behaviour of the same protein was measured by the assay, and the same inhibitors were tested on both cell types. Therefore, sperm HDACs may also have recovered activity in the time frame of the assay resulting in levels of measured deacetylase activity that were higher than if the inhibitors were present

throughout the assay. Future experiments could seek to clarify the level to which inhibitors of HDACs can lower deacetylase activity in sperm by measuring activity in their presence. Nevertheless, the findings show that sperm exhibit detectable levels of HDAC activity, which can be lowered by treatment with tubacin and TSA.

4.3.3 Conclusions

The results presented in this chapter demonstrate the detection of HDAC6 activity in murine sperm. However, the high baseline levels of acetylated α-tubulin in sperm, and the insensitivity of sperm α-tubulin to treatment with TSA/tubacin suggested that the activity of HDAC6 was low. Therefore, the maintenance of sperm α-tubulin in such a highly acetylated state may be a consequence of the low HDAC6 activity, with important implications for sperm functionality. As α-tubulin acetylation has been shown to be a marker of microtubule stability, it was postulated that this stability may be a requirement for normal sperm function. To investigate this hypothesis, sperm microtubules were subjected to treatment with a destabilising drug, and the consequences for sperm structure and motility were examined; the results of these investigations are discussed in the following chapter.

Chapter 5

Chapter 5 – The role of microtubule stability in sperm motility

5.1 Introduction

The findings reported in the previous chapter demonstrated that murine sperm exhibit detectable levels of HDAC6 activity and concurrent high baseline levels of acetylated α-tubulin. These results, interpreted alongside the finding of sperm insensitivity to HDAC inhibitor treatments, suggest low HDAC6 activity in sperm and as a result, maximal acetylation of sperm α-tubulin. This highly acetylated state of sperm α-tubulin may therefore serve an important purpose in the maintenance of normal sperm function. However, the mechanisms through which α-tubulin acetylation contributes to sperm function are currently unknown.

Research in other cell lines has indicated a link between the presence of acetylated α-tubulin and microtubule stability. Webster and Borisy reported that acetylated α-tubulin accumulated in stable, long-lived microtubules (Webster and Borisy, 1989), whilst others found that microtubule acetylation could aid in resistance to cold-induced depolymerisation (Cambray-Deakin and Burgoyne, 1987). Furthermore, chemical stabilisation of microtubules in fibroblasts enhanced the number of acetylated microtubules (Palazzo, Ackerman and Gundersen, 2003). These studies all contribute to the widely-accepted notion that acetylation acts as a marker of stable microtubules. Therefore, the highly acetylated state of α-tubulin in sperm suggests that dynamic instability does not occur in sperm microtubules to a significant degree. The stability of the microtubules may therefore be important for the regulation of sperm functions such as motility, in which the microtubules play a central role.

5.1.1 Aims

The main aim of the experiments reported in this chapter was to investigate whether microtubule stability plays a role in the regulation of sperm motility. Therefore, murine sperm

were treated with nocodazole with the aim of destabilising the microtubules, and the effects on sperm motility were examined. In addition, the consequences of nocodazole treatment for α-tubulin organisation and acetylation in sperm were also assessed.

5.2 Results

5.2.1 Impact of nocodazole treatment on murine sperm

5.2.1.1 Nocodazole alters murine sperm motility parameters

To initially determine whether a response to nocodazole could be detected in sperm, preliminary experiments were carried out in which murine sperm were treated with 5, 10 and 25 µM nocodazole for 3 hours and assessed using CASA. The results demonstrated alterations to sperm motility parameters following exposure to 25 µM nocodazole, and so this concentration was used in subsequent experiments. **Figure 5.1** shows the mean motility parameters from five independent experiments in which sperm were treated with 25 µM nocodazole for 3 hours during capacitation. Treatment with nocodazole led to significant increases of approximately 26% ($P < 0.05$), 25% ($P < 0.05$), and 21% ($P < 0.01$) in curvilinear velocity, average path velocity, and amplitude of lateral head displacement, respectively when compared to vehicle controls using an unpaired T-test. Straight line velocity and beat cross frequency were also increased by nocodazole treatment, whereas straightness, linearity and wobble exhibited small reductions, though these changes did not reach statistical significance (**Figure 5.1**). The percentages of sperm exhibiting hyperactivated and progressive motility (**Figure 5.2**) were both approximately 5% higher in the nocodazole-treated group compared to vehicle-treated sperm; the increase in progressive motility was enhanced significantly when compared using an unpaired T-test ($P < 0.05$). The results demonstrated that nocodazole treatment exerted an influence on murine sperm motility parameters.

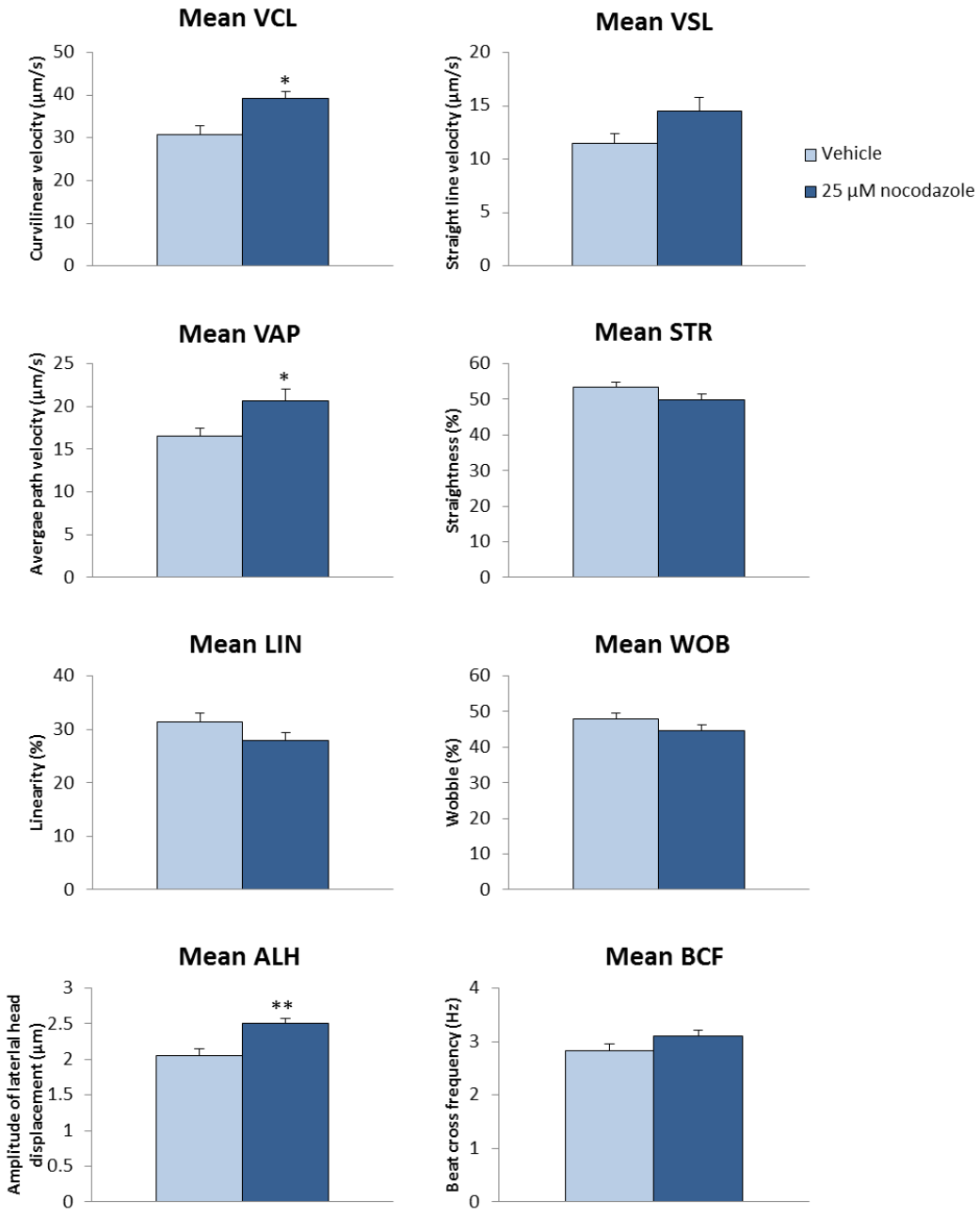

Figure 5.1: Motility parameters following treatment of sperm with nocodazole for 3 hours during capacitation.

Epididymal sperm were treated with vehicle or 25 µM nocodazole for 3 hours, and motility characteristics were assessed using computer-assisted sperm analysis. Sperm treated with nocodazole exhibited significant increases in VCL – curvilinear velocity, VAP - average path velocity and ALH - amplitude of lateral head displacement; whilst STR - straightness, LIN - linearity and WOB – wobble decreased slightly. VSL - straight line velocity and BCF - beat cross frequency exhibited small increases in response to nocodazole when compared to control. Values are mean ± SEM, n=5, compared by unpaired T-test, *$P < 0.05$, **$P < 0.01$.

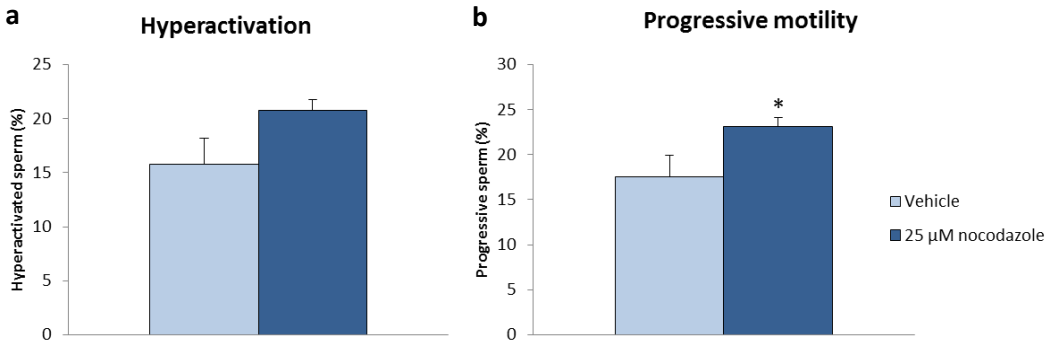

Figure 5.2: Hyperactivation and progressive motility in sperm following treatment with nocodazole for 3 hours during capacitation.

Analysis of sperm motility following treatment with vehicle and 25 µM nocodazole for 3 hours showed the percentage of sperm exhibiting (a) hyperactivated and (b) progressive motility was higher in the nocodazole-treated group. Hyperactivated sperm are shown as a percentage of the total motile sperm; progressive sperm are shown as a percentage of total sperm in the analysed sample. Values shown are mean ± SEM, n=5, compared by unpaired T-test, *$P < 0.05$.

5.2.1.2 Nocodazole alters sperm motility in viscous media

A Kremer assay was used to investigate whether nocodazole treatment altered sperm motility in conditions mimicking the female reproductive tract by assessing the ability of sperm to penetrate artificial mucus. For a schematic illustration of the experimental procedure, see **Chapter 3, Figure 3.5a**. Sperm were treated with 25 μM nocodazole for 3 hours during capacitation, and subsequently examined for their ability to penetrate artificial mucus in 1 hour. Overall, the mean number of sperm reaching a distance of 1 cm was less than the mean number of sperm entering the viscous media at 0 cm by approximately 17% and 31% in vehicle- and nocodazole-treated conditions respectively (**Figure 5.3**). Assessment of the effects of nocodazole demonstrated that treatment for 3 hours resulted in a significant increase in the mean number of sperm entering the media at 0 cm when compared to control using an unpaired T-test ($P < 0.05$). The mean number of sperm progressing to 1 cm was also higher in the nocodazole-treated group, however this was not statistically significant (**Figure 5.3**). These results demonstrate that exposure to nocodazole significantly enhanced the ability of sperm to swim in viscous media, suggesting that the drug could influence motility patterns required for navigation of the female reproductive tract.

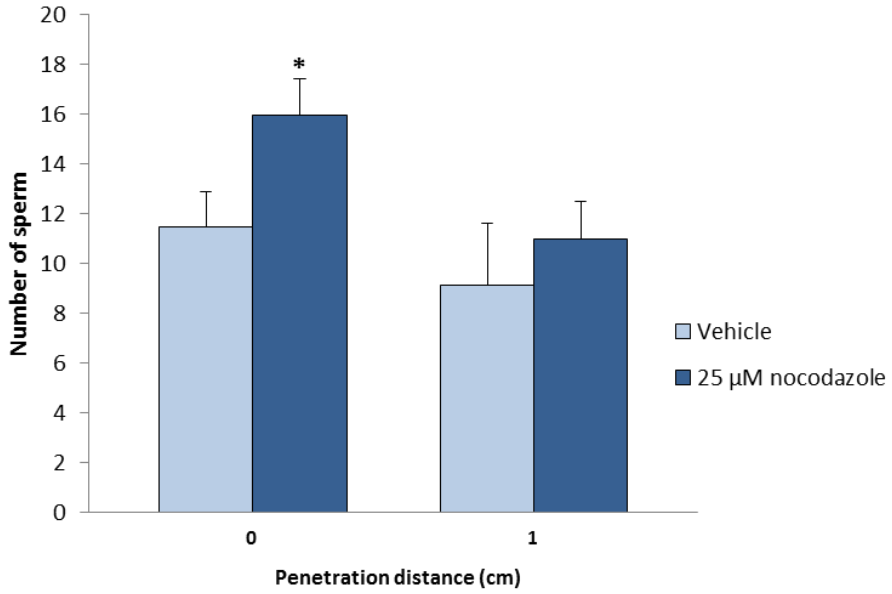

Figure 5.3: Penetration distance of sperm in viscous media following treatment with nocodazole for 3 hours during capacitation.

Sperm treated with vehicle or 25 µM nocodazole for 3 hours were assessed for their ability to enter and penetrate viscous media. The mean number of sperm entering the media at 0 cm and penetrating to 1 cm was increased by treatment with nocodazole. Values shown are mean ± SEM, n=6, compared by unpaired T-test, *$P < 0.05$.

5.2.1.3 Organisation of α-tubulin in sperm microtubules is not visibly affected by nocodazole

As changes to sperm motility parameters were exhibited in the presence of nocodazole, immunofluorescence analysis was used to investigate the action of the drug on microtubule structure by assessing the organisation of α-tubulin. **Figure 5.4** shows representative images of sperm labelled for α-tubulin following treatment with vehicle (**Figure 5.4a**), 25 μM nocodazole (**Figure 5.4b**), or 1 μM TSA as a control (**Figure 5.4c**) for 3 hours. Sperm treated with nocodazole and TSA were not observed to display any changes to the gross microtubule organisation in the sperm tail; microtubule structures appeared to remain intact and were comparable to that of vehicle-treated sperm. To control for the effects of the drug, HEK-MSR cells were also treated with vehicle, 25 μM nocodazole, or 1 μM TSA for 3 hours, labelled for α-tubulin, and visualised using immunofluorescence. Cells treated with 1 μM TSA (**Figure 5.4f**) exhibited α-tubulin organisation that was comparable to vehicle-treated cells (**Figure 5.4d**), with microtubule polymers observed in all cells examined. In contrast, following treatment of HEK-MSR cells with 25 μM nocodazole, microtubule polymer structures were lost, and punctate aggregates of α-tubulin were visible throughout the cytoplasm of cells (**Figure 5.4e**). The representative image in **Figure 5.4e** also shows aggregates of α-tubulin, which may correspond to abnormal spindle formation.

Overall, α-tubulin organisation and microtubule structure in HEK cells was severely disrupted following treatment with 25 μM nocodazole for 3 hours. This contrasted with the effects of nocodazole on sperm microtubules and suggests that nocodazole does not cause the complete disassembly of sperm microtubules. Instead, nocodazole may influence sperm motility parameters via subtle changes in the microtubule structure that were not detectable using this methodology.

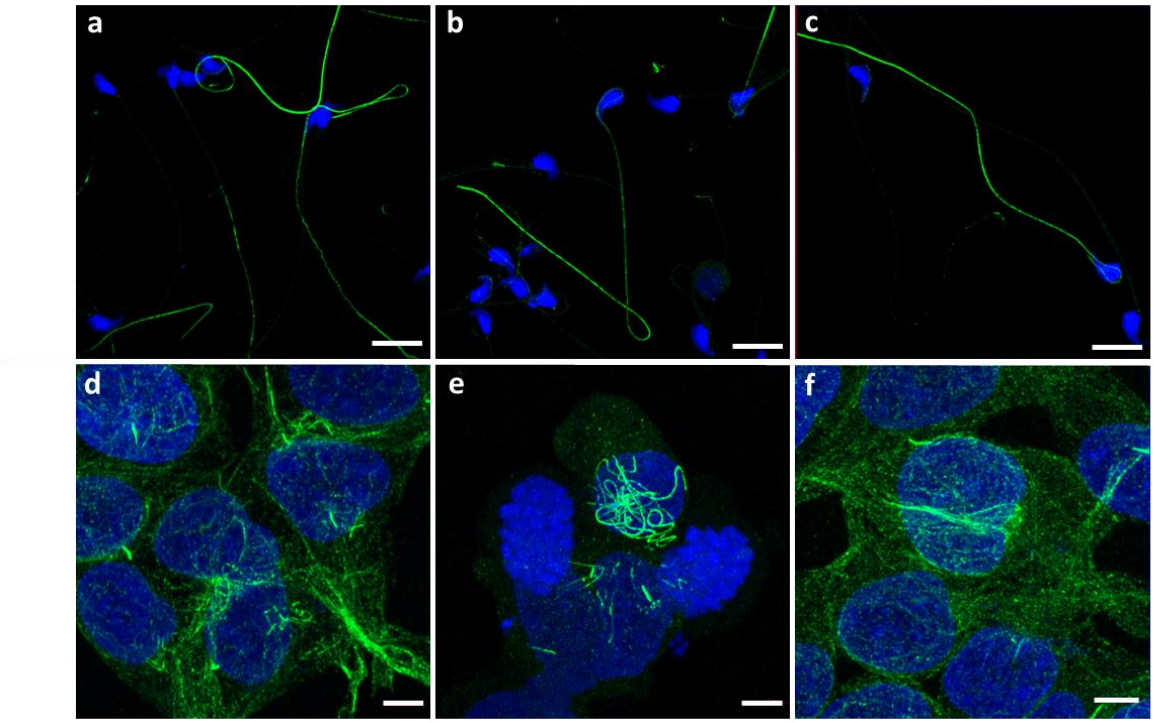

Figure 5.4: Immunofluorescence examination of α-tubulin localisation in sperm and HEK-MSR cells following treatment with nocodazole.

Sperm and HEK-MSR cells were treated with either (a, d) vehicle, (b, e) 25 µM nocodazole, or (c, f) 1 µM TSA for 3 hours and were labelled with α-tubulin antibody (green) and DAPI (blue) for nuclei staining. Sperm treated with nocodazole and TSA exhibited α-tubulin labelling comparable to that of vehicle-treated sperm. HEK-MSR cells exhibited substantial disruption to α-tubulin localisation and microtubule structure following treatment with 25 µM nocodazole when compared to vehicle-treated cells. Organisation of α-tubulin in HEK cells treated with TSA appeared comparable to control. Images are representative of two independent experiments. Scale bars: sperm – 10 µm; HEK cells – 5 µm.

As analysis of the sperm tail by immunofluorescence did not show any changes to the organisation of α-tubulin following treatment with nocodazole, TEM was employed for a higher resolution examination of the sperm axoneme structure. **Figure 5.5** shows representative electron micrographs of transverse and longitudinal sections through the sperm tail following 3 hour treatments with vehicle (**Figure 5.5a, d**), nocodazole (**Figure 5.5b, e**) and TSA (**Figure 5.5c, f**). The location and structure of sperm axoneme components were observed to be comparable across the conditions; microtubules occupied their central position in the axoneme and maintained their characteristic 9+2 arrangement even in the presence of nocodazole. This indicated that the microtubule depolymerising drug did not disrupt microtubule organisation in the sperm flagellum which is in agreement with the results from the immunofluorescence analysis (**Figure 5.4**). These findings therefore suggest that nocodazole exerted its influence upon sperm motility via a mechanism other than microtubule depolymerisation.

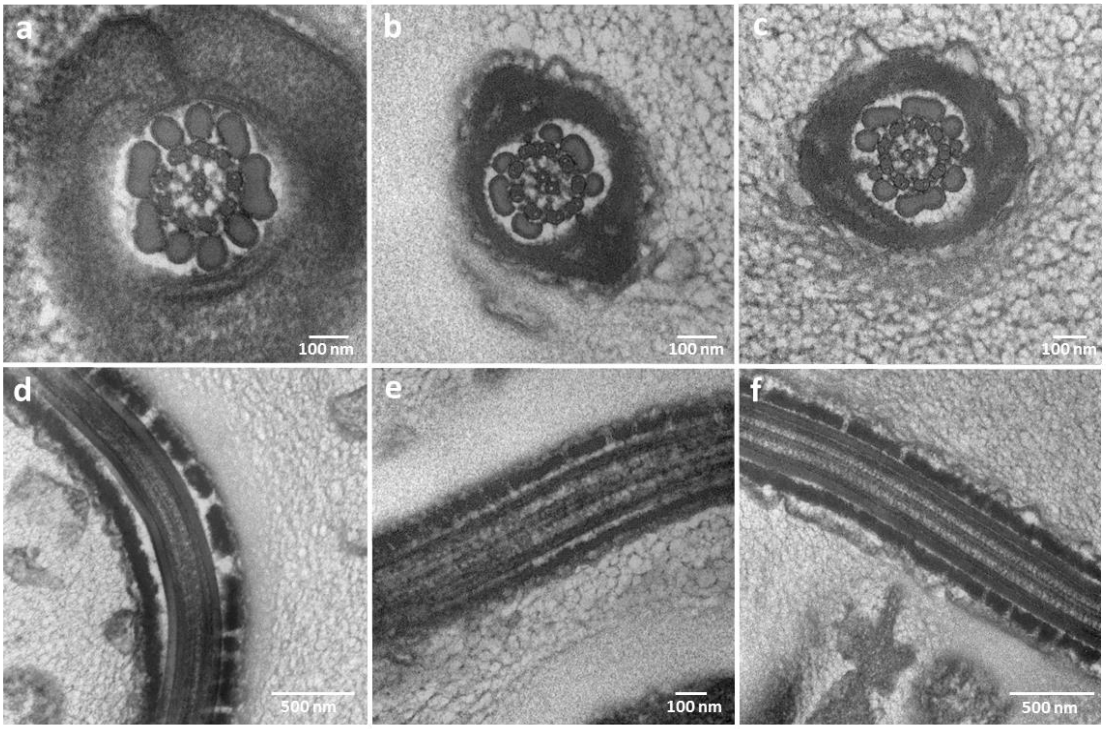

Figure 5.5: Transmission electron micrographs examining the ultrastructure of the murine sperm tail following treatment with nocodazole.

Sperm were treated with either vehicle (a, d), 25 µM nocodazole (b, e), or 1 µM TSA (c, f) for 3 hours during capacitation and were fixed for examination of their axonemal structures using transmission electron microscopy. Micrographs of transverse (a-c) and longitudinal (d-f) sections through the sperm tail revealed that the ultrastructure was comparable across all conditions, with microtubules maintaining a 9+2 arrangement, and accessory structures unaffected following treatment with nocodazole and TSA.

5.2.1.4 Levels of acetylated α-tubulin in sperm are unaffected by nocodazole

The findings from experiments detailed so far demonstrated that treatment with nocodazole altered sperm motility parameters, but did not lead to any demonstrable effects on the sperm microtubule structure when assessed using confocal microscopy. As no change in the organisation of α-tubulin was detected by immunofluorescence, sperm were analysed by Western blot to determine whether the acetylation state of α-tubulin was influenced by exposure to nocodazole. **Figure 5.6a** shows a representative Western blot with sperm lysates from two independent experiments in which sperm were treated with 25 μM nocodazole for 3 hours, and demonstrates that acetylation of α-tubulin appears comparable between vehicle- and nocodazole-treated sperm. Bands at approximately 55 kDa corresponding to acetylated α-tubulin were subject to densitometric analysis; **Figure 5.6c** shows the mean results from five sets of lysates. The data demonstrate a small, non-significant 0.2-fold increase in the abundance of acetylated α-tubulin following treatment with nocodazole when compared to control. Reprobing blots for total α-tubulin and subsequent densitometric analysis of bands at approximately 55 kDa showed that the abundance of α-tubulin was also slightly increased in the nocodazole-treated condition (**Figure 5.6d**). Therefore, a slight increase in the protein loaded onto the gel in this condition could account for the elevation in acetylated α-tubulin abundance. A representative blot demonstrating total α-tubulin abundance is shown in **Figure 5.6b**. The results therefore demonstrate that nocodazole did not exert a significant influence on the levels of α-tubulin acetylation in sperm.

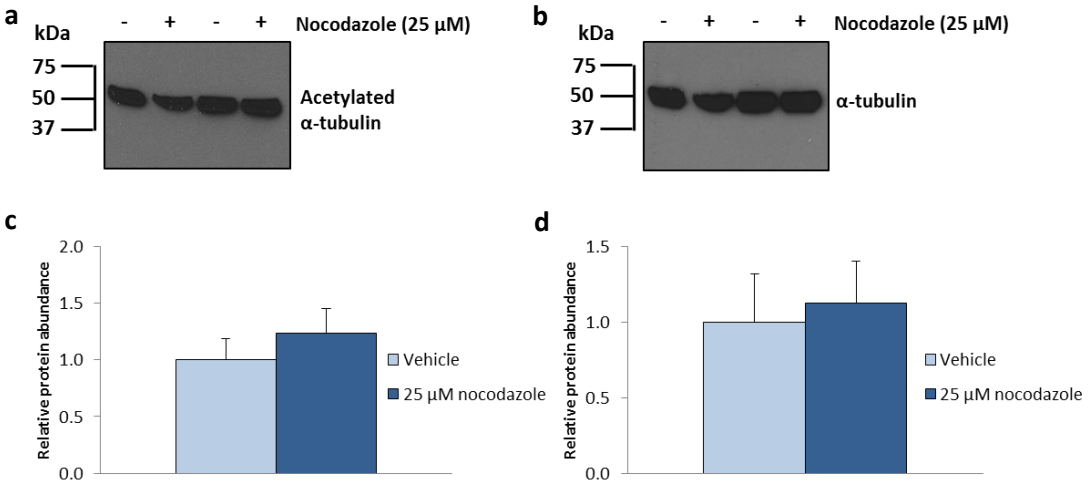

Figure 5.6: Acetylation of α-tubulin in sperm following treatment with nocodazole for 3 hours during capacitation.

(a) Representative Western blot of acetylated protein from sperm treated with either vehicle or 25 µM nocodazole for 3 hours in 2 independent experiments. Protein from approximately 0.5 million sperm was loaded in each lane. Bands at approximately 55 kDa correspond to acetylated α-tubulin. (b) All blots were reprobed for total α-tubulin as a loading control; bands at approximately 55 kDa correspond to α-tubulin. (c) Bar graph shows densitometric analysis of bands corresponding to acetylated α-tubulin (n=5). (d) Bar graph shows densitometric analysis of bands corresponding to total α-tubulin (n=5). Values are shown as mean ± SEM and were compared using an unpaired T-test.

5.2.1.5 Treatment with nocodazole reduces levels of acetylated α-tubulin in HEK-MSR cells

In contrast to sperm where microtubule structure was unchanged by nocodazole treatment, α-tubulin organisation in HEK-MSR cells was severely disrupted following exposure to nocodazole. Therefore, the effect of nocodazole upon the levels of acetylated α-tubulin in HEK cells was examined. **Figure 5.7a** shows the results from Western blot analysis of lysates from HEK cells treated with 25 μM nocodazole for 3 hours in three independent experiments. The blot demonstrated a reduction in the abundance of acetylated α-tubulin following treatment with nocodazole. This finding was confirmed by the densitometric analysis of bands at approximately 55 kDa corresponding to acetylated α-tubulin as shown in **Figure 5.7c**. This analysis demonstrated that treatment with nocodazole led to a significant 10-fold reduction in acetylated α-tubulin in HEK-MSR cells as analysed using an unpaired T-test ($P < 0.001$). Reprobing the blot for total α-tubulin demonstrated a slight reduction in the level of α-tubulin in the nocodazole-treated condition compared to control, however this was not significant (**Figure 5.7b, d**). These results indicate that the disruption of α-tubulin organisation observed in HEK cells upon treatment with nocodazole is accompanied by a reduction in the abundance of acetylated α-tubulin.

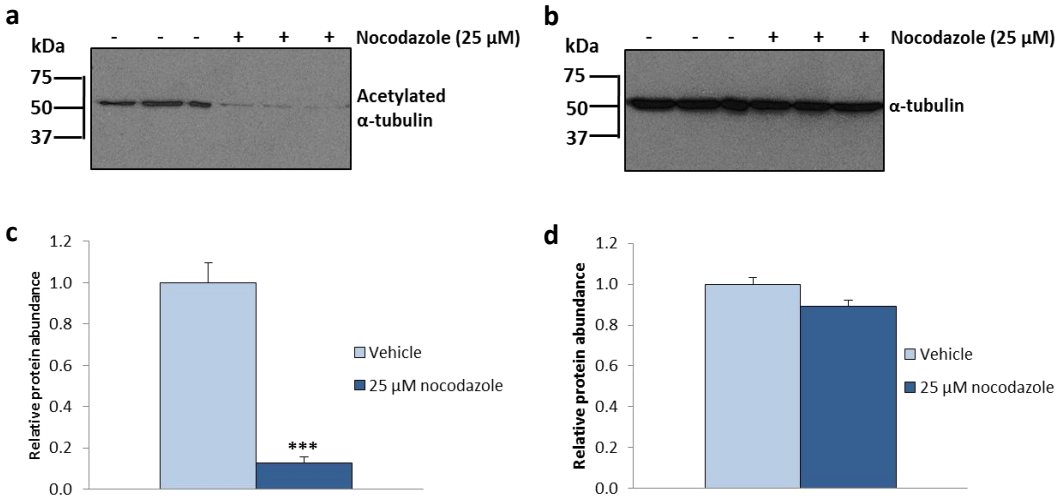

Figure 5.7: Acetylation of α-tubulin in HEK-MSR cells following treatment with nocodazole for 3 hours.

(a) Representative Western blot of acetylated protein from HEK-MSR cells treated with 25 µM nocodazole for 3 hours. Approximately 20 µg of protein was loaded into each lane. Bands at approximately 55 kDa correspond to acetylated α-tubulin. (b) All blots were reprobed for total α-tubulin as a loading control; bands at approximately 55 kDa correspond to α-tubulin. (c) Bar graph shows densitometric analysis of bands corresponding to acetylated α-tubulin in HEK cells treated with 25 µM nocodazole for 3 hours (n=3). (d) Bar graph shows densitometric analysis of bands corresponding to α-tubulin in HEK cells treated with 25 µM nocodazole for 3 hours (n=3). Values shown are mean ± SEM and were compared by unpaired T-test, ***$P < 0.001$.

5.2.1.6 Levels of acetylated α-tubulin in spermatids are unaffected by nocodazole

As an indication of the response of microtubules to nocodazole in developing sperm for control purposes, spermatids were assessed for levels of acetylated α-tubulin following treatment with nocodazole. **Figure 5.8a** shows a representative Western blot following analysis of lysates from spermatids treated with 25 μM nocodazole for 3 hours in two independent experiments. The blot and subsequent densitometric analysis of bands at approximately 55 kDa from three experiments demonstrated that the abundance of acetylated α-tubulin was only very slightly reduced by treatment with nocodazole, and this change was not significant (**Figure 5.8a, c**). Western blots were reprobed for total α-tubulin, which demonstrated that levels of α-tubulin were comparable between vehicle- and nocodazole-treated spermatid lysates (**Figure 5.8b, d**). The results demonstrated that the level of α-tubulin acetylation in spermatids was not significantly affected by treatment with nocodazole which is in accordance with the findings in sperm. Therefore, whilst sperm exhibited changes to motility parameters in response to nocodazole, α-tubulin organisation in sperm, and α-tubulin acetylation in sperm and spermatids were unaffected by the treatment.

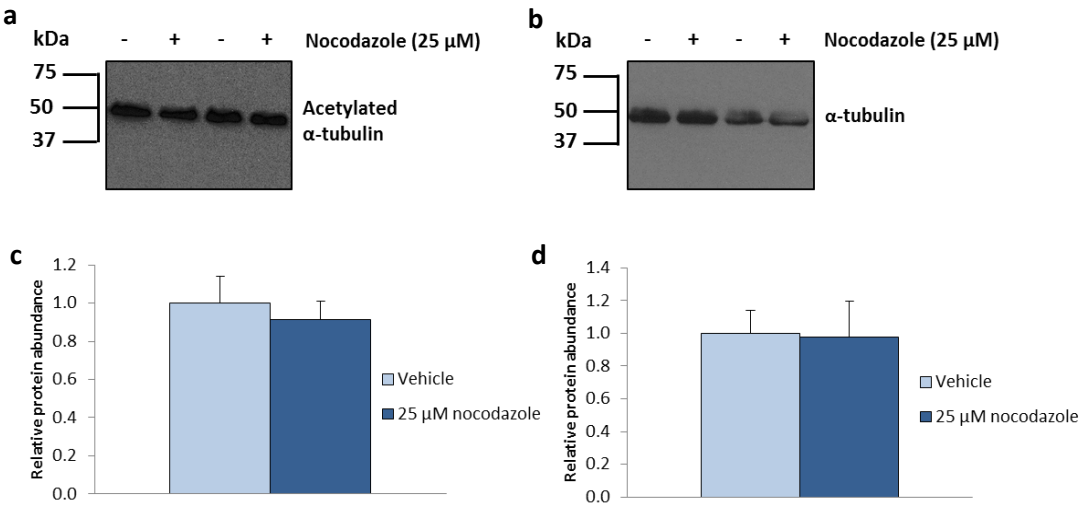

Figure 5.8: Acetylation of α-tubulin in spermatids following treatment with nocodazole for 3 hours.

(a) Representative Western blot of acetylated protein from spermatids treated with 25 µM nocodazole for 3 hours in two independent experiments. Approximately 20 µg of protein was loaded into each lane. Bands at approximately 55 kDa correspond to acetylated α-tubulin. (b) All blots were reprobed for total α-tubulin as a loading control; bands at approximately 55 kDa correspond to α-tubulin. (c) Bar graph shows densitometric analysis of bands corresponding to acetylated α-tubulin in spermatids treated with 25 µM nocodazole for 3 hours (n=3). (d) Bar graph shows densitometric analysis of bands corresponding to α-tubulin in spermatids treated with 25 µM nocodazole for 3 hours (n=3). Values are shown as mean ± SEM, and were compared by unpaired T-test.

5.3 Discussion

The findings reported in the preceding chapters demonstrated that sperm exhibit high baseline levels of acetylated α-tubulin, and whilst HDAC6 activity is detectable, the insensitivity of sperm to treatment with HDAC inhibitors indicates that this activity is low. As acetylation of α-tubulin is linked with microtubule stability, the main aim of the experiments detailed in this chapter was to examine whether the stability of sperm microtubules was an important factor in the regulation of sperm motility.

To investigate this hypothesis, sperm were exposed to nocodazole for 3 hours, and motility parameters were assessed. Treatment with nocodazole resulted in a significant increase in certain sperm motility parameters, namely curvilinear velocity, average path velocity, and amplitude of lateral head displacement (**Figure 5.1**). Changes to the velocity parameters indicated an increase in swimming speed in response to nocodazole, whilst the increase in ALH indicated that the drug induced a stronger bend in the proximal region of the sperm tail (Mortimer, 2000). The increase in velocity was also apparent upon assessment of progressive motility; the percentage of sperm exhibiting progressive motility was significantly higher in the nocodazole-treated condition compared to vehicle-treated sperm (**Figure 5.2b**). In addition, as both curvilinear velocity and amplitude of lateral head displacement were increased by nocodazole and are motility parameters involved in determining hyperactivation, it follows that the percentage of sperm exhibiting hyperactivation was higher in the nocodazole-treated condition compared to the vehicle-treated group (**Figure 5.2a**). Whilst this result was not statistically significant, it seemed to be biologically relevant as demonstrated by the significant increase in the number of sperm that were able to enter viscous media following exposure to nocodazole during the Kremer assay (**Figure 5.3**). As murine sperm are able to move through viscoelastic substances more easily when hyperactivated (Suarez and Dai, 1992), the increase in hyperactivation may play a part in the enhanced ability of nocodazole-treated sperm to enter the viscous media. The number of sperm able to penetrate to 1 cm in the media was also

increased following exposure to nocodazole which further indicates that nocodazole influenced the ability of sperm to navigate the artificial mucus. Overall, the results from the motility assessments demonstrated that treatment with nocodazole altered sperm motility parameters; these effects are summarised in **Figure 5.9a**. This suggested that the stability of the sperm microtubule structure may play an important regulatory role in sperm motility. Whilst others have postulated that an increase in microtubule stability may lead to lower flagellar motility (Parab *et al.*, 2015), this is the first study to demonstrate that sperm motility can be influenced by the direct application of nocodazole.

As treatment with nocodazole was found to influence sperm motility, the effect of the drug on the organisation of α-tubulin in the sperm tail was examined to determine the extent to which treatment disrupted microtubule structure. Unexpectedly, visualisation of α-tubulin using immunofluorescence showed that the microtubules remained intact throughout the flagellum in nocodazole-treated sperm, and α-tubulin organisation was comparable to that of vehicle- and TSA-treated sperm (**Figure 5.4 a-c**). In accordance with these findings, higher resolution examination of the sperm tail following treatment with nocodazole using TEM revealed that sperm maintained their characteristic 9+2 microtubule arrangement, with the location and structure of all axoneme components remaining comparable to control in the presence of the depolymerising drug (**Figure 5.5**). The maintenance of normal microtubule structures in the sperm contrasted significantly with the results from the immunofluorescence analysis of HEK cells following treatment with 25 μM nocodazole for 3 hours. Exposure to nocodazole completely disrupted the HEK cell microtubule network when compared to vehicle- and TSA-treated cells, leaving only aggregates of disordered α-tubulin (**Figure 5.4 d-f**). The findings in HEK cells demonstrated that a nocodazole concentration of 25 μM and a 3 hour treatment period were sufficient to cause depolymerisation of microtubules in HEK cells. The lack of α-tubulin disruption found in sperm following nocodazole treatment therefore suggests that sperm microtubules may be resistant to disassembly in the presence of a depolymerising drug. Indeed, research has suggested that acetylated microtubules are much more resistant to

disassembly by depolymerizing drugs than non-acetylated microtubules (LeDizet and Piperno, 1986). However, the ability of nocodazole to influence sperm motility parameters suggests that treatment may have affected an aspect of microtubule function, or caused partial destabilisation. Although the possibility exists that limitations in the resolving power of the microscopes may have prevented visualisation of changes to sperm α-tubulin organisation, the substantial effect that nocodazole exerted upon the gross microtubule structure in HEK cells was clearly visible using immunofluorescence, suggesting similar changes to sperm microtubules would have been observed using this methodology. Therefore, it appears that sperm microtubules may be resistant to the depolymerising effects of nocodazole.

The difference in the response of sperm and HEK cell microtubules to nocodazole identified by immunofluorescence is also mirrored by the variation in α-tubulin acetylation following treatment, as assessed biochemically. Western blot analysis of sperm and HEK cells treated with 25 μM nocodazole for 3 hours demonstrated that acetylation of α-tubulin persisted in nocodazole-treated sperm to levels matching that of controls (**Figure 5.6**, and summarised in **Figure 5.9**), whereas HEK cells exhibited an approximate 10-fold reduction in the abundance of acetylated α-tubulin (**Figure 5.7**). These results indicated that the levels of acetylated α-tubulin in sperm were not affected by treatment with nocodazole, suggesting that this aspect of microtubule structure was not significantly disrupted by the drug, supporting the findings from immunofluorescence and TEM analysis. Since acetylation is deemed to be a marker of microtubule stability (Janke and Montagnac, 2017), it seems that exposure to nocodazole did not lead to the depolymerisation of sperm microtubules as the treatment did in HEK cells. Similarly, Western analysis of spermatids treated with 25 μM nocodazole for 3 hours also showed that nocodazole did not significantly affect the abundance of acetylated α-tubulin in this cell type (**Figure 5.8**). This finding suggests that, like sperm, microtubule structure in spermatids may not have been disrupted by nocodazole treatment. However, analysis of α-tubulin organisation in spermatids would be required to determine whether the structure of

the microtubule network was affected by treatment with nocodazole. Nevertheless, if acetylation of α-tubulin signifies microtubule stability, the microtubules of both developing and mature murine sperm appear to be resistant to destabilisation following a 3 hour treatment with 25 μM nocodazole, in contrast to the complete microtubule depolymerisation observed in HEK cells following treatment.

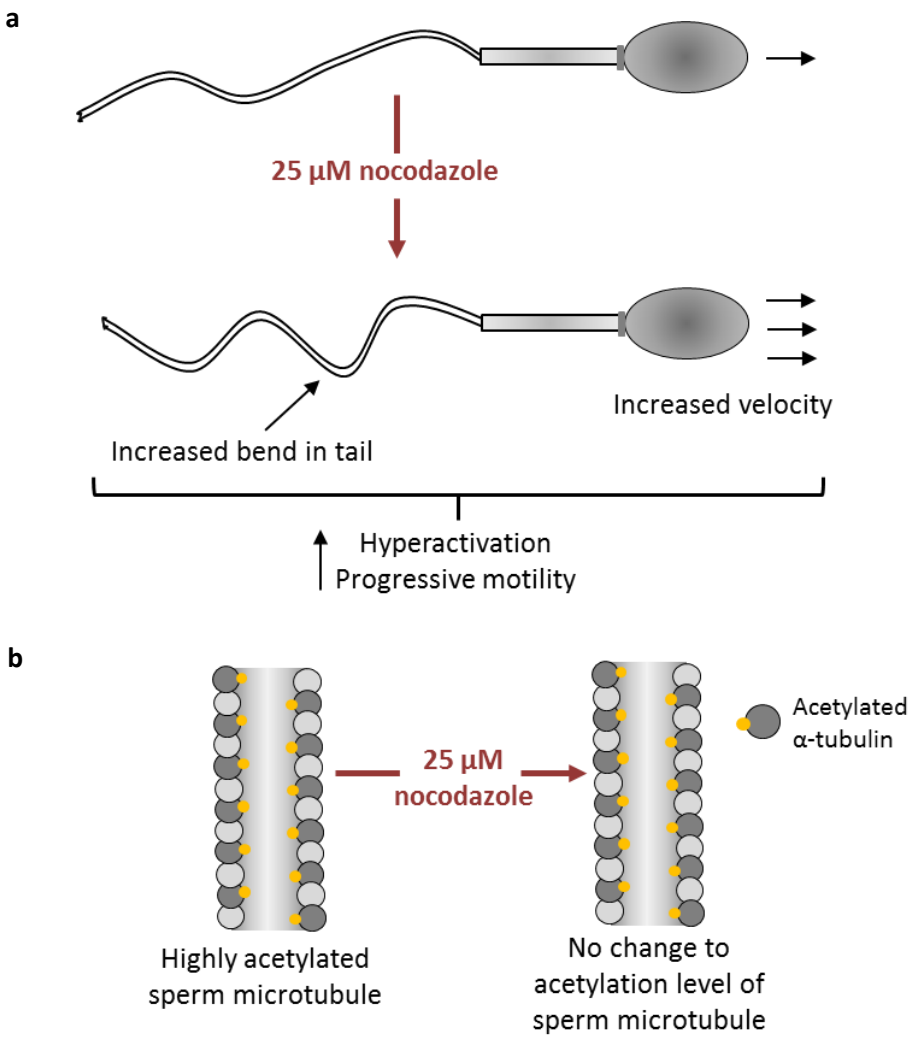

Figure 5.9: Summary schematic illustrating the effects of nocodazole on sperm motility and acetylated α-tubulin.

(a) Murine sperm treated with 25 µM nocodazole for 3 hours during capacitation exhibited significant increases in curvilinear velocity, average path velocity, and amplitude of lateral head displacement, resulting in a rise in hyperactivation, and a significant increase in progressive motility. (b) Treatment with nocodazole did not have any effect on the high levels of acetylated α-tubulin in the sperm, suggesting that microtubule structure was not disrupted by the treatment to a great extent.

5.3.1 Conclusions

Overall, the results described in this chapter demonstrated the novel finding that treatment with the microtubule depolymerising drug, nocodazole, influenced murine sperm motility parameters, inducing an increase in velocity and a stronger bend in the tail, culminating in increased progressive and hyperactive motility. Furthermore, these changes in motility characteristics in the presence of nocodazole may have important biological significance as indicated by the enhancement of sperm motility in artificial mucus. Interestingly, treatment with nocodazole did not cause the complete disassembly of sperm microtubules as it did in HEK-MSR cells, nor did exposure to the drug affect the levels of α-tubulin acetylation in sperm. Therefore, the mechanisms through which nocodazole exerted its influence upon sperm motility parameters are unclear; further discussion of this point follows in the next chapter.

Chapter 6

Chapter 6 – Discussion and future work

6.1 Background and aims

Microtubules, made up of protofilaments of α- and β-tubulin heterodimers which assemble laterally to form tubes, are a central component of the sperm axoneme, a cytoskeletal structure present in cilia and flagella. Components of the axoneme underpin the mechanical mechanism of sperm motility; adjacent microtubule doublets interact via dynein arms which are activated in response to intracellular rises in Ca^{2+}, cAMP and ATP as a result of external cues such as an increase in pH. Subsequent activity of the dynein ATPase results in the generation of a power stroke by the dynein arms, causing the microtubules to slide past one another, creating a bend in the flagellum (Turner, 2006). Therefore, microtubules play a central role in motility; however, the mechanisms involved in the regulation of microtubule function are not well understood. Identification of the K40 acetylation site on α-tubulin (L'Hernault and Rosenbaum, 1985; LeDizet and Piperno, 1987), and subsequent findings of the involvement of the PTM in cell migration raised the possibility that the acetylation state of α-tubulin may exert an influence on sperm motility. This implicated the counterbalancing activities of the α-tubulin acetyltransferase, α-TAT1, and the deacetylases, HDAC6 and SIRT2, in sperm motility. Therefore, the overall aim of this thesis was to explore the role that the state of α-tubulin acetylation plays in the regulation of sperm motility using a murine model. This was achieved by assessing the effect of inhibitors of deacetylases on motility and α-tubulin acetylation, as well as investigating the activity of Class I and II HDACs in murine sperm. In addition, the role of microtubule stability which has been correlated with α-tubulin acetylation was examined to determine its part in sperm motility.

6.2 Murine sperm as a model for sperm motility studies

Due to the ease of breeding and maintenance, and the physiological similarities and genetic homology with humans, mice have been utilised extensively to model human biology and

disease (Perlman, 2016). With the additional potential for creation of transgenic and knockout/knockin mice, many research areas have benefitted greatly from the availability of the species for investigative and screening purposes prior to the use of drugs and technologies on humans. One such area in which the use of mice has vastly contributed to the development of knowledge and techniques is reproductive science; rodent models have traditionally been used to study the most fundamental aspects of reproduction leading to advances in the technologies used in ART (Quinn and Horstman, 1998; Menezo, 2002). In addition, the use of mouse models has also led to the identification of over 400 genes that are essential for male fertility, increasing the knowledge of processes such as spermatogenesis, capacitation, and fertilisation (Jamsai and O'Bryan, 2011). Furthermore, mouse sperm have been widely used to examine flagellum abnormalities and subsequent motility defects (Miki *et al.*, 2002; Escalier, 2006; Dong *et al.*, 2018), as the structural plan of the sperm tail varies little between mice and humans (Fawcett, 1970). For this reason, in addition to the availability of fresh samples, mouse sperm were used in the research comprising this thesis to study the role of α-tubulin acetylation in motility regulation.

Sperm from other animal species have also been developed as models in reproductive science research such as that from boar and cattle. Sperm from these animals may be more comparable in morphology to human sperm – they are of a similar size and exhibit paddle-shaped heads (Barkalina, Jones and Coward, 2016). In addition, sperm can be isolated from the ejaculate of these animals as opposed to epididymal excision required to obtain murine sperm. However, the nature of this retrieval means that sperm from livestock are maintained in semen extenders for sperm preservation, and these may exert artificial effects on sperm parameters such as motility and viability (Raseona *et al.*, 2017; Raheja *et al.*, 2018). As motility was the focus of research in this thesis, the accessibility of fresh mouse sperm avoided the need for any additional additives to the sperm that may have influenced their motility, and therefore the mouse was deemed a good model in which to examine the regulation of this motility.

6.3 HDACs in sperm

6.3.1 The effect of HDAC inhibitors on sperm motility and α-tubulin acetylation

The results presented in this thesis demonstrated that treatment with a HDAC6 specific inhibitor (tubacin), an inhibitor of Class I and II HDACs (TSA), and a Class III HDAC inhibitor (nicotinamide) did not exert a significant influence on motility parameters or α-tubulin acetylation in capacitated or capacitating murine sperm. Another important finding from the investigations in this thesis was the high baseline level of acetylated α-tubulin exhibited by sperm in the absence of any inhibitors. In fact, the results presented in Chapter 4 suggested that all of the α-tubulin detected by Western blot in sperm lysates was acetylated. **Figure 6.1** summarises the response of the highly acetylated sperm microtubules to tubacin, TSA and nicotinamide. Baseline levels of sperm α-tubulin acetylation were also found to be approximately 6-fold higher than that of HEK-MSR cells. Published studies have stated that α-tubulin in sperm is highly acetylated (Nereo Kalebic *et al.*, 2013), however the results presented in this thesis provide a direct comparison of α-tubulin acetylation between sperm and HEK cells, allowing the extent of the difference between different cell types to be visualised.

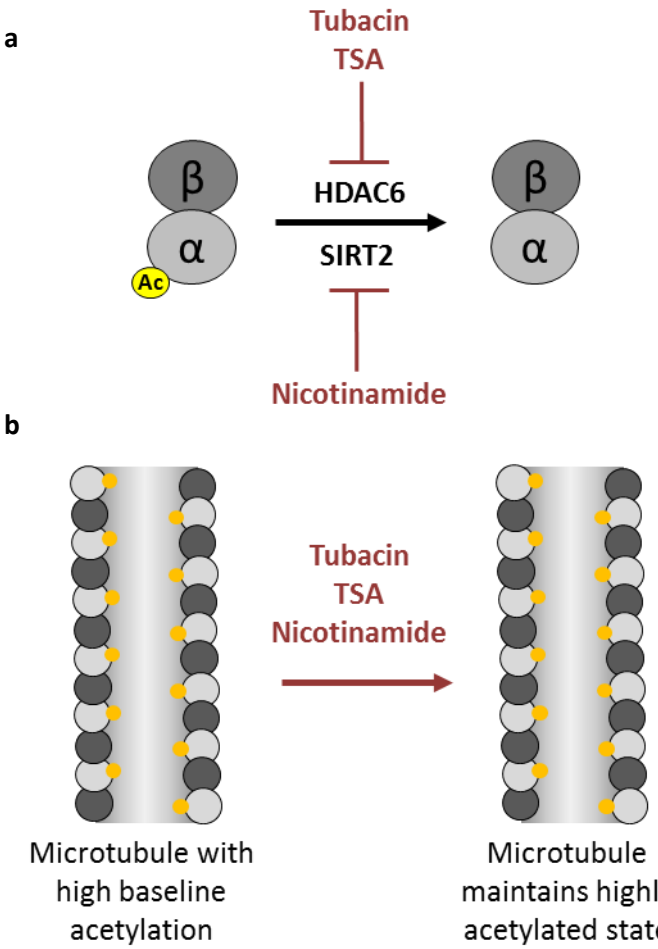

Figure 6.1: The effects of HDAC inhibitors on sperm microtubules.

(a) α-tubulin acetylation at the K40 site can be reversed by the deacetylase action of HDAC6 and SIRT2. The deacetylase activity of HDAC6 can be inhibited by the specific inhibitor, tubacin, or the general Class I and II HDAC inhibitor trichostatin A (TSA). Activity of SIRT2 can be inhibited by the general Class III HDAC inhibitor, nicotinamide. (b) Sperm microtubules were found to exhibit high baseline levels of acetylated α-tubulin which were insensitive to treatment with the inhibitors. Deacetylation of the microtubules was therefore postulated to be inactive, or occur at very low levels, and so inhibition of this process would not exert significant effects on the overall levels of acetylated α-tubulin.

Normal motility (including levels of hyperactivation) and unchanged levels of acetylated α-tubulin following treatment with tubacin were found in sperm from BALB/c and C57 mice. Conversely, whilst treatment with TSA (reported in Chapter 4) did not produce significant changes to sperm motility, small increases in the amplitude of lateral head displacement; beat cross frequency; curvilinear, straight line, and average path velocities; hyperactivation; and progressive motility were observed following exposure of sperm to 1 μM TSA for 1 hour. This was matched by slight increases in the levels of acetylated α-tubulin in all TSA treatment conditions (1 μM for 1 and 3 hour, 10 μM for 1 hour) compared to their relevant controls. This effect was not seen in tubacin-treated sperm. The data therefore suggest that members of the Class I and II HDACs other than HDAC6 could play a minor role in modifying sperm motility and α-tubulin acetylation. Indeed, knockdown of HDAC3 has been shown to increase levels of acetylated α-tubulin in a prostate cancer cell line to a similar extent as HDAC6 knockdown (Bacon *et al.*, 2015). Whilst the fact that the published results were obtained using a cancer cell line should be taken into consideration, the findings provide evidence that other HDACs may have an indirect role in the modulation of α-tubulin acetylation. However, as TSA is an inhibitor of HDAC6, the possibility that the minor effects on acetylated α-tubulin abundance and motility in the presence of TSA were due to HDAC6 inhibition cannot be ruled out. For confirmation, further studies using inhibitors such as sodium butyrate which acts upon Class I and IIa HDACs, but not the Class IIb member, HDAC6 (Davie, 2003) would be required. Nevertheless, the changes to motility and α-tubulin acetylation following exposure to TSA were very slight, not statistically significant, and did not affect the results of the Kremer assay – a method designed to evaluate sperm motility in a viscoelastic environment more closely related to the female reproductive tract. The ability of sperm to enter and penetrate the viscous media present in the assay was unchanged by exposure to TSA. This indicated that the slight alterations to motility parameters and acetylated α-tubulin abundance following TSA treatment did not affect overall sperm motility in artificial mucus and so were unlikely to be biologically significant.

These findings are in agreement with results from Parab and colleagues who demonstrated that sperm motility and levels of acetylated α-tubulin in the sperm from Holtzman rats were not significantly affected by treatment with TSA (Parab *et al.*, 2015). However, Parab *et al*. also reported that the specific inhibition of HDAC6 using tubastatin A resulted in a statistically significant reduction in progressive motility, an increase in beat frequency, and a significant increase in acetylated α-tubulin (Parab *et al.*, 2015). This implicated HDAC6 in the modulation of sperm motility which contrasts with the results presented in this thesis demonstrating that exposure of sperm to tubacin had no effect on motility or acetylation of α-tubulin. Variations in the protocols could have influenced the disparity between the outcomes of the two studies. Whilst incubation periods and inhibitor concentrations used in this thesis were equivalent to those utilised by Parab *et al*., the group used tubastatin A to inhibit HDAC6 rather than tubacin which may underlie the difference in effects. However, tubastatin A is more selective for HDAC6 than tubacin (Butler *et al.*, 2010), and so the results reported by Parab *et al*. regarding HDAC6 inhibition should not be due to an off-target effect. Alternatively, the disparity in the results may have been due to the different animal species used in the studies. Nevertheless, to ensure that the tubacin used in the experiments described in this thesis was able to inhibit HDAC6, the inhibitor was tested in control cells. Significant increases in acetylated α-tubulin abundance in HEK-MSR cells exposed to tubacin over a 3 hour time course indicated that the inhibitor concentration and treatment periods used were appropriate to elicit significant inhibition of α-tubulin deacetylation in cells. This effect was also observed following exposure of HEK-MSR cells to TSA, indicating that this inhibitor could also demonstrably inhibit α-tubulin deacetylation.

The effects of tubacin and TSA were also assessed in spermatids. Like sperm, spermatids showed no change in the abundance of acetylated α-tubulin following treatment with tubacin or TSA. These results are consistent with published findings of strong tubulin acetylation in

condensing and elongating spermatids in both HDAC6-deficient and wild-type mice (Zhang et al., 2008), and indicate that HDAC6 may not actively deacetylate α-tubulin in spermatids.

Overall, the results presented in Chapters 3 and 4 demonstrate that sperm are largely insensitive to treatment with TSA and tubacin. Therefore, no evidence has been found to support an active role for HDAC6 in sperm motility or α-tubulin deacetylation in sperm. Whilst this conclusion challenges the data from Parab *et al.*, it provides support for findings that demonstrate spermatogenesis and fertility in HDAC6-deficient mice to be comparable to wild-type mice (Zhang *et al.*, 2008). Data from Zhang and colleagues indicate that HDAC6 activity is not a requirement for normal sperm development and function, or overall viability of the mouse. However, whilst the researchers assessed the fertility of the mice based on sperm numbers and litter sizes following mating experiments, they did not assess sperm motility directly. Therefore whilst the mice were found to be fertile, conclusions cannot be drawn regarding the motility aspect of sperm function. Nevertheless, the work of Zhang *et al*. indicates that removal of HDAC6 does not exert detrimental effects on sperm function, which is in agreement with the findings of this study that indicate sperm motility is normal even in the presence of an inhibitor of HDAC6.

Haberland and colleagues suggested that the lack of an *in vivo* phenotype in HDAC6-deficient mice may have arisen due to redundancy with HDAC10 (Haberland, Montgomery and Olson, 2009). HDAC10 is the only other member of the Class IIb HDACs, alongside HDAC6, and its cellular role is still under debate. Research has implicated HDAC10 in various biological processes including angiogenesis (Duan *et al.*, 2017), lysosomal exocytosis (Ridinger *et al.*, 2018) and cell cycle regulation (Yang *et al.*, 2016); although many studies into HDAC10 function have been carried out in the context of cancer. Therefore, the localisation and suggested roles of HDAC10 may differ between cancerous and non-cancerous cells. Nevertheless, HDAC10 has been found in the testis tissue of normal mice (Kao *et al.*, 2002), and so the deacetylase may have a role in sperm development or function. The small changes

in sperm motility and abundance of acetylated α-tubulin demonstrated in this thesis in response to TSA, but not tubacin, suggests that one or more members of the Class I and II HDACs may have a minor role in sperm function, which could include HDAC10. However, further inhibitory studies using a combination of inhibitors would be required to determine whether other HDACs were involved. Nonetheless, whilst the substitution of HDAC6 with HDAC10 may provide a possible explanation for the lack of phenotype in HDAC6-deficient mice, the fact that many HDAC6-deficient tissues showed hyperacetylation of α-tubulin in the knockout mice compared to wild-type (Zhang *et al.*, 2008) indicates that the function of α-tubulin deacetylation was not replaced by the activity of another HDAC, or at least to the same extent.

The finding that treatment with HDAC inhibitors did not impact upon sperm motility may have important wider implications for the growing number of conditions with the potential for treatment using therapies based upon HDAC inhibition. Whilst many HDAC inhibitors are undergoing clinical trials, and some have been approved for the treatment of cancer (Li and Seto, 2016), the interest in such agents as potential therapeutics in various other conditions such as neurodegenerative disorders including Parkinson's disease (Didonna and Opal, 2015), and mood disorders such as bipolar disorder (Machado-Vieira *et al.*, 2011) is mounting. Given the emergence of new applications for HDAC inhibitors, the effects of treatment with this type of drug on fertility are an important consideration. Research in this area is limited, and the studies published have mainly focussed on the Class I and II HDAC inhibitor, vorinostat (suberoylanilide hydroxamic acid, SAHA), which is currently used in the therapy of cutaneous T-cell lymphoma. Sperm counts, motility, and overall fertility were found to be normal in rats following oral administration of vorinostat for 14 weeks (Wise *et al.*, 2008). Similarly, fertility in male mice was comparable to control following intraperitoneal injection of vorinostat for 7 weeks, with sperm concentrations and morphology unaffected by the treatment (Kläver *et al.*, 2015). As TSA belongs to the hydroxymate group alongside vorinostat, the results presented in

this thesis provide support for the findings that treatment with a Class I and II general HDAC inhibitor does not exert detrimental effects on sperm motility. Furthermore, treatment with tubacin did not influence motility either as shown in Chapter 3, indicating that the more specific HDAC inhibitor may not be detrimental to aspects of male fertility. However, in these experiments, both inhibitors were directly applied to sperm, in contrast to the method of administration if inhibitors were to be used as therapeutics. Nevertheless, a growing body of evidence suggests that HDAC inhibitors may not be detrimental to male fertility.

As no evidence was found in this thesis to demonstrate that HDAC6 was involved in sperm motility, or actively deacetylated α-tubulin in sperm, it was hypothesised that another α-tubulin deacetylase, the Class III HDAC, SIRT2 (North *et al.*, 2003), may play a role in sperm function. However, a similar lack of effect on sperm motility and levels of acetylated α-tubulin was found following treatment with the Class III HDAC inhibitor, nicotinamide. Therefore, the notion that SIRT2 actively deacetylates α-tubulin in sperm was not supported. Furthermore, the levels of acetylated α-tubulin in sperm treated with tubacin and nicotinamide in combination were comparable to the control, indicating that at least in terms of α-tubulin deacetylation, SIRT2 and HDAC6 did not appear to be substituting for one another in murine sperm. However, the abundance of acetylated α-tubulin in HEK cells exposed to nicotinamide as a control was also unchanged by treatment. This was unexpected, as published findings demonstrated that siRNA-mediated knockdown of SIRT2 in 293T cells resulted in an increase in acetylated α-tubulin compared to control (North *et al.*, 2003). However, knockout of SIRT2 in fibroblasts resulted in levels of acetylated α-tubulin comparable to wild-type cells, indicating genetic inactivation of SIRT2 did not affect α-tubulin acetylation (Zhang *et al.*, 2008). Similarly, SIRT2-deficient mice exhibited levels of acetylated α-tubulin in brain samples that were comparable to that of wild-type samples (Bobrowska *et al.*, 2012). The findings suggest that SIRT2 may only have a role in α-tubulin deacetylation under specific conditions in certain cell types, which may not include murine sperm. Nevertheless, in order to reinforce the

conclusions drawn from the treatment of sperm with nicotinamide presented in Chapter 3, an independent positive control would be required to confirm that the nicotinamide used in this study was able to inhibit SIRT2 in other cell types. To further investigate the role of SIRT2, assessment of sperm and primary cells such as fibroblasts from SIRT2 knockout mice would be useful in determining whether the absence of the Class III HDAC affected motility or levels of α-tubulin acetylation in sperm and other cell types, aiding to define the role of this deacetylase.

Overall, the general insensitivity of sperm motility and α-tubulin acetylation to treatment with HDAC inhibitors reported in this thesis suggested that α-tubulin in sperm is not actively deacetylated to a significant extent by HDAC6. Furthermore, a role for HDAC6 in motility regulation was not demonstrated. These results indicated that there may be little or no HDAC6 activity in sperm - a hypothesis that was subsequently investigated.

6.3.2 The activity of HDACs in sperm

To investigate whether HDACs are active in sperm, an assay was utilized in which HDAC activity was measured fluorometrically following the addition of a cell-permeable HDAC substrate. Importantly, detectable levels of HDAC activity were demonstrated in murine sperm. Furthermore, the treatment of sperm with tubacin resulted in a reduction in HDAC activity, indicating the presence of active HDAC6. Exposure to TSA also decreased HDAC activity, to a greater extent than tubacin, which suggested the presence of other active Class I and II HDACs. Whilst the reductions in activity were not statistically significant, the results were reproducible and notably demonstrated the presence of active HDAC6 in murine sperm. Accordingly, Parab *et al*. also showed a reduction in HDAC activity following treatment with TSA, tubastatin A and sodium butyrate using lysates of rat sperm as a source of HDACs (Parab *et al.*, 2015). The enhanced reduction of activity following TSA exposure compared with tubastatin A, coupled with the ability of sodium butyrate to significantly lower HDAC activity compared to control, indicated the contribution of HDACs other than HDAC6 (Parab *et al.*, 2015). This is in

agreement with the results demonstrated in Chapter 4. However, whilst Parab and colleagues demonstrated HDAC activity in sperm lysates (Parab *et al.*, 2015), the data presented in this thesis importantly shows that inhibition of HDAC activity in live sperm can be detected. In addition, the increased inhibition of HDAC activity by TSA over that of tubacin is consistent with the minor effects on motility following exposure to TSA but not tubacin. Therefore, it is possible that other HDACs may play a minor role in sperm function; substantiation of this hypothesis would require evidence from further inhibitor studies. One such candidate to examine would be the Class IIb member, HDAC10. As HDAC10-specific inhibitors are unavailable, a combination of HDAC inhibitors would be required to reveal the effects of HDAC10, such as sodium butyrate to inhibit all Class I and IIa HDACs, in conjunction with tubacin or tubastatin A to inhibit HDAC6. Alternatively, the assessment of sperm from knockout mouse models would help to define the role of HDACs in sperm function further.

The results from the HDAC activity assay taken together with the finding of high baseline levels of α-tubulin acetylation in sperm indicated that whilst HDAC activity is present, the extent of HDAC6 activity in sperm is low. As a result, sperm α-tubulin is likely to be maximally acetylated as indicated in Chapter 4, thus explaining the lack of response to treatment with HDAC inhibitors. The contribution of low HDAC6 activity to the maintenance of α-tubulin in an acetylated state may therefore be a requirement for normal sperm function. Indeed, correlations have been found between levels of acetylated α-tubulin and sperm motility; individuals exhibiting impaired sperm motility have been shown to also display hypoacetylation of sperm α-tubulin (Gentleman *et al.*, 1996; Bhagwat *et al.*, 2014). Furthermore, loss of the α-tubulin acetyltransferase, α-TAT1 in mice led to defects in sperm morphology, impairments in motility, and an overall infertile phenotype in male mice (Nereo Kalebic *et al.*, 2013). This published study indicates the requirement for α-TAT1 in normal sperm development in mice, implicating acetylation of α-tubulin as an important factor in sperm function. However, α-TAT1 has another role in the regulation of microtubule dynamicity independent of its acetyltransferase activity; overexpression of α-TAT1 has been shown to

decrease microtubule stability, which was not dependent on the levels of α-tubulin acetylation (N. Kalebic *et al.*, 2013). This brings into question whether it is the catalytic activity of α-TAT1, or its role in microtubule dynamics that is a necessary requirement for normal sperm function. Further to this question, Kalebic and colleagues demonstrated that loss of α-TAT1 was detrimental to sperm development. In their study, sperm from knockout mice exhibited significant reductions in flagellar length, and dramatic increases in the presence of cytoplasmic droplets associated with impaired sperm maturation (Nereo Kalebic *et al.*, 2013). Therefore, acetylation of α-tubulin may be important during spermatogenesis for normal microtubule assembly, but the subsequent impairment of motility in mature sperm could result from the abnormal morphology, rather than an α-TAT1 deficiency. To date, no inhibitors have been developed that target α-TAT1, therefore it is not currently possible to distinguish the point at which a loss of activity causes the observed effects. The availability of an α-TAT1 inhibitor would allow evaluation of the consequences of α-TAT1 inhibition in mature sperm to determine the role of the acetyltransferase in sperm functions such as motility.

The findings of low HDAC6 activity and high baseline levels of α-tubulin acetylation in sperm presented in this thesis support the notion that microtubule acetylation plays an important role in an aspect of sperm function, whether as a by-product of another regulatory process such as microtubule stability, or as an independent regulatory mechanism. One such mechanism which influences levels of α-tubulin acetylation in microtubules has recently come to light, and may be applicable to sperm. Research by Portran *et al.* demonstrated that microtubules are softened by K40 acetylation as the presence of the PTM weakens lateral interactions between tubulin protofilaments (Portran *et al.*, 2017). As microtubules are rigid structures that can rupture under stress (Hawkins *et al.*, 2010), Portran and colleagues proposed that acetylation renders microtubules less susceptible to breakage in areas subject to repeated bending (Portran *et al.*, 2017). In addition, Xu *et al.* demonstrated that regions of microtubules undergoing high curvature exhibited enhanced acetylation, increasing flexibility, and allowing the microtubules to better resist mechanical stress (Xu *et al.*, 2017). As the sole

function of the sperm relies on its ability to swim towards an oocyte requiring intense periods of flagellar bending, it is possible that the highly acetylated state of α-tubulin found in sperm is a consequence of a protective mechanism against breakage. In addition, research by Alper and colleagues demonstrated that K40 acetylation increased the motility of outer arm axonemal dynein and regulated ciliary beat (Alper *et al.*, 2014). Given the similarity between the structure and motility mechanisms of cilia and flagella, the findings by Alper *et al.* may be applicable to the sperm flagellum. Therefore, α-tubulin acetylation may play various roles in the regulation of microtubule function in sperm. Previous studies have also shown a correlation between α-tubulin acetylation and microtubule stability, with the enrichment of acetylation in stable microtubules (Webster and Borisy, 1989) deemed likely to be a consequence rather than a cause of stability (Palazzo, Ackerman and Gundersen, 2003; Szyk *et al.*, 2014b). The highly acetylated state of α-tubulin in sperm may therefore be indicative of stable microtubules, and so the role of this stability in sperm motility was investigated using a microtubule depolymerising drug, nocodazole.

6.4 The role of microtubule stability in sperm motility

Treatment of sperm with nocodazole for 3 hours resulted in a significant increase in certain motility parameters, namely, curvilinear and average path velocities which indicated faster swimming speeds, as well as amplitude of lateral head displacement which indicated that the drug induced a stronger bend in the proximal region of the sperm tail (Mortimer, 2000). As a consequence, progressive motility was significantly increased by the presence of nocodazole. To the best of the researcher's knowledge, the only other study to investigate the effect of nocodazole on sperm found that boar sperm motility was unaffected by treatment (Rashid, 2017). However, the study does not detail methodology, including drug concentrations, incubation times or measures of motility, and does not include data from the experiment, making it difficult to assess the conclusions drawn from the investigation. The results presented in this thesis therefore demonstrate a novel finding that treatment with a drug to

induce microtubule destabilisation influenced sperm motility. However, upon immunofluorescence and TEM analysis of microtubule structure and arrangement, exposure to nocodazole was not found to disrupt α-tubulin or gross microtubule organisation in sperm. In fact, the microtubule arrangement remained intact and comparable to control throughout the sperm tail following treatment. Whilst limitations in the resolution of the microscopy may have prevented the detection of subtle changes (as discussed in Chapter 5, section 5.3), acetylation of α-tubulin also persisted in nocodazole-treated sperm and spermatids to levels matching that of controls, supporting the notion that microtubule structure was not disrupted by nocodazole. In stark contrast, HEK cells treated with nocodazole exhibited highly disrupted microtubule structures, and a significant reduction in acetylated α-tubulin compared to vehicle-treated cells.

The difference in the response of sperm and HEK cells to nocodazole may be explained by the initial acetylation state of their respective α-tubulin; research has found that acetylated microtubules are much more resistant to disassembly by depolymerising drugs than non-acetylated microtubules (LeDizet and Piperno, 1986). Piperno and colleagues also demonstrated that nocodazole and colchicine caused depolymerisation of microtubules in HeLa and NIH 3T3 cells, however residual microtubules remaining at the end of treatment were acetylated (Piperno, LeDizet and Chang, 1987). In addition, microtubules with high α-tubulin acetylation induced by HDAC inhibition were found to be more resistant to depolymerisation by nocodazole (Asthana *et al.*, 2013) and demecolcin (Matsuyama *et al.*, 2002a) compared to their control counterparts. The high levels of acetylation in sperm microtubules which are likely to indicate microtubule stability could therefore have provided resistance against nocodazole-induced depolymerisation. In contrast, the more dynamic microtubules in HEK cells displaying lower levels of α-tubulin acetylation were more susceptible to disassembly. Further investigations into the effects of a HDAC6 inhibitor and nocodazole in combination may help to clarify whether the different responses to nocodazole between the two cell types were a result of the different states of microtubule stability, or

levels of acetylation itself. However, as research suggests that acetylation marks microtubule stability rather than causing it, it is likely that the different effects observed on microtubule organisation are a result of the different states of microtubule dynamicity between HEK cells and sperm.

As the results appear to demonstrate that the gross structure of the sperm microtubules and the levels of acetylated α-tubulin in sperm are unchanged following exposure to nocodazole, the finding that sperm motility is significantly altered by the drug is surprising. Nocodazole is known to bind deeply in the β-tubulin subunit, overlapping the characterised colchicine binding site slightly (Wang *et al.*, 2016; Aguayo-Ortiz *et al.*, 2017). The mechanism of action of nocodazole is therefore predicted to be similar to that of colchicine; binding is likely to induce a conformational change in the β-tubulin subunit, reducing the interaction with α-tubulin. This subsequently results in the generation of a heterodimer with a curved conformation (Aguayo-Ortiz *et al.*, 2013) which is unable to bind another heterodimer to produce the protofilament (Barbier *et al.*, 2010). In cells with dynamic microtubules, nocodazole therefore inhibits the polymerisation of microtubules. However, as sperm microtubules are highly acetylated (indicative of stability) and the nature of sperm motility relies upon stable, persistent microtubules, it is unlikely that sperm microtubules undergo a significant degree of polymerisation/depolymerisation. Therefore, the alterations to sperm motility parameters in the absence of any change to microtubule structure may not have arisen from the inhibition of polymerisation, but rather, from conformational changes to the tubulin subunits within the microtubule protofilaments. Exposure of the sperm microtubules to nocodazole may therefore have weakened the interactions between tubulin subunits, effectively "loosening" the lattice and increasing microtubule flexibility. As a consequence, stronger bends were produced by the sperm tail leading to the increased velocity and pattern of motility observed. **Figure 6.2** illustrates the reported and postulated mechanisms of nocodazole action and the effects of the drug on sperm motility. It is also possible that the action of nocodazole may have affected interactions between microtubules and other proteins such as motor proteins, and so the

effects observed may be due to an alternative, unidentified mechanism. Overall, whilst the exact mechanism requires elucidation, nocodazole was notably found to influence sperm motility parameters without discernible effects on the sperm microtubule structure.

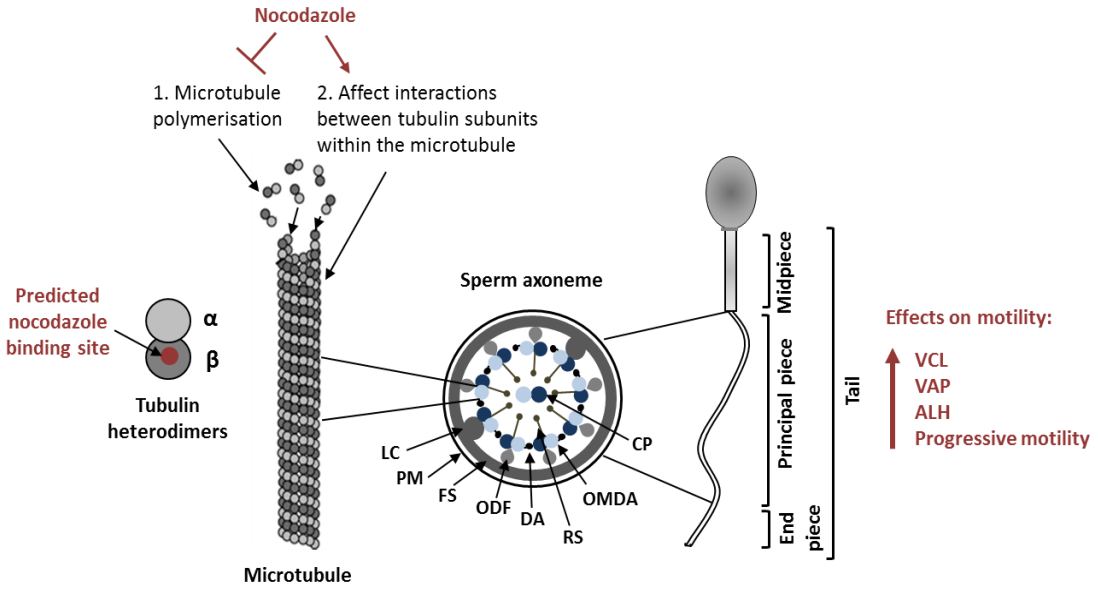

Figure 6.2: Overview of the effects of nocodazole on sperm.

The microtubules comprise one component of the sperm axoneme which runs through the entire length of the sperm tail and plays a central role in sperm motility. For simplicity, only a cross-section of the axoneme through the principal piece of the sperm tail is shown. Microtubules are made up of heterodimers of α- and β-tubulin which join to form protofilaments that subsequently associate and fold to produce the cylindrical microtubules. Nocodazole is predicted to bind deeply within the β-tubulin subunit and is reported to (1) prevent microtubule polymerisation. As treatment of murine sperm with nocodazole led to significant increases in curvilinear velocity (VCL), average path velocity (VAP), amplitude of lateral head displacement (ALH), and progressive motility, without discernible effects on tubulin organisation, it is postulated that nocodazole may have (2) bound to β-tubulin within the microtubule, causing subtle changes to the conformation of the microtubule and the subsequent effects on sperm motility. LC - longitudinal columns, PM - plasma membrane, FS - fibrous sheath, ODF - outer dense fibres, DA - dynein arms, RS - radial spokes, OMDA - outer microtubule doublets of the axoneme, CP - central pair of microtubules.

6.5 Conclusions and future work

In summary, the findings presented in this thesis have shown that the α-tubulin of murine epididymal sperm is highly acetylated, which is likely maintained by low levels of HDAC6 activity. Furthermore, the results demonstrated that the inhibition of HDACs does not significantly influence sperm motility parameters, opposing a role for α-tubulin deacetylation in this sperm function. It is therefore postulated that acetylation is likely to play an important role in the maintenance of microtubule function in sperm, either during sperm development, or during maturity when acetylation may protect microtubules from breakage or regulate flagellar beat. As limitations in the research arising from the semi quantitative nature of Western blots, and the highly acetylated state of sperm α-tubulin meant that small differences in levels of α-tubulin acetylation following treatment with HDAC inhibitors may not have been detected; future research could seek to confirm whether α-tubulin acetylation is important for the functioning of sperm by evaluating the role of α-TAT1 in mature sperm. This research would be valuable as it could aid in determining whether the highly acetylated state of α-tubulin in sperm is a product of microtubule assembly during spermatogenesis, or whether α-TAT1 actively acetylates microtubules in mature sperm.

The data presented in this thesis also highlight a role for the regulation of microtubule organisation and structure in the modulation of murine sperm motility. Alterations to motility parameters in response to nocodazole suggested that subtle changes in the conformation of the sperm microtubules may influence flagellar motion. This finding could be useful for further studies into the mechanisms regulating sperm motility; future work could seek to elucidate the mechanism by which nocodazole exerted the observed effects on motility parameters. Techniques such as stochastic optical reconstruction microscopy (STORM) or further TEM focussing on the ends of the microtubules may be helpful in providing a higher resolution view of the mechanisms of nocodazole action on microtubule structure (Miller *et al.*, 2018). However, limitations in the resolving power of the microscopes may prevent the identification

of any subtle changes to the microtubule conformation in the presence of nocodazole. An alternative avenue of research could include investigations into the effects that nocodazole may have had on microtubule interactions with other proteins; biochemical techniques such as immunoprecipitation and mass spectrometry could be utilised to identify binding partners of α-tubulin in the presence and absence of nocodazole. Any differences found could potentially aid in elucidating the molecular pathways affected by the drug. In addition, for further confirmation of the role of microtubule stability in sperm motility regulation, microtubule depolymerising drugs that target different ligand binding sites on tubulin could be tested for their effects on motility. One well-characterised site is the vinca-site of β-tubulin located at the interface between two longitudinally-interacting dimers, which is targeted by members of the vinca-alkaloid family, such as vincristine and vinblastine (Steinmetz and Prota, 2018). On the other hand, drugs such as paclitaxel that stabilise the microtubules could be investigated for their effects on sperm motility. Additionally, as detyrosination has also been found to accumulate in long-lived microtubules like acetylation (Brown *et al.*, 1993; Palazzo, Ackerman and Gundersen, 2003), assessment of this PTM may provide a useful second marker of microtubule stability. Research using other model cells may also be useful in further clarifying the role of acetylation in microtubules. The acetylation of α-tubulin was initially identified in *Chlamydomonas* (L'Hernault and J L Rosenbaum, 1983; McKeithan *et al.*, 1983; L'Hernault and Rosenbaum, 1985; Piperno and Fuller, 1985), a unicellular, biflagellate organism with an axonemal structure and function remarkably comparable to mammalian flagella, and with flagellar proteins similar to those found in human sperm (Silflow and Lefebvre, 2001). *Chlamydomonas reinhardtii* may therefore provide an advantageous model for studying the role of α-tubulin acetylation in flagellar function further in future research.

Overall, the findings in this thesis of high baseline α-tubulin acetylation and low HDAC6 activity in murine sperm are important as they suggest that deacetylation of α-tubulin is not a requirement for the normal motility of murine sperm. Furthermore, the finding that nocodazole increased sperm velocity and tail bend, culminating in increases in hyperactivation

and progressive motility, and an enhanced ability to navigate viscous media, could have important implications for future research into therapies for male infertility caused by impaired sperm motility. Of course, experiments to validate the findings from murine sperm would be required in human sperm. Although mice represent a good species in which to model human sperm motility research given the genetic homology and comparable sperm tail structure, differences such as head morphology and the tendency of mouse sperm to form 'trains' - a behaviour not found in human sperm - mean that the applicability of these research findings to humans requires verification. Nevertheless, the results obtained in this study indicating that sperm motility can be significantly influenced by a microtubule depolymerising drug represent a valuable contribution to the endeavour of elucidating the mechanisms regulating sperm motility. Although the introduction of ICSI into fertility treatment circumvents the requirement for sperm motility, research into the modulation of this sperm function remains imperative in order to develop alternative management strategies for male infertility which do not place the burden of treatment on the female partner (Barratt, De Jonge and Sharpe, 2018). Furthermore, with recent evidence showing that young males conceived by ICSI exhibit sperm concentrations half that of men conceived naturally, with two-fold lower total motile sperm counts, the concerns that ICSI-conceived children inherit sperm defects from their fathers are founded (Belva *et al.*, 2016). Therefore, the requirement for alternative ways to manage male infertility such as drug treatments (Martins da Silva *et al.*, 2017) is ever-increasing, necessitating a drive for further research into the complex processes regulating sperm function. With asthenozoospermia being the most common sperm defect in infertile males (Curi *et al.*, 2003), the findings presented in this thesis contribute to the knowledge of sperm motility regulation, with a view to aiding in the development of future therapies for male infertility.

Chapter 7

Chapter 7 – References

Abou-Haila, A. and Tulsiani, D. R. P. (2000) 'Mammalian sperm acrosome: Formation, contents, and function', *Archives of Biochemistry and Biophysics*, 379(2), pp. 173–182.

Agarwal, A. *et al.* (2015) 'A unique view on male infertility around the globe', *Reproductive Biology and Endocrinology*, 13(1), p. 37.

Aguayo-Ortiz, R. *et al.* (2013) 'Towards the identification of the binding site of benzimidazoles to β-tubulin of Trichinella spiralis: Insights from computational and experimental data', *Journal of Molecular Graphics and Modelling*, 41, pp. 12–19.

Aguayo-Ortiz, R. *et al.* (2017) 'Structure-based approaches for the design of benzimidazole-2-carbamate derivatives as tubulin polymerization inhibitors', *Chemical Biology & Drug Design*, 90(1), pp. 40–51.

Aguilar, A. *et al.* (2014) 'Alpha-Tubulin K40 acetylation is required for contact inhibition of proliferation and cell-substrate adhesion', *Molecular Biology of the Cell*, 25(12), pp. 1854–1866.

Aillaud, C. *et al.* (2017) 'Vasohibins/SVBP are tubulin carboxypeptidases (TCPs) that regulate neuron differentiation', *Science*, 358(6369), pp. 1448–1453.

Akella, J. S. *et al.* (2010) 'MEC-17 is an α-tubulin acetyltransferase', *Nature*, 467(7312), pp. 218–222.

Al-Bassam, J. and Corbett, K. D. (2012) '-Tubulin acetylation from the inside out', *Proceedings of the National Academy of Sciences*, 109(48), pp. 19515–19516.

Alberts, B. *et al.* (2002) *Molecular Biology of the Cell*. Garland Science.

Alper, J. D. *et al.* (2014) 'The Motility of Axonemal Dynein Is Regulated by the Tubulin Code', *Biophysical Journal*, 107(12), pp. 2872–2880.

Amaral, A. *et al.* (2013) 'Mitochondria functionality and sperm quality.', *Reproduction (Cambridge, England)*. Society for Reproduction and Fertility, 146(5), pp. R163-74.

Asthana, J. *et al.* (2013) 'Inhibition of HDAC6 deacetylase activity increases its binding with microtubules and suppresses microtubule dynamic instability in MCF-7 cells', *Journal of Biological Chemistry*, 288(31), pp. 22516–22526.

Austin, C. R. (1951) 'Observations on the penetration of the sperm in the mammalian egg.', *Australian journal of scientific research. Ser. B: Biological sciences*, 4(4), pp. 581–596.

Austin, C. R. (1952) 'The capacitation of the mammalian sperm.', *Nature*, 170(4321), p. 326.

Avalos, J. L., Bever, K. M. and Wolberger, C. (2005) 'Mechanism of sirtuin inhibition by nicotinamide: Altering the NAD+cosubstrate specificity of a Sir2 enzyme', *Molecular Cell*, 17(6), pp. 855–868.

Bacon, T. *et al.* (2015) 'Histone deacetylase 3 indirectly modulates tubulin acetylation.', *The Biochemical journal*, 472(3), pp. 367–77.

Baibakov, B. *et al.* (2007) 'Sperm binding to the zona pellucida is not sufficient to induce acrosome exocytosis.', *Development (Cambridge, England)*, 134(5), pp. 933–43.

Balhorn, R., Brewer, L. and Corzett, M. (2000) 'DNA condensation by protamine and arginine-rich peptides: analysis of toroid stability using single DNA molecules.', *Molecular reproduction and development*, 56, pp. 230–234.

Barbier, P. *et al.* (2010) 'Stathmin and interfacial microtubule inhibitors recognize a naturally curved conformation of tubulin dimers.', *The Journal of biological chemistry*, 285(41), pp. 31672–81.

Barkalina, N., Jones, C. and Coward, K. (2016) 'Nanomedicine and mammalian sperm: Lessons from the porcine model', *Theriogenology*, 85(1), pp. 74–82.

Barratt, C. L. R. *et al.* (2011) 'Diagnostic tools in male infertility-the question of sperm dysfunction.', *Asian journal of andrology*, 13(1), pp. 53–8.

Barratt, C. L. R., De Jonge, C. J. and Sharpe, R. M. (2018) '"Man Up": the importance and strategy for placing male reproductive health centre stage in the political and research agenda', *Human Reproduction*, 33(4), pp. 541–545.

Battistone, M. A. *et al.* (2013) 'Functional human sperm capacitation requires both bicarbonate-dependent PKA activation and down-regulation of Ser/Thr phosphatases by Src family kinases', *Molecular Human Reproduction*, 19(9), pp. 570–580.

Baur, P. S. and Stacey, T. R. (1977) 'The use of PIPES buffer in the fixation of mammalian and marine tissues for electron microscopy', *Journal of Microscopy*, 109(3), pp. 315–327.

Belva, F. *et al.* (2016) 'Semen quality of young adult ICSI offspring: the first results', *Human Reproduction*, 31(12), pp. 2811–2820.

Bertos, N. R. *et al.* (2004) 'Role of the tetradecapeptide repeat domain of human histone deacetylase 6 in cytoplasmic retention', *Journal of Biological Chemistry*, 279(46), pp. 48246–48254.

Bhagwat, S. *et al.* (2014) 'Acetylated α-tubulin is reduced in individuals with poor sperm motility', *Fertility and Sterility*, 101(1), pp. 95–104.

Bitterman, K. J. *et al.* (2002) 'Inhibition of silencing and accelerated aging by nicotinamide, a putative negative regulator of yeast Sir2 and human SIRT1', *Journal of Biological Chemistry*, 277(47), pp. 45099–45107.

Bobrowska, A. *et al.* (2012) 'SIRT2 ablation has no effect on tubulin acetylation in brain, cholesterol biosynthesis or the progression of Huntington's disease phenotypes in vivo.', *PloS one*. Edited by H. Okazawa, 7(4), p. e34805.

Boivin, J. *et al.* (2007) 'International estimates of infertility prevalence and treatment-seeking: Potential need and demand for infertility medical care', *Human Reproduction*, 22(6), pp. 1506–1512.

Vander Borght, M. and Wyns, C. (2018) 'Fertility and infertility: Definition and epidemiology', *Clinical Biochemistry*, 62, pp. 2–10.

Boskovic, A. and Torres-Padilla, M.-E. (2013) 'How mammals pack their sperm: a variant matter.', *Genes & development*, 27(15), pp. 1635–9.

Boyault, C. *et al.* (2006) 'HDAC6-p97/VCP controlled polyubiquitin chain turnover', *EMBO Journal*, 25(14), pp. 3357–3366.

Boyault, C. *et al.* (2007) 'HDAC6, at the crossroads between cytoskeleton and cell signaling by acetylation and ubiquitination', *Oncogene*. Nature Publishing Group, 26(37), pp. 5468–5476.

Boyle, C. A. *et al.* (1992) 'The relation of computer-based measures of sperm morphology and motility to male infertility', *Epidemiology*, 3(3), pp. 239–246.

Braun, R. E. (1998) 'Post-transcriptional control of gene expression during spermatogenesis', *Seminars in Cell and Developmental Biology*, 9, pp. 483–489.

Bré, M. H. *et al.* (1996) 'Axonemal tubulin polyglycylation probed with two monoclonal antibodies: widespread evolutionary distribution, appearance during spermatozoan maturation and possible function in motility.', *Journal of cell science*, 109, pp. 727–738.

Bressac, C. *et al.* (1995) 'A massive new posttranslational modification occurs on axonemal

tubulin at the final step of spermatogenesis in Drosophila', *Eur J Cell Biol*, 67(4), pp. 346–355.

Breucker, H., Schafer, E. and Holstein, A.-F. (1985) 'Morphogenesis and fate of the residual body in human spermiogenesis', *Cell Tissue Res*, 240, pp. 303–309.

Brouhard, G. and Sept, D. (2012) 'Microtubules: Sizing Up the GTP Cap', *Current Biology*, 22(18), pp. R802–R803.

Brown, A. *et al.* (1993) 'Composite microtubules of the axon: quantitative analysis of tyrosinated and acetylated tubulin along individual axonal microtubules', *Journal of Cell Science*, 104, pp. 339–352.

Buffone, M. G., Hirohashi, N. and Gerton, G. L. (2014) 'Unresolved questions concerning mammalian sperm acrosomal exocytosis.', *Biology of reproduction*, 90(5), p. 112.

Butler, K. V *et al.* (2010) 'Rational design and simple chemistry yield a superior, neuroprotective HDAC6 inhibitor, tubastatin A.', *Journal of the American Chemical Society*, 132(31), pp. 10842–6.

Calvin, H. I., Hwang, F. H. and Wohlrab, H. (1975) 'Localization of zinc in a dense fiber-connecting piece fraction of rat sperm tails analogous chemically to hair keratin', *Biology of Reproduction*, 13, pp. 228–239.

Cambray-Deakin, M. A. and Burgoyne, R. D. (1987) 'Acetylated and detyrosinated alpha-tubulins are co-localized in stable microtubules in rat meningeal fibroblasts.', *Cell motility and the cytoskeleton*, 8(3), pp. 284–291.

Carlson, A. E., Hille, B. and Babcock, D. F. (2007) 'External Ca2+ acts upstream of adenylyl cyclase SACY in the bicarbonate signaled activation of sperm motility', *Developmental Biology*, 312(1), pp. 183–192.

Carrell, D. T., Emery, B. R. and Hammoud, S. (2007) 'Altered protamine expression and diminished spermatogenesis: What is the link?', *Human Reproduction Update*, 13(3), pp. 313–327.

Caudron, F. *et al.* (2010) 'Mutation of Ser172 in yeast β tubulin induces defects in microtubule dynamics and cell division.', *PloS one*, 5(10), p. e13553.

Chang, M. C. (1951) 'Fertilizing capacity of spermatozoa deposited into the fallopian tubes [9]', *Nature*, pp. 697–698.

Cho, C. and Vale, R. D. (2012) 'The mechanism of dynein motility: Insight from crystal

structures of the motor domain', *Biochimica et Biophysica Acta - Molecular Cell Research*, pp. 182–191.

Choudhary, C. *et al.* (2009) 'Lysine acetylation targets protein complexes and co-regulates major cellular functions.', *Science*, 325(5942), pp. 834–40.

Chretien, D. *et al.* (1992) 'Lattice defects in microtubules: Protofilament numbers vary within individual microtubules', *Journal of Cell Biology*, 117(5), pp. 1031–1040.

Chu, C.-W. *et al.* (2011) 'A novel acetylation of β-tubulin by San modulates microtubule polymerization via down-regulating tubulin incorporation.', *Molecular biology of the cell*, 22(4), pp. 448–56.

Chung, J.-J. *et al.* (2014) 'Structurally distinct Ca(2+) signaling domains of sperm flagella orchestrate tyrosine phosphorylation and motility.', *Cell*, 157(4), pp. 808–22.

Conacci-Sorrell, M., Ngouenet, C. and Eisenman, R. N. (2010) 'Myc-nick: a cytoplasmic cleavage product of Myc that promotes alpha-tubulin acetylation and cell differentiation.', *Cell*, 142(3), pp. 480–93.

Coombes, C. *et al.* (2016) 'Mechanism of microtubule lumen entry for the α-tubulin acetyltransferase enzyme αTAT1.', *Proceedings of the National Academy of Sciences of the United States of America*, 113(46), pp. E7176–E7184.

Cooper, T. G. *et al.* (2010) 'World Health Organization reference values for human semen characteristics', *Human Reproduction Update*, 16(3), pp. 231–245.

Creppe, C. *et al.* (2009) 'Elongator Controls the Migration and Differentiation of Cortical Neurons through Acetylation of α-Tubulin', *Cell*, 136(3), pp. 551–564.

Curi, S. M. *et al.* (2003) 'Asthenozoospermia: Analysis of a large population', *Archives of Andrology*, 49(5), pp. 343–349.

Dacheux, J. L. and Dacheux, F. (2014) 'New insights into epididymal function in relation to sperm maturation', *Reproduction*, 147(2), pp. R27-42.

Davie, J. R. (2003) 'Inhibition of Histone Deacetylase Activity by Butyrate', *The Journal of Nutrition*, 133(7), p. 2485S–2493S.

Didonna, A. and Opal, P. (2015) 'The promise and perils of HDAC inhibitors in neurodegeneration.', *Annals of clinical and translational neurology*, 2(1), pp. 79–101.

van Dijk, J. *et al.* (2007) 'A targeted multienzyme mechanism for selective microtubule polyglutamylation.', *Molecular cell*, 26(3), pp. 437–48.

Dong, F. N. *et al.* (2018) 'Absence of CFAP69 Causes Male Infertility due to Multiple Morphological Abnormalities of the Flagella in Human and Mouse', *The American Journal of Human Genetics*, 102(4), pp. 636–648.

Duan, B. *et al.* (2017) 'HDAC10 promotes angiogenesis in endothelial cells through the PTPN22/ERK axis.', *Oncotarget*, 8(37), pp. 61338–61349.

Dutcher, S. K. (2001) 'Motile organelles: The importance of specific tubulin isoforms', *Current Biology*, 11(11), pp. R419-22.

Dvoráková, K. *et al.* (2005) 'Cytoskeleton localization in the sperm head prior to fertilization.', *Reproduction*, 130(1), pp. 61–9.

Escalier, D. (2006) 'Knockout mouse models of sperm flagellum anomalies', *Human Reproduction Update*, 12(4), pp. 449–461.

ESHRE (2018) *ART fact sheet*.

Estiu, G. *et al.* (2008) 'Structural origin of selectivity in class II-selective histone deacetylase inhibitors', *Journal of Medicinal Chemistry*, 51(10), pp. 2898–2906.

Fawcett, D. W. (1970) 'A comparative view of sperm ultrastructure.', *Biology of reproduction. Supplement*, 2, pp. 90–127.

Fawcett, D. W. (1975) 'The mammalian spermatozoon', *Developmental Biology*, 44(2), pp. 394–436.

Fayomi, A. P. and Orwig, K. E. (2018) 'Spermatogonial stem cells and spermatogenesis in mice, monkeys and men', *Stem Cell Research*, 29, pp. 207–214.

Ferrer, M. *et al.* (2012) 'MMP2 and acrosin are major proteinases associated with the inner acrosomal membrane and may cooperate in sperm penetration of the zona pellucida during fertilization.', *Cell and tissue research*, 349(3), pp. 881–95.

Finnin, M. S. *et al.* (1999) 'Structures of a histone deacetylase homologue bound to the TSA and SAHA inhibitors', *Nature*, 401(6749), pp. 188–193.

Firman, R. C. *et al.* (2013) 'No evidence of sperm conjugate formation in an Australian mouse bearing sperm with three hooks.', *Ecology and evolution*, 3(7), pp. 1856–63.

Fourest-Lieuvin, A. *et al.* (2006) 'Microtubule regulation in mitosis: tubulin phosphorylation by the cyclin-dependent kinase Cdk1.', *Molecular biology of the cell*, 17(3), pp. 1041–50.

Francis, S. *et al.* (2014) 'Aberrant protamine content in sperm and consequential implications for infertility treatment.', *Human fertility (Cambridge, England)*, 17(2), pp. 80–9.

Fraser, L. R. and Quinn, P. J. (1981) 'A glycolytic product is obligatory for initiation of the sperm acrosome reaction and whiplash motility required for fertilization in the mouse.', *Journal of reproduction and fertility*, 61(1), pp. 25–35.

Friedmann, D. R. *et al.* (2012) 'Structure of the alpha-tubulin acetyltransferase, alphaTAT1, and implications for tubulin-specific acetylation', *Proceedings of the National Academy of Sciences*, 109(48), pp. 19655–19660.

Fuentes-Mascorro, G., Serrano, H. and Rosado, A. (2000) 'Sperm chromatin', *Archives of Andrology*, 45, pp. 215–225.

Fukushige, T. *et al.* (1999) 'MEC-12, an alpha-tubulin required for touch sensitivity in C. elegans.', *Journal of cell science*, 112, pp. 395–403.

Galjart, N. (2010) 'Plus-end-tracking proteins and their interactions at microtubule ends.', *Current biology : CB*, 20(12), pp. R528-37.

García-Peiró, A. *et al.* (2011) 'Protamine 1 to protamine 2 ratio correlates with dynamic aspects of DNA fragmentation in human sperm', *Fertility and Sterility*, 95(1), pp. 105–109.

Gentleman, S. *et al.* (1996) 'Ultrastructural Analysis of Sperm Flagella Biochemical Analysis of Sperm Flagella Case Study', *Human Pathology*, 27(1), pp. 80–84.

Gershey, E. L., Vidali, G. and Allfrey, V. G. (1968) 'Chemical studies of histone acetylation. The occurrence of epsilon-N-acetyllysine in the f2a1 histone.', *The Journal of biological chemistry*, 243(19), pp. 5018–22.

Greenbaum, M. P. *et al.* (2011) 'Germ cell intercellular bridges', *Cold Spring Harbor Perspectives in Biology*, 3(8), pp. 1–18.

Greer, K. *et al.* (1985) 'Alpha-tubulin acetylase activity in Isolated Chlamydomonas Flagella', *The Journal of Cell Biology*, 101, pp. 2081–2084.

Grozinger, C. M., Hassig, C. A. and Schreiber, S. L. (1999) 'Three proteins define a class of human histone deacetylases related to yeast Hda1p.', *Proceedings of the National Academy of Sciences of the United States of America*, 96(9), pp. 4868–4873.

Haberland, M., Montgomery, R. L. and Olson, E. N. (2009) 'The many roles of histone deacetylases in development and physiology: Implications for disease and therapy', *Nature Reviews Genetics*, pp. 32–42.

Haggarty, S. J. *et al.* (2003) 'Domain-selective small-molecule inhibitor of histone deacetylase 6 (HDAC6)-mediated tubulin deacetylation', *Proceedings of the National Academy of Sciences*, 100(8), pp. 4389–4394.

Haigis, M. C. *et al.* (2006) 'SIRT4 Inhibits Glutamate Dehydrogenase and Opposes the Effects of Calorie Restriction in Pancreatic β Cells', *Cell*, 126(5), pp. 941–954.

Hallak, M. E. *et al.* (1977) 'Release of tyrosine from tyrosinated tubulin. Some common factors that affect this process and the assembly of tubulin.', *FEBS letters*, 73(2), pp. 147–50.

Hawkins, T. *et al.* (2010) 'Mechanics of microtubules', *Journal of Biomechanics*, 43(2010), pp. 23–30.

HFEA (2014) *Fertility treatment in 2013: Trends and figures*. Available at: https://www.hfea.gov.uk/media/2081/hfea-fertility-trends-2013.pdf (Accessed: 4 June 2018).

HFEA (2016) *HFEA Fertility treatment 2014: Trends and figures*.

HFEA (2018) *Fertility treatment 2014–2016: Trends and figures*. Available at: https://www.hfea.gov.uk/media/2563/hfea-fertility-trends-and-figures-2017-v2.pdf (Accessed: 3 May 2018).

Ho, H. C. and Suarez, S. S. (2001) 'Hyperactivation of mammalian spermatozoa: Function and regulation', *Reproduction*, 122(4), pp. 519–526.

Howes, S. C. *et al.* (2014) 'Effects of tubulin acetylation and tubulin acetyltransferase binding on microtubule structure', *Molecular Biology of the Cell*, 25(2), pp. 257–266.

Hubbert, C. *et al.* (2002) 'HDAC6 is a microtubule-associated deacetylase', *Nature*, 417(6887), pp. 455–458.

Hull, M. G. *et al.* (1985) 'Population study of causes, treatment, and outcome of infertility.', *British medical journal (Clinical research ed.)*, 291(6510), pp. 1693–7.

Iftode, F. *et al.* (2000) 'Tubulin polyglycylation: A morphogenetic marker in ciliates', *Biology of the Cell*, 92(8–9), pp. 615–628.

Jamsai, D. and O'Bryan, M. K. (2011) 'Mouse models in male fertility research.', *Asian journal*

of andrology, 13(1), pp. 139–51.

Janke, C. (2014) 'The tubulin code: Molecular components, readout mechanisms, functions', *Journal of Cell Biology*, 206(4), pp. 461–472.

Janke, C. and Montagnac, G. (2017) 'Causes and Consequences of Microtubule Acetylation', *Current Biology*, 27(23), pp. R1287–R1292.

Jin, M. *et al.* (2011) 'Most fertilizing mouse spermatozoa begin their acrosome reaction before contact with the zona pellucida during in vitro fertilization.', *Proceedings of the National Academy of Sciences of the United States of America*, 108(12), pp. 4892–6.

De Jonge, C. (2005) 'Biological basis for human capacitation', *Human Reproduction Update*, pp. 205–214.

Joshi, H. C. and Cleveland, D. W. (1989) 'Differential utilization of beta-tubulin isotypes in differentiating neurites', *Journal of Cell Biology*, 109(2), pp. 663–673.

Kalebic, N. *et al.* (2013) 'Tubulin Acetyltransferase TAT1 Destabilizes Microtubules Independently of Its Acetylation Activity', *Molecular and Cellular Biology*, 33(6), pp. 1114–1123.

Kalebic, N. *et al.* (2013) 'αTAT1 is the major α-tubulin acetyltransferase in mice', *Nature Communications*, 4(1), p. 1962.

Kalinina, E. *et al.* (2007) 'A novel subfamily of mouse cytosolic carboxypeptidases.', *The FASEB journal*, 21(3), pp. 836–850.

Kao, H. Y. *et al.* (2002) 'Isolation and characterization of mammalian HDAC10, a novel histone deacetylase', *Journal of Biological Chemistry*, 277(1), pp. 187–193.

Kaul, N., Soppina, V. and Verhey, K. J. (2014) 'Effects of α-tubulin K40 acetylation and detyrosination on kinesin-1 motility in a purified system.', *Biophysical journal*, 106(12), pp. 2636–43.

Kawaguchi, Y. *et al.* (2003) 'The deacetylase HDAC6 regulates aggresome formation and cell viability in response to misfolded protein stress', *Cell*, 115(6), pp. 727–738.

Kierszenbaum, A. L. (2002) 'Sperm axoneme: A tale of tubulin posttranslation diversity', *Molecular Reproduction and Development*, 62(1), pp. 1–3.

Kim, E. *et al.* (2005) 'Identification of a hyaluronidase, Hyal5, involved in penetration of mouse

sperm through cumulus mass.', *Proceedings of the National Academy of Sciences of the United States of America*, 102(50), pp. 18028–33.

Kim, G.-W. and Yang, X.-J. (2011) 'Comprehensive lysine acetylomes emerging from bacteria to humans', *Trends in Biochemical Sciences*, 36(4), pp. 211–220.

Kim, G. W. *et al.* (2013) 'Mice lacking alpha-tubulin acetyltransferase 1 are viable but display alpha-tubulin acetylation deficiency and dentate gyrus distortion', *Journal of Biological Chemistry*, 288(28), pp. 20334–20350.

Kläver, R. *et al.* (2015) 'Direct but No Transgenerational Effects of Decitabine and Vorinostat on Male Fertility', *PLOS ONE*, 10(2), p. e0117839.

Konno, A. *et al.* (2015) 'Branchial cilia and sperm flagella recruit distinct axonemal components', *PLoS ONE*, 10(5), p. e0126005.

Kovacs, J. J. *et al.* (2005) 'HDAC6 regulates Hsp90 acetylation and chaperone-dependent activation of glucocorticoid receptor.', *Molecular cell*, 18(5), pp. 601–7.

Kubo, T. *et al.* (2010) 'Tubulin polyglutamylation regulates axonemal motility by modulating activities of inner-arm dyneins.', *Current biology : CB*, 20(5), pp. 441–5.

L'Hernault, S. W. and Rosenbaum, J. L. (1983) 'Chlamydomonas a-tubulin is posttranslationally modified in the flagella during assembly', *Journal of Cell Biology*, 97(July), pp. 258–263.

L'Hernault, S. W. and Rosenbaum, J. L. (1983) 'Chlamydomonas alpha-tubulin is posttranslationally modified in the flagella during flagellar assembly.', *The Journal of cell biology*, 97(1), pp. 258–63.

L'Hernault, S. W. and Rosenbaum, J. L. (1985) 'Chlamydomonas alpha-tubulin is posttranslationally modified by acetylation on the epsilon-amino group of a lysine.', *Biochemistry*, 24(2), pp. 473–8.

Lalle, M. *et al.* (2011) 'Giardia duodenalis 14-3-3 protein is polyglycylated by a tubulin tyrosine ligase-like member and deglycylated by two metallocarboxypeptidases.', *The Journal of biological chemistry*, 286(6), pp. 4471–84.

Lazarus, J. E. *et al.* (2013) 'Dynactin subunit p150(Glued) is a neuron-specific anti-catastrophe factor.', *PLoS biology*, 11(7), p. e1001611.

LeDizet, M. and Piperno, G. (1986) 'Cytoplasmic microtubules containing acetylated alpha-tubulin in Chlamydomonas reinhardtii: Spatial arrangement and properties', *Journal of Cell*

Biology, 103(1), pp. 13–22.

LeDizet, M. and Piperno, G. (1987) 'Identification of an acetylation site of Chlamydomonas alpha-tubulin.', *Proceedings of the National Academy of Sciences of the United States of America*, 84(16), pp. 5720–4.

Lefièvre, L. *et al.* (2007) 'Counting sperm does not add up any more: time for a new equation?', *Reproduction*, 133, pp. 675–684.

Leroux, M. R. (2010) 'Tubulin acetyltransferase discovered: ciliary role in the ancestral eukaryote expanded to neurons in metazoans.', *Proceedings of the National Academy of Sciences of the United States of America*, 107(50), pp. 21238–9.

Levine, H. *et al.* (2017) 'Temporal trends in sperm count: a systematic review and meta-regression analysis', *Human Reproduction Update*, 23(6), pp. 646–659.

Lewis, S. A., Gu, W. and Cowan, N. J. (1987) 'Free intermingling of mammalian β-tubulin isotypes among functionally distinct microtubules', *Cell*, 49(4), pp. 539–548.

Li, L. and Yang, X. J. (2015) 'Tubulin acetylation: Responsible enzymes, biological functions and human diseases', *Cellular and Molecular Life Sciences*, pp. 4237–4255.

Li, Y. and Seto, E. (2016) 'HDACs and HDAC inhibitors in cancer development and therapy', *Cold Spring Harbor Perspectives in Medicine*, 6(10).

Lindemann, C. B. and Lesich, K. A. (2016) 'Functional anatomy of the mammalian sperm flagellum', *Cytoskeleton*, pp. 652–669.

Lindemann, C. B., Orlando, A. and Kanous, K. S. (1992) 'The flagellar beat of rat sperm is organized by the interaction of two functionally distinct populations of dynein bridges with a stable central axonemal partition.', *Journal of cell science*, 102(Pt 2), pp. 249–260.

Lishko, P. V *et al.* (2012) 'The control of male fertility by spermatozoan ion channels.', *Annual review of physiology*, 74, pp. 453–75.

Lishko, P. V, Botchkina, I. L. and Kirichok, Y. (2011) 'Progesterone activates the principal Ca 2+ channel of human sperm', *Nature*, 471(7338), pp. 387–392.

Lishko, P. V and Kirichok, Y. (2010) 'The role of Hv1 and CatSper channels in sperm activation', *Journal of Physiology*, pp. 4667–4672.

Lu, J. *et al.* (2000) 'Regulation of skeletal myogenesis by association of the MEF2 transcription

factor with class II histone deacetylases.', *Molecular cell*, 6(2), pp. 233–44.

Luconi, M. *et al.* (2004) 'Increased phosphorylation of AKAP by inhibition of phosphatidylinositol 3-kinase enhances human sperm motility through tail recruitment of protein kinase A', *Journal of Cell Science*, 117(7), pp. 1235–1246.

Luconi, M. *et al.* (2011) 'Role of a-kinase anchoring proteins (AKAPs) in reproduction.', *Frontiers in bioscience (Landmark edition)*, 16, pp. 1315–30.

Ly, N. *et al.* (2016) 'αTAT1 controls longitudinal spreading of acetylation marks from open microtubules extremities', *Scientific Reports*, 6, p. 35624.

Machado-Vieira, R. *et al.* (2011) 'Histone deacetylases and mood disorders: epigenetic programming in gene-environment interactions.', *CNS neuroscience & therapeutics*, 17(6), pp. 699–704.

Martins da Silva, S. J. *et al.* (2017) 'Drug discovery for male subfertility using high-throughput screening: a new approach to an unsolved problem', *Human Reproduction*, 32(5), pp. 974–984.

Mascarenhas, M. N. *et al.* (2012) 'National, Regional, and Global Trends in Infertility Prevalence Since 1990: A Systematic Analysis of 277 Health Surveys', *PLoS Medicine*. Edited by N. Low, 9(12).

Matsuyama, A. *et al.* (2002a) 'In vivo destabilization of dynamic microtubules by HDAC6-mediated deacetylation.', *The EMBO journal*, 21(24), pp. 6820–31.

Matsuyama, A. *et al.* (2002b) 'In vivo destabilization of dynamic microtubules by HDAC6-mediated deacetylation', *The EMBO journal*, 21(24), pp. 6820–6831.

McKeithan, T. W. *et al.* (1983) 'Multiple forms of tubulin in Polytomella and Chlamydomonas: evidence for a precursor of flagellar alpha-tubulin.', *The Journal of cell biology*, 96(4), pp. 1056–63.

McKeithan, T. W. and Rosenbaum, J. L. (1981) 'Multiple forms of tubulin in the cytoskeletal and flagellar microtubules of Polytomella.', *The Journal of cell biology*, 91(2 Pt 1), pp. 352–60.

McKinsey, T. A., Zhang, C. L. and Olson, E. N. (2001) 'Identification of a signal-responsive nuclear export sequence in class II histone deacetylases.', *Molecular and cellular biology*, 21(18), pp. 6312–21.

Menezo, Y. (2002) 'Mouse and bovine models for human IVF', *Reproductive BioMedicine Online*, 4(2), pp. 170–175.

Meurer-Grob, P., Kasparian, J. and Wade, R. H. (2001) 'Microtubule structure at improved resolution', *Biochemistry*, 40(27), pp. 8000–8008.

Michishita, E. *et al.* (2005) 'Evolutionarily Conserved and Nonconserved Cellular Localizations and Functions of Human SIRT Proteins', *Molecular Biology of the Cell*, 16(10), pp. 4623–4635.

Miki, K. *et al.* (2002) 'Targeted disruption of the Akap4 gene causes defects in sperm flagellum and motility.', *Developmental biology*, 248(2), pp. 331–42.

Miki, K. *et al.* (2004) 'Glyceraldehyde 3-phosphate dehydrogenase-S, a sperm-specific glycolytic enzyme, is required for sperm motility and male fertility.', *Proceedings of the National Academy of Sciences of the United States of America*, 101(47), pp. 16501–6.

Miller, D. J., Gong, X. and Shur, B. D. (1993) 'Sperm require beta-N-acetylglucosaminidase to penetrate through the egg zona pellucida.', *Development*, 118(4), pp. 1279–89.

Miller, M. *et al.* (2018) 'Asymmetrically Positioned Flagellar Control Units Regulate Human Sperm Rotation', *Cell Reports*, 24(10), pp. 2606–2613.

Miller, M. R. *et al.* (2016) 'Unconventional endocannabinoid signaling governs sperm activation via the sex hormone progesterone', *Science*, 352(6285), pp. 555–559.

Miyake, Y. *et al.* (2016) 'Structural insights into HDAC6 tubulin deacetylation and its selective inhibition', *Nature Chemical Biology*, 12(9), pp. 748–754.

Mohri, H. *et al.* (2012) 'Tubulin-dynein system in flagellar and ciliary movement.', *Proceedings of the Japan Academy. Series B, Physical and biological sciences*, 88(8), pp. 397–415.

Montagnac, G. *et al.* (2013) 'αTAT1 catalyses microtubule acetylation at clathrin-coated pits', *Nature*, 502(7472), pp. 567–570.

Moore, H. *et al.* (2002) 'Exceptional sperm cooperation in the wood mouse', *Nature*, 418(6894), pp. 174–177.

Moritz, M. *et al.* (1995) 'Microtubule nucleation by γ-tubulin-containing rings in the centrosome', *Nature*, 378(6557), pp. 638–640.

Morley, S. J. *et al.* (2016) 'Acetylated tubulin is essential for touch sensation in mice', *eLife*, 5, p. 25.

Mortimer, S. T. (2000) 'CASA--practical aspects.', *Journal of andrology*, 21(4), pp. 515–524.

Nallella, K. P. *et al.* (2006) 'Significance of sperm characteristics in the evaluation of male

infertility', *Fertility and Sterility*, 85(3), pp. 629–634.

Neesen, J. *et al.* (2001) 'Disruption of an inner arm dynein heavy chain gene results in asthenozoospermia and reduced ciliary beat frequency.', *Human molecular genetics*, 10(11), pp. 1117–28.

NICE (2013) *Fertility problems: assessment and treatment. Clinical Guidelines*. Available at: https://www.nice.org.uk/guidance/cg156/resources/fertility-problems-assessment-and-treatment-35109634660549 (Accessed: 4 June 2018).

Nieuwenhuis, J. *et al.* (2017) 'Vasohibins encode tubulin detyrosinating activity', *Science*, 358(6369), pp. 1453–1456.

Nishimura, H. and L'Hernault, S. W. (2017) 'Spermatogenesis', *Current Biology*, pp. R988–R994.

Nogales, E. *et al.* (1999) 'High-resolution model of the microtubule', *Cell*, 96(1), pp. 79–88.

Nogales, E. (2000) 'Structural Insights into Microtubule Function', *Annual Review of Biochemistry*, 69(1), pp. 277–302.

North, B. J. *et al.* (2003) 'The human Sir2 ortholog, SIRT2, is an NAD+-dependent tubulin deacetylase.', *Molecular cell*, 11(2), pp. 437–44.

O'Donnell, L. *et al.* (2011) 'Spermiation: The process of sperm release.', *Spermatogenesis*, 1(1), pp. 14–35.

O'Donnell, L. (2014) 'Mechanisms of spermiogenesis and spermiation and how they are disturbed', *Spermatogenesis*, 4(2), p. e979623.

Odde, D. (1998) 'Diffusion inside microtubules', *European Biophysics Journal*, 27(5), pp. 514–520.

Ohkawa, N. *et al.* (2008) 'N-acetyltransferase ARD1-NAT1 regulates neuronal dendritic development', *Genes to Cells*, 13(11), pp. 1171–1183.

Okamura, N. *et al.* (1985) 'Sodium bicarbonate in seminal plasma stimulates the motility of mammalian spermatozoa through direct activation of adenylate cyclase', *Journal of Biological Chemistry*, 260(17), pp. 9699–9705.

Oko, R. and Sutovsky, P. (2009) 'Biogenesis of sperm perinuclear theca and its role in sperm functional competence and fertilization', *Journal of Reproductive Immunology*, 83(1–2), pp. 2–7.

Olson, G. E. and Winfrey, V. P. (1985) 'Substructure of a cytoskeletal complex associated with the hamster sperm acrosome', *Journal of Ultrastructure Research and Molecular Structure Research*, 92(3), pp. 167–179.

Palazzo, A., Ackerman, B. and Gundersen, G. G. (2003) 'Cell biology: Tubulin acetylation and cell motility.', *Nature*, 421(6920), p. 230.

Parab, S. *et al.* (2015) 'HDAC6 deacetylates alpha tubulin in sperm and modulates sperm motility in Holtzman rat', *Cell and Tissue Research*, 359(2), pp. 665–678.

Park, I. Y., Powell, R. T., *et al.* (2016) 'Dual Chromatin and Cytoskeletal Remodeling by SETD2.', *Cell*, 166(4), pp. 950–962.

Park, I. Y., Chowdhury, P., *et al.* (2016) 'Methylated α-tubulin antibodies recognize a new microtubule modification on mitotic microtubules', *mAbs*, 8(8), pp. 1590–1597.

Paturle-Lafanechère, L. *et al.* (1991) 'Characterization of a Major Brain Tubulin Variant Which Cannot Be Tyrosinated', *Biochemistry*, 30(43), pp. 10523–10528.

Perlman, R. L. (2016) 'Mouse models of human disease: An evolutionary perspective.', *Evolution, medicine, and public health*. Oxford University Press, 2016(1), pp. 170–6.

Perrod, S. *et al.* (2001) 'A cytosolic NAD-dependent deacetylase, Hst2p, can modulate nucleolar and telomeric silencing in yeast', *EMBO Journal*, 20(1–2), pp. 197–209.

Piperno, G. and Fuller, M. T. (1985) 'Monoclonal Antibodies Specific for an Acetylated Form of a-Tubulin Recognize the Antigen in Cilia and Flagella from a Variety of Organisms', *The Journal of Cell Biology*, 101(37), pp. 2085–2094.

Piperno, G., LeDizet, M. and Chang, X. J. (1987) 'Microtubules containing acetylated alpha-tubulin in mammalian cells in culture.', *Journal of Cell Biology*, 104(2), pp. 289–302.

Portran, D. *et al.* (2017) 'Tubulin acetylation protects long-lived microtubules against mechanical ageing', *Nature Cell Biology*, 19(4), pp. 391–398.

Prota, A. E. *et al.* (2013) 'Structural basis of tubulin tyrosination by tubulin tyrosine ligase', *Journal of Cell Biology*, 200(3), pp. 259–270.

Quinn, P. and Horstman, F. C. (1998) 'Is the mouse a good model for the human with respect to the development of the preimplantation embryo in vitro?', *Human Reproduction*, 13(SUPPL. 4), pp. 173–183.

Raff, E. C. *et al.* (1997) 'Microtubule architecture specified by a β-tubulin isoform', *Science*, 275(5296), pp. 70–73.

Raff, E. C. *et al.* (2000) 'Conserved axoneme symmetry altered by a component β-tubulin', *Current Biology*, 10(21), pp. 1391–1394.

Raff, E. C. *et al.* (2008) 'Axoneme β-Tubulin Sequence Determines Attachment of Outer Dynein Arms', *Current Biology*, 18(12), pp. 911–914.

Raheja, N. *et al.* (2018) 'A review on semen extenders and additives used in cattle and buffalo bull semen preservation', *JOURNAL OF ENTOMOLOGY AND ZOOLOGY STUDIES*, 6(3), pp. 239–245.

Ramkumar, A., Jong, B. Y. and Ori-McKenney, K. M. (2018) 'ReMAPping the microtubule landscape: How phosphorylation dictates the activities of microtubule-associated proteins', *Developmental Dynamics*, 247(1), pp. 138–155.

Raseona, A. M. *et al.* (2017) 'Viability of bull semen extended with commercial semen extender and two culture media stored at 24 °C', *South African Journal of Animal Science*, 47(1), p. 49.

Rashid, A. (2017) 'Sperm Motility as a Screening Strategy for the Identification of Microtubule Targeting Drugs', *International Journal of Trend in Scientific Research and Development*, 1(4), pp. 2456–6470.

Reed, N. A. *et al.* (2006) 'Microtubule Acetylation Promotes Kinesin-1 Binding and Transport', *Current Biology*, 16(21), pp. 2166–2172.

Ren, D. *et al.* (2001) 'A sperm ion channel required for sperm motility and male fertility', *Nature*, 413(6856), pp. 603–609.

Ridinger, J. *et al.* (2018) 'Dual role of HDAC10 in lysosomal exocytosis and DNA repair promotes neuroblastoma chemoresistance.', *Scientific reports*, 8(1), p. 10039.

Rocha, C. *et al.* (2014) 'Tubulin glycylases are required for primary cilia, control of cell proliferation and tumor development in colon', *The EMBO Journal*, 33(19), pp. 2247–2260.

Rogowski, K. *et al.* (2009) 'Evolutionary Divergence of Enzymatic Mechanisms for Posttranslational Polyglycylation', *Cell*, 137(6), pp. 1076–1087.

Rogowski, K. *et al.* (2010) 'A family of protein-deglutamylating enzymes associated with neurodegeneration.', *Cell*, 143(4), pp. 564–78.

Rojas, J. R. *et al.* (1999) 'Structure of Tetrahymena GCN5 bound to coenzyme A and a histone H3 peptide', *Nature*, 401(6748), pp. 93–98.

Roldan, E. R. S., Murase, T. and Shi, Q.-X. (1994) 'Exocytosis in spermatozoa in respones to progesterone and zona pellucida', *Science*, 266(5190), pp. 1578–1581.

Saling, P. M., Sowinski, J. and Storey, B. T. (1979) 'An ultrastructural study of epididymal mouse spermatozoa binding to zonae pellucidae in vitro: Sequential relationship to the acrosome reaction', *Journal of Experimental Zoology*, 209(2), pp. 229–238.

Schaap, I. A. T., De Pablo, P. J. and Schmidt, C. F. (2004) 'Resolving the molecular structure of microtubules under physiological conditions with scanning force microscopy', *European Biophysics Journal*, 33(5), pp. 462–467.

Schaedel, L. *et al.* (2015) 'Microtubules self-repair in response to mechanical stress', *Nature Materials*, 14(11), pp. 1156–1163.

Schwer, H. D. *et al.* (2001) 'A lineage-restricted and divergent beta-tubulin isoform is essential for the biogenesis, structure and function of blood platelets.', *Current biology*, 11(8), pp. 579–86.

Seetapun, D. *et al.* (2012) 'Estimating the microtubule GTP cap size in vivo.', *Current biology*, 22(18), pp. 1681–7.

Seigneurin-Berny, D. *et al.* (2001) 'Identification of Components of the Murine Histone Deacetylase 6 Complex: Link between Acetylation and Ubiquitination Signaling Pathways', *Molecular and Cellular Biology*, 21(23), pp. 8035–8044.

Shah, N. *et al.* (2018) 'TAK1 activation of alpha-TAT1 and microtubule hyperacetylation control AKT signaling and cell growth', *Nature Communications*, 9(1), p. 1696.

Shahbazian, M. D. and Grunstein, M. (2007) 'Functions of Site-Specific Histone Acetylation and Deacetylation', *Annual Review of Biochemistry*, 76(1), pp. 75–100.

Shida, T. *et al.* (2010) 'The major alpha-tubulin K40 acetyltransferase alphaTAT1 promotes rapid ciliogenesis and efficient mechanosensation.', *Proceedings of the National Academy of Sciences of the United States of America*, 107(50), pp. 21517–22.

Silflow, C. D. and Lefebvre, P. A. (2001) 'Assembly and Motility of Eukaryotic Cilia and Flagella. Lessons from Chlamydomonas reinhardtii', *PLANT PHYSIOLOGY*, 127(4), pp. 1500–1507.

Sirajuddin, M., Rice, L. M. and Vale, R. D. (2014) 'Regulation of microtubule motors by tubulin

isotypes and post-translational modifications.', *Nature cell biology*. NIH Public Access, 16(4), pp. 335–44.

Skinner, B. M. and Johnson, E. E. P. (2017) 'Nuclear morphologies: their diversity and functional relevance', *Chromosoma*. Chromosoma, 126(2), pp. 195–212.

Skoge, R. H. and Ziegler, M. (2016) 'SIRT2 inactivation reveals a subset of hyperacetylated perinuclear microtubules inaccessible to HDAC6', *Journal of Cell Science*, 129(15), pp. 2972–2982.

Solinger, J. A. *et al.* (2010) 'The Caenorhabditis elegans Elongator complex regulates neuronal alpha-tubulin acetylation.', *PLoS genetics*, 6(1), p. e1000820.

Song, Y. *et al.* (2013) 'Transglutaminase and polyamination of tubulin: posttranslational modification for stabilizing axonal microtubules.', *Neuron*, 78(1), pp. 109–23.

Steczkiewicz, K. *et al.* (2006) 'Eukaryotic domain of unknown function DUF738 belongs to Gcn5-related N-acetyltransferase superfamily', *Cell Cycle*, pp. 2927–2930.

Steinmetz, M. O. and Prota, A. E. (2018) 'Microtubule-Targeting Agents: Strategies To Hijack the Cytoskeleton', *Trends in Cell Biology*, 28(10), pp. 776–792.

Storey, B. T. and Kayne, F. J. (1975) 'Energy metabolism of spermatozoa. V. The Embden-Myerhof pathway of glycolysis: activities of pathway enzymes in hypotonically treated rabbit epididymal spermatozoa.', *Fertility and sterility*, 26(12), pp. 1257–65.

Suarez, S. S. (2008) 'Control of hyperactivation in sperm', *Human Reproduction Update*, 14(6), pp. 647–657.

Suarez, S. S. and Dai, X. (1992) 'Hyperactivation Enhances Mouse Sperm Capacity for Penetrating Viscoelastic Media', *Biology of Reproduction*, 46(4), pp. 686–691.

Sun, G. *et al.* (2014) 'Insights into the lysine acetylproteome of human sperm', *Journal of Proteomics*, 109(1), pp. 199–211.

Suryavanshi, S. *et al.* (2010) 'Tubulin Glutamylation Regulates Ciliary Motility by Altering Inner Dynein Arm Activity', *Current Biology*, 20(5), pp. 435–440.

Suzuki, K. and Koike, T. (2007) 'Mammalian Sir2-related protein (SIRT) 2–mediated modulation of resistance to axonal degeneration in slow Wallerian degeneration mice: A crucial role of tubulin deacetylation', *Neuroscience*, 147(3), pp. 599–612.

Szyk, A. *et al.* (2014a) 'Molecular basis for age-dependent microtubule acetylation by tubulin acetyltransferase', *Cell*, 157(6), pp. 1405–1415.

Szyk, A. *et al.* (2014b) 'Molecular basis for age-dependent microtubule acetylation by tubulin acetyltransferase', *Cell*, 157(6), pp. 1405–1415.

Taes, I. *et al.* (2013) 'HDAC6 deletion delays disease progression in the SOD1g93a mouse model of ALS', *Human Molecular Genetics*, 22(9), pp. 1783–1790.

Tourmente, M., Zarka-Trigo, D. and Roldan, E. R. S. (2016) 'Is the hook of muroid rodent's sperm related to sperm train formation?', *Journal of Evolutionary Biology*, 29(6), pp. 1168–1177.

Travis, A. J. *et al.* (1998) 'Targeting of a Germ Cell-specific Type 1 Hexokinase Lacking a Porin-binding Domain to the Mitochondria as Well as to the Head and Fibrous Sheath of Murine Spermatozoa', *Molecular Biology of the Cell*, 9, pp. 263–276.

Turner, R. M. (2003) 'Tales from the Tail: What Do We Really Know about Sperm Motility?', *Journal of Andrology*, 24(6), pp. 790–803.

Turner, R. M. (2006) 'Moving to the beat: a review of mammalian sperm motility regulation', *Reproduction, Fertility and Development*, 18(2), p. 25.

Valenzuela-Fernández, A. *et al.* (2008) 'HDAC6: a key regulator of cytoskeleton, cell migration and cell-cell interactions', *Trends in Cell Biology*, 18(6), pp. 291–297.

Valenzuela, P. *et al.* (1981) 'Nucleotide and corresponding amino acid sequences encoded by α and β tubulin mRNAs', *Nature*, 289(5799), pp. 650–655.

Varea-Sanchez, M. *et al.* (2016) 'Unraveling the Sperm Bauplan: Relationships Between Sperm Head Morphology and Sperm Function in Rodents', *Biology of Reproduction*, 95(1), pp. 25–25.

Verdel, A. *et al.* (2000) 'Active maintenance of mHDA2/mHDAC6 histone-deacetylase in the cytoplasm', *Current Biology*, 10(12), pp. 747–749.

Verhey, K. J. and Gaertig, J. (2007) 'The Tubulin Code', *Cell*, 6(17), pp. 2152–2160.

Verma, P. *et al.* (2017) 'Developmental Testicular Expression, Cloning, and Characterization of Rat HDAC6 In Silico', *BioMed Research International*, 2017, p. 5170680.

Wandernoth, P. M. *et al.* (2010) 'Role of carbonic anhydrase IV in the bicarbonate-mediated activation of murine and human sperm', *PLoS ONE*, 5(11), p. e15061.

Wang, A. H. and Yang, X. J. (2001) 'Histone deacetylase 4 possesses intrinsic nuclear import and export signals.', *Molecular and cellular biology*, 21(17), pp. 5992–6005.

Wang, Y. *et al.* (2016) 'Structures of a diverse set of colchicine binding site inhibitors in complex with tubulin provide a rationale for drug discovery', *FEBS Journal*, 283(1), pp. 102–111.

Webster, D. D. R. and Borisy, G. G. (1989) 'Microtubules are acetylated in domains that turn over slowly', *J. Cell Sci.*, 92(1), pp. 57–65.

Webster, D. R. *et al.* (1990) 'Detyrosination of Alpha Tubulin Does Not Stabilize Microtubules In Vivo', *The Journal of Cell Biology*, 111, pp. 113–122.

Westhoff, D. and Kamp, G. (1997) 'Glyceraldehyde 3-phosphate dehydrogenase is bound to the fibrous sheath of mammalian spermatozoa.', *Journal of cell science*, 110, pp. 1821–9.

WHO (2010) *WHO laboratory manual for the Examination and processing of human semen, 5th edition*. Available at: http://apps.who.int/iris/bitstream/handle/10665/44261/9789241547789_eng.pdf;jsessionid=4B03AE343E6B6BED57DFD9C4164A03F2?sequence=1 (Accessed: 18 June 2018).

Wise, L. D. *et al.* (2008) 'Assessment of female and male fertility in Sprague–Dawley rats administered vorinostat, a histone deacetylase inhibitor', *Birth Defects Research Part B: Developmental and Reproductive Toxicology*, 83(1), pp. 19–26.

Wloga, D., Joachimiak, E. and Fabczak, H. (2017) 'Tubulin post-translational modifications and microtubule dynamics', *International Journal of Molecular Sciences*, p. 2207.

Xu, W., Parmigiani, R. and Marks, P. (2007) 'Histone deacetylase inhibitors: molecular mechanisms of action', *Oncogene*, 26(37), pp. 5541–5552.

Xu, Z. *et al.* (2017) 'Microtubules acquire resistance from mechanical breakage through intralumenal acetylation', *Science*, 356(6335), pp. 328–332.

Yanagimachi, R. (1970) 'The movement of golden hamster spermatozoa before and after capacitation', *Journal of reproduction and fertility*, 23, pp. 193–196.

Yang, X.-J. and Grégoire, S. (2005) 'Class II histone deacetylases: from sequence to function, regulation, and clinical implication.', *Molecular and cellular biology*, 25(8), pp. 2873–2884.

Yang, Y. *et al.* (2016) 'HDAC10 promotes lung cancer proliferation via AKT phosphorylation.', *Oncotarget*, 7(37), pp. 59388–59401.

Yu, H. *et al.* (2015) 'Acetylproteomic Analysis Reveals Functional Implications of Lysine Acetylation in Human Spermatozoa (sperm)', *Molecular & Cellular Proteomics*, 14(4), pp. 1009–1023.

Zhang, D. *et al.* (2014) 'Activation of histone deacetylase-6 induces contractile dysfunction through derailment of α-tubulin proteostasis in experimental and human atrial fibrillation', *Circulation*, 129(3), pp. 346–358.

Zhang, M. *et al.* (2014) 'HDAC6 deacetylates and ubiquitinates MSH2 to maintain proper levels of MutSα', *Molecular Cell*, 55(1), pp. 31–46.

Zhang, X. *et al.* (2007) 'HDAC6 modulates cell motility by altering the acetylation level of cortactin.', *Molecular cell*, 27(2), pp. 197–213.

Zhang, Y. *et al.* (2002) 'Identification of genes expressed in C. Elegans touch receptor neurons', *Nature*, 418(6895), pp. 331–335.

Zhang, Y. *et al.* (2003) 'HDAC-6 interacts with and deacetylates tubulin and microtubules in vivo', *EMBO Journal*, 22(5), pp. 1168–1179.

Zhang, Y. *et al.* (2006) 'Two catalytic domains are required for protein deacetylation.', *The Journal of biological chemistry*, 281(5), pp. 2401–4.

Zhang, Y. *et al.* (2008) 'Mice lacking histone deacetylase 6 have hyperacetylated tubulin but are viable and develop normally.', *Molecular and cellular biology*, 28(5), pp. 1688–701.

Zhao, Z., Xu, H. and Gong, W. (2010) 'Histone deacetylase 6 (HDAC6) is an independent deacetylase for alpha-tubulin.', *Protein and peptide letters*, 17(5), pp. 555–8.

Zilberman, Y. *et al.* (2009) 'Regulation of microtubule dynamics by inhibition of the tubulin deacetylase HDAC6', *Journal of Cell Science*, 122(19), pp. 3531–3541.